

# JEMS

JOURNAL OF ETA MARITIME SCIENCE



[www.jemsjournal.org](http://www.jemsjournal.org)



Volume: **12** Issue: **4**

December **2024**

E-ISSN: 2148-9386



## Editorial Board

### ■ On Behalf of UCTEA The Chamber of Marine Engineers

**Yaşar CANCA**

UCTEA Chamber of Marine Engineers,  
Chairman of the Board

### ■ EDITOR-IN-CHIEF

**Prof. Dr. Selçuk NAS**

Dokuz Eylül University Maritime Faculty,  
Department of Maritime Education and  
Training, İzmir/Türkiye

### ■ DEPUTY EDITOR

**Assoc. Prof. Dr. Remzi FİŞKİN**

Ordu University Faculty of Marine Sciences,  
Department of Marine Transportation  
Engineering, Ordu/Türkiye

## Section Editors

### Marine Transportation Engineering

**Prof. Dr. Ender ASYALI**

Maine Maritime Academy, Marine Transportation Operations,  
Castine Maine/United States

**Prof. Dr. Özkan UĞURLU**

Ordu University Faculty of Marine Science, Department of Maritime  
Transportation and Management Engineering, Ordu/Türkiye

**Prof. Dr. Selçuk ÇEBİ**

Yıldız Technical University Faculty of Mechanical Engineering, Department of  
Industrial Engineering, İstanbul/Türkiye

**Prof. Dr. Emre AKYÜZ**

İstanbul Technical University Maritime Faculty, Department of Maritime  
Transportation and Management, İstanbul/Türkiye

**Assoc. Prof. Dr. Momoko KITADA**

World Maritime University, Department of Maritime Education and Training,  
Malmö/Sweden

### Marine Engineering

**Prof. Dr. Alper KILIÇ**

Bandırma Onyedi Eylül University Maritime Faculty, Department of Marine  
Business Management and Ship Machines Operational Engineering,  
Balıkesir/Türkiye

**Assoc. Prof. Dr. Görkem KÖKKÜLÜNK**

Yıldız Technical University Faculty of Naval Architecture and Maritime,  
Department of Marine Engineering, İstanbul/Türkiye

**Assoc. Prof. Dr. Burak ZİNCİR**

İstanbul Technical University Maritime Faculty, Department of Marine Engineering,  
İstanbul/Türkiye

**Asst. Prof. Dr. Olgun KONUR**

Dokuz Eylül University Maritime Faculty, Department of Marine Engineering,  
İzmir/Türkiye

**Dr. Jing YU**

Dalian Maritime University Maritime Faculty Engineering, Dalian/China

**Asst. Prof. Dr. Onur YÜKSEL**

Zonguldak Bulent Ecevit University, Maritime Faculty, Department of Marine  
Engineering, Zonguldak/Türkiye

### Maritime Business Administration

**Assoc. Prof. Dr. Abdullah AÇIK**

Dokuz Eylül University Maritime Faculty, Department of Maritime Business  
Administration, İzmir/Türkiye

**Asst. Prof. Dr. Cemile SOLAK FİŞKİN**

Ordu University Faculty of Marine Sciences, Department of Maritime Business  
Administration, Ordu/Türkiye

### Naval Architecture

**Prof. Dr. Ahmet TAŞDEMİR**

Piri Reis University Maritime Faculty, Department of Marine Engineering,  
İstanbul/Türkiye

**Prof. Dr. Ercan KÖSE**

Karadeniz Technical University Faculty of Marine Science,  
Department of Shipbuilding and Marine Engineering, Trabzon/Türkiye

**Prof. Dimitrios KONOVESSIS**

University of Strathclyde, Department of Naval Architecture, Ocean and Marine  
Engineering, Scotland/United Kingdom

**Dr. Rafet Emek KURT**

University of Strathclyde Faculty of Engineering, Department of Naval  
Architecture Ocean and Marine Engineering, Glasgow/United Kingdom

**Dr. Sefer Anıl GÜNBEYAZ**

University of Strathclyde Faculty of Engineering, Department of Naval  
Architecture, Ocean and Marine Engineering, Glasgow/United Kingdom

**Assoc. Prof. Dr. Gökhan BUDAK**

İzmir Katip Çelebi University, Department of Shipbuilding and Ocean Engineering,  
İzmir/Türkiye

### Coastal and Port Engineering

**Assoc. Prof. Dr. Kubilay CİHAN**

Kırıkkale University Faculty of Engineering and Architecture,  
Department of Hydraulics, Kırıkkale/Türkiye

### Logistic and Supply Chain Management

**Assoc. Prof. Dr. Ceren ALTUNTAŞ VURAL**

Chalmers University of Technology, Department of Technology Management and  
Economics, Division of Service Management and Logistics, Göteborg/Sweden

### Marine Tourism

**PhD Eng. Aleksandra LAPKO**

Maritime University of Szczecin, Faculty of Economics and Transport Engineering,  
Szczecin/Poland



## Editorial Board

### Prof. Dr. Ersan BAŞAR

Karadeniz Technical University, Sürmene Faculty of Marine Sciences, Department of Maritime Transportation and Management Engineering, Trabzon/Türkiye

### Prof. Dr. Masao FURUSHO

Director of the National Institute of Technology, Oshima Maritime College, Japan

### Prof. Dr. Metin ÇELİK

Istanbul Technical University Maritime Faculty, Department of Marine Machinery Management Engineering, İstanbul/Türkiye

### Prof. Dr. Nikitas NIKITAKOS

University of the Aegean School of Business, Department of Shipping Trade and Transport, Mytilene/Greece

### Assoc. Prof. Dr. Ghiorghe BATRINCA

Maritime University of Constanta Faculty of Navigation and Naval Transport, Department of Economic Engineering in Transports, Constanta/Romania

### Assoc. Prof. Dr. Marcella Castells-SANABRA

Polytechnic University of Catalonia, Barcelona School of Nautical Studies, Department of Nautical Science and Engineering, Barcelona/Spain

### Assoc. Prof. Dr. Radu HANZU-PAZARA

Constanta Maritime University, Vice-Rector, Constanta/Romania

### Dr. Angelica M BAYLON

Maritime Academy of Asia and the Pacific (MAAP), Central Luzon/Philippines

### Dr. Iraklis LAZAKIS

University of Strathclyde Faculty of Engineering, Department of Naval Architecture, Ocean and Marine Engineering, Glasgow/United Kingdom

## Associate Editors

### Asst. Prof. Dr. Emin Deniz ÖZKAN

Dokuz Eylül University Maritime Faculty, Department of Marine Transportation Engineering, İzmir/Türkiye

### Asst. Prof. Dr. Ömer ARSLAN

Çanakkale Onsekiz Mart University Faculty of Marine Science and Technology, Department of Maritime Transportation and Management Engineering, Çanakkale/Türkiye

### Dr. Pelin ERDEM

University of Strathclyde Faculty of Engineering, Department of Naval Architecture, Ocean and Marine Engineering, Glasgow/United Kingdom

### Res. Asst. Dr. Burak KUNDAKÇI

İskenderun Technical University Faculty of Barbaros Hayrettin Naval Architecture and Maritime, Department of Marine Transportation Engineering, Hatay/Türkiye

### Res. Asst. Dr. Coşkan SEVGİLİ

Zonguldak Bülent Ecevit University Maritime Faculty, Department of Marine Transportation Management Engineering, Zonguldak/Türkiye

### Res. Asst. Dr. Elif ARSLAN

Dokuz Eylül University Maritime Faculty, Department of Marine Transportation Engineering, İzmir/Türkiye

### Asst. Prof. Dr. Gizem KAYIŞOĞLU

Istanbul Technical University Maritime Faculty, Department of Marine Transportation Engineering, İstanbul/Türkiye

### Res. Asst. Merve GÜL ÇIVGIN

Istanbul Technical University Maritime Faculty, Marine Engineering Department, İstanbul/Türkiye

## Advisory Board

### Prof. Dr. Ali Muzaffer FEYZİOĞLU

Karadeniz Technical University Sürmene Faculty of Marine Sciences, Department of Marine Sciences and Technology Engineering, Trabzon/Türkiye

### Prof. Dr. Şermin AÇIK ÇINAR

Dokuz Eylül University Maritime Faculty, Department of Maritime Business Management, İzmir/Türkiye

### Prof. Dr. Özcan ARSLAN

Istanbul Technical University Maritime Faculty, Marine Transportation Engineering, İstanbul/Türkiye

### Prof. Dr. Murat YAYLACI

Recep Tayyip Erdoğan University Maritime Faculty, Rize/Türkiye

### Prof. Dr. Özkan UĞURLU

Ordu University Faculty of Marine Science, Department of Maritime Transportation and Management Engineering, Ordu/Türkiye

### Prof. Dr. Mehmet BİLGİN

Istanbul University Faculty of Engineering, Department of Chemical Engineering, İstanbul/Türkiye

### Prof. Dr. Osman TURAN

University of Strathclyde Faculty of Engineering, Department of Naval Architecture Ocean and Marine Engineering, Glasgow/United Kingdom



Please refer to the journal's webpage ([www.jemsjournal.org](http://www.jemsjournal.org)) for "About Us", "Aim and Scope", "Guide for Authors" and "Ethical Policy".

JEMS is currently indexed in Web of Science Emerging Sources Citation Index (ESCI), Tubitak Ulakbim Science Database, Transport Research International Documentation (TRID), Directory of Open Access Journals (DOAJ), EBSCO, J-Gate, Scopus and CNKI.

### Owner UCTEA The Chamber of Marine Engineers

Address: Sahrayıcedit Mah. Halk Sk. Golden Plaza No: 29 C Blok K:3 D:6 Kadıköy/İstanbul - Türkiye  
Web: [gemimo.org](http://gemimo.org) E-mail: [bilgi@gemimo.org](mailto:bilgi@gemimo.org) Phone: +90 216 747 15 51 Fax: +90 216 747 34 35

### Publisher Galenos Publishing House

Address: Molla Gürani Mah. Kaçamak Sk. No: 21/1 34093 İstanbul, Türkiye  
Phone: +90 (530) 177 30 97 E-mail: [info@galenos.com.tr](mailto:info@galenos.com.tr) Web: [www.galenos.com.tr](http://www.galenos.com.tr)



JEMS apply the Creative Commons Attribution NonCommercial 4.0 International Licence to all manuscripts to be published.

### Journal website:

[www.jemsjournal.org](http://www.jemsjournal.org)

### Submit Article:

[jag.journalagent.com/jems](http://jag.journalagent.com/jems)

### E-ISSN: 2148-9386

### Online Publication Date:

December 2024

### Cover Photo:

2024 / Volume 12 / Issue 4

2024 Burak Reis YAVUZ. Strait of Istanbul, Yavuz Sultan Selim Bridge



<b>ED</b>	<b>Editorial</b>	<b>357</b>
	Selçuk Nas	
<b>AR</b>	<b>Astern Running of Heavy-Tonnage Vessels in an Ice Channel</b>	<b>358</b>
	Aleksei Dobrodeev, Kirill Sazonov	
<b>AR</b>	<b>State Estimation and Control for a Model Scale Passenger Ship using an LQG Approach</b>	<b>365</b>
	Ferdi Çakıcı, Ahmad Irham Jambak, Emre Kahramanoğlu, Ahmet Kaan Karabüber, Bünyamin Ustalı, Mehmet Utku Öğür, Fuat Peri, Ömer Sinan Şahin, Mehmet Akif Uğur, Afşin Baran Bayezit	
<b>AR</b>	<b>A Conceptual COLREGs-based Obstacle Avoidance Algorithm Implementing Dynamic Path Planning and Collision Risk Assessment</b>	<b>377</b>
	Hasan Uğurlu, Omar Djecevic, İsmail Çiçek	
<b>AR</b>	<b>Strategic Ship Fleet Planning for Crude Palm Oil Marine Transportation: A Case Study in Indonesia</b>	<b>395</b>
	Achmad Riadi, Muhammad Hanif Fajri Ramadhan	
<b>AR</b>	<b>A Dynamic Discretization Algorithm for Learning BN Model: Predicting Causation Probability of Ship Collision in the Sunda Strait, Indonesia</b>	<b>404</b>
	Iis Dewi Ratih, Ketut Buda Artana, Heri Kuswanto, Dhimas Widhi Handani, Renata Zahabiya	
<b>AR</b>	<b>Analysis of the Strain-Dependent Damping of Paulownia Wood to Reduce Vibrations in Maritime Transport</b>	<b>418</b>
	Jürgen Göken, Nicolas Saba	
<b>AR</b>	<b>Strategic Management Modeling for Offshore Tugboat and Support Vessel Operations: A Hybrid SWOT-TOWS Fuzzy DEMATEL-TOPSIS Framework</b>	<b>427</b>
	Ali Burçin Eke, Ozan Batmaz, Muhammed Fatih Gülen, Esmâ Uflaz, Özcan Arslan	
<b>AR</b>	<b>Close Contact Tracing and Risky Area Identification Using Alpha Shape Algorithm and Binary Contact Detection Model Based on Bluetooth 5.1</b>	<b>446</b>
	Qianfeng Lin, Jooyoung Son	
<b>AR</b>	<b>Challenges and Facilitators in Professional Pursuits: A Qualitative Exploration of Work Experiences in Türkiye and Perspectives of Seaborne Professionals</b>	<b>466</b>
	Özgür Sert, İbrahim Sani Mert	
<b>IN</b>	<b>2024 Reviewer Index</b>	
<b>IN</b>	<b>2024 Author Index</b>	
<b>IN</b>	<b>2024 Subject Index</b>	

Dear Readers,

With great pleasure, I present to our esteemed readers JEMS 12 (4). We are delighted to see that our publications are becoming more and more worldwide with each issue. Additionally, we see that the articles tend to focus on marine engineering subjects. We strive to be discriminating and only publish 9-10 articles per issue, even with the high volume of article submissions. This issue contains some interesting and valuable studies. There is no doubt that the maritime sector will benefit from these investigations.

In the upcoming year, we intend to host online seminars for our authors. Prof. Dr. Tahsin Tezdođan, esteemed editor of Ocean Engineering, will start off our opening seminar. "Publishing in journals included in Q1 quarter and journal publication processes" is the title of the seminar that will take place in January. I hope our authors will benefit from it.

I thank the editorial board, the section editors, the authors who carefully followed our publication standards to produce articles of the highest quality, and the reviewers whose insightful investigations were accepted for publication in this issue.

Best regards,

**Prof. Dr. Selçuk NAS**  
**Editor in Chief**



**Address for Correspondence:** Selçuk Nas, Dokuz Eylül University Maritime Faculty, Department of Maritime Education and Training, İzmir, Türkiye  
**E-mail:** snas@deu.edu.tr  
**ORCID iD:** orcid.org/0000-0001-5053-4594

**Received:** 25.12.2024

**Last Revision Received:** 25.12.2024

**Accepted:** 25.12.2024



Copyright© 2024 the Author. Published by Galenos Publishing House on behalf of UCTEA Chamber of Marine Engineers.  
This is an open access article under the Creative Commons AttributionNonCommercial 4.0 International (CC BY-NC 4.0) License

# Astern Running of Heavy-Tonnage Vessels in an Ice Channel

✉ Aleksei Dobrodeev, ✉ Kirill Sazonov

Krylov State Research Centre, St. Petersburg, Russia

## Abstract

One of the most important tasks in raising the efficiency of marine transport systems is to make heavy-tonnage vessels move at faster speeds in channels laid by icebreakers. Studies conducted in the Krylov State Research Center (KSRC) Ice Basin have shown that broken ice is a significant factor that restricts vessel speed through ice channels. Wide breadths of heavy-tonnage vessels make it difficult to push ice pieces aside, resulting in their accumulation ahead of the bow. Ice blocks can be removed from the bow area only if they are immersed and passed along the hull underwater. With increasing speed, these processes require increasing amounts of energy. Possibly, easy ice passage along the underwater hull and speed improvements can be achieved if large-size vessels go stern first in ice channels. In this mode of operation, we have a number of factors contributing to the more efficient passage of ice provided by the small angle of the sternpost, making it easier for ice floes to dive under the hull, as well as the suction produced by the propellers. Moreover, the propeller slipstreams wash away the submerged ice outside the channel edges and reduce the ice friction of the underwater hull. This paper provides some theoretical assessments regarding the efficiency of running a large-sized vessel astern in an ice channel. Model studies have been undertaken in the KSRC Ice Basin to confirm that the suggested mode of operation is effective. During these experiments, models of large vessels were run through an ice channel to determine their ice resistance and speed. The theoretical estimates were compared with the model test results obtained for the Ice Basin. The analysis of all results proves that the described mode of operation promises faster vessels through ice channels.

**Keywords:** Heavy-tonnage vessel, Propulsion in ice, Hull form, Ice basin, Model tests

## 1. Introduction

Shipping in the Arctic region and freezing seas play an important role in economics. The XXI century saw substantial changes in the methods of marine operations under ice conditions, primarily related to a wider application of heavy-tonnage vessels. Unlike previously used vessels in the Arctic, modern ships have larger principal dimensions (beam, length, displacement), which make traditional icebreaker practice not very suitable for leading these vessels on ice. The breadth of modern large vessels is much greater than that of any existing icebreaker. For this reason, the vessel running behind the icebreaker has to complete ice breaking and widen the channel [1,2]. This effort requires substantial power from the propulsion plant and gives rise to new effects that affect ship motion in a narrow ice channel. One of these effects is the asymmetric ship motion with respect to the channel's central axis due to the interaction between the hull and the channel edges [3].

When a heavy-tonnage vessel moves through an ice channel laid by an icebreaker, there is also a higher resistance of broken ice. This effect is due to two factors. The first factor arises in connection with channel edges, making it difficult for the hull to push aside small ice pieces, as is well known [4]. The second factor is the bow shape of the heavy-tonnage vessels, which is less suitable for pushing ice floes aside than conventional ice-class vessels. This generates an area of broken ice, which is towed by the ship, thus increasing its ice resistance. The ship moving ahead in an ice channel was considered by the Sazonov and Dobrodeev [5]. It should be noted that at faster speeds in the ice channel, the resistance of broken ice to heavy-tonnage vessels is increased according to experimental results [6].

At present, one of the critical tasks addressed by Arctic navigators is to increase the average speed of heavy-tonnage vessels in ice [6,7]. Certain problems are encountered when



**Address for Correspondence:** Aleksei Dobrodeev, Krylov State Research Centre, St. Petersburg, Russia

**E-mail:** stamukha@yandex.ru

**ORCID iD:** orcid.org/0000-0001-6305-5090

**Received:** 17.01.2024

**Last Revision Received:** 20.07.2024

**Accepted:** 19.08.2024

**To cite this article:** A. Dobrodeev, and K. Sazonov "Astern Running of Heavy-Tonnage Vessels in an Ice Channel." *Journal of ETA Maritime Science*, vol. 12(4), pp. 358-364, 2024.



Copyright© 2024 the Author. Published by Galenos Publishing House on behalf of UCTEA Chamber of Marine Engineers. This is an open access article under the Creative Commons AttributionNonCommercial 4.0 International (CC BY-NC 4.0) License

ships run in channels made of ice more than 1.5 m thick. Therefore, the analysis of various tactical methods that can potentially increase the average speed of heavy-tonnage vessels could be of interest.

This paper considers the advantages and disadvantages of running heavy-tonnage vessels astern in an ice channel. The considerations herein primarily refer to ships equipped with propulsion pods, but are also applicable to vessels with a traditional arrangement of propellers and rudders.

## 2. Experimental Facility

Studies regarding the astern operation of commercial vessels in ice channels filled with broken ice were carried out based on model test data obtained in the Ice Basin of Krylov State Research Center (KSRC). KSRC Ice Basin has the following dimensions: test section length: 80 m, width: 10 m, depth: 2.0 m. For experiments the fine-grained (FG-type) ice was frozen [8]. Ice resistance experiments were carried out by towing tests of ship models with running propellers according to the International Towing Tank Conference (ITTC) Guidelines [9].

In compliance with the ITTC Guidance [8], a channel packed with broken ice was modeled by freezing solid-level ice followed by forming the ice channel. The ice channel width was chosen to be 10% wider than the tested breadth of the ship. The ice pieces in the channel were mainly square, measuring from 5 to 8 m in length. Such ice fragments are classified as an ice cake typical of channels cut into solid-level ice. The ice concentration in the channel was 9/10 (Figure 1).

## 3. Ship Models

Ice resistance studies were conducted for five ice-class carriers equipped with propulsion and steering pods. The ships have different dimensions, purposes, hull forms, and numbers of thrusters. The main aspects are summarized in Table 1.



**Figure 1.** Model ice channel filled with broken ice (concentration 9/10)

The most important hull-form parameters for ice-resistance estimates are frame angles  $\beta$ , stem and sternpost angles  $\phi_b$  and  $\phi_c$ , respectively, and the angle of waterline  $\alpha$  (Figure 2).

The waterline slope angle  $\alpha$  is measured at the buttock attachment point at a  $B/4$  distance from the centerline plane. The angles of stem  $\gamma_b$  and sternpost  $\gamma_c$  are measured in the centerline plane. All vessels under consideration have a stern skeg in the centerline plane. It should be noted that ship no. 3 has a pronounced forefoot to accommodate transverse thrusters. Table 1 lists the main characteristics of the ships tested in the Ice Basin.

## 4. Model Tests

Model tests were conducted under different ice conditions, which were chosen by taking into consideration each vessel's ice-going capabilities, operation areas, and propulsion power requirements. To analyze the efficiency of the stern-first operation, experiments were conducted on models running both astern and ahead on ice of equal thickness at the same speeds. The proposed approach enables the comparison of the ship ice resistance in ice channels under astern and ahead running conditions.

Movement in an ice channel is one of the most common modes of transport vessel navigation under ice conditions. It ensures efficient operation at high speed. At the same time, the risk of damage to the propellers and projections increases [10]. Therefore, studies of the hull interaction with broken ice in an ice basin are model tests for specification design.

Table 2 lists the characteristics of the ice and ship speeds modeled in the Ice Basin.

Figures 3-7 below show pictures illustrating the main episodes of the model tests in an ice channel filled with broken ice.

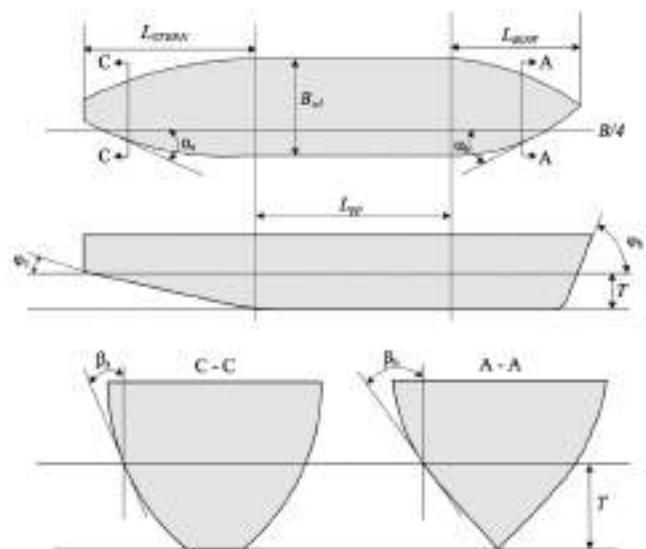


**Figure 2.** Definition of the angles of the hull elements



Table 1. Main specifications of the ships

Description	Symbol	Ship 1	Ship 2	Ship 3	Ship 4	Ship 5
Number of pods	1	2	3	2	3	3
Model scale	$\lambda$	1:20	1:34.4	1:22.5	1:34.4	1:33.3
Length between perpendiculars	$L_{pp}$ , m	114.0	280.0	109.0	285.0	284.0
Waterline breadth	$B_{wl}$ , m	24.0	49.0	25.0	47.0	42.0
Length of entrance	$L_{BOW}$ , m	38.0	95.0	33.0	72.0	58.0
Length of run	$L_{STERN}$ , m	23.0	77.0	22.0	58.0	41.0
Drafts at midships	$T$ , m	7.0	12.0	8.0	12.0	12.0
Displacement	$D$ , m <sup>3</sup>	14 000	135 000	13 000	126 000	100 000
Angle of the stem	$\phi_b$ , degree	60	23	20	25	32
Angle of the sternpost	$\phi_s$ , degree	47	22	34	22	20
Waterline run slope at $B/4$ distance	$\alpha_b$ , degree	33	52	35	48	44
Waterline entrance slope at $B/4$ distance	$\alpha_s$ , degree	55	46	60	43	55
Frame angle and bow	$\beta_b$ , degree	-	-	-	-	-
at $0.5 \cdot B_{wl}$	$\beta_{b-0.5}$ , degree	28	80	75	72	60
at $0.4 \cdot B_{wl}$	$\beta_{b-0.4}$ , degree	25	71	67	69	52
at $0.3 \cdot B_{wl}$	$\beta_{b-0.3}$ , degree	22	60	60	65	50
at $0.2 \cdot B_{wl}$	$\beta_{b-0.2}$ , degree	12	53	45	57	44
at $0.1 \cdot B_{wl}$	$\beta_{b-0.1}$ , degree	7	44	30	46	30
Frame angle, stern	$\beta_s$ , degree	-	-	-	-	-
at $0.5 \cdot B_{wl}$	$\beta_{s-0.5}$ , degree	86	75	80	78	80
at $0.4 \cdot B_{wl}$	$\beta_{s-0.4}$ , degree	82	67	76	74	77
at $0.3 \cdot B_{wl}$	$\beta_{s-0.3}$ , degree	77	65	71	70	74
at $0.2 \cdot B_{wl}$	$\beta_{s-0.2}$ , degree	64	63	58	68	70
at $0.1 \cdot B_{wl}$	$\beta_{s-0.1}$ , degree	52	51	35	54	58

## 5. Model Testing Data

The model test data are shown as the relative ice resistance  $R_{I \text{ Ahead}}/R_{I \text{ Astern}}$  (where  $R_{I \text{ Astern}}$  - ice resistance of model's running astern at a given speed,  $R_{I \text{ Ahead}}$  - ice resistance of model's running ahead at the same speed) as a function of Froude number with respect to ice thickness  $Fr_h = v/\sqrt{gH}$  (Figure 8).

The obtained results provide conclusive evidence that four out of five ships go more efficiently through the ice channel in the astern running mode than in the ahead running mode. The highest efficiency was achieved for ship no. 3 because the forefoot caused additional ice resistance in the ahead running mode. Figure 7 intensive interaction of the forefoot with ice. While in astern running mode, the forefoot of a similar design is not exposed to the ice effect as strongly as that because it is washed with propeller slipstreams.

Practically the same results were obtained for ships 2 and 4 as they have similar hull forms in terms of the main criteria and

absolutely identical test conditions and full-scale correlation. These are heavy-tonnage vessels with icebreaker bow and stern lines. It should be noted that the bow concept of these vessels differs. Ship no. 2 had a spoon-type bow, while ship no. 4 had a wedge-type bow. However, the angles of the stem, waterline, and frames at the standard measurement points are quite similar. Obviously, different bow concepts have little influence on ships moving in a fresh ice channel if their other hull form characteristics are somewhat similar. The test data show that the level of ice resistance in astern mode for both ship types was reduced by 15-20%.

Ship no. 1 is slightly more effective in reducing ice resistance than large-size vessels with an icebreaker's hull form. This ship has a low block coefficient and a slender bow, giving her advantages for sailing through broken ice because this vessel is capable of pushing ice cake aside. However, these effects were observed only at low ice concentrations below 6/10 and in open water. All experiments in the ice basin were performed in an ice channel of limited width with an ice concentration

**Table 2. Test conditions**

Description	Symbol	Ship 1	Ship 2	Ship 3	Ship 4	Ship 5
Ice thickness A	$H_A$ , m	0.6	1.5	1.5	1.5	1.2
Speed A1	$V_{SA1}$ , knots	8.0	11.0	8.0	11.0	12.0
Speed A2	$V_{SA2}$ , knots	6.0	9.0	6.0	9.0	9.0
Speed A3	$V_{SA3}$ , knots	4.0	7.0	4.0	7.0	6.0
Speed A4	$V_{SA4}$ , knots	-	-	-	-	4.0
Ice thickness B	$H_B$ , m	0.9	2.1	2.0	2.1	1.7
Speed B1	$V_{SB1}$ , knots	8.0	9.0	6.0	9.0	12.0
Speed B2	$V_{SB2}$ , knots	6.0	7.0	4.0	7.0	9.0
Speed B3	$V_{SB3}$ , knots	4.0	5.0	2.0	5.0	6.0
Speed B4	$V_{SB4}$ , knots	-	-	-	-	4.0



*a) Running ahead:*

*b) Running the astern*

**Figure 3. Model tests of ship 1**



*a) Running ahead:*

*b) Running the astern*

**Figure 4. Model tests of ship 2**



*a) Running ahead:*

*b) Running the astern*

**Figure 5. Model tests of ship 3**

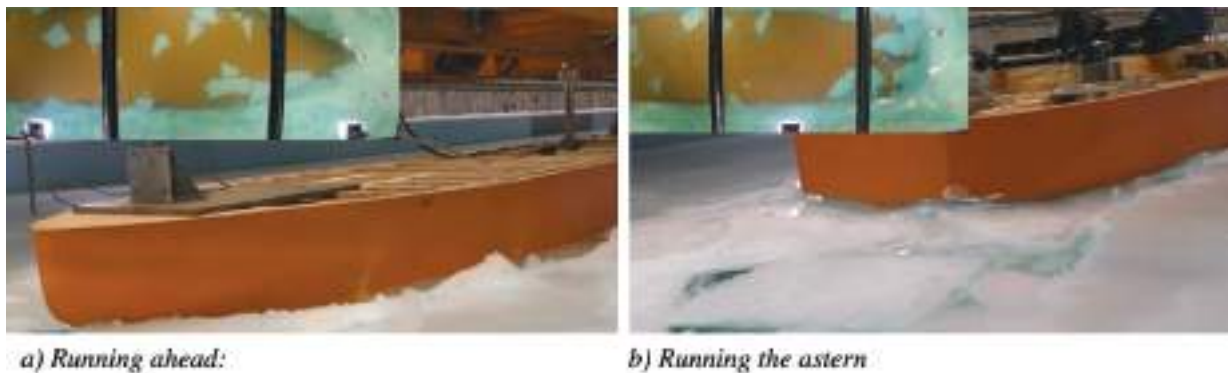


Figure 6. Model tests of ship 4

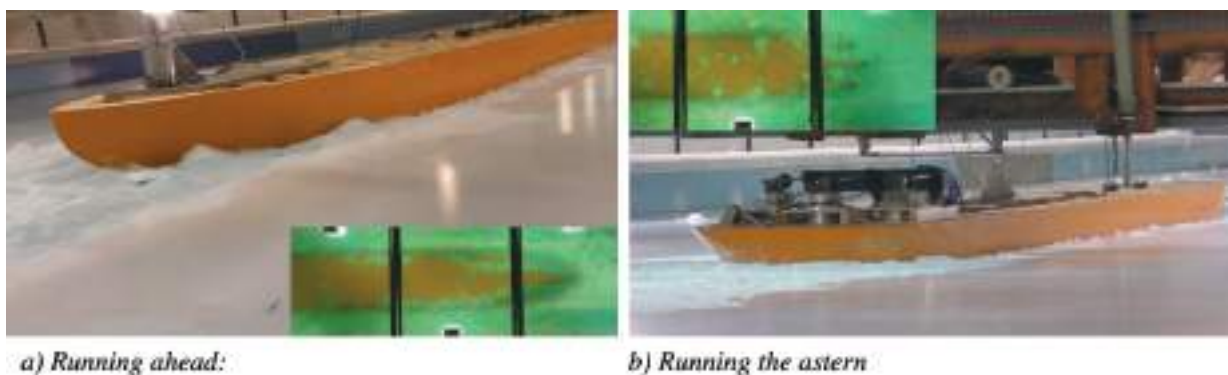


Figure 7. Model tests of ship 5

of 9/10. When concentrated ice is brushed aside by stems, an ice crushing effect occurs in the pathway of the transition from entrance to parallel middle body. Thus, the icebreaker's stern also provides vessel advantages in astern mode.

The relationship between ship resistance and speed is of some interest. The linear trends seen in the test data in Figure 8 show that vessels with a forefoot and spoon bow tend to have more ice resistance in ahead running mode than in astern running mode. For ships with a more slender bow, the trend was reversed. It was indicated above that the test data for ships no. 2 and no. 4 was practically the same. However, it is expected that at faster speeds, the difference between these two vessels will become more vivid.

According to the model test results, ship no. 5 has a 5-10% reduction in ice resistance when moving ahead. Differing from other results, this outcome has established an important criterion that may have a significant impact on better ship ice propulsion under astern running conditions compared to ahead running conditions. This criterion is the hull form. Ship no. 5 had a shorter aft entrance, which was 1.5 times smaller than that of ships no. 2 and 4, which had similar dimensions. In this case, the distance from the waterline to the propulsion pod struts is considerably reduced, which prevents ice pieces submerged by the hull from being arranged in such a way as to have the least influence on the struts of the ship control

surfaces. The effects obtained are described in detail in Lee's [11] study. Also, the reduction in ice resistance when running ahead can be explained by a somewhat different bow shape from that of ships no. 2 and 4. In this case, the ship has a clear wedge-shaped hull and lower frame angles, which promotes the submergence of ice by the hull and also exerts an additional lateral force to throw ice under the ice

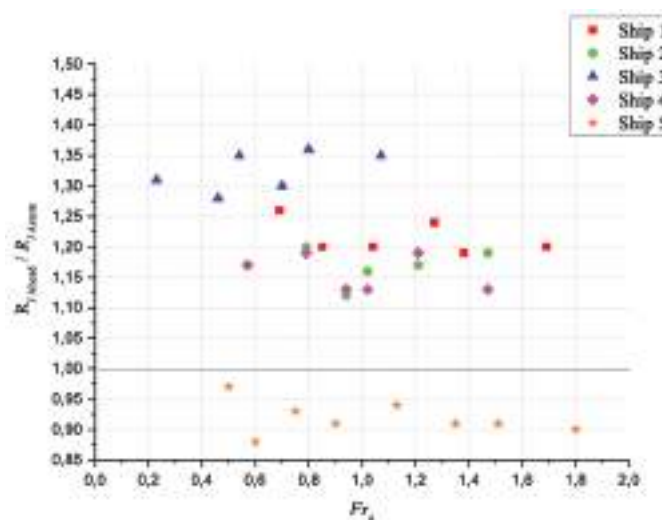


Figure 8. Relative ice resistance as a function of Froude number with respect to ice thickness

channel edge. Thus, the resistance component depending on the ice friction against the hull plating is reduced because the underwater hull is cleared of broken ice.

### 6. Discussion of Results

Let us consider in more detail the physical processes that may reduce ice resistance during astern running of a heavy-tonnage vessel under ice conditions, including ice channels filled with broken ice. Commonly, three groups of factors that may lead to the reduction of ice resistance are distinguished. First, it is the hull form of a heavy-tonnage vessel, which, as a rule, features a lower angle of the sternpost than the stem angle. Second, the propeller suction changes the flow pattern. The propeller suction is associated with the thrust deduction arising from the hull of the ship moving ahead in open water. Third, it was washed by propeller slipstreams. Let us make some assessments of these factors on the ice resistance of a heavy-tonnage vessel moving through an ice channel.

The angle between the stem and sternpost, under all other conditions being equal (ship speed and thickness of broken ice are constant), only influences the diving of ice pieces under the hull.

The elementary consideration of ice pieces sliding on an inclined plane without taking into account friction forces gives the following relation:

$$tg\varphi \leq \frac{R_w(V)}{h_l S_{lf} (\rho_w - \rho_i)} \tag{1}$$

where  $\varphi$  - angle of stem of sternpost;  $R_w(V) = C_w \frac{\rho_w V^2}{2} S_{ic}$  - resistance of water at the ice floe being towed by the bow or stern of the ship running in channel;  $C_w$  - resistance coefficient of the ice floe being towed;  $V$  is the ship speed;  $S_{ic} \approx B l_{ic}$  - area of the ice feature in front of the bow or stern;  $B$  - ship beam;  $\rho_w, \rho_i$  - density of water or ice, respectively;  $S_{lf} \approx B l_{lf}$  - area of the ice layer submerged by the bow or stern;  $l_{lf}$  - length of the ice layer equal to the length of individual ice floes.

The obtained relation makes it possible to determine the influence of the stem and sternpost angles on the ice resistance at constant ship speed and ice thickness. In this case, the function can be rewritten as follows:

$$tg\varphi \leq K \frac{l_{ic}}{l_{lf}}, \quad K = \frac{C_w V^2}{2h_l (1 - \frac{\rho_i}{\rho_w})} \tag{2}$$

With this formula, it can be shown, for instance, that the length of accumulated ice in front of the 22° bow will be less than that in front of the 18° sternpost  $l_{ic}(22) \approx 1.24 l_{ic}(18)$ . In this case, the floe lengths are assumed to be the same.

The influence of propeller operation on the flow pattern around has been thoroughly studied in Ignatev's study [12] concerning the application of bow propellers in icebreakers. Below, we quote some results drawn from this investigation. The graphs given below show the relative longitudinal velocity  $k_{\parallel} = \frac{V}{w_{\infty}}$ , (Figure 9) and the pressure coefficient in induced flow  $\xi = \frac{p}{\rho_w w_{\infty}^2}$  (Figure 10), where  $w_{\infty} = V(\sqrt{1 + \sigma_p} - 1)$  - total induced velocity in the propeller jet at infinity;  $\sigma_p = \frac{2T}{\rho_w V^2 F}$  - thrust load coefficient;  $T$  - propeller thrust;  $F$  - area of the propeller hydraulic section;  $p$  - fluid pressure taking account of the atmospheric pressure. In the graphs, the origin of the axes coincides with the propeller location, X-axis is positive in the ship's motion direction, the Y-axis is positive upward, and  $r$  is a polar coordinate with respect to the propeller axis.

Figure 9 shows the relative longitudinal velocity for an unlimited flow. The ice cover values on the graph should be multiplied by 2.

From the calculation results presented here, it follows that the longitudinal force has only a local effect of increasing velocity near the propeller, which is more favorable for ice pieces that

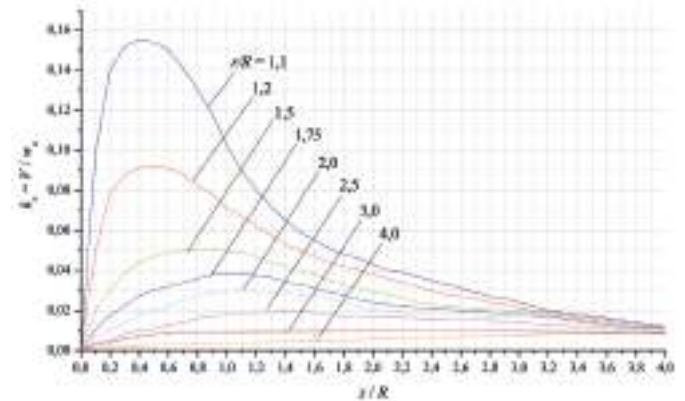


Figure 9. Values of the propeller-induced longitudinal force

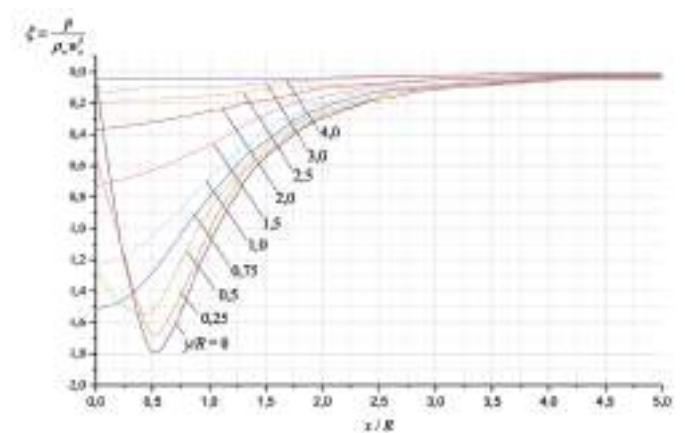


Figure 10. Pressure coefficient  $\xi = f(\frac{x}{R}, \frac{h}{R})$  for  $h = 1.2R$  at propeller operation under an ice cover

are diving under the hull. The negative pressure produced by the propeller is small and cannot affect the diving of ice pieces in any noticeable way; however, it promotes this process.

Obviously, the effects associated with propeller-induced velocities and propeller suction strongly depend on the stern lines and design characteristics of a heavy-tonnage ice-class vessel. Nevertheless, a positive influence on the stern-broken ice interaction in the channel, as described above, will remain.

For a ship running astern in a channel, an important role is played by washing the hull with propeller slipstreams. It is difficult to assess the influence of this effect. However, our visual observations of the models in the Ice Basin strongly confirm this assumption. Figures 3-7 show photos of the underwater hulls investigated during these Ice Basin model experiments of heavy-tonnage vessels moving astern and ahead in the ice channel, illustrating this conclusion.

## 7. Conclusion

Studies based on calculations and experiments have proven that heavy-tonnage vessels can effectively run asterns in ice channels filled with broken ice. According to the model test data obtained for a series of heavy-tonnage vessels in the Ice Basin, three groups of factors promoting the reduction of ice resistance can be identified: vessel stern lines, propeller suction, and hull washing by propeller slipstreams. The theoretical appraisals of these factors on the ice resistance of heavy-tonnage vessels in ice channels were fully validated by the Ice Basin model test data, which also provided additional insight into the effects associated with propeller suction on ships in astern running mode.

### Footnotes

### Authorship Contributions

Concept design: A. Dobrodeev, Data Collection or Processing: A. Dobrodeev, Analysis or Interpretation: K. Sazonov, Literature Review: K. Sazonov, Writing, Reviewing and Editing: A. Dobrodeev, and K. Sazonov.

**Funding:** The research was funded by a grant no.: 23-19-00039 of Russian Research Fund “Theoretical basis and application tools for developing a system of intellectual fleet planning and support of decisions on Arctic navigation” (<https://rscf.ru/project/23-19-00039/>).

## References

- [1] K. E. Sazonov, and A. A. Dobrodeev, “*Propulsion of heavy-tonnage vessels in ice*”. SPb., 2017. (in Russian).
- [2] F. Li, M. Suominen, and P. Kujala, “Ship performance in ice channels narrower than ship beam: Model test and numerical investigation”. *Ocean Engineering*, vol. 240, 109922, Nov 2021.
- [3] A. A. Dobrodeev, N. Y. Klementyeva, and K. E. Sazonov, “Large ship motion mechanics in “narrow” ice channel”, *IOP Conference Series: Earth and Environmental Science, Institute of Physics Publishing*, pp. 12017, 2018.
- [4] V. I. Kashtlyan, I. I. Poznyak and A. Ya. Ryvlin, “*Ship ice resistance*”, Leningrad, 1968. (in Russian).
- [5] K. E. Sazonov, and A. A. Dobrodeev, “Ice resistance assessment for a large size vessel running in a narrow ice channel behind an icebreaker”. *Journal of Marine Science and Application*, vol. 20, pp. 446-455, 2021.
- [6] K. E. Sazonov, and A. A. Dobrodeev, “Fast-speed escorting of heavy tonnage vessels by icebreakers: researching in ice model tank”. *Arctic: Ecology and Economy*, vol. 3, pp. 76-83, 2018. (In Russian).
- [7] K. E. Sazonov, and A. A. Dobrodeev, “Fast sailing in ice - the new goal of model studies”. *Naval Architect*, pp. 22-24, 2018.
- [8] *General Guidance and Introduction to Ice Model Testing, Recommended Procedures and Guidelines, ITTC 7.5-02-04-01*, pp. 1-9, 2021.
- [9] *Resistance tests in Ice Model Testing. Recommended Procedures and Guidelines, ITTC 7.5-02-04-02.1*, 8 p, 2017.
- [10] A. Bozkurt, and M. Ertogan, “Analysis of the structure of marine propeller blades for ice navigation”. *Journal of ETA Maritime Science*, vol. 12, pp. 74-82, Mar 2024.
- [11] S. K. Lee, “Engineering practice on ice propeller strength assessment based on iacs polar ice rule”. *UR13, ABS Technical Papers*, 2007.
- [12] M.A. Ignatev, “*Propellers of ice going ships*”. Leningrad, Sudostroenie, 1966. (in Russian).

# State Estimation and Control for a Model Scale Passenger Ship using an LQG Approach

© Ferdi Çakıcı<sup>1</sup>, © Ahmad Irham Jambak<sup>2</sup>, © Emre Kahramanoğlu<sup>3</sup>, © Ahmet Kaan Karabüber<sup>4</sup>,  
© Bünyamin Ustalı<sup>5</sup>, © Mehmet Utku Öğür<sup>6</sup>, © Fuat Peri<sup>7</sup>, © Ömer Sinan Şahin<sup>8</sup>, © Mehmet Akif Uğur<sup>4</sup>,  
© Afşin Baran Bayezit<sup>9</sup>

<sup>1</sup>Yıldız Technical University, Department of Naval Architecture and Marine Engineering, İstanbul, Türkiye

<sup>2</sup>İstanbul Technical University, Department of Mechatronics Engineering, İstanbul, Türkiye

<sup>3</sup>İstanbul Technical University, Department of Marine Engineering, İstanbul, Türkiye

<sup>4</sup>Yıldız Technical University, Department of Control and Automation Engineering, İstanbul, Türkiye

<sup>5</sup>Yıldız Technical University, Department of Mechatronics Engineering, İstanbul, Türkiye

<sup>6</sup>Yıldız Technical University, Department of Civil Engineering, İstanbul, Türkiye

<sup>7</sup>İstanbul Technical University, Department of Naval Architecture and Marine Engineering, İstanbul, Türkiye

<sup>8</sup>Recep Tayyip Erdoğan University Faculty of Maritime, Department of Marine Engineering, Rize, Türkiye

<sup>9</sup>İstanbul Technical University, Department of Shipbuilding and Ocean Engineering, İstanbul, Türkiye

## Abstract

Reducing the roll response of ships between irregular waves is an important issue for the operational requirement. This study presents a roll dynamics model for a passenger ship equipped with active fins. In this study, a Kalman Filter was applied to accurately estimate all states from the measurement of total roll motion and roll velocity (based on fins and waves), even in the presence of measurement noise. Synchronously, a linear quadratic gaussian (LQG) controller actively drives the fins to minimize roll motion and velocity by taking the fin amplitude and rate saturations together. Two different sea states were modeled for the simulation purpose. Results demonstrate the success of the state estimation approach and the remarkable potential of the LQG strategy in roll reduction.

**Keywords:** Roll stabilization, Kalman filter, LQG

## 1. Introduction

The challenge of managing roll motion on ships in demanding marine environments is crucial for maintaining safety and comfort standards. Excessive ship rolling raises significant concerns. It can create lateral acceleration that hinder the efficiency of crew operations, increase the duration of tasks, and, in severe cases, render the vessel non-functional. Moreover, the pronounced roll motion can induce vertical acceleration that lead to seasickness in both the crew and passengers, thereby affecting their comfort and operational capabilities. For cargo ships transporting delicate goods, like perishable items, excessive rolling can cause damage to the cargo. Additionally, extreme roll angles can limit the operation of vital equipment,

an issue of particular importance for naval vessels engaged in tasks such as weapon system operations, deployment and recovery processes, and sonar functionality in warships.

In pursuit of minimizing ship roll, studies for many years have led to the creation of various technologies designed to mitigate roll, including fins, bilge keels, and antirolling tanks, which differ in their motion mechanisms, placement, and weight. In particular, fins, which work based on acceleration and interaction with the surrounding fluid mass, have become a widely adopted solution [1]. They are particularly effective due to their ability to alter the initially symmetric foil into asymmetry by altering its angle, which generates lift and moment that stabilizes the ship.



**Address for Correspondence:** Ferdi Çakıcı, Yıldız Technical University, Department of Naval Architecture and Marine Engineering, İstanbul, Türkiye

**E-mail:** fcakici@yildiz.edu.tr

**ORCID iD:** orcid.org/0000-0001-9752-1125

**Received:** 17.04.2024

**Last Revision Received:** 04.09.2024

**Accepted:** 20.09.2024

**To cite this article:** F. Çakıcı, et al. "State Estimation and Control for a Model Scale Passenger Ship using an LQG Approach." *Journal of ETA Maritime Science*, vol. 12(4), pp. 365-376, 2024.



Copyright© 2024 the Author. Published by Galenos Publishing House on behalf of UCTEA Chamber of Marine Engineers. This is an open access article under the Creative Commons AttributionNonCommercial 4.0 International (CC BY-NC 4.0) License

Numerous experiments and research projects have been conducted to investigate and improve the efficiency of fins and rudders in diminishing roll motion. These include Sharif et al.'s [2,3] experimental research, Wu et al.'s [4] implementation of a proportional-integral-derivative (PID) control mechanism, and the utilization of artificial neural networks and fuzzy logic controllers in simulation studies by Liut [5] and Liut et al. [6]. Model predictive controllers have been introduced to address non-linear phenomena, for example, dynamic stalls [7,8]. To design roll motion mitigation fins under random beam-sea scenarios, parallel multi-pattern control approaches and applied computational fluid dynamics have been proposed [9,10]. The effectiveness of both PID and Linear Quadratic Gaussian (LQG) controllers in reducing roll and pitch motions was examined by Kim and Kim [11]. Additional developments include control algorithms customized to ship velocity, encounter angles, and wave conditions by Koshkouei and Nowak [12], along with various robust control techniques by Moradi and Malekizade [13]. Further advancements in this field include Hinojosa et al.'s [14] focus on optimal control with environmental disturbances, Li et al.'s [15] adoption of adaptive neural networks, Luo et al.'s [16] modification of the mathematical model for control design, and Huang et al.'s [17] enhancement of hydrodynamic coefficient estimation online. Recent innovations include improved MPC designs by Jimoh et al. [18], Three-degree-of-freedom (3DOF) motion control strategies by Cakici [19], active adaptive fractional-order sliding mode control (FOSMC) by Lee et al. [20], non-linear feedback controller development by Liang et al. [21], Optimal  $H_\infty$  controller designs by Taskin et al. [22], and advanced MPC algorithms by Hu et al. [23]. Rezaei and Tabatabaei [24] demonstrated the effectiveness of an adaptive FOSMC for roll motion control, underscoring the advantages of integrating fractional-order derivatives.

The objective of this research is to investigate the application of an LQG controller that integrates state estimations from Kalman Filters (KFs) with linear quadratic regulator (LQR) control. First, all states (roll motions and rates induced by fins and waves) are separated in the time domain using a KF. A full-state feedback controller is then used to reduce the magnitude of the states. This approach aims to optimize the operation of active fins to significantly reduce the roll motion of the ship. A 3-m Gulet model, which is a class of passenger ships, was used in the simulations. The same model also physically exists in the Yıldız Technical University Hydrodynamic Research Laboratory for the experimental validation of control strategies in future works.

The remainder of this paper is summarized as follows: Section 2 discusses the modeling of system dynamics, focusing on the roll motion of a passenger ship with midship fins and the equations governing this motion. Section 3 details the

implementation of the LQG control strategy, which integrates a KF for state estimation and LQR to optimize control actions. Section 4 presents simulation results that validate the effectiveness of the control system by comparing scenarios with and without fins. Section 5 concludes the paper by summarizing the research findings, noting significant reductions in roll motion and rate, and proposing future research directions.

## 2. System Dynamics Modeling

This paper investigates roll-motion reduction through the utilization of one pair of midship fins under the impact of irregular waves on the beams of states 3 and sea state 4. The proactive manipulation of these fins generates a counteractive moment that mitigates the wave-induced roll. The spatial configuration of the fins is illustrated in Figure 1a, and the Gulet model is shown in Figure 1a, b.

Here, the forces exerted by the port and starboard fins are denoted by  $F_1$  and  $F_2$  respectively, while  $M_4$  signifies the total roll moment resulting from fin action. As the ship's roll motion around the  $x$ -axis transpires, the fins must pivot around the  $y$ -axis to engender vertical force. Table 1 lists the parameters of the utilized ships and fins.

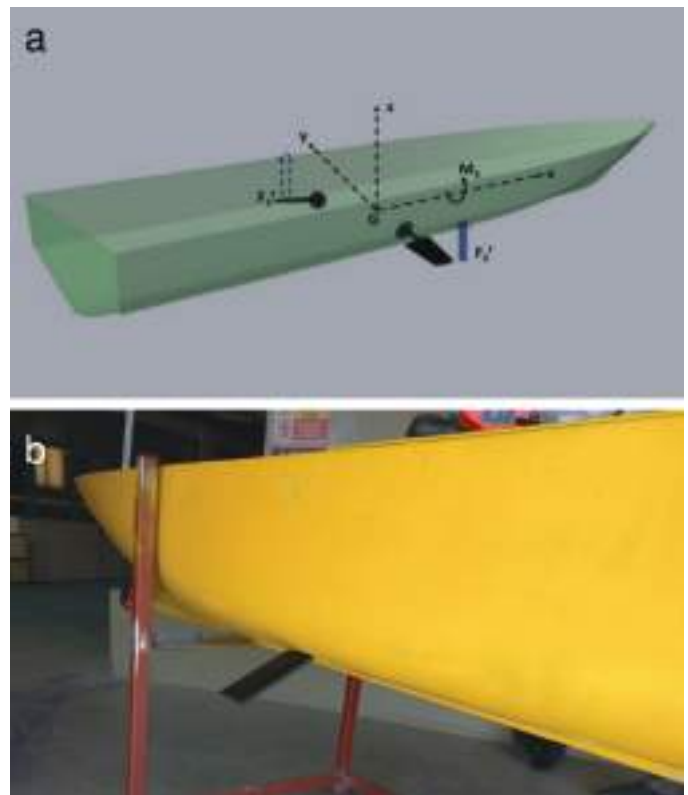


**Figure 1.** a) Standard configuration of fins on a ship [25]. b) Gulet and fins

**Table 1.** Parameters of the ship and fins

Parameter	Unit	Value
Waterline length	m	3
Surge speed, $U$	m/s	1.4
Displacement	kg	115.6
Vertical center of gravity (kg)	m	0.30
The transverse metacentric height	m	0.10
Moment of inertia $I_{44}$	kgm <sup>2</sup>	6.6
Natural Roll Period	s	1.66
Fin area	m <sup>2</sup>	2 x 0.013
Aspect ratio (Span/Chord)	-	2
Moment arm, $r_f$	M	0.41
$C_L$ (Lift coefficient of the fins)	1/deg	$\approx 0.046$
$K_p$ (Ship added mass)	kgm <sup>2</sup>	0.1997 x I44
$K_p$ (Ship linear damping)	kgm <sup>2</sup> /s	4.4

### 2.1. Passenger Ship Roll Motion Equation

The control system design involves modeling the roll motion dynamics using either a one-degree-of-freedom (1DOF) or complex four-degree-of-freedom (4DOF) approach. For simplicity, the 1DOF model for roll motion was employed as follows (Equations 1 and 2):

$$\dot{\phi} = p \quad (1)$$

$$I_{44}\dot{p} = K_h + K_w + K_c \quad (2)$$

where  $\phi$ ,  $p$  and  $I_{44}$  denote the roll angle, roll velocity (or rate), and moment of inertia about the x-axis.  $K_h$  encapsulates hydrostatic and hydrodynamic moments,  $K_w$  denotes the moment from wave forces while  $K_c$  the control moment from the fins.  $K_h$  is approximated as follows (Equation 3):

$$K_h \approx K_p\dot{p} + K_p p + K(\phi) \quad (3)$$

Here,  $K_p$  signifies the roll motion added mass coefficient,  $K_p$  denotes linear damping coefficient, and  $K(\phi)$  denotes the restoring terms generated by gravity and buoyancy forces. Obtaining these coefficients generally involves a combination of experimental measurements, empirical formulas, numerical simulations, and loading conditions, each of which is suitable for capturing different aspects of ship behavior in water.

The term  $K_w$  in active control system literature is often omitted due to the complexity associated with the ‘‘force superposition method.’’ Instead, this study employs the ‘‘motion superposition method’’, treating ship and wave models separately and combining them to determine the

total roll motion and rate [26]. A further exposition of the state space model of the system is provided in the following sections.

### 2.2. Dynamics of Fin Roll Stabilizer

The investigations into fin stabilizer performances indicate that their effectiveness is reduced under severe sea conditions due to nonlinear effects. In contrast, under milder conditions, the static behavior serves as a sufficient descriptor. Consequently, the focus is placed on the steady behavior of the fins, and the fin-induced roll moment is formulated as [7] (Equation 4):

$$K_c = 0.5\rho r_f V^2 A_f C_L(\alpha_e) \quad (4)$$

where  $\rho$  denotes the water density,  $r_f$  signifies the roll moment arm, and  $V$  represents the relative velocity between fin and flow.  $A_f$ ,  $C_L$  and  $\alpha_e$  stand for fin projection area, lift coefficient, and effective angle of attack. The fin section is a NACA 0015 profile, and the aspect ratio (Span length divided by chord length) of the fin is two.

The lift force and angle of attack are linearly related until the stall angle, where the lift force is typically represented as  $C_L(\alpha_e) \approx \tilde{C}_L \alpha_e$  with  $\tilde{C}_L \approx \frac{\partial C_L}{\partial \alpha_e}$  at  $\alpha_e = 0$ . This value was taken as 0.046 (1/deg) for the present fins. The effective angle is calculated as (Equation 5):

$$\alpha_e = -\alpha_{pu} - \alpha_m \quad (5)$$

where  $\alpha_{pu}$  is generated by forward velocity and roll rate of the ship while  $\alpha_m$  denotes mechanical angle of the fin (Equation 6).

$$\alpha_{pu} = \arctan\left(\frac{V_{roll}}{U}\right) = \arctan\left(-\frac{r_f \dot{p}}{U}\right) \approx -\frac{r_f \dot{p}}{U} \quad (6)$$



Thus, the fins' total roll moments is given by (Equations 7, 8):

$$K_c = K_{c_p} + K_{c_s} \approx K_{\alpha} \left( -\frac{r_f \beta - \alpha_m^p}{\nu} \right) + K_{\alpha} \left( -\frac{r_f \beta - \alpha_m^{sf}}{\nu} \right) \quad (7)$$

$$K_{\alpha} \approx 0.5 \rho r_f U^2 A_f \bar{C}_L \quad (8)$$

Here,  $\alpha_m^p$  and  $\alpha_m^{sf}$  represent the mechanical angles of the port and starboard fins, respectively. A schematic of the ship and its fins is shown in Figure 2.

### 3. Implementation of LQG in Ship Roll Motion Control

The LQG control strategy stands out among control methods due to its effective blend of two key elements: the LQR and the KF. LQR is adept at optimizing control actions to reduce a specific cost function while balancing performance goals and control efforts. In contrast, the KF improves decision making in the presence of noise and uncertainties. The comprehensive LQG controller approach is illustrated in Figure 3.

#### 3.1. Model Derivation for LQG Control

The dynamics of an unforced ship roll can be characterized through a state-space model, where the state equation, as detailed in a numerical study by [25], is described as follows (Equation 9):

$$\dot{\eta}(t) = A_{fin} \eta(t) \quad (9)$$

In this context, the state vector  $\eta(t) = [\phi_{fin}(t), P_{fin}(t)]^T$  comprises the fin generated roll angle  $\phi_{fin}(t)$  and the roll rate  $P_{fin}(t)$ . The system matrix is defined as follows (Equation 10):

$$A_{fin} = \begin{bmatrix} 0 & 1 \\ R & D \end{bmatrix} \quad (10)$$

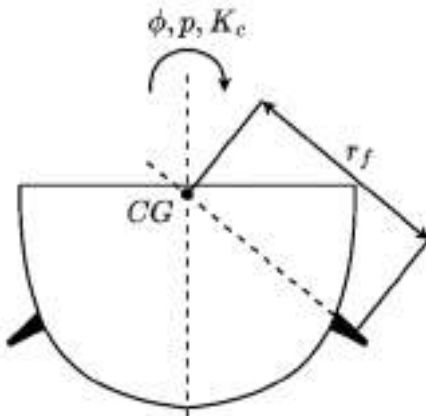


Figure 2. Representation of ship and fins

where  $R$  and  $D$  denote the restoring and damping terms, respectively, which are calculated as follows (Equations 11, 12)

$$R = \frac{-GM_T \Delta}{I_{44} + K_p} \quad (11)$$

$$D = \frac{-K_p - 2K_{\alpha} r_f / U}{I_{44} + K_p} \quad (12)$$

This model was adapted to include the effects of ship fins as roll-stabilizing actuators and wave-induced effects. The fin model is integrated using the term  $B_{fin}$ , resulting in the following modified ship-motion model (Equations 13, 14):

$$\dot{\eta}(t) = A_{fin} \eta(t) + B_{fin} u_{fin}(t) + B_{wave} u_{wave}(t) \quad (13)$$

where,

$$B_{fin} = \begin{bmatrix} 0 & 1 \\ \frac{K_{\alpha}}{I_{44} + K_p} & -\frac{K_{\alpha}}{I_{44} + K_p} \end{bmatrix} \quad (14)$$

Because wave-induced forces are challenging to quantify precisely, the model does not directly incorporate these forces but instead utilizes a motion-based approach encapsulated within the system matrix  $A_{wave}$  and  $B_{wave}$  as follows (Equation 15):

$$A_{wave} = \begin{bmatrix} 0 & 1 \\ -w_0^2 & -2\zeta w_0 \end{bmatrix} \quad (15)$$

$$B_{wave} = \begin{bmatrix} 0 \\ 2\zeta w_0 \sigma \end{bmatrix}$$

where  $w_0$  is the natural frequency and  $\zeta$  represents the damping ratio of the wave. Please note that the parameters of the  $A_{wave}$  matrix is calculated with spectral factorization method with respect to sea state level. A reader interested in the proposed approach can obtain detailed information about the proposed approach [7]. To effectively integrate the ship and wave models, an augmented system is proposed as follows (Equations 16-19):

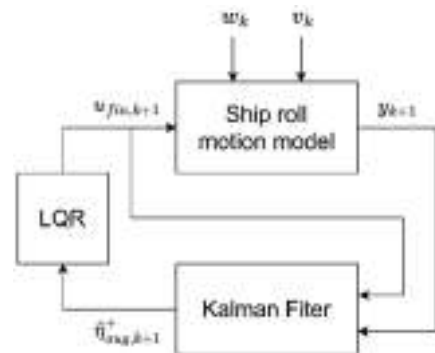


Figure 3. Flow diagram of an lqg controller for ship roll motion stabilization

$$\dot{\eta}_{aug}(t) = A_{aug}\eta_{aug}(t) + B_{augf}u_{fin}(t) + B_{augw}u_{wave}(t) \quad (16)$$

$$A_{aug} = \begin{bmatrix} 0 & 1 & 0 & 0 \\ R & D & 0 & 0 \\ 0 & 0 & 0 & 1 \\ 0 & 0 & -w & -2\zeta w_0 \end{bmatrix} \quad (17)$$

$$B_{augf} = \begin{bmatrix} 0 & 1 \\ \frac{v_x}{1+\kappa_f} & -\frac{v_y}{1+\kappa_f} \\ 0 & 0 \\ 0 & 0 \end{bmatrix} \quad (18)$$

$$B_{augw} = \begin{bmatrix} 0 \\ 0 \\ 0 \\ 2\zeta w_0 \sigma \end{bmatrix} \quad (19)$$

Here,  $\eta_{aug} = [\phi_{fin}(t), P_{fin}(t), \phi_{wave}(t), P_{wave}(t)]^T$  represents the augmented state vector, encompassing both ship- and wave-induced motions and rates.

For digital control systems that operate in discrete intervals, Equation (16) must be discretized (Equation 20):

$$\eta_{aug,k} = A_{aug}\eta_{aug,k} + B_{augf}u_{fin,k} \quad (20)$$

Applying the Euler Forward method, the state at the next time step ( $k + 1$ ) is predicted as follows (Equation 21):

$$\eta_{aug,k+1} = \begin{bmatrix} \phi_{aug,k} + P_{aug,k}\Delta t \\ P_{aug,k} + \Delta t(P_{aug,k}R + P_{aug,k}D) \\ \phi_{aug,k} + P_{aug,k}\Delta t \\ P_{aug,k} + \Delta t(-wP_{aug,k} + 2\zeta w_0 P_{aug,k}) \end{bmatrix} + \begin{bmatrix} 0 \\ \frac{\Delta t v_x}{1+\kappa_f} \\ \frac{\Delta t v_y}{1+\kappa_f} \\ 0 \end{bmatrix} u_{fin,k} + \begin{bmatrix} 0 \\ 0 \\ 0 \\ \Delta t \cdot 2\zeta w_0 \sigma \end{bmatrix} \quad (21)$$

This leads to the discretized state space representation as follows (Equation 22):

$$\eta_{aug,k+1} = A_{aug,d}\eta_{aug,k} + B_{augf,d}u_{fin,k} + B_{augw,d}u_{wave,k} \quad (22)$$

Where  $A_{aug,d}$  and  $B_{aug,d}$  denote discretized matrices of  $A_{aug}$  and  $B_{aug}$  formulated as follows (Equations 23-25):

$$A_{aug,d} = \begin{bmatrix} 1 & \Delta t & 0 & 0 \\ R\Delta t & D\Delta t + 1 & 0 & 0 \\ 0 & 0 & 1 & \Delta t \\ 0 & 0 & -w\Delta t & -2\zeta w_0 \Delta t + 1 \end{bmatrix} \quad (23)$$

$$B_{augf,d} = \begin{bmatrix} 0 & \Delta t \\ \frac{\Delta t v_x}{1+\kappa_f} & -\frac{\Delta t v_y}{1+\kappa_f} \\ 0 & 0 \\ 0 & 0 \end{bmatrix} \quad (24)$$

$$B_{augw,d} = \begin{bmatrix} 0 \\ 0 \\ 0 \\ \Delta t \cdot 2\zeta w_0 \sigma \end{bmatrix} \quad (25)$$

### 3.2. Incorporating KF and LQR into LQG Framework

In practical scenarios, models cannot perfectly capture the dynamics of physical systems. Moreover, imperfections in sensor technologies, which result in inaccuracies, limited precision, and stochastic variations, further increase the discrepancies in Equation (21). In this context, the KF is a crucial tool for providing optimal state estimates under these less-than-ideal conditions.

In this study, physical experiments were not conducted. Instead, the true-state measurements were simulated by using the theoretical model established in the previous section. This model is enhanced by incorporating Gaussian process noise to mimic uncertainties that occur in real life. In addition, noise was also added to the measurement model. The complete model is expressed as follows (Equation 26):

$$\left. \begin{aligned} \eta_{aug,k+1} &= A_{aug}^D \eta_{aug,k} + B_{augf}^D u_{fin,k} + B_{augw}^D u_{wave}(t) \\ y_{k+1} &= C \eta_{aug,k+1} + v_k \\ w_k &\sim \mathcal{N}(0, Q_{KF}) \\ v_k &\sim \mathcal{N}(0, R_{KF}) \end{aligned} \right\} \quad (26)$$

Here  $w_k$  and  $v_k$  represent process and measurement noise, respectively, following Gaussian distributions with covariance matrices  $Q_{KF}$  and  $R_{KF}$ . The observation  $C$  matrix is given as (Equation 27):

$$C = [1 \ 0 \ 1 \ 0; 0 \ 1 \ 0 \ 1] \quad (27)$$

where is the measured total roll motion and rate derived from the combined ship dynamics and wave effect.

The KF state estimation algorithm can be divided into two phases: prediction and estimation. In the prediction phase, the future system state  $\hat{\eta}_{aug,k+1}^-$  is computed using the current estimated state  $\hat{\eta}_{aug,k}^+$  adjusting (22) as follows (Equation 28):

$$\hat{\eta}_{aug,k+1}^- = A_{aug,d} \hat{\eta}_{aug,k}^+ + B_{aug,d} u_{aug,k} \quad (28)$$

The predicted covariance matrix  $P_{k+1}^-$  and the Kalman gain  $K_{KF,k+1}$  computed as follows (Equations 29, 30):

$$P_{k+1}^- = A_{aug,d} P_k^+ A_{aug,d}^T + Q_{KF} \quad (29)$$

$$K_{KF,k+1} = P_{k+1}^- C^T (C P_{k+1}^- C^T + R_{KF})^{-1} \quad (30)$$

Using the  $K_{KF,k+1}$ , estimated state  $\hat{\eta}_{aug,k+1}^+$  and covariance matrix  $P_{k+1}^+$  is calculated as follows (Equations 31, 32):

$$\hat{\eta}_{aug,k+1}^+ = \hat{\eta}_{aug,k+1}^- + K_{KF,k+1} (y_{k+1} - C \hat{\eta}_{aug,k+1}^-) \quad (31)$$

$$P_{k+1}^+ = (I - K_{KF,k+1} C) P_{k+1}^- \quad (32)$$

Now that the estimated state from the KF is available, the control input  $u_k$  is obtained using LQR, which minimizes the cost function  $J$  (Equation 33):

$$J = \sum_{k=0}^{\infty} (\eta_{aug,k}^T Q_{aug} \eta_{aug,k} + u_{fin,k}^T R_{fin} u_{fin,k}) \quad (33)$$

In the standard LQR framework, the cost function  $J$  aims to minimize a combination of the state error weighted by  $Q$  and the control effort weighted by  $R$ . In addition,  $\eta_{fin,k} = [\phi_{fin,k} \ P_{fin,k}]$  is the state vector for the ship motion.  $Q_{fin}$ ,  $R_{fin}$  are symmetric, positive semi-definite weighting matrices for the state variables and control inputs in each subsystem. The optimal control law for minimizing the cost function  $J$  is (Equation 34):

$$u_k = -K_{LQR} \hat{\eta}_{aug,k}^+ \quad (34)$$

Here, instead of feeding the control law with true state  $\eta_{aug,k}$  like typical a LQR control law,  $u_{fin,k}$  is computed with the estimated state  $\hat{\eta}_{aug,k}^+$  obtained from the KF.  $K_{LQR}$  is the optimal gain matrix obtained by first solving the following Discrete Algebraic Riccati Equation 35:

$$P = A_{aug,d}^T P A_{aug,d} - A_{aug,d}^T P B_{aug,d} (B_{aug,d}^T P B_{aug,d} + R_{fin})^{-1} B_{aug,d}^T P A_{aug,d} + Q_{fin} \quad (35)$$

Then,  $K_{LQR}$  can be calculated as follows (Equation 36):

$$K_{LQR} = (R_{fin} + B_{aug,d}^T P B_{aug,d})^{-1} B_{aug,d}^T P A_{aug,d} \quad (36)$$

#### 4. Simulation Results

In this section, the performance of the ship roll stabilization controller is rigorously assessed by simulating its operation under two environmental conditions, specifically, sea state 3 and state 4. These conditions represent moderate and rough sea states, respectively, thus providing a diverse test framework. The simulations were designed to evaluate the controller's ability to maintain stability and effectively respond to varying degrees of wave-induced disturbance. First, the effectiveness of the fins in stabilizing the roll motion of the ship was evaluated. Before these simulations, the effects of active fins were demonstrated in calm water at a 1.4 m/s surge speed while the fins are  $\pm 25$  degrees and Figure 4 shows the results. As shown in the figure,  $4^\circ$  roll motion is recorded after transition of the response.

The simulation involved two scenarios: one in which the ship was subjected to wave disturbances with passive fins and another in which active stabilizing fins. In the scenario involving active fins, the fin angles were limited to a maximum of  $\pm 25$  degrees, and the rate of change was capped at  $\pm 75$  degrees per second. This constraint was implemented to realistically simulate the mechanical limitations of the fins under actual maritime conditions on a model scale. Results from both scenarios were compared to assess the impact of the fins on roll stabilization. Table 2 lists the parameters for sea states 3 and 4. These parameters can be calculated using the spectral factorization method for each sea state. The detailed information about these parameters can be found in [7].

In addition, the KF algorithm was initialized with  $Q_{KF} = \text{diag}([10^{-4}, 10^{-4}, 10^{-4}, 10^{-4}])$  and  $R_{KF} = \text{diag}([10^{-4}, 10^{-4}])$ . The simulation length is 50s with time step size of 0.02s. The LQR controller was parameterized differently based on the sea state in which the ship was simulated. Table 3 lists the parameters used to obtain the LQR gain.

Consequently, by solving (35)-(41), the LQR gain matrix for both sea state  $K_{LQR,SS3}$  and  $K_{LQR,SS4}$  are obtained as follows (Equations 37, 38):

$$K_{LQR,SS3} = \begin{bmatrix} -0.2670 & -1.7160 & -0.2330 & -1.9624 \\ 0.2670 & 1.7160 & 0.2330 & 1.9624 \end{bmatrix} \quad (37)$$

$$K_{LQR,SS4} = \begin{bmatrix} -0.2687 & -1.6956 & -0.1991 & -1.6304 \\ 0.2687 & 1.6956 & 0.1991 & 1.6304 \end{bmatrix} \quad (38)$$

It can be observed that variations in the weighting matrices influence the resulting control gains  $K_{LQR,SS3}$  and  $K_{LQR,SS4}$  which correspondingly exhibit higher and lower gain values. These gain values were employed for controlling in an active fin scenario, and the outcomes were subsequently compared

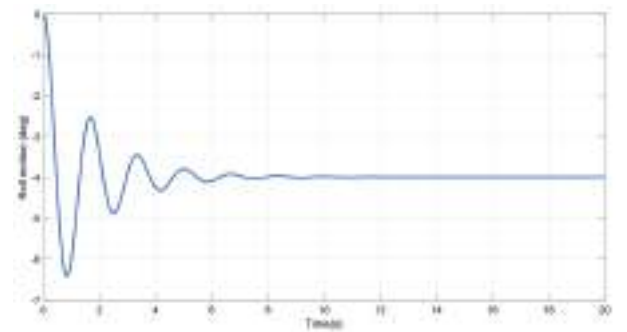


Figure 4. Demonstration of fins in calm water

Table 2. Parameters for sea states 3 and 4

Parameter	Sea state 3:	Sea state 4:
$\zeta$	0.1603	0.1617
$\sigma$	0.1596	0.2678

with those of a passive fin scenario. The comparative results are shown in Figures 5 to 7. The root mean square (RMS) values are detailed in Tables 4 and 5 to quantify the outcomes of the simulation.

In Figure 5, corresponding to the milder sea state 3, the roll motion and roll rate graphs show that active fins, controlled by a more aggressive LQR strategy, significantly reduced the amplitude of roll compared to passive fins. This approach leverages less severe conditions to apply more aggressive

control actions that effectively mitigate smaller disturbances and result in smoother, more damped responses. In contrast, Figure 7 where represents rougher sea state 4, where the control strategy is less aggressive but more robust and tailored to cope with larger disturbances typical of harsher sea conditions. Despite the increased severity, the active fins still outperformed the passive fins, maintaining better control over roll motion and rate. Tuning the LQR parameters in sea state 4 aims for durability and sustained performance under

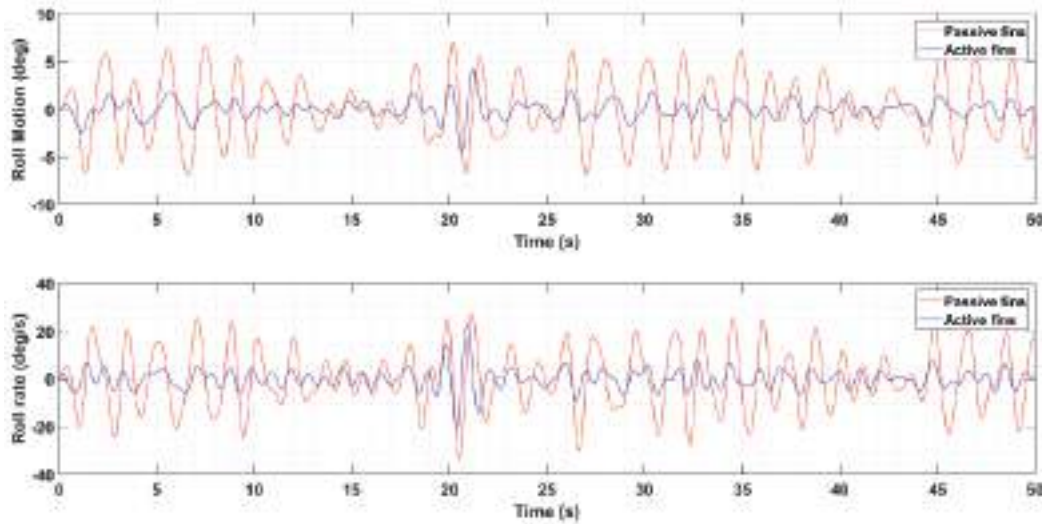


Figure 5. Comparison of ship roll motion and rate with passive and active fins in sea state 3

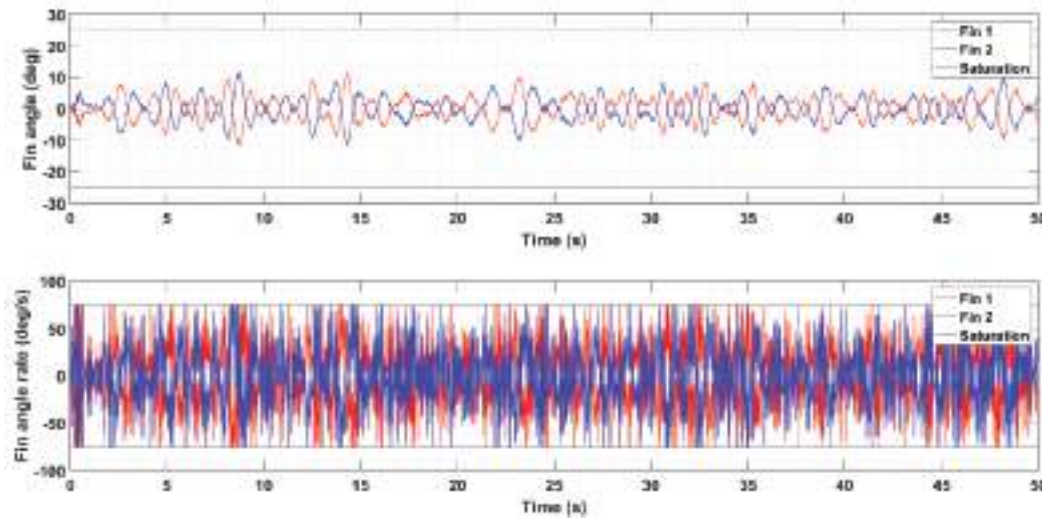
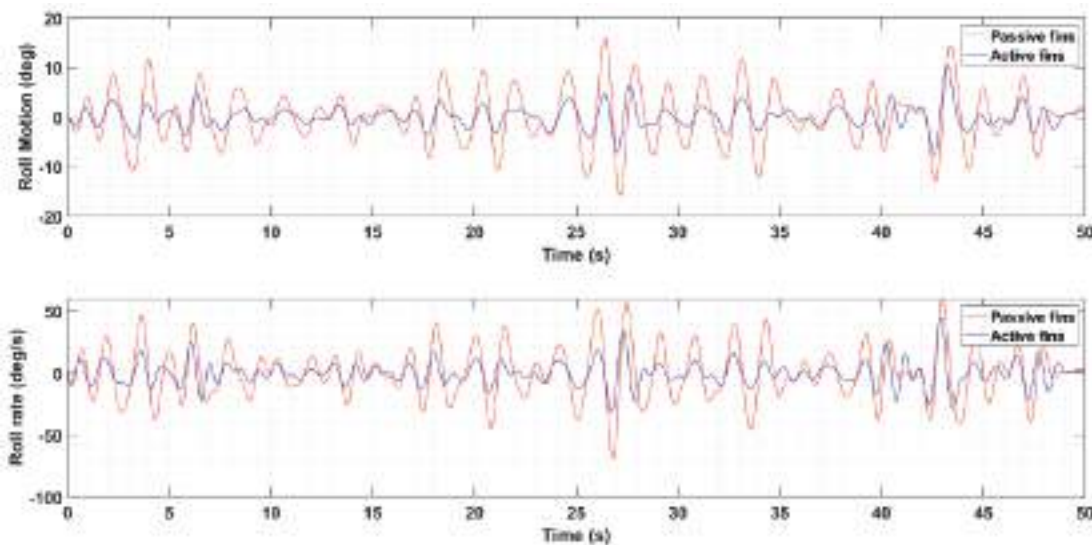


Figure 6. Fin angular motion and rate in active fin scenario in sea state 3

Table 3. LQR parameters

Parameter	Sea state 3:	Sea state 4:
$Q_{fin}$	$diag([1,1])$	$diag([1,1])$
$Q_{wave}$	$diag([18,18])$	$diag([9,9])$
$R_{fin}$	$diag([0.1,0.1])$	$diag([0.1,0.1])$



**Figure 7.** Comparison of ship roll motion and rate with passive and active fins for sea state 4

stress, rather than finer control under milder conditions. These findings are further elucidated in Figures 6 and 8, respectively, depict the fin angular motion and rate in sea states 3 and 4, respectively. In sea state 3, fins exhibited higher frequency movements, as indicated by the denser angular rate plot compared to sea state 4. Additionally, in sea state 4, due to harsher conditions, the fins occasionally reached and maintained their maximum angular rate, indicating the struggle as they stabilized the ship's motion.

In Table 4, the reduction percentages for roll motion and rate are quite substantial, at approximately 72.855% and 70.181%, respectively, in sea state 3. This significant reduction underscores the effectiveness of the more aggressive control strategy applied under milder conditions, whereas in Table 5, which presents harsher conditions, the RMS values for both roll motion and roll rate in sea state 4 are higher than those in sea state 3. Despite this, the reductions are still notable, at 57.413% for roll motion and 51.517% for roll rate. Considering the increased environmental challenges, this outcome is satisfactory. The less aggressive, more robust control strategy in sea state 4 is designed not merely to minimize immediate disturbances but to ensure steady and sustained ship stability over time. This approach is particularly important under harsh conditions, where over-reactive control responses can potentially lead to system instability or increased wear and tear on the control mechanisms.

Promising results are observed in Figures 5 and 7, which are quantified in Tables 4 and 5, are controlled based on estimated values  $\hat{\eta}_{aug,k}^+$  obtained from a KF algorithm, as derived in section 3. KF is crucial because it filters out noise from measurements and compensates for process disturbances, thus providing a refined estimate of the system's state. To validate the reliability and accuracy of these estimates, the KF's performance was validated. The results are presented in Figures 9-12.

However, it is difficult to observe the performance of KF directly, as illustrated in Figures 9 and 11, the overall error in the KF estimation was generally smaller than that in the raw measurements, as shown in Figures 10 and 12. To better understand the performance of KF estimation compared to measurement data with respect to the true value, the RMS values of the errors are presented in Table 6.

Table 6 presents a quantitative assessment of the errors associated with the measured and estimated states for the roll motion and roll rate in sea states 3 and 4, utilizing the KF for the estimation process. The RMS errors for both roll motion and roll rate in sea state 3 indicate a reduction in the error from measurement to estimation, with the roll motion decreasing from  $0.576^\circ$  to  $0.437^\circ$  and the roll rate decreasing from  $0.581^\circ$  to  $0.491^\circ$ . In sea state 4, the results were somewhat consistent, with the roll motion error modestly reduced from  $0.579^\circ$  in raw measurements to  $0.442^\circ$  in estimation.

**Table 4.** Roll motion (deg) and rate (deg/s) RMS in sea state 3

State	Passive fins	Active fins	Reduction (%)
Roll motion	3.053	0.829	72.855
Roll rate	11.926	3.556	70.181

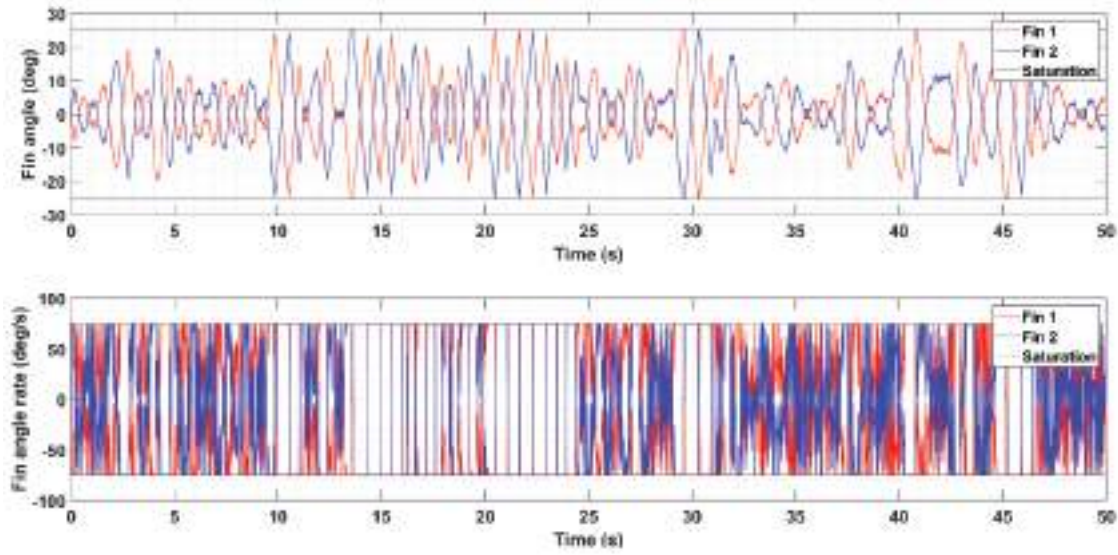


Figure 8. Fin angular motion and rate in active fin scenario in sea state 4

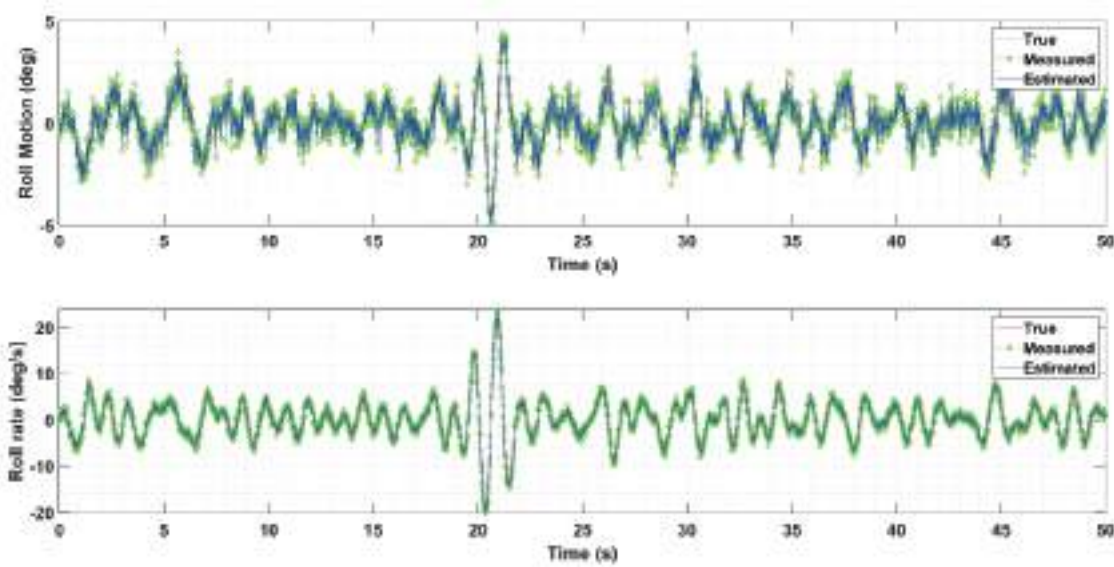


Figure 9. True, measured, and estimated states in sea state 3 simulation

Table 5. Roll motion (deg) and rate (deg/s) of RMS in sea state 4

State	Passive fins	Active fins	Reduction (%)
Roll motion	5.534	2.356	57.413
Roll rate	21.045	10.203	51.517

Table 6. RMS of measured vs. estimated roll motion (deg) and rate (deg/s) errors

	State	Measurement	Estimation
Sea State 3	Roll motion	0.576	0.437
	Roll rate	0.581	0.491
Sea State 4	Roll motion	0.579	0.442
	Roll rate	0.577	0.567

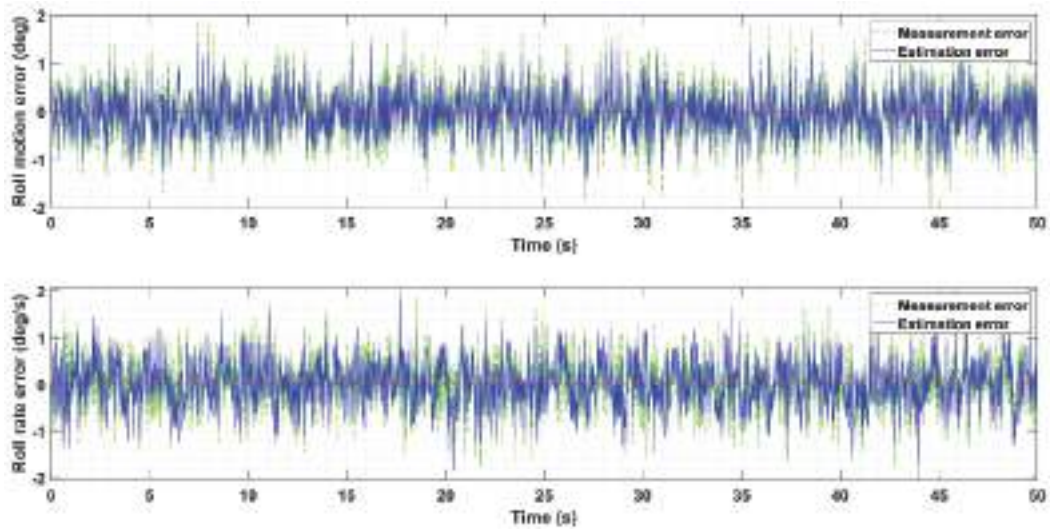


Figure 10. Measurement and estimation errors in the sea state 3 simulation

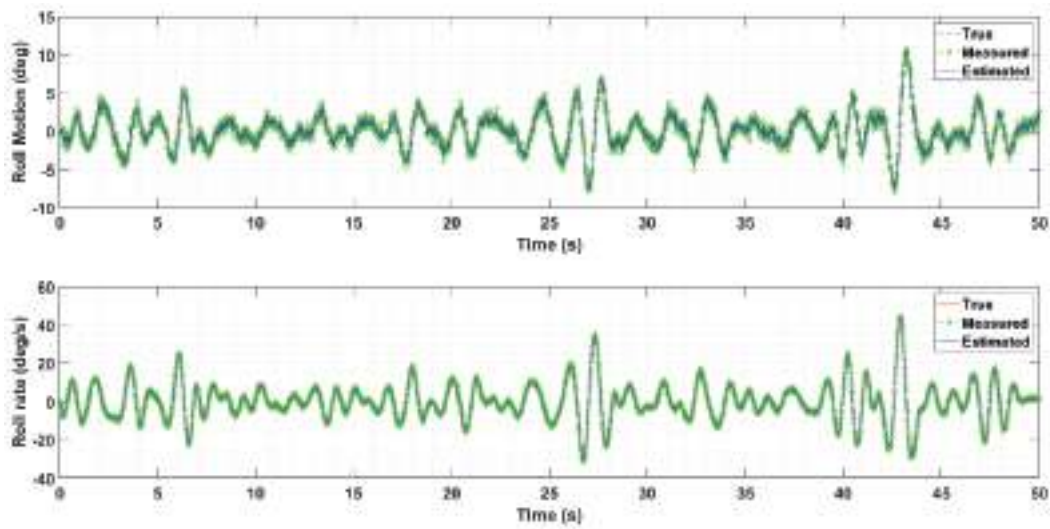


Figure 11. True, measured, and estimated states in the sea state 4 simulation

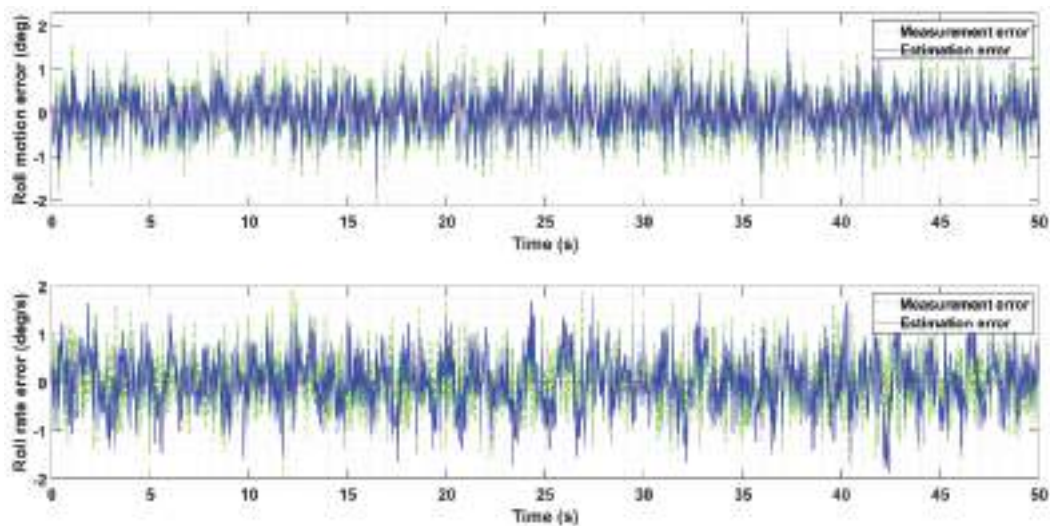


Figure 12. Measurement and estimation errors in the sea state 4 simulation

However, the roll rate error exhibits a smaller reduction from 0.577 to 0.567 deg/s. The smaller improvement in roll rate estimation under rougher conditions for sea state 4 might be indicative of the KF reaching its performance limits in more challenging environments.

## 5. Conclusion

In conclusion, this study successfully demonstrated the effectiveness of an LQG controller for roll motion reduction and its rate of change under wave-disturbed conditions for sea states 3 and 4. The integration of active fins as stabilizers, controlled by the LQG algorithm, led to significant improvements in the vessel's roll response, as evidenced by substantial reductions in roll motion and rate. The accuracy of state estimation through the KF plays a pivotal role in this context, ensuring that the controller inputs are based on precise estimations of the ship's state. This approach provides a more reliable and effective control strategy, highlighting the importance of accurate state estimation in the overall control system design. Furthermore, the results underscore the potential of using advanced control strategies, such as LQG, in marine applications, especially under challenging environmental conditions. This study not only contributes to the field of naval engineering by providing a viable solution for roll stabilization but also sets the groundwork for future research in this area.

Future work could focus on exploring the robustness of this approach under varying sea conditions and ship configurations, as well as integrating real-time environmental data to further enhance the system's adaptive capabilities. In addition, exploring more complex control strategies or integrating other types of stabilizers could provide additional improvements to ship stability and safety.

## Footnotes

### Authorship Contributions

Concept design: F. Çakıcı, A. I. Jambak, E. Kahramanoğlu, Ö. S. Şahin, A. Baran Bayezit, Data Collection or Processing: F. Çakıcı, A. I. Jambak, A. K. Karabüber, B. Ustalı, M. U. Öğür, F. Peri, M. A. Uğur, Analysis or Interpretation: F. Çakıcı, A. I. Jambak, A. K. Karabüber, M. U. Öğür, F. Peri, Literature Review: A. I. Jambak, A. K. Karabüber, B. Ustalı, M. A. Uğur, Writing, Reviewing and Editing: F. Çakıcı, A. I. Jambak, E. Kahramanoğlu, B. Ustalı, F. Peri, Ö. S. Şahin, M. A. Uğur, A. B. Bayezit.

**Funding:** This research was supported by the Scientific and Technological Research Council of Türkiye (project number 123M482).

## References

- [1] J. H. Chadwick, "On the stabilization of roll". *Transactions of the Society of Naval Architects and Marine Engineers*, vol. 63, pp. 237-280, 1955.
- [2] M. T. Sharif, G. N. Roberts, and R. Sutton, "Final experimental results of full scale fin/rudder roll stabilisation sea trials". *Control Engineering Practice*, vol. 4, pp. 377-384, Mar 1996.
- [3] M. T. Sharif, G. N. Roberts, and R. Sutton, "Sea-trial experimental results of fin/rudder roll stabilisation". *Control Engineering Practice*, vol. 3, pp. 703-708, May 1995.
- [4] T. Wu, J. Guo, Y.-N. Chen, and W.-C. Chen, "Control system design and performance evaluation of anti-pitching fins". *Journal of Marine Science and Technology*, vol. 4, pp. 117-122, Dec 1999.
- [5] D. A. Liut, *Neural-network and fuzzy-logic learning and control of linear and nonlinear dynamic systems*. Virginia Polytechnic Institute and State University, 1999.
- [6] D. Liut, D. Mook, K. Weems, and A. Nayfeh, "A numerical model of the flow around ship-mounted fin stabilizers". *International Shipbuilding Progress*, vol. 48, pp. 19-50, Apr 2001.
- [7] T. Perez, *Ship motion control: course keeping and roll stabilisation using rudder and fins*. Springer Science & Business Media, 2006.
- [8] T. Perez and G. C. Goodwin, "Constrained predictive control of ship fin stabilizers to prevent dynamic stall". *Control Engineering Practice*, vol. 16, pp. 482-494, Apr 2008.
- [9] G. N. Roberts, V. Cournou, B. Vinsonneau, and K. J. Burnham, "Parallel multi-model switched control for ship roll stabilization". *Proceedings of the Institution of Mechanical Engineers, Part M: Journal of Engineering for the Maritime Environment*, vol. 220, pp. 53-65, Jun 2006.
- [10] S. Surendran, S. K. Lee, and S. Y. Kim, "Studies on an algorithm to control the roll motion using active fins". *Ocean Engineering*, vol. 34, pp. 542-551, Mar 2007.
- [11] J. H. Kim and Y. H. Kim, "Motion control of a cruise ship by using active stabilizing fins". *Proceedings of the Institution of Mechanical Engineers, Part M: Journal of Engineering for the Maritime Environment*, vol. 225, pp. 311-324, Oct 2011.
- [12] A. J. Koshkouei, and L. Nowak, "Stabilisation of ship roll motion via switched controllers". *Ocean Engineering*, vol. 49, pp. 66-75, Aug 2012.
- [13] M. Moradi and H. Malekizade, "Robust adaptive first-second-order sliding mode control to stabilize the uncertain fin-roll dynamic". *Ocean Engineering*, vol. 69, pp. 18-23, Sep 2013.
- [14] M. A. Hinostroza, W. Luo, and C. G. Soares, "Robust fin control for ship roll stabilization based on L2-gain design". *Ocean Engineering*, vol. 94, pp. 126-131, Jan 2015.
- [15] R. Li, T. Li, W. Bai, and X. Du, "An adaptive neural network approach for ship roll stabilization via fin control". *Neurocomputing*, vol. 173, pp. 953-957, Jan 2016.
- [16] W. Luo, B. Hu, and T. Li, "Neural network based fin control for ship roll stabilization with guaranteed robustness". *Neurocomputing*, vol. 230, pp. 210-218, Mar 2017.
- [17] L. Huang, Y. Han, W. Duan, Y. Zheng, and S. Ma, "Ship pitch-roll stabilization by active fins using a controller based on onboard hydrodynamic prediction". *Ocean Engineering*, vol. 164, pp. 212-227, Sep 2018.
- [18] I. A. Jimoh, I. B. Küçükdemiral, and G. Bevan, "Fin control for ship roll motion stabilisation based on observer enhanced MPC with disturbance rate compensation". *Ocean Engineering*, vol. 224, 108706, Mar 2021.



- [19] F. Cakici, "Vertical acceleration control using LQG approach for a passenger ship". *Ocean Engineering*, vol. 241, 110040, Dec 2021.
- [20] S.-D. Lee, S.-S. You, X. Xu, and T. N. Cuong, "Active control synthesis of nonlinear pitch-roll motions for marine vessels". *Ocean Engineering*, vol. 221, 108537, Feb 2021.
- [21] L. Liang, Q. Cheng, J. Li, Z. Le, P. Cai, and Y. Jiang, "Design of the roll and heel reduction controller on ship's turning motion". *Ocean Engineering*, vol. 284, 115093, Sep 2023.
- [22] M. Taskin, R. Guclu, and A. O. Ahan, " $H_\infty$  optimal control of DTMB 5415 combatant roll motion by using active fins with actuator saturations". *Ocean Engineering*, vol. 276, 114255, Mar 2023.
- [23] L. Hu, M. Zhang, X. Yu, Z.-M. Yuan, and W. Li, "Real-time control of ship's roll motion with gyro stabilisers". *Ocean Engineering*, vol. 285, 115348, 2023.
- [24] A. Rezaei and M. Tabatabaei, "Ship roll stabilization using an adaptive fractional-order sliding mode controller". *Ocean Engineering*, vol. 287, p. 115883, Oct 2023.
- [25] F. Cakici, and E. Kahramanoglu, "Numerical roll motion control by using fins based on the linear quadratic regulator and dynamic mode decomposition". *Applied Ocean Research*, vol. 142, 103828, Jan 2024.
- [26] T. Perez, and M. Blanke, "Ship roll damping control". *Annual Reviews in Control*, vol. 36, pp. 129-147, Apr 2012.

# A Conceptual COLREGs-based Obstacle Avoidance Algorithm Implementing Dynamic Path Planning and Collision Risk Assessment

Hasan Uğurlu<sup>1</sup>, Omar Djecevic<sup>2</sup>, İsmail Çiçek<sup>3</sup>

<sup>1</sup>Ordu University Fatsa Faculty of Marine Sciences, Department of Marine Transportation Management Engineering, Ordu, Türkiye

<sup>2</sup>Codeus Inc., Studentska, bb. Lamela 8, 81000 Podgorica, Montenegro

<sup>3</sup>Istanbul Technical University Faculty of Maritime, Department of Marine Engineering, İstanbul, Türkiye

## Abstract

This paper introduces an algorithm for collision avoidance systems intended for Maritime Autonomous Surface Ships. The algorithm takes into account the rules defined by the International Regulations for Preventing Collisions at Sea (COLREGs) and is tailored for real-world maritime environments. Analysis of collision accidents highlights human error and non-compliance with COLREGs as primary contributing factors. Employing the COLREGs as foundational design criteria can mitigate these factors. The algorithm also has the potential to serve as a decision support system on currently manned vessels, enhancing safe navigation. The study proposes a novel rule-based collision avoidance algorithm that adheres to COLREGs, utilizes the Collision Risk Index and ship domain for safety assessment, and combines dynamic path planning for collision-free navigation. Leveraging the Automatic Identification System, which is present on all ships navigating international waters, the algorithm achieves target detection. The algorithm was applied to simulate past ship-to-ship collision incidents, considering the ship kinematics, dynamics, and maneuverability resulting in successful prevention of such accidents through the proposed approach.

**Keywords:** Collision avoidance, Collision Risk Index (CRI), COLREGs, Dynamic path planning, Ship domain

## 1. Introduction

Human error has been recognized as a primary contributing factor in more than 75% of maritime accidents, according to the findings of [1]. In studies [2] and [3], the incidence of human error in marine accidents was identified as 78% and 80%, respectively. A recent comprehensive analysis of major collision accidents since 1977 has found that reduced crew numbers, the adoption of swift loading and unloading equipment, and the resultant increase in seafarers' workload and duty hours have contributed significantly to these incidents, with human error identified as the primary cause in 94.7% of cases [4]. A bridge watch entails a multifaceted process demanding simultaneous and continuous consideration and assessment of numerous elements. These encompass maintaining a lookout, coordinating with the

bridge team, managing bridge resources, utilizing navigational equipment for observing maritime traffic, adhering to the International Regulations for Preventing Collisions at Sea (COLREGs) during maneuvering, and engaging in effective communication with other vessels. There is a requirement to develop algorithms and methods that can assist human operators in collision avoidance strategies, a pivotal component of ensuring ships' safe navigation. This need arises from the limitations of human operators as discussed earlier, compounded by commercial pressures [5]. These algorithms and methods will not only aid human operators but also serve as the foundation for future systems that are anticipated to replace human involvement.

The literature contains a plenty of techniques, algorithms, and applications for collision avoidance and path planning



**Address for Correspondence:** Hasan Uğurlu, Ordu University Fatsa Faculty of Marine Sciences,

Department of Marine Transportation Management Engineering, Ordu, Türkiye

**E-mail:** dr.hasan.ugurlu@hotmail.com

**ORCID iD:** orcid.org/0000-0002-0778-9265

**Received:** 20.08.2024

**Last Revision Received:** 11.11.2024

**Accepted:** 15.11.2024

**To cite this article:** H. Uğurlu, O. Djecevic, and İ. Çiçek. "A Conceptual COLREGs-based Obstacle Avoidance Algorithm Implementing Dynamic Path Planning and Collision Risk Assessment." *Journal of ETA Maritime Science*, vol. 12(4), pp. 377-394, 2024.



Copyright© 2024 the Author. Published by Galenos Publishing House on behalf of UCTEA Chamber of Marine Engineers.

This is an open access article under the Creative Commons AttributionNonCommercial 4.0 International (CC BY-NC 4.0) License

in autonomous surface vehicles. By excluding variations of these methods, the authors have identified a total of 37 distinct approaches (Table 1). However, in comparison to collision avoidance and path planning for aviation, land, and underwater vehicles, addressing these challenges for

Maritime Autonomous Surface Ships (MASSs) presents a more intricate undertaking. The methods listed in Table 1 can be classified into two categories: those that offer vector-based visual solutions [6-14], and those that rely on numerical mathematical models [15-24]. While

**Table 1.** Methods, algorithms, and functions used for ship collision avoidance and path planning in the literature

Method	Purpose	Research
Artificial Potential Field (APF)	Collision avoidance	[6]
Velocity Obstacle (VO)	Path plan. + Collision avoidance	[7]
Dynamic Window (DW)	Collision avoidance	[8]
Voronoi Diagram	Path planning	[9]
Fast Marching Method	Path plan. + Collision avoidance	[10]
Swarm Intelligence	Path plan. + Collision avoidance	[11]
Dynamic Optimization Algorithm	Path plan. + Collision avoidance	[11]
Rapidly-Exploring Random Tree (RRT)	Path plan. + Collision avoidance	[12]
Branch and Bound Method	Collision avoidance	[13]
Grid-based Method	Path plan. + Collision avoidance	[14]
Fuzzy Logic	Collision avoidance	[15]
Model Predictive Control (MPC)	Path plan. + Collision avoidance	[16]
Neural Networks	Path plan. + Collision avoidance	[17]
Game Theory	Collision avoidance	[18]
Dijkstra Algorithm	Path plan. + Collision avoidance	[19]
Evolutionary Algorithm	Path plan. + Collision avoidance	[20]
Case-based Reasoning	Collision avoidance	[21]
Inevitable Collision State	Path plan. + Collision avoidance	[22]
Control Barrier Function	Collision avoidance	[23]
Barrier Lyapunov Function	Path plan. + Collision avoidance	[24]
Gauss Mix Model	Collision avoidance	[25]
Bayesian Networks	Collision avoidance	[26]
Deterministic Method	Path plan. + Collision avoidance	[27]
Line of Sight (LOS)	Path plan. + Collision avoidance	[28]
Interval Programming (IvP)	Collision avoidance	[29]
Non-linear Programming	Path planning	[30]
Constrained Convex Optimization	Collision avoidance	[31]
Danger Immune Algorithm	Collision avoidance	[32]
Distributed Search Algorithm (DSA)	Collision avoidance	[33]
Linear Extension Algorithm	Collision avoidance	[34]
Local Reactive Obstacle Avoidance Based on Region Analysis (LROABRA)	Collision avoidance	[35]
Local Normal Distributed Based Trajectory	Path plan. + Collision avoidance	[36]
Recursive Algorithm	Path plan. + Collision avoidance	[37]
Pseudospectral Optimal Control	Path planning	[38]
Probabilistic Approach	Collision avoidance	[39]
Observation Inference Prediction Decision Model	Collision avoidance	[40]
Pontryagin's Maximum Principle	Path plan. + Collision avoidance	[41]

visual solution methods are advantageous for their ease of calculation and interpretability, they are generally inadequate for providing safe recommendations in areas with heavy traffic. Conversely, methods based on mathematical models can yield safe outcomes under all conditions when accurately modeled, but they face challenges such as delayed results due to the complexities involved in modeling and numerous calculations. A limitation common to many algorithms for collision prevention is that they are restricted to the collision avoidance function alone [8,18,25,26] and cannot perform local route planning, which is essential for comprehensive collision prevention.

Despite the frequent use of methods like Artificial Potential Field (APF) [6], Velocity Obstacle (VO) [7], and Model Predictive Control (MPC) [16] in the literature, each has significant drawbacks concerning safe collision avoidance. APF can become trapped in local minimum regions; in the VO method, inaccurate trajectory prediction can result in unsafe recommendations; and in MPC, the approach cannot guarantee safe collision avoidance if the modeling is flawed or an unmodeled scenario arises. In comparison, the proposed method addresses both collision avoidance and local route planning, overcoming limitations such as the need for trajectory estimation and susceptibility to local minima. It operates independently of modeling assumptions by utilizing a rule-based system coupled with real-time risk analysis, thereby enhancing adaptability to unforeseen situations. The proposed method has certain limitations, primarily stemming from its exclusive reliance on Automatic Identification System (AIS) as the target detection sensor and its inability to detect obstacles, such as landmasses, due to the use of non-vectorized electronic charts. However, considering that the study introduces a conceptual system, it offers significant contributions to the literature. These include the incorporation of Rule 18, and the evaluation of interactions with other vessels on a case-by-case basis in compliance with COLREGs.

Collision risk must be identified to enable ships to recognize potential risks in various encountered situations and make suitable collision avoidance decisions. Once the collision risk is calculated during ship encounters, the decision of whether to maneuver or not becomes a crucial aspect that demands careful consideration. Not all ship encounters necessitate maneuvering, as some instances where ships approach each other closely (but still maintain a safe threshold) may not pose an immediate danger. Therefore, continuous monitoring of nearby vessels is essential, and avoidance maneuvers should be executed when deemed necessary based on the identification of collision risks.

This study represents the initial phase of a multi-stage project and within this phase, it has contributed the following advancements to the existing literature. The combination

of the updated ship domain and the Collision Risk Index (CRI) serves to signal the initiation and termination points of collision avoidance maneuvers. As far as the available literature indicates, this study stands as the pioneering endeavor to encompass and adhere to all rules complying with COLREG Rules 5, 7, 8, and 13-18, which pertain to navigation and maneuvering aspects. Moreover, practical safety zones have been recommended, aligning with the guidance laid out in [42]. This study's innovation extends to enhancing the objectivity of regulations for autonomous vehicles. This is achieved by aggregating data from various studies that offer numerical interpretations of the COLREG Rules from diverse perspectives.

The primary objective of this study is to introduce a system capable of adhering to the COLREGs, capable of autonomous decision-making that transcends human subjectivity, pre-evaluating collision risk, and executing avoidance actions. The overarching goal of this study is to enhance navigation safety and curtail the frequency of collision incidents leading to loss of life, substantial environmental damage, and property loss. Upon the completion of the project, the proposed system holds the potential for real-world implementation in actual maritime conditions. Additionally, the deployment of this system on manned vessels aims to alleviate the cognitive burden on bridge personnel, streamlining collision prevention measures. The forthcoming section delves into the methodology and approach applied for developing the collision avoidance algorithms. This narrative continues in Section 3, explaining the framework of the envisaged rule-based collision avoidance system. In Section 4, the kinematic and dynamic characteristics of the vessels are presented. The algorithms are exemplified through case studies in Section 5. Section 6 encapsulates the outcomes and fosters a discourse on the results, contextualizing their significance. Section 6 encapsulates the principal takeaways drawn from the study.

## 2. Preliminaries

In this section, an explanation is provided regarding the devices utilized in the application, as well as the rules and data that are taken into consideration.

### 2.1. Devices Used for Target Detection and Environment Sensing

The MASSs must be equipped with devices that can simply detect the target's location and acquire images and/or data of the vehicle's surrounding environment. Numerous device options are employed for target detection and environmental sensing on board ships. Alongside external detection sensors like radar [6], lidar [30], and cameras [43], transponder-based sensors like AIS [44], location-providing sensors such as GPS [45], and sensors supplying depth and underwater environmental images like sonar [46] are widely utilized. However, the harsh conditions at high sea pose significant

challenges in using some of these devices. Especially cameras and lidars are not well-suited for the demanding sea conditions of MASSs [47].

AIS equipment is more cost-effective than radar and is widely employed as a sensor onboard ship, boasting a detection range greater than conventional shipboard radar. Particularly when combined with the Electronic Chart Display and Information System (ECDIS), AIS has the potential to supplant radar as the primary collision avoidance device for vessels equipped with AIS technology. This attribute positions AIS as an effective collision avoidance solution for ships [48]. AIS messages can be received from numerous ships, encompassing target vessels that might evade radar detection due to range limitations, obstruction, or other factors. Especially in areas with restricted visibility, like fjord-type regions, where radar and visual observers encounter obscured sections, AIS broadcasts generally demonstrate improved reception performance [49]. The direct usability of data from an AIS device, without the need for interpretation, enhances its appeal. However, AIS has limitations, such as data gaps and instances of not receiving data. To handle these limitations of AIS, the system we propose calculates the positions of target vessels using Dead Reckoning positions in place of missing or corrupted data from the moment it detects abnormal values in the data until the data returns to normal. Given these advantages, the AIS device was selected as the target detection sensor for this study. ECDIS, which synergizes well with the AIS device and offers reliable environmental information, played a crucial role.

## 2.2. COLREG Rules

Statheros et al. [50] demonstrated that 56% of marine accidents were attributed to violations of the COLREGs. Likewise, in the investigation conducted by [4], violation of the COLREG Rules emerged as the foremost contributing factor to ship-to-ship collisions. The outcomes derived from the implemented algorithm in this research underscore the imperative and critical significance of complying with the COLREGs to ensure the safety of ship navigation.

Studies purporting to account for the COLREG Rules commonly declare their adherence to COLREGs by focusing solely on three distinct encounter scenarios, as exemplified by [44] and [51]. However, COLREGs are not just about the situations specified by a few rules that delineate the encounters, i.e. by Rules 13, 14, and 15. The COLREGs also include regulations directly related to steering and sailing [52]. For instance, depending on the traffic-specific responsibilities of the ships, Rule 18 alone might be the predominant rule to apply, rendering other rules inapplicable. In this study, Rule 18 is recognized to exert a significant influence on collision avoidance. Nevertheless, the majority of the COLREG Rules related to navigation and maneuvering are incorporated into

the algorithm development study, and they are itemized in Table 2.

## 2.3. Data Set

Recorded AIS data was utilized for both modeling and testing the algorithms. The data underwent sequential analysis with a focus on time and adherence to the COLREGs was established as the primary criteria. As a result, the same algorithm can be effectively applied in real-world scenarios, utilizing AIS-derived data.

For each collision accident, a simulation was created using the collision accident reports sourced from the Japan Transport Safety Board's (JTSB) database. The data extracted from the JTSB database included details such as the date, time, latitude, longitude, Speed Over Ground (SOG), Course Over Ground (COG), ship name, ship length, and the ship's navigational status. These data were employed in the simulation study. Additionally, parameters like Distance of Closest Point of Approach (DCPA), Time of Closest Point of Approach (TCPA), and Variation of Compass Degree (VCD) were computed using the formulas described in subsequent sections. The location data of the nearby ships was integrated and visually depicted on the map using the Webmap function of MATLAB/Simulink®, thereby facilitating the simulation

*Table 2. COLREG rules considered in the study*

Rule	Definition	Implementation status	Implementation method
5	Look-out	√	AIS data
6	Safe speed	X	-
7	Risk of collision	√	CRI and ship domain
8	Action to avoid collision	√	Developed algorithm
9	Narrow channels	X	-
10	Traffic separation schemes	X	-
13	Overtaking	√	Developed algorithm
14	Head-on situation	√	Developed algorithm
15	Crossing situation	√	Developed algorithm
16	Action by give-way vessel	√	Proposed rule-base
17	Action by stand-on vessel	√	Proposed rule-base
18	Responsibilities between vessels	√	Navigation status from AIS
COLREG: International Regulations for Preventing Collisions at Sea, AIS: Automatic Identification System, CRI: Collision Risk Index			

of the collision accidents. The accidents and the specific COLREG Rules violated in this study are displayed in Table 3.

### 3. Rule-Based Collision Avoidance

This section comprehensively elucidates various aspects, including the quantification of the COLREG Rules, the determination of ships' relative positions, the assignment of right-of-way between ships, and the calculation of the CRI.

#### 3.1. Quantification of COLREG Rules

The algorithm developed in this study incorporated the following COLREGs, each accompanied by a concise outline

**Table 3.** Simulated collision accidents and COLREG rules violated in accidents

Scenario no	Violated COLREG rule	Collision accident	Year
1	Rule 13	APL Pusan-Shoutokumaru	2019
2	Rule 14	Jia Hui-Eifuku Maru	2013
3	Rule 15	ACX Crystal-USS Fitzgerald	2017
4	Rule 15	Sulphur Garland-Wakomaru	2015
5	Rule 18	Aquamarin-Hirashin Maru	2011

COLREG: International Regulations for Preventing Collisions at Sea

of its collision avoidance requirements. The implementation of the COLREG Rules was carried out in specific stages within the framework of the study. These stages are illustrated in Figure 1.

##### 3.1.1. Receiving initial data of own ship and target ship

In this stage, the algorithm gathers the following input parameters from the target ships that are within the range of the AIS device:

- Date and time,
- Position as latitude and longitude,
- SOG,
- COG,
- Navigation status of target ships,
- Ship sizes,
- True bearing of the target ship ( $BRG_{TS}$ ),
- Distance (range) of target ship ( $RNG_{TS}$ ) and,
- CPA and TCPA.

##### 3.1.2. Determination of the target ship's position relative to COLREGs

Sectors A, B, and D in Figure 2 are explicitly defined in Rules 13 and 15, respectively. However, Sector C is not precisely defined in Rule 14. In this study, an angular area of 12 degrees was adopted and applied for Rule 14.

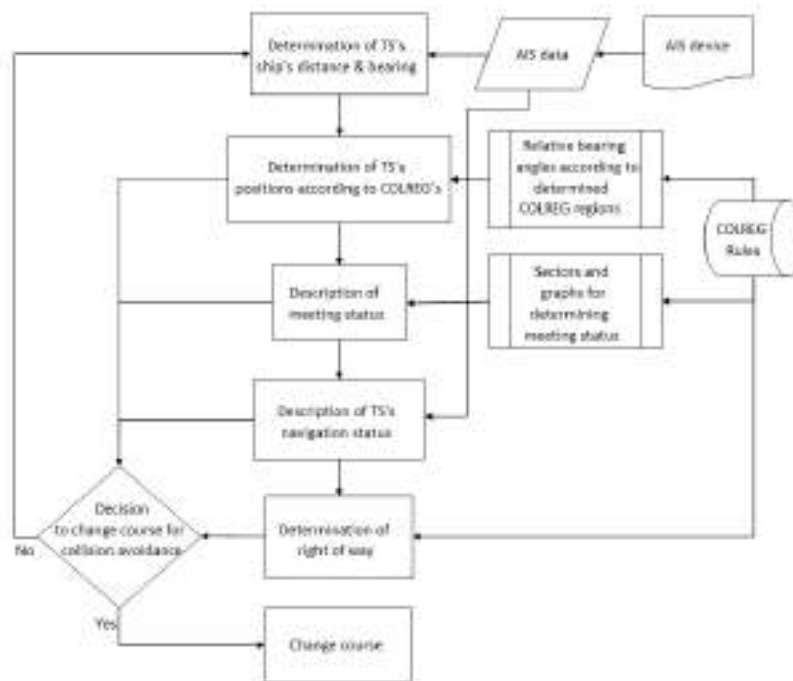


**Figure 1.** Flowchart of the algorithm for quantifying COLREG rules

COLREG: International Regulations for Preventing Collisions at Sea, TS: Target ship, AIS: Automatic Identification System

Sector A is defined in COLREG Rule 13/b as follows: “A vessel shall be deemed to be overtaking when coming up with another vessel from a direction more than 22.5° abaft her beam, that is, in such a position with reference to the vessel she is overtaking, that at night she would be able to see only the sternlight of that vessel but neither of her sidelights”. Sector C is defined in COLREG Rule 14/b as follows: “When a vessel sees the other ahead or nearly ahead and by night, she could see the masthead lights of the other in line or nearly in a line and/or both sidelights and by day she observes the corresponding aspect of the other vessel”. Considering the definitions of Sector A and C, as well as the statement in COLREG Rule 15 regarding the responsibility of the Give-Way (GW) vessel, we can describe Sector B and D as depicted in Figure 2.

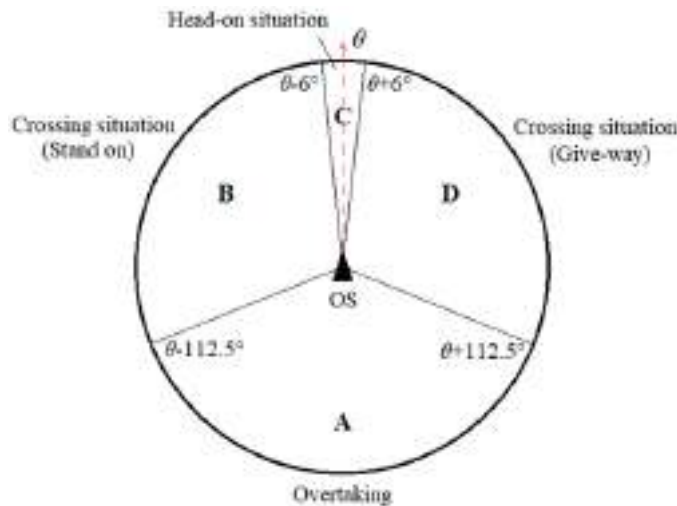


**Figure 2.** Ship encounter situations according to COLREGs

*COLREG: International Regulations for Preventing Collisions at Sea*

Sector A designates the region in which the TS is moving at a higher speed than the OS, signifying an overtaking situation. Sector A covers the relative bearing span ranging from 112.5° to 247.5°, considering the OS’s heading as 000°. This can be mathematically represented as follows (Equation 1):

$$P \text{ Sec}_A = \theta + 112.5^\circ \leq BRG_{TS} \leq \theta - 112.5^\circ \quad (1)$$

In the provided equation, where: P represents the position of the TS, BRG<sub>TS</sub> denotes the true bearing of the TS, θ indicates the course of the OS relative to the ground. Sector B pertains to the situation where the OS is considered the Stand-On (SO) vessel during a crossing situation. Sector B covers the relative bearing range between 247.5° and 354° and can be expressed using the following relationship (Equation 2):

$$P \text{ Sec}_B = \theta - 112.5^\circ < BRG_{TS} < \theta - 6^\circ \quad (2)$$

Sector C denotes the region where the OS and the TS are in a Head-On (HO) situation upon sighting the target ship. Sector C covers the relative bearing range from 354° to 006° [52] and can be represented using the following Equation 3:

$$P \text{ Sec}_C = \theta - 6^\circ \leq BRG_{TS} \leq \theta + 6^\circ \quad (3)$$

Sector D covers the relative bearing region of the OS between 006° and 112.5°. If a collision risk arises, a TS within sector D is considered a SO vessel and should be avoided. The position of the TS within sector D can be described using the following Equation 4:

$$P \text{ Sec}_D = \theta + 6^\circ < BRG_{TS} < \theta + 112.5^\circ \quad (4)$$

### 3.1.3. Determining the type of encounter

The subsequent conditional statements ascertain the type of the encounter situation, whether it corresponds to Rules 13, 14, or 15. These regulations are exclusively relevant when there is an imminent risk of collision. A comparable approach was adopted for identifying encounter types, as employed by [54].

#### Overtaking (Overtaken), Rule 13 (Algorithm Function Rule 13a):

IF  $TS_{\text{posn}} \subset \text{Sec A}$ ,

THEN Execute Function Rule 13a.

In the formula  $TS_{\text{posn}}$  signifies the position of the TS, and Sec A denotes the sector labeled as A in Figure 2.

When the TS is positioned within sector A, it indicates that the TS is moving at a higher speed than the OS. In such a situation, the TS is considered the GW vessel. An interesting aspect of this rule is that it remains applicable irrespective of the ship’s type or the navigational area.

#### Overtaking (Overtaking), Rule 13 (Algorithm Function Rule 13b):

IF  $TS_{\text{posn}} \subset \text{Sec B, C or D}$ ,

THEN Execute Function Rule 13b.

COLREG Rule 13 applies if the TS is in sectors B, C, or D and the OS is faster than the TS. In this case, OS is in the status of a GW vessel. COLREG Rule 13 comes into effect when the TS is located within sectors B, C, or D, while the OS has a higher speed than the TS. In this situation, the OS assumes the role of the GW vessel.

#### HO situation, Rule 14 (Algorithm Function Rule 14):

IF  $TS_{\text{posn}} \subset \text{Sec C}$ ,

AND  $COG_{OS} - COG_{TS} \approx 180^\circ$ ,

THEN Execute Function Rule 14.

If the TS is situated within sector C, COLREG Rule 14 will be applicable when both ships are on reciprocal or nearly reciprocal courses.

**Crossing situation (GW), Rule 15, 16 (Algorithm Function Rule 15a):**

IF  $TS_{Posn} \subset Sec D$ ,  
 THEN Execute Function Rule 15a.

COLREG Rule 15 is applied when the TS is located within sector D. This rule dictates that the OS must take evasive action, while the TS should maintain its course and speed.

**Crossing situation (SO), Rule 15, 17 (Algorithm Function Rule 15b):**

IF  $TS_{Posn} \subset Sec B$ ,  
 THEN Execute Function Rule 15b.

When the TS is situated in sector B and both vessels are power-driven, COLREG Rule 15 comes into effect, designating the OS as the SO vessel. However, if the TS is not a power-driven vessel underway, Rule 18, which addresses responsibilities between vessels, should be applied.

The preceding paragraphs explain the occurrence of encounter situations. The following section provides graphical illustrations that highlight possible situations and their corresponding occurrence times. The identified areas presented here are modeled after the delineations in the work conducted by [55]. The classification process commences by categorizing targets according to the instantaneous heading of the OS and its relative position within the zones identified in Figure 3.

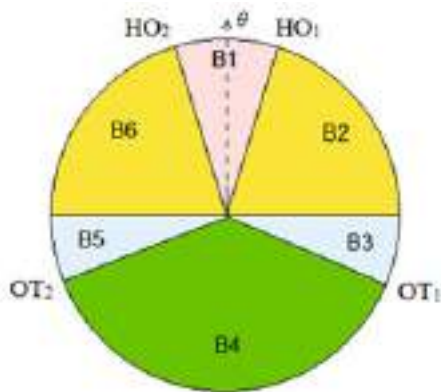


**Figure 3.** Zones used to classify the TS's location where the OS is in the center [55]  
 OT: Overtaking, HO: Head-On, TS: Target ship, OS: Own ship

Zones B1 to B6 are the zones we designate created according to the COLREG Rules, where  $\{HO_1, HO_2, OT_1, OT_2\} = \{\theta+6^\circ, \theta-6^\circ, \theta+112.5^\circ, \theta-112.5^\circ\}$ . The angular expression of the regions according to the heading of the OS: B1 =

$(\theta-6^\circ\_ \theta+6^\circ)$ , B2 =  $(\theta+6^\circ\_ \theta+90^\circ)$ , B3 =  $(\theta+90^\circ\_ \theta+112.5^\circ)$ , B3 =  $(\theta+112.5^\circ\_ \theta-112.5^\circ)$ , B5 =  $(\theta-112.5^\circ\_ \theta-90^\circ)$ , B6 =  $(\theta-90^\circ\_ \theta-6^\circ)$ .

TSs are also classified according to their relative directions determined by the direction of the OS. Figure 4 identifies the categorized regions HGB1 and HGB6, where  $\{HO_1, HO_2, OT_1, OT_2\} = \{\theta+67.5^\circ, \theta-67.5^\circ, \theta+174^\circ, \theta-174^\circ\}$  (HGB: Target Ship Region).

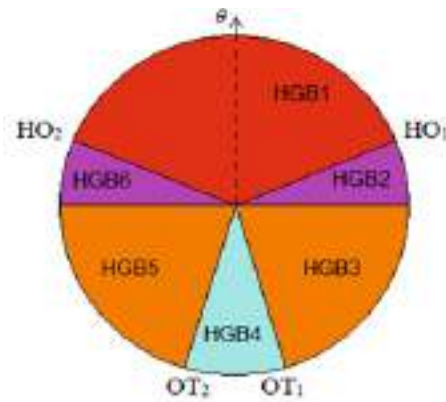


**Figure 4.** Zones used to classify the direction of the TS [55]  
 TS: Target ship, OT: Overtaking

Targets detected within the yellow zone in Figure 3 are assigned abbreviated encounter statuses: Overtaking (OT), Crossing SO, Crossing GW, HO, and Safe (SF). In regions

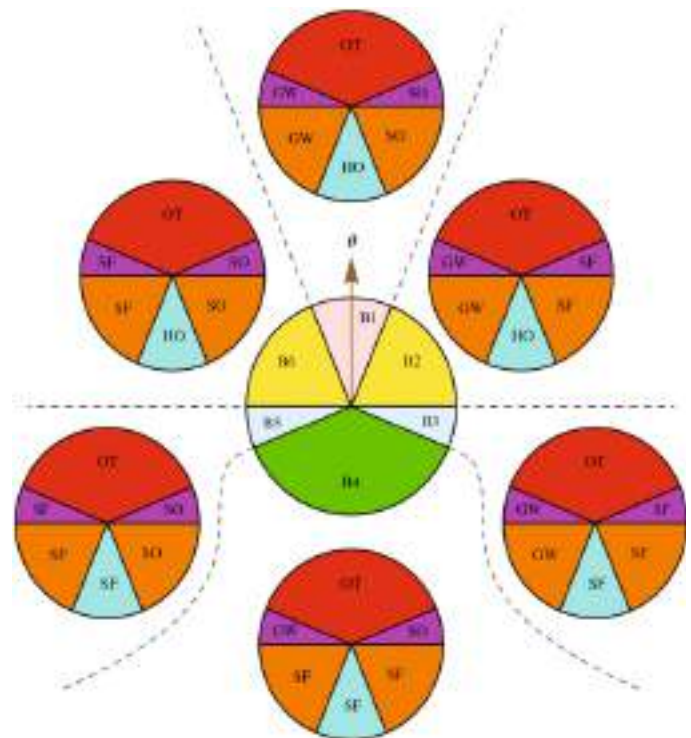


**Figure 5.** Determining the type of encounter [55]  
 OT: Overtaking, GW: Give-Way, HO: Head-On, SF: Safe



designated as SF, the OS is not required to take immediate action. Each target ship is categorized into an encounter type based on its bearing and relative position to the OS. To illustrate, if the TS is situated in zone B2 (as depicted in Figure 5) and its heading falls within zone HGB1, indicating a course between  $292.5^\circ$  and  $67.5^\circ$ , the resultant encounter type would be Overtaking (OT) as per the graph, considering the OS's course of  $000^\circ$ . The depicted encounter situations on the graph are determined by the OS's location.

### 3.1.4. Determination of the navigational status of the target ship

At sea, determining the right of way is not solely governed by COLREG Rules 13, 14, and 15, as the ship's navigational status derived from the AIS plays a crucial role. Navigational status is a piece of information accessible to all nearby ships equipped with AIS. According to COLREGs, AIS provides the navigation statuses for ships:

According to COLREG Rule 18, ships are assigned distinct priorities over other vessels based on their navigational status. This rule supersedes Rules 14 and 15, which are only applicable in situations where there is a potential collision involving power-driven vessels. The ship identification process outlined in this study establishes the respective responsibilities between the ships, as described in the subsequent sections.

### 3.1.5. Determination of the navigational status of the target ship

In accordance with the COLREGs, the SO vessel is required to maintain its current course and speed, while the GW vessel is responsible for executing the necessary evasive maneuver. The obligations of the OS differ across various navigational circumstances. The algorithm produces one of two potential outcomes: the right of way assigned to either the TS or the OS.

In the case of Rule 13 ( $\theta \approx \text{COG}_{\text{TS}}$  and  $\text{SOG}_{\text{OS}} > \text{SOG}_{\text{TS}}$ ), the right-of-way (SO) vessel is the overtaken vessel. If the OS intends to overtake another vessel, it must do so without impeding the course of that vessel and ensuring a safe clearance during the overtaking maneuver.

In the case of Rule 14 ( $\theta - \text{COG}_{\text{TS}} \approx 180^\circ$ ) there is no right of way between vessels. Both vessels are obliged to pass clear from each other.

In the case of Rule 14 ( $\theta - \text{COG}_{\text{TS}} \approx 180^\circ$ ), there is no established right of way between the vessels. Both vessels are obliged to navigate in a manner that ensures they pass clear of each other.

In the case of Rule 15, if the OS detects the TS on its starboard side, the TS has the right of way, meaning the OS is obligated to give way to the TS. Conversely, if the OS detects the TS on

its port side, the right of way belongs to the OS, and the TS is then obligated to give way.

Under Rule 18, when dealing with a power-driven vessel underway, the obligation to give way falls upon that vessel, irrespective of the zone in which the TS is detected. In this case, the right of way is granted to the TS, which is considered a vessel restricted in her ability to maneuver.

### 3.1.6. Determination of the action to be made by the own ship

In this section, we will discuss the movement of the OS based on the data obtained in the previous stages. The areas identified in this study, as illustrated in Figure 6, conform to [17]. According to International Maritime Organization's (IMO) recommendation [42], the yellow, orange, and red areas correspond to "caution", "warning", and "alarm", respectively. The region outside the yellow area is considered the "safe" zone.

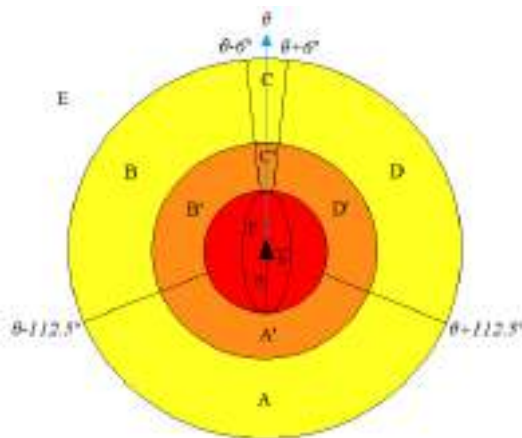


**Figure 6.** Zones determined according to the COLREGs and the action to be taken by the OS

COLREG: International Regulations for Preventing Collisions at Sea, OS: Own ship

Among the regions specified by IMO, the red/alarm area in our study has been designated as a "restricted zone", and the measurement of this area has been determined considering the maneuvering characteristics, including the maximum turning radius of a commercial vessel. It's important to note that merchant ships typically require a turning circle with a maximum diameter of 4.5 times their length when they are navigating at full ahead speed [56].

The orange/warning area has been designated as the "close-quarters situation zone". In navigation practice and theoretical calculations, the term "point of the latest minute action" [17] or "last moment maneuver" [57] typically refers to the distance at which two vessels in a close-quarters situation at sea are positioned, which is usually between two to three nautical miles (NM). This point represents the latest

possible moment at which the vessel responsible for avoiding a collision can initiate a maneuver, taking into account the maneuverability of the vessel. If the maneuver is executed later than this critical point, there is a risk that the vessels may not have enough distance to pass each other safely [58].

In the algorithm developed, since the regions in Figure 6 are calculated separately for each of the two vessels, taking a reference of an average merchant vessel length of 185 m, a warning zone of three NM in total has been established. In addition, the values explained and evidenced by [59] in their study were also taken into account in determining the diameter of the orange zone.

The yellow zone, where the monitoring of surrounding vessels will begin, has been set at three NM or 30 ship lengths, considering an average commercial vessel length, especially in regions with heavy traffic. Since this zone will be created for each vessel, a total warning area of 12 NM will be obtained. This measure is taken to ensure that the computer and algorithm's performance is not significantly affected, particularly in busy traffic areas.

The radius of color-coded circular zones relative to the length of the ship, "L":

The radius of the red ellipse  $\Rightarrow a = \min(4.5L)$  and  $b = 1.5L$ ,

The radius of the orange circle  $\Rightarrow 30L - \min 4.5L$ ,

The radius of the yellow circle  $\Rightarrow 30L - 60L$ .

In maritime collision avoidance, two primary methods are employed: altering course and/or changing speed. This study focuses exclusively on course alterations as the preferred strategy for collision avoidance in open sea, given the impracticality of relying on speed changes.

To assess collision risks, we establish a specific area called the "ship domain", which is determined based on the turning circle's diameter, representing the ship's maneuvering capabilities. The calculation method for determining the ship domain is elaborated in detail in Section Referring to Figure 6, the tracking process begins with targets detected within the yellow zone. When these targets enter the orange zone, the relevant COLREGs come into play to avoid potential collisions. If the OS maintains the SO position and the TS does not yield as they approach the red zone, the OS will initiate the necessary maneuver to prevent a collision, even if it means deviating from strict COLREGs compliance. The goal is to prevent the TS from entering the red zone. The OS executes turns with a rudder angle of  $30^\circ$  to ensure a clear course while adhering to COLREGs Rule 8/b.

Table 4 identified the OS's behavior when detecting TSs within the zones illustrates in Figure 6. According to the rule-based collision avoidance method, the appropriate action is

**Table 4.** The action is to be taken by OS according to the area where the TS was detected

Zone of the TS	Navigation status of TS	Speed of TS as per OS	Course of TS as per OS	Position of TS as per OS	COLREG rule(s) to comply with	Action to be taken by OS
A	Underway	Faster	Parallel	-	Rule 13	Keep speed & course
A'	Underway	Faster	Parallel	Port	Rule 13 + Rule17-a-ii/b	Change course to starboard
A'	Underway	Faster	Parallel	Starboard	Rule 13 + Rule17-a-ii/b	Change course to port
B	Underway	-	Crossing	Port	Rule 15 + Rule17-a-i	Keep speed & course
B	Restricted maneuver	-	Crossing	Port	Rule 16 + Rule 18	Change course to safe side*
B'	Underway	-	Crossing	Port	Rule 15 + Rule17-a-ii/b	Change course to safe side*
C	Underway	-	Reciprocal	-	Rule 14 + Rule 16	Change course to starboard
C	Restricted maneuver	-	Reciprocal	-	Rule 16 + Rule 18	Change course to safe side*
C'	Underway	-	Reciprocal	-	Rule 14	Change course to safe side*
D	Underway	-	Crossing	Starboard	Rule 15 + Rule 16	Change course to safe side* (do not pass ahead)
D'	Underway	-	Crossing	Starboard	Rule 13 + Rule17-a-ii/b	Change course to safe side* (do not pass ahead)
E	-	-	-	-	-	-
E	-	-	-	-	-	Change course to safe side*

\*CRI and ship domain determine the safe side  
CRI: Collision Risk Index, TS: Target ship, OS: Own ship, COLREG: International Regulations for Preventing Collisions at Sea

determined based on the zone where the target is detected and the corresponding action specified in Table 4. For instance, if a target moves from zone A to zone B' in Figure 6, the OS will continue to adhere to the rules applicable in zone A but will not follow the rules for zone B'.

### 3.2. Identifying the Risk of Collision

To facilitate ships' ability to recognize the risk and make appropriate collision avoidance decisions when encountering different collision scenarios, it is essential to assess collision risk. The determination of when and how to execute evasive maneuvers is typically guided by collision risk assessment methods. Despite the presence of these promising methods, classical parameters like DCPA and TCPA continue to serve as industry standards for collision avoidance and decision support systems. The ship domain, which is widely used, is mainly employed in warning-based collision avoidance decision-making applications. On the other hand, CPA-based methods may not always ensure collision avoidance with certainty, but they have their own advantages.

In this study, we aimed to address the limitations of these methods by incorporating CPA and TCPA, along with VCD, as proposed by [60]. Additionally, we introduced the concept of CRI, which takes into account various factors influencing collision risk, such as the distance between ships.

#### 3.2.1. Calculation of the CRI

CRI is among the most commonly employed methods for assessing collision risk in land, marine, and air vehicles [48]. CRI quantifies the probability of collision for each ship in the vicinity with respect to the OS. This calculation takes into account various parameters, including the ship's length, maneuvering characteristics, environmental factors like current and wind, ship domain, safe area diameters, ship speed, VCD between ships, DCPA, and TCPA (Equation 5). An advantage of determining the CRI is that it identifies ships that do not pose a collision risk, even when they are in close proximity to the OS. In such cases, no avoidance maneuver is required, which can result in savings in both fuel and time [61]. What sets CRI apart from other collision risk assessment methods is its ability to provide a quantitative and real-time view of the risk associated with each ship, without necessitating immediate action.

Because the COLREGs are designed for ship-to-ship encounters, calculating the collision risk for multiple ships within a specific sea area or zone, as well as grouping ships together, can create challenges in adhering to COLREG Rules [62]. Therefore, in this study, the CRI is computed individually for each target, and collision avoidance maneuvers are executed based on ship-to-ship encounter situations as defined by the COLREGs.

The significance of the CRI obtained in this study, in accordance with COLREG Rules, aligns with Rule 7/d/i, which addresses the risk of collision. Specifically, it refers to "the risk deemed to exist if the compass bearing of an approaching vessel does not appreciably change" and takes into account the change of bearing between ships. While there are fundamental differences, such as the consideration of VCD and the use of different coefficients depending on encounter situations, the CRI calculation technique outlined in the study by [63] was adopted. However, in contrast to this study, elliptical ship domains were defined instead of the quadrilateral ship domain. The CRI proposed in this study assesses real-time collision risk and is dynamically updated based on changes in the parameters involved in its computation.

$$VCD = |Bearing_{i-1} - Bearing_i| \quad (5)$$

The asymmetric Gaussian function was employed to calculate the collision risk using the following Equation 6:

$$\sigma_a = \frac{r_a}{\log(\frac{1}{r_0}) \times (\frac{1}{r})^2} \quad (6)$$

In the Equation,  $\sigma_a$  is the longitudinal collision risk,  $r_a$  is the long side of the ellipse ship domain,  $r$  is the collision risk coefficient according to the distance between the ships,  $r_0$  is the coefficient of the point where the risk will start to be calculated, and it is accepted as 0.6 in this study. The transverse collision risk is calculated with the asymmetric Gaussian function as follows (Equation 7):

$$\sigma_b = \frac{r_b}{\log(\frac{1}{r_0}) \times (\frac{1}{r})^2} \quad (7)$$

where  $\sigma_b$  is the longitudinal collision risk and  $r_b$  is the short side of the elliptical ship domain.

Transverse and longitudinal collision risks obtained from Equations 6 and 7 are substituted in Equation 8 and collision risk is calculated for a single ship:

$$R = \exp\left(-\left(\frac{x}{\sigma_a}\right)^2 + \left(\frac{y}{\sigma_b}\right)^2\right) \quad (8)$$

Since DCPA and TCPA are important parameters in the determination of collision, the effects of the risks created by these values in the calculation of the collision risk were also calculated with the following Equations 9 and 10:

$$R_{DCPA} = \exp^{-|DCPA|} \quad (9)$$

$$R_{TCPA} = \exp^{\frac{-TCPA}{10}} \quad (10)$$

In this study, the following Equation 11 is proposed as an additional condition to obtain the collision risk value more effectively:

$$\text{If } TCPA < 0 \text{ then } R_{TCPA} = 0 \quad (11)$$

Instead of using a summation of product approach, the preferred method involved multiplying factors, specifically those related to DCPA, TCPA, and degrees of danger as a function of the type of encounter [64]. The CRI value was calculated by applying the CR, RDCPA, RTCPA, and VCD values as follows (Equation 12):

$$CRI = CR \cdot R_{DCPA} \cdot R_{TCPA} \cdot VCD \quad (12)$$

The CRI is calculated for ships when they enter the yellow zone, as depicted in Figure 6. COLREG Rules come into effect to avoid the TSs detected in the orange zone. If the OS is the SO vessel and the TS fails to give way within the orange zone, attempting to enter the red zone while surpassing a CRI threshold of 0.6, the OS must execute the necessary maneuver to avoid collision and strictly prevent the TS from entering the red zone. In this study, the CRI parameter is set to one at the boundary of the ship domain and assigned a smaller value (with a minimum of 0) as the distance from the OS increases. The CRI value range is predetermined, with its maximum value indicating a collision situation. Consequently, the CRI can be easily correlated with the actual probability of collision, facilitating the quantification of collision risk.

The threshold value of 0.6 established for the CRI was determined through the formulation of scenarios involving target vessels across each region corresponding to the columns in Table 4 and within six distinct regions depicted in Figure 5. To assess the robustness of the proposed methodology, scenarios necessitating adherence to multiple COLREG Rules and encounter situations concurrently, including those involving multiple target vessels, were incorporated. Totally 22 analyses/scenario practice performed according to Imazu Problem [65]. The primary objective is to prioritize collision risk and thereby ascertain the collision avoidance risk for each target vessel. Upon comprehensive evaluation of all devised and tested scenarios, it was found that the safer outcomes, which effectively mitigate the overlap of red/alarm zones, were achieved with a CRI coefficient of 0.6.

### 3.2.2. Calculation of ship domain

When determining the elliptical ship domain [66], various criteria were taken into consideration in this study. To determine the long diameter of the ellipse, the “advance” distance, which reflects a ship’s turning maneuver characteristic, was used as a reference. The maximum value recommended by the IMO for ships, which is 4.5 times the ship’s length, was adopted as the long radius of the ellipse. Reference [67] have noted that the distance between ships passing side by side in narrow channels should be at least one ship length to mitigate their adverse hydrodynamic effects. In this study, a short radius of 1.5 times the ship’s length was

chosen for added safety. The radii of the elliptical ship domain are determined using the following Equations 13 and 14:

$$\begin{cases} (SOG_{OS} + SOG_{TS}) \times 28sec & \text{if } (SOG_{OS} + SOG_{TS}) \times 28sec \geq 4.5 L_{OS} \\ 4.5 L_{OS} & \text{otherwise} \end{cases} \quad (13)$$

$$b = 1.5L_{OS} \quad (14)$$

$SOG_{OS}$  represents the speed of the OS,  $SOG_{TS}$  is the speed of the TS, and  $L_{OS}$  is the length of the OS. The reason for choosing 28 seconds in Equation 13 is because it is the average maximum time that merchant ships can perform a

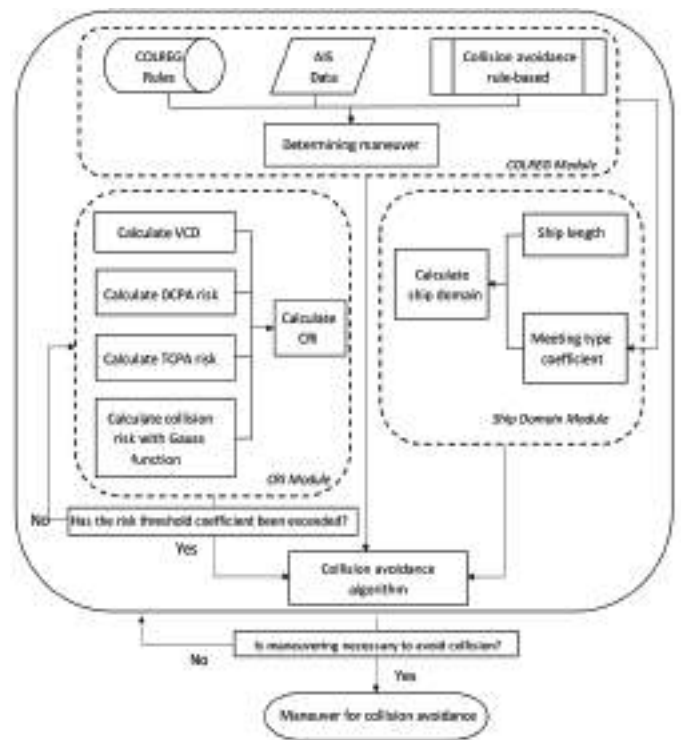


**Figure 7.** Rule-based collision avoidance system flowchart

CRI: Collision Risk Index, COLREG: International Regulations for Preventing Collisions at Sea, AIS: Automatic Identification System, DCPA: Distance of Closest Point of Approach, TCPA: Time of Closest Point of Approach, VCD: Variation of Compass Degree

hard to starboard to port, or vice versa, with a single rudder engine. The flow chart of the proposed rule-based collision avoidance system is shown in Figure 7.

## 4. Case Studies

The MATLAB/Simulink® software was employed to code the equations, data, and calculation process in a structured manner, following the flow diagram depicted in Figure



Figure 8. Legend for the collision avoidance scenarios

8. A simulation study was conducted to demonstrate the execution of COLREG Rules 13, 14, 15, and 18 for accident scenarios, as detailed in the subsequent subsections. The magenta, green, yellow, and light blue colors in the depicted ship routes within the scenarios signify their trajectories leading up to the moment of collision. In the context of the study, it is presumed that other vessels failed to adhere to their responsibilities outlined in the COLREG Rules. Consequently, the own ship avoids the potential collision accident by proactively implementing avoidance measures in adherence to the COLREG Rules. Figure 9 illustrates representative lines and areas delineating the simulated routes of ships, ship domains, as well as monitoring and avoidance zones.

#### 4.1. HO Situation

In event scenario 2, as outlined in Table 3, the OS is the vessel navigating along a magenta-colored course. When the TS enters the orange circle and reaches a CRI of 0.6 or higher (as shown in Figure 9), the OS promptly alters its course following the established rules. To ensure clarity, the course change is executed with a  $30^\circ$  rudder angle, in accordance with Rule 8(b) of the COLREGs. After successfully completing the collision avoidance maneuver and confirming that there is no longer a risk of collision  $CRI < 0.6$  and keep clear of TS  $TCPA < 0$ , the OS resumes its course along the new route leg, determined through dynamic path planning, toward the designated waypoint that should have been reached prior to the avoidance maneuver.

#### 4.2. Overtaking

The rule-based collision avoidance algorithm faced a challenge when identifying land areas in the Webmap function of MATLAB/Simulink<sup>®</sup>. Consequently, in the simulation for Scenario 1 from Table 3, the ship following the magenta course was designated as the OS. As depicted in Figure 10, at the outset of the simulation, the vessel following the green trajectory came under observation due to the ships' current positions. This led to the initiation of a collision avoidance maneuver in accordance with COLREG Rule 13 and the process outlined in Figure 8. The black line represents the new course determined as a result of the dynamic path planning process.

#### 4.3. Crossing Situation

Two distinct simulations have been generated for Rule 15 because the crossing situation rule encompasses two separate scenarios: GW and SO.

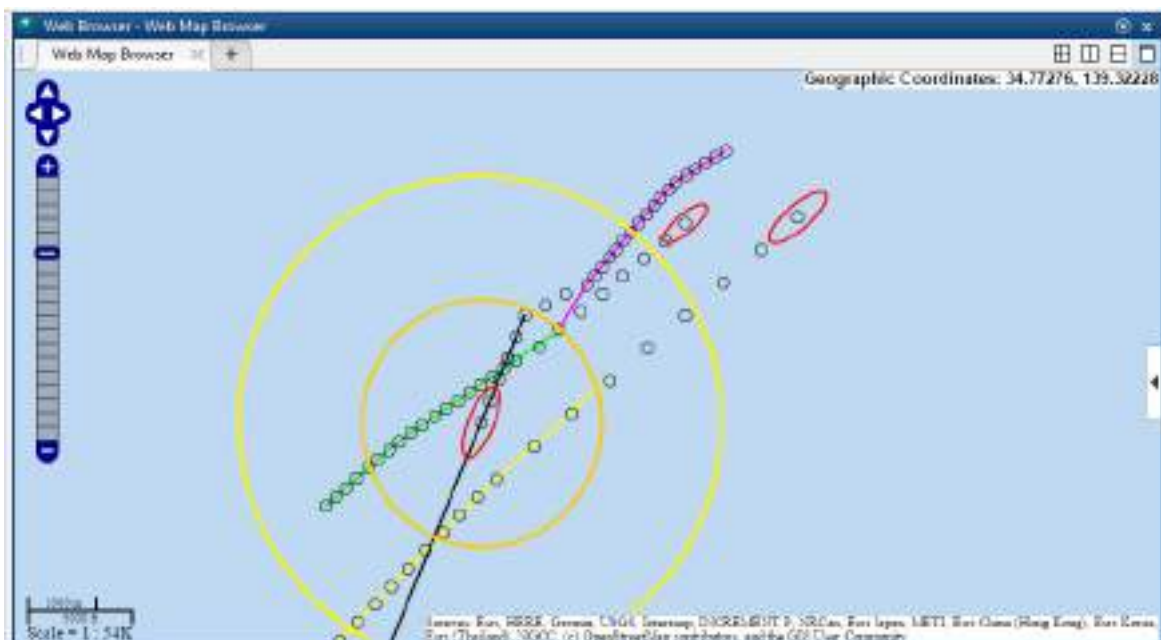


Figure 9. A collision avoidance maneuver with a rule-based method for Head-On situation (Rule 14)

#### 4.3.1. Behavior of the GW vessel

As depicted in Figure 11, the simulation for Scenario 3 in Table 3 involves three distinct ships. The vessel following the magenta-colored route is designated as the OS, while the ships entering the yellow circle are being monitored as TSs.

Figure 11 presents a simulation image depicting the OS taking evasive action when there was a risk of collision with the TS proceeding on the green course and the CRI reached

0.6. To avoid a collision, the OS altered its course to port, ensuring it did not cross in front of the other two vessels. This collision avoidance maneuver involved a rudder angle of  $30^\circ$  in accordance with COLREG Rule 16.

#### 4.3.2. Behavior of the GW vessel

In the simulation generated for Scenario 4 in Table 3, a total of four vessels were involved at the time of the accident. The magenta-colored vessel was designated as the OS. Once the



Figure 10. Collision avoidance maneuver with rule-based method for overtaking (Rule 13)



Figure 11. Rule-based collision avoidance maneuver for a vessel crossing Give-Way (Rule 15)

surrounding vessels entered the yellow circle, they began to be monitored, and their courses were plotted as shown in Figure 12.

In this scenario, a TS specified in COLREG Rules 15 and 17 did not give way when it was supposed to. As soon as it entered the orange circle, its CRI value exceeded 0.6. Consequently, the OS had to change its course to avoid a collision, even though it was the SO vessel. This situation is visualized in Figure 12. After the TS became clear and its CRI value decreased to 0, the OS resumed its original route. The ships following the yellow and blue trajectories did not pose a collision risk to the OS, with CRI values below 0.6, so the OS did not need to change course for these vessels' positions and courses.

#### 4.4. Responsibilities Between Vessels

In the scenario described in Table 3, a magenta-colored vessel was selected as the OS. According to AIS information, the vessel following the green trajectory was identified as a fishing vessel. The rule-based algorithm determined that Rule 18 applied, requiring the OS to maneuver and give way. Figure 13 illustrates that the OS executed a collision avoidance maneuver by altering her course to the port side to avoid crossing the path of the fishing vessel.

#### 5. Results and Discussions

While COLREG Rules are typically designed for single-ship encounters, this study addresses the behavior of OS in multi-ship encounters through the calculated CRI. The



Figure 12. The path followed by own ship for the vessel crossing Stand-On (Rule 15)



Figure 13. Rule-based collision avoidance maneuver for responsibilities between vessels (Rule 18)

TS is identified as the highest collision risk and is the primary focus of avoidance actions. However, real-world efficiency necessitates monitoring and evaluating CRIs continuously, rather than relying solely on route changes. Despite limited rule-based data, the study successfully provides collision-free paths based on the OS's CRI value and computes the dynamic ship domain for both the OS and TS. The rules determine the turning direction for the OS, which, once executed, proceeds along the avoidance course while continually assessing collision risk criteria. The deviation caused by the avoidance maneuver prompts the creation of a new route to reach the next waypoint. These rules encompass the entire process of determining and monitoring collision risk criteria, acting as objective functions to ensure flexibility and guarantee the optimal collision-free path.

While the primary goal of this study is to prevent collisions in open waters, it is worth noting that most of the accident scenarios presented in the research occurred in restricted waters and congested sea lanes. This observation indicates that the algorithm developed in this study has applicability in both open seas and confined waterways (in areas without traffic separation schemes and narrow waterways). The algorithm focuses its monitoring efforts on vessels within the specified COLREGs region, thereby reducing the unnecessary processing of extensive data sets that could otherwise lead to confusion and sluggish computations.

This study has genuine outcomes with the following important aspects:

- a) Unlike similar studies [29,36], Rule 18 under the COLREGs (responsibilities between vessels) has been used in the algorithm set. The following example depicts the importance of Rule 18. A TS that is detected on the port side of the OS and that is at risk of collision must give way to the OS under Rule 15. However, if the navigation status of the vessel is a "fishing vessel", then Rule 18 becomes the rule to follow and the OS is obliged to give way to this TS. That is, the detected ship at the port side being a fishing vessel invalidates Rule 15.
- b) To test the effectiveness of the outcomes of this study, real-world accident events were simulated by creating scenarios with data recorded during these accidents. These accidents were selected to test each of the developed algorithms that coincide with each COLREG Rule considered for maneuvering. Scenarios demonstrated that all four accidents would be prevented.
- c) Demonstrations also prove that the CRIs are monitored after the primary route change actions.
- d) To increase the efficiency, an index different from the existing CRIs [62,63] in the literature was calculated with the help of criteria that are effective in preventing collision

to determine only the targets posing collision risk, not every determined target.

e) Different from the ship domains in the literature [66,68], improved dynamic mutual ship domains have been obtained and applied, taking into account the COLREGs.

f) Risk calculations can be made for all of the many ships in the vicinity and it does not require manual plotting.

## 6. Study Limitations

There are also limitations of the study. The biggest shortcoming of the study is that it can only detect targets with AIS devices. In this conceptual study, the authors acknowledge that AIS alone may not fulfill the "Lookout" requirements. Nevertheless, due to its capability to detect all ships equipped with AIS, the study exclusively employed AIS as the target detection sensor. It cannot interpret when faced with a situation outside the suggested rule base. Such situations often occur in narrow waterways and areas with heavy traffic. However, these regions are not the areas intended for the study. Finally, since the primary purpose of the route changes is to ensure the safe passage of the ships, the route change optimization that will increase the efficiency of the turns is not discussed in the study. An elliptical ship domain was preferred over a quaternion ship domain to improve the algorithm's processing speed, even though the quaternion ship domain provides more accurate results. The last constraint arises from the limitations of the electronic chart function, which does not allow for the detection of land areas and depths, leading to the disregard of this data.

## 7. Conclusion

Maritime operations being human-centric systems, with human error being the dominant factor in maritime accidents despite precautions, highlights the need for fundamental changes in the maritime industry. The introduction of autonomous ships is a key element of this transformation. While autonomous ships involve many systems, collision avoidance stands out as one of the most critical and challenging tasks. To address this, a set of rule-based collision avoidance algorithms, considering relevant COLREG Rules, has been proposed. The scenarios demonstrated in this study have shown the effectiveness of these algorithms in preventing collisions in real-world accident events. The research suggests that the algorithm can also serve as a decision support system for collision avoidance on manned ships. Implementation of this algorithm helps reduce collision risks.

Every ship equipped with an AIS device becomes a data source for maritime authorities, but processing this data is essential as it can be overwhelming. The proposed system not only acts as a collision prevention system but also provides valuable real-time data to shore authorities. Ships equipped



with this system calculate dynamic CRI using collected data, enhancing collision avoidance and safe navigation. This advancement marks a significant step in improving safety and efficiency in maritime transportation.

This study is expected to offer valuable insights and a fresh perspective to researchers, shipyards, classification societies, IMO's navigators and the broader maritime community involved in autonomous ships.

Despite the various limitations, the proposed study has managed to achieve the intended results in terms of collision accidents. This study represents the initial phase of a multi-stage project. As the project progresses, the subsequent phase will incorporate a route optimization feature into the algorithm, utilizing electronic maps that account for bathymetry in relation to static target data. Radar will then complement AIS for both target and environment detection. Furthermore, grounding prevention will be encompassed in the study's scope. In the project's final stage, the accumulation of knowledge will culminate in field tests and research regarding helm commands, conducted with an unmanned surface vehicle. This will bring the project to its ultimate completion, offering comprehensive insights and advancements in the field.

## Footnotes

### Authorship Contributions

Concept design: H. Uğurlu, Data Collection or Processing: H. Uğurlu, and İ. Çiçek, Analysis or Interpretation: H. Uğurlu, Literature Review: H. Uğurlu, Writing, Reviewing and Editing: H. Uğurlu, and O. Djecevic.

**Funding:** The authors did not receive any financial support for the research, authorship and /or publication of this article.

## References

- [1] I. Acejo, H. Sampson, N. Turgo, N. Ellis, and L. Tang, "The causes of maritime accidents in the period 2002-2016". *Cardiff: Seafarers International Research Centre (SIRC)*. Nov 2018.
- [2] European Maritime Safety Agency. Safety analysis of EMCIP data. Analysis of navigation accidents. Summary Report. 2022. Available: [https://safety4sea.com/wp-content/uploads/2022/09/EMSA-EMCIP-Navigation-Accidents-2022\\_09.pdf](https://safety4sea.com/wp-content/uploads/2022/09/EMSA-EMCIP-Navigation-Accidents-2022_09.pdf) [Accessed: Oct. 12, 2024].
- [3] I. C. Ishak, M. F. Azlan, S. B. Ismail, and N. M. Zainee, "A study of human error factors on maritime accident rates in maritime industry". *Asian Academy of Management Journal*, vol. 24(Supp. 2), pp. 17-32, Oct 2019.
- [4] H. Ugurlu, and I. Cicek, "Analysis and assessment of ship collision accidents using fault tree and multiple correspondence analysis". *Ocean Engineering*, vol. 245, 110514, Feb 2022.
- [5] H. Uğurlu, "Application of combined SWOT and AHP (A'WOT): A case study for maritime autonomous surface ships". *Turkish Journal of Maritime and Marine Sciences*, vol. 9, pp. 129-147, Dec 2023.
- [6] F. Ma, Y. W. Chen, Z. C. Huang, X. P. Yan, and J. Wang, "A novel approach of collision assessment for coastal radar surveillance". *Reliability Engineering & System Safety*, vol. 155, pp. 179-195, Nov 2016.
- [7] L. Du, O. A. V. Banda, Y. Huang, F. Goerlandt, P. Kujala, and W. Zhang, "An empirical ship domain based on evasive maneuver and perceived collision risk". *Reliability Engineering & System Safety*, vol. 213, 107752, Sep 2021.
- [8] P. Tang, R. Zhang, D. Liu, Q. Zou, and C. Shi, "Research on near-field obstacle avoidance for unmanned surface vehicle based on heading window". Published in 24th Chinese Control and Decision Conference (CCDC), IEEE, pp. 1262-1267, May 2012.
- [9] H. Niu, Y. Lu, A. Savvaris, and A. Tsourdos, "An energy-efficient path planning algorithm for unmanned surface vehicles". *Ocean Engineering*, vol. 161, pp. 308-321, Aug 2018.
- [10] X. Sun, G. Wang, Y. Fan, D. Mu, and B. Qiu, "A formation autonomous navigation system for unmanned surface vehicles with distributed control strategy". *IEEE Transactions on Intelligent Transportation Systems*, vol. 22, pp. 2834-2845, Mar 2020.
- [11] X. Wang, K. Feng, G. Wang, and Q. Wang, "Local path optimization method for unmanned ship based on particle swarm acceleration calculation and dynamic optimal control". *Applied Ocean Research*, vol. 110, 102588, May 2021.
- [12] T. T. Enevoldsen, and R. Galeazzi, "Grounding-aware RRT\* for path planning and safe navigation of marine crafts in confined waters". *IFAC-PapersOnLine*, vol. 54, pp. 195-201, 2021.
- [13] H. Fukushima, K. Kon, and F. Matsuno, "Model predictive formation control using branch-and-bound compatible with collision avoidance problems". *IEEE Transactions on Robotics*, vol. 29, pp. 1308-1317, May 2013.
- [14] M. Blaich, M. Rosenfelder, M. Schuster, O. Bittel, and J. Reuter, "Extended grid based collision avoidance considering colregs for vessels". *IFAC Proceedings Volumes*, vol. 45, pp. 416-421, Sep 2012.
- [15] L. Song, X. Shi, H. Sun, K. Xu, and L. Huang, "Collision avoidance algorithm for USV based on rolling obstacle classification and fuzzy rules". *Journal of Marine Science and Engineering*, vol. 9, 1321, Nov 2021.
- [16] M. Abdelaal, M. Fränzle, and A. Hahn, "Nonlinear model predictive control for trajectory tracking and collision avoidance of underactuated vessels with disturbances". *Ocean Engineering*, vol. 160, pp. 168-180, Jul 2018.
- [17] S. Li, Z. Zheng, and J. Mi, "The latest minute action of ship". 5th International Conference on Traffic Engineering and Transportation System (ICTETS 2021), SPIE, Dec 2021.
- [18] J. Lisowski, "Game strategies of ship in the collision situations". *TransNav*, vol. 8, pp. 69-77, Mar 2014.
- [19] M. Zyczkowski, and R. Szlapczynski, "Collision risk-informed weather routing for sailboats". *Reliability Engineering & System Safety*, vol. 232, 109015, Apr 2023.
- [20] L. Wang, Z. Zhang, Q. Zhu, and S. Ma, "Ship route planning based on double-cycling genetic algorithm considering ship maneuverability constraint". *IEEE Access*, vol. 8, pp. 190746-190759, Oct 2020.
- [21] Y. Liu, C. Yang, Y. Yang, F. Lin, X. Du, and T. Ito, "Case learning for CBR-based collision avoidance systems". *Applied Intelligence*, vol. 36, pp. 308-319, Mar 2012.

- [22] M. Blaich, S. Weber, J. Reuter, and A. Hahn, "Motion safety for vessels: An approach based on inevitable collision states". Published in 2015 IEEE/RSJ International Conference on Intelligent Robots and Systems (IROS), pp. 1077-1082, Oct 2015.
- [23] N. Åsheim, "Autonomous ship maneuvering with guaranteed safety". NTNU, 2021.
- [24] Y. Yan, X. Zhao, S. Yu, and C. Wang, "Barrier function-based adaptive neural network sliding mode control of autonomous surface vehicles". *Ocean Engineering*, vol. 238, 109684, Oct 2021.
- [25] X. Jin, and M. J. Er, "Dynamic collision avoidance scheme for unmanned surface vehicles under complex shallow sea environments". *Ocean Engineering* vol. 218, 108102, Dec 2020.
- [26] Y. Cho, J. Kim, and J. Kim, "Intent inference of ship collision avoidance behavior under maritime traffic rules". *IEEE Access*, vol. 9, pp. 5598-5608, Jan 2021.
- [27] A. Lazarowska, "Verification of a deterministic ship's safe trajectory planning algorithm from different ships' perspectives and with changing strategies of target ships". *TransNav*, vol. 15, pp. 623-628, Sep 2021.
- [28] N. Khaled and R. Alkhatib, "Novel formulation for line of sight guidance and obstacle avoidance for under-actuated ships". *WSEAS TRANSACTIONS on CIRCUITS and SYSTEMS*, vol. 20, pp. 1-9, Mar 2021.
- [29] K. Woerner, "COLREGS-compliant autonomous collision avoidance using multi-objective optimization with interval programming". *Massachusetts Institute of Technology*, 2014.
- [30] W. Zhang, F. Jiang, C. F. Yang, Z. P. Wang, and T. J. Zhao, "Research on unmanned surface vehicles environment perception based on the fusion of vision and lidar". *IEEE Access*, vol. 9, pp. 63107-63121, Feb 2021.
- [31] R. Hedjar, and M. Bounkhel, "An automatic collision avoidance algorithm for multiple marine surface vehicles". *International Journal of Applied Mathematics and Computer Science*, vol. 29, pp. 759-768, Jul 2019.
- [32] Q. Xu, "Collision avoidance strategy optimization based on danger immune algorithm". *Computers & Industrial Engineering*, vol. 76, pp. 268-279, Oct 2014.
- [33] K. Hirayama, K. Miyake, T. Shiota, and T. Okimoto, "DSSA+: distributed collision avoidance algorithm in an environment where both course and speed changes are allowed". *TransNav*, vol. 13, pp. 117-123, Mar 2019.
- [34] S. Ni, Z. Liu, and Y. Cai, "Ship manoeuvrability-based simulation for ship navigation in collision situations". *Journal of Marine Science and Engineering*, vol. 7, pp. 2-21, Mar 2019.
- [35] R. Guardoño, M. J. López, J. Sánchez, and A. Consegliere, "AutoTuning environment for static obstacle avoidance methods applied to USVs". *Journal of Marine Science and Engineering*, vol. 8, pp. 2-29, Apr 2020.
- [36] Y. Wang, X. Yu, X. Liang, and B. Li, "A COLREGs-based obstacle avoidance approach for unmanned surface vehicles". *Ocean Engineering*, vol. 169, pp. 110-124, Dec 2018.
- [37] L. You, S. Xiao, Q. Peng, C. Claramunt, X. Han, and Z. Guan, "ST-Seq2Seq: A spatio-temporal feature-optimized Seq2Seq model for short-term vessel trajectory prediction". *IEEE Access*, vol. 8, pp. 218565-218574, Dec 2020.
- [38] D. Ma, S. Hao, W. Ma, H. Zheng, and X. Xu, "An optimal control-based path planning method for unmanned surface vehicles in complex environments". *Ocean Engineering*, vol. 245, 110532, Feb 2022.
- [39] X. Xin, K. Liu, Z. Yang, J. Zhang, and X. Wu, "A probabilistic risk approach for the collision detection of multi-ships under spatiotemporal movement uncertainty". *Reliability Engineering & System Safety*, vol. 215, 107772, Nov 2021.
- [40] T. Wang, Q. Wu, J. Zhang, B. Wu, and Y. Wang, "Autonomous decision-making scheme for multi-ship collision avoidance with iterative observation and inference". *Ocean Engineering*, vol. 197, 106873, Feb 2020b.
- [41] Y. Melhaoui, A. Kamil, M. Riouali, K. Mansouri, and M. Rachik, "Optimal control of ship collision avoidance problem". *Journal of Mathematical and Computational Science*, vol. 12, 91, Feb 2022.
- [42] IMO, "Adoption of the revised performance standards for Integrated Navigation Systems (INS)". MSC 252 (83), 2007.
- [43] M. Knébel, "Detecting obstacles from camera image at open sea". Master's thesis, Aalto University, Aug 2020.
- [44] J. Zhang, J. Liu, S. Hirdaris, M. Zhang, and W. Tian, "An interpretable knowledge-based decision support method for ship collision avoidance using AIS data". *Reliability Engineering & System Safety*, 230, 108919, Feb 2023.
- [45] J. Zhou, C. Wang, and A. Zhang, "A COLREGs-based dynamic navigation safety domain for unmanned surface vehicles: A case study of Dolphin-I". *Journal of Marine Science and Engineering*, vol. 8, pp. 1-21, Apr 2020.
- [46] G. West, and N. Swift, "Enhancing ship safety with the navigation and obstacle avoidance sonar". *OCEANS 2017 - Anchorage*, IEEE, 1-6, Sep 2017.
- [47] X. Chen, Y. Liu, and K. Achuthan, "WODIS: water obstacle detection network based on image segmentation for autonomous surface vehicles in maritime environments". *IEEE Transactions on Instrumentation and Measurement*, vol. 70, pp. 1-13, Jun 2021.
- [48] M. Cai, J. Zhang, D. Zhang, X. Yuan, and CG. Soares, "Collision risk analysis on ferry ships in jiangsu section of the Yangtze River based on ais data". *Reliability Engineering & System Safety*, vol. 215, 107901, Nov 2021.
- [49] A. G. Bole, A. Wall, and A. Norris, "Radar and ARPA manual: radar, AIS and target tracking for marine radar users", Butterworth-Heinemann, 2013.
- [50] T. Statheros, G. Howells, and K. M. Maier, "Autonomous ship collision avoidance navigation concepts, technologies and techniques". *Journal of Navigation*, vol. 61, pp. 129-142, Jan 2008.
- [51] M. Li, J. Mou, P. Chen, H. Rong, L. Chen, and P. Van Gelder, "Towards real-time ship collision risk analysis: An improved R-TCR model considering target ship motion uncertainty". *Reliability Engineering & System Safety*, vol. 226, 108650, Oct 2022.
- [52] IMO, "Convention on the International Regulations for Preventing Collisions at Sea (COLREGs)", 1972.
- [53] H. Uğurlu, "Quantification of the head-on situation under Rule 14 of COLREGs with modeling of ships". *Ocean & Coastal Management*, vol. 255, 107261, Sep 2024.
- [54] T. Brcko, "Determining the most immediate danger during a multi-vessel encounter". In Proceedings of the 18th International Conference on Transport Science (ICTS 2018), Portorož, Slovenia. 2018.
- [55] C. Tam, and R. Bucknall, "Collision risk assessment for ships". *Journal of Marine Science and Technology*, vol. 15, pp. 257-270, Apr 2010.

- [56] Standards for Ship Manoeuvrability; International Maritime Organization (IMO); Resolution MSC.137(76)4. Available: [https://wwwcdn.imo.org/localresources/en/KnowledgeCentre/IndexofIMOResolutions/MSCResolutions/MSC.137\(76\).pdf](https://wwwcdn.imo.org/localresources/en/KnowledgeCentre/IndexofIMOResolutions/MSCResolutions/MSC.137(76).pdf)
- [57] J. Koszelew, and P. Wolejsza, "Determination of the last moment manoeuvre for collision avoidance using standards for ships manoeuvrability". *Annual of Navigation*, vol. 24, pp. 301-313, Dec 2017.
- [58] P. Krata and J. Montewka, "Assessment of a critical area for a give-way ship in a collision encounter". *Archives of Transport*, vol. 34, pp. 51-60, Jun 2015.
- [59] W. Dong, P. Zhang, and J. Li, "Safety first - a critical examination of the lights and shapes in COLREGs". *Journal of Marine Science and Engineering*, vol. 11, 1508, Dec 2023.
- [60] A. C. Bukhari, I. Tusseyeva, and Y. G. Kim, "An intelligent real-time multi-vessel collision risk assessment system from VTS view point based on fuzzy inference system". *Expert Systems with Applications*, vol. 40, pp. 1220-1230, Mar 2013.
- [61] K. Zhou, J. Chen, and X. Liu, "Optimal collision-avoidance manoeuvres to minimise bunker consumption under the two-ship crossing situation". *The Journal of Navigation*, vol. 71, pp. 151-168, Oct 2018.
- [62] Z. Liu, Z. Wu, and Z. Zheng, "A novel framework for regional collision risk identification based on AIS data". *Applied Ocean Research*, vol. 89, pp. 261-272, Aug 2019.
- [63] Z. Qiao, Y. Zhang, and S. Wang, "A collision risk identification method for autonomous ships based on field theory". *IEEE Access*, vol. 9, pp. 30539-30550, Feb 2021.
- [64] J. M. Mou, C. Van Der Tak, and H. Ligteringen, "Study on collision avoidance in busy waterways by using AIS data". *Ocean Engineering*, vol. 37, pp. 483-490, Apr 2010.
- [65] H. Imazu, "Research on collision avoidance manoeuvre". Ph.D. thesis, The University of Tokyo, 1987.
- [66] Y. Fujii, and K. Tanaka, "Traffic capacity", *The Journal of Navigation*, vol. 24, pp. 543-552, Oct 1971.
- [67] C. K. Lee, S. B. Moon, and T. G. Jeong, "The investigation of ship maneuvering with hydrodynamic effects between ships in curved narrow channel". *International Journal of Naval Architecture and Ocean Engineering*, vol. 8, pp. 102-109, Jan 2016.
- [68] J. Liu, F. Zhou, Z. Li, M. Wang, and R. W. Liu, "Dynamic ship domain models for capacity analysis of restricted water channels". *The Journal of Navigation*, vol. 69, pp. 481-503, Oct 2015.

# Strategic Ship Fleet Planning for Crude Palm Oil Marine Transportation: A Case Study in Indonesia

© Achmad Riadi, © Muhammad Hanif Fajri Ramadhan

Universitas Indonesia Faculty of Engineering, Department of Mechanical Engineering, Depok, Indonesia

## Abstract

This paper presents the application of strategic ship fleet planning for the maritime transportation of crude palm oil. This study aims to determine the optimal number of chemical tankers required, their capacity (in deadweight tonnage), and the appropriate timing for chartering, buying, or selling vessels within the fleet. To achieve this, mixed integer linear programming is utilized as the optimization framework for strategic ship fleet planning. To ensure a more authentic approach, the investigation utilized a case study focused on the export of Indonesian crude palm oil. The research findings indicate that several export routes cannot be serviced due to higher transportation costs, which could potentially be anticipated through an increase in freight rates. In addition, decisions regarding the quantity and categories of fleets required for each transportation route were also made. The importance of this study is highlighted by its capacity to offer valuable insights to exporters, shipping companies, and the government regarding tanker fleet deployment, management, and regulatory considerations. Furthermore, these findings provide a clearer understanding of the necessity of a tanker fleet for transporting crude palm oil. This supports the Indonesian government's "beyond cabotage" policy, which mandates the use of vessels operated by national shipping companies for crude palm oil exports, making it a relevant case study for examining the effectiveness of such measures.

**Keywords:** Strategic ship fleet planning, Crude palm oil, Beyond cabotage policy, Mixed integer linear programming, Optimization, Marine transportation

## 1. Introduction

The expansion of palm oil plantations in regions like Southeast Asia has significantly contributed to the increase in its global trade volume, although it raises concerns regarding deforestation and biodiversity loss [1]. Additionally, the growing utilization of crude palm oil (CPO) in biofuel production, driven by policies promoting renewable energy sources, has propelled its international trade, highlighting its significance in the context of energy sustainability. As a result, the intricate interplay between economic, environmental, and social factors underscores the complex dynamics influencing the escalating trade of CPO the global stage.

In the context of global CPO trade via marine transportation, the size of ships plays a pivotal role in the strategic decisions of shipping companies operating as ship operators. The

choice between purchasing or chartering vessels involves meticulous consideration of cargo volume, transportation efficiency, and operational costs. Optimal ship size selection influences economies of scale, impacting loading capacities and voyage expenses, thereby allowing shipping companies to effectively meet market demands while maximizing profitability in the competitive landscape of CPO transportation.

Meeting fleet requirements requires strategic fleet planning, which involves activities like acquiring new vessels or chartering existing ones. In addition, addressing the specific characteristics of the CPO export shipping markets is crucial given their competitive and highly volatile nature. Therefore, planning should include both the timing for expanding the fleet capacity and the appropriate moments for reducing it, which can be accomplished by selling or scrapping



**Address for Correspondence:** Achmad Riadi, Universitas Indonesia Faculty of Engineering, Department of Mechanical Engineering, Depok, Indonesia  
**E-mail:** achmadriadi@ui.ac.id  
**ORCID iD:** orcid.org/0000-0002-1697-2299

**Received:** 08.08.2024

**Last Revision Received:** 22.10.2024

**Accepted:** 19.11.2024

**To cite this article:** A. Riadi, and M. H. F. Ramadhan, "Strategic Ship Fleet Planning for Crude Palm Oil Marine Transportation: A Case Study in Indonesia." *Journal of ETA Maritime Science*, vol. 12(4), pp. 395-403, 2024.



Copyright© 2024 the Author. Published by Galenos Publishing House on behalf of UCTEA Chamber of Marine Engineers. This is an open access article under the Creative Commons AttributionNonCommercial 4.0 International (CC BY-NC 4.0) License

ships. Hence, the optimization of fleet planning is crucial for determining the appropriate timing for the chartering, purchasing, or selling of vessels within the fleet. Ship fleet planning in maritime transportation can be categorized based on its planning level into three main stages: strategic, tactical, and operational fleet planning [2]. Strategic fleet planning primarily focuses on critical decisions related to ship acquisition, sales, chartering, and scrapping [3]. Numerous research papers have explored strategic fleet planning in liner shipping [4-13], and tramp shipping contexts [3,14-17]. One study concentrated on strategic maritime fleet planning, incorporating the potential for retrofitting and uncertainties related to future fuel and carbon prices [18].

Strategic ship fleet planning using Mixed-Integer Linear Programming (MILP) optimization is a critical approach in the shipping industry, addressing various operational challenges, such as fleet deployment, scheduling, and cost management. This method allows for the simultaneous consideration of multiple objectives, including economic efficiency and environmental impact, thereby enhancing decision-making processes in fleet management. MILP models can optimize service schedules, vessel speeds, and cargo allocation while balancing costs and emissions. For instance, a model that integrates CO<sub>2</sub> emissions and operational costs demonstrates the trade-offs between economic and environmental objectives [19]. A previous study developed a MILP formulation for shuttle tankers that incorporates variable travel times to improve scheduling efficiency under logistical constraints [20]. Another study proposed a model that considers multimode investments for fleet capacity expansion to address market fluctuations and operational needs [21].

This section presents the development of a strategic ship fleet planning model tailored specifically for CPO transportation. The MILP optimization model is designed to maximize the overall profit and to offer recommendations regarding the ideal timing for chartering, buying, or selling vessels in the fleet. To be more realistic, the research was carried out using a case study of Indonesian CPO exports.

The present study differs from previous studies on strategic fleet planning of tankers [3]. The previous study primarily focused on contract analysis for tanker shipping, where strategic fleet planning was based on the existence of freight contracts in tramp shipping, such as spot charter, Contract of Affreightment, and time charter [22]. Consequently, the objective function of the optimization model is to maximize profit by determining which transportation contracts to serve. In contrast, the present study focuses on strategic fleet planning to meet the optimal fleet requirements for transporting CPOs, specifically using Indonesia as a case study. The proposed approach provides a comparative

analysis between existing and optimal fleet requirements. Unlike previous studies, the present study considers the transportation demand to be fully met without regard to the form of transportation contracts. This study provides novel insights into strategic ship fleet planning by emphasizing the practical implications of MILP for both the government and shipping companies. By providing recommendations based on robust analytical models, this study aims to address specific fleet needs for exporting cargo, particularly Indonesian CPO cargo. Furthermore, the outcomes of this study align with government policies, especially beyond cabotage policy. This policy enhances the competitiveness of national shipping companies by allowing them to operate in international markets. By understanding and optimizing fleet requirements, policymakers can facilitate trade and improve the competitive position of local shipping companies in the global market. The recommendations derived from this study will not only support the implementation of the policy but also enhance the overall economic performance of the maritime sector.

The remainder of this study is organized as follows. Section 2 outlines the materials and methods, Section 3 discusses the results and analysis, and Section 4 provides the conclusions.

## 2. Materials and Methods

### 2.1. Study Area

The CPO is a key export commodity for Indonesia. It is exported to various countries, including India and several European Union nations, while the remainder is sold domestically. Hence, it was selected as our study case. Statistics on Indonesia's CPO exports reveal a consistent upward trend from 2016 to 2019, with annual growth rates ranging from 12.03% to 19.44% [23]. Given the growing global demand for CPO, Indonesia's CPO export volume is expected to continue to rise [24].

With the increasing volume of CPO exports, the Indonesian government took steps to establish a national maritime transportation policy. This policy was introduced through a series of Minister of Trade Regulations, including Number 82 of 2017, Number 80 of 2018, Number 40 of 2020, and Number 65 of 2020 [25-28]. Among these regulations, one significant policy stipulates that exporters are obligated to utilize vessels under the control of national shipping companies when exporting certain commodities, including CPOs. The rationale behind implementing this policy is rooted in various factors, such as challenging global economic conditions and Indonesia's trade deficit in the services sector [29]. This policy is commonly called the "beyond cabotage policy", and it has been in effect since July 2020 [30].

Currently, the fleet of chemical tankers registered under the Indonesian flag and operated by national shipping companies

primarily serves the transportation of CPO between domestic ports for domestic transportation needs. In contrast, foreign shipping companies appointed by CPO importers largely handle the transportation of CPO for export purposes. The trade of CPO exports from Indonesia generally uses International Commercial Terms (INCOTERMS) of the Free on Board (FOB) terms, with the Cost Insurance and Freight (CIF) terms being very rarely used [31].

The Beyond Cabotage policy implemented by the Indonesian government aligns with the government's desire to propose a shift in international shipping INCOTERMS, specifically for CPO, from FOB to CIF. Implementing the beyond cabotage policy for CPO exports presents considerable challenges if not supported by an adequate fleet of chemical tankers. According to the Indonesian Ministry of Transportation, only 65 Indonesian-flagged chemical tankers suitable for transporting CPO is only 65 units, representing a mere 3.4% of the total tanker fleet [32]. Figure 1 shows the descriptive statistics (box-plot) of the fleet of chemical tankers transporting CPO. It can be seen that the average gross tonnage (GT) was 3,600 GT, and the average Length Overall (LOA) of the fleet was 94 meters. Only a few chemical tankers have a capacity above 10,000 GT and a length above 120 meters.

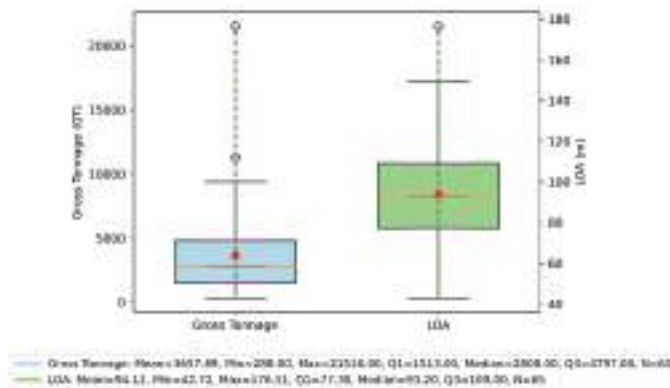


**Figure 1.** Descriptive statistics (box-plot) of the fleet of chemical tankers transporting CPO

CPO: Crude Palm Oil, LOA: Length Overall

## 2.2. Research Framework

In this study, a strategic ship fleet planning model was developed to determine the optimal number of chemical tankers required, their capacities, and the suitable timing for chartering, purchasing, and selling the fleet for transporting Indonesian CPO exports. Figure 2 depicts a schematic representation of the research framework.

This study began with data collection, including demand data for Indonesia's CPO export, chemical tanker fleet, and shipping cost data. Each dataset was then used for statistical

analysis and clustering models to determine alternative chemical tankers to be considered in fleet planning. Subsequently, an optimization process was conducted using MILP to generate objectives in the form of the optimal number of chemical tankers required, their capacities, and the suitable timing for chartering, purchasing, and selling the fleet. In the optimization process conducted using MILP, there are several optimization conditions grouped as objective functions, decision variables, and constraints, as can be seen in Table 1.

## 2.3. Model Assumptions

The developed strategic ship fleet planning model considers CPO export demands from Indonesia to various export destinations over multiple years. This approach addresses challenges in determining the number of ships to operate, when acquiring or chartering vessels, and optimizing ship capacity.

To address this challenge, optimization-based fleet planning aims to maximize profits by considering the revenue generated from freight costs charged to shippers and shipping costs based on the export destination and the used fleet.

Several model assumptions are made, including those pertaining to CPO export destination routes. Specifically, the model considers the five largest CPO export destinations: India, China, Pakistan, the Netherlands, and the United States. Data on CPO export demand in these countries were obtained from the microdata service of the Indonesian Central Bureau of Statistics [33]. Using the obtained data, CPO export demand forecasting was conducted for the 10-year fleet planning period (2023 to 2032). The forecasting model used is exponential smoothing forecasting based on the Additive Error, Additive Trend, and Additive Seasonality for Exponential Triple Smoothing algorithm. This algorithm mitigates minor fluctuations in historical data trends by identifying seasonal patterns and establishing confidence intervals [34].

To determine the optimal vessel capacity, a vessel alternative approach is employed, which is obtained by applying the K-Means clustering algorithm. Over 100 Indonesian and foreign-flagged chemical tankers are used for both domestic and international CPO shipments [32]. Ship data, including GT, LOA, and service speed ( $V_s$ ), are used as attributes in the clustering method. The clustering results yield 6 clusters, each represented by the vessel closest to the cluster centroid. The clustering results are visualized in Figure 3, and vessel alternatives are derived from the vessels representing each cluster, as shown in Table 2. The table also presents several variables, such as dead weight tonnage (DWT), Draft, Main Engine (M/E) capacity, and Auxiliary Engine (A/E) capacity. These variables are used to calculate the cost of operating each vessel.

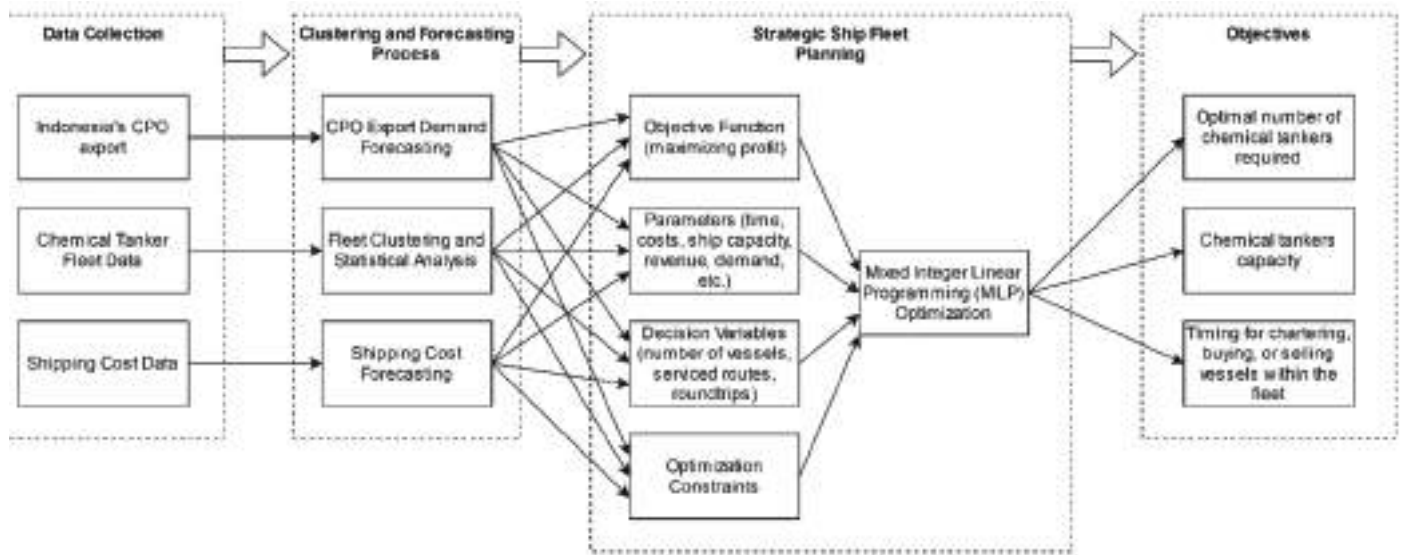


Figure 2. Research framework

CPO: Crude Palm Oil

Table 1. Optimization conditions

Objective Function	Decision Variables	Constraints
Maximizing profit to serve the export transportation of CPOs from Indonesia to several export destination countries.	<ul style="list-style-type: none"> <li>The number and capacity of vessels chartered.</li> <li>Number and capacity of owned vessels, including newly built and secondary acquired vessels.                             <ul style="list-style-type: none"> <li>Number of round trips.</li> <li>Serviced and non-serviced routes.</li> </ul> </li> </ul>	<ul style="list-style-type: none"> <li>Vessels must have sufficient capacity to meet the CPO requirements for serviced routes.</li> <li>The total time spent on all round trips for each vessel type does not exceed the available time.</li> </ul>

CPO: Crude Palm Oil

Table 2. Alternative chemical tankers to be considered in fleet planning

Cluster	Vessel alternatives	DWT (ton)	Gross tonnage (GT)	LOA (m)	Vs (knots)	Draft (m)	M/E (kW)	A/E (kW)
0	v1	9,045	5,256	110	10	7.5	2,720	1,341
1	v2	49,539	29,965	183	12	12.5	12,750	3,600
2	v3	12,975	8,448	127	12	8.7	4,440	1,680
3	v4	25,086	16,202	160	14	10.5	5,200	1,800
4	v5	19,992	11,925	146	12	9.5	6,150	1,649
5	v6	3,974	2,432	85	5	4.1	462	240

Before presenting the optimization model’s formulation, the notations are defined in Tables 3-5.

2.4. Model Formulations

Equation 1 defines the objective function, which maximizes profit. The initial component assesses the revenue generated from servicing existing CPO export routes from Indonesia to various destinations or evaluates the feasibility of servicing these routes. The second component calculates the revenue

obtained from chartering and selling vessels, considering the number of vessels and transaction values. The third component determines the costs associated with chartering and acquiring new vessels. The fourth component estimates the expenses related to new vessel purchases. The fifth component addresses the costs incurred during voyages. The sixth component includes both the operational and capital expenses associated with owned vessels.

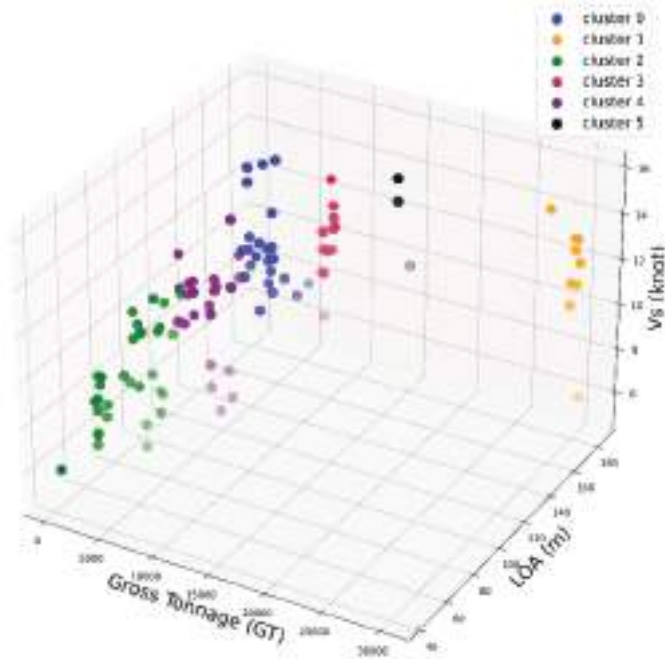


Figure 3. Visualization of chemical tanker clustering results

$$\begin{aligned}
 \sum_{v \in V} N_{v,0}^{OWN} &= \sum_{v \in V} N_{v,t-1}^{OWN} + \sum_{v \in V} N_{v,t}^{BY} - \sum_{v \in V} N_{v,t}^{SL} + \sum_{v \in V} N_{v,t}^{NW} \\
 &- \sum_{v \in V} N_{v,t}^{CIN} - \sum_{v \in V} N_{v,t}^{COUT} \quad \forall v \in V, t \in T \quad (1)
 \end{aligned}$$

Equation 2 maintains the total count of owned vessels, and Equation 3 guarantees the total count of controlled and operated vessels. Equation 4 specifies that only owned vessels can be chartered. Equations 5 and 6 define the initial fleet, and Equation 7 restricts the acquisition of newly built vessels in the early stages due to delivery time requirements.

$$N_{v,t}^{OWN} = N_{v,t-1}^{OWN} + N_{v,t}^{BY} - N_{v,t}^{SL} + N_{v,t}^{NW} \quad \forall v \in V, t \in T \quad (2)$$

$$N_{v,t}^{TOT} = N_{v,t}^{OWN} + N_{v,t}^{CIN} - N_{v,t}^{COUT} \quad \forall v \in V, t \in T \quad (3)$$

$$N_{v,t}^{OWN} \geq N_{v,t}^{COUT} \quad \forall v \in V, t \in T \quad (4)$$

$$N_{v,0}^{OWN} = F_v^0 \quad \forall v \in V \quad (5)$$

$$N_{v,0}^{TOT} = N_{v,0}^{OWN} + N_{v,0}^{CIN} - N_{v,0}^{COUT} \quad \forall v \in V \quad (6)$$

$$N_{v,1}^{NW} = 0 \quad \forall v \in V \quad (7)$$

Equations 8 and 9 represent CPO demand and fleet capacity constraints. Equation 8 guarantees that the fleet has sufficient capacity to meet the CPO demands for the serviced routes, while Equation 9 ensures that the total time spent on all round trips for each vessel type on a route does not exceed the available time.

$$\sum_{v \in V} P_v A_{vr} y_{vrt} \geq D_{rt} \alpha_r \quad \forall t \in T, r \in R \quad (8)$$

$$T_{vt}^{TOT} N_{vt}^{TOT} \geq \sum_{r \in R} T_{vr} y_{vrt} \quad \forall v \in V, t \in T \quad (9)$$

Equations 10-12 define the characteristics of variables such as Boolean and integer.

$$\alpha_r \in \{0,1\} \quad \forall r \in R \quad (10)$$

$$N_{vt}^{TOT}, N_{vt}^{OWN}, N_{vt}^{CIN}, N_{vt}^{COUT}, N_{vt}^{BY}, N_{vt}^{NW}, N_{vt}^{SL} \geq 0 \text{ and integer } \forall v \in V, t \in T \quad (11)$$

$$y_{vrt} \geq 0 \text{ and integer } \forall v \in V, r \in R, t \in T \quad (12)$$

### 3. Results

The MILP optimization model was solved using the MILP solver available in Matrix Laboratory (MATLAB) software [38]. Table 6 presents the results of the decision variable  $\alpha_r$ , where 1 indicates that route  $r$  is serviced, and 0 indicates otherwise. It is noteworthy that CPO export routes to India and Pakistan are not currently serviced. Optimization models aim to maximize profits by finding optimal solutions. Thus, these two routes have higher shipping costs than the revenue generated by them.

Table 3. Sets and indices

Set	Index	Description
$T$	$t$	The time periods are denoted as $T = \{0,1,2,3, \dots, T_{max}\}$ , where period 0 represents the initial planning phase, and $T_{max}$ indicates the maximum time period considered.
$R$	$r$	Available CPO export routes from Indonesia to other countries
$V$	$v$	Available vessel types



Table 4. Parameters

Parameter	Description	Unit	Data collection
$T_{vr}$	The total duration of a roundtrip of vessel type $v$ on route $r$ , encompassing both the time spent at sea and the time spent in port.	Days	[35]
$T_{vt}^{TOT}$	Total time available for vessel type $v$ during the period $t$	Days	Depends on the vessel docking time (14 to 30 days)
$D_{rt}$	Demand for CPO on route $r$ during the period $t$	Ton	[33]
$P_v$	The cargo capacity (Payload) of the vessel $v$	Ton	90% of the DWT
$A_{vr}$	This binary parameter is set to 1 if assigning vessel type $v$ on route $r$ is feasible. Draft-related constraints typically define this parameter.	-	Port bathymetry along each route
$F_v^0$	Quantity of vessels of type $v$ that are owned during the planning period	Ship	set to 0, implying that no vessel was owned during the planning period.
$R_r^{SV}$	Revenue from the servicing route $r$	USD	Based on forecasted CPO export demand and calculated freight rate for each route
$R_{vt}^{SL}$	Revenue generated from sale of vessel type $v$ during the period $t$	USD	Based on depreciation calculation (5% per year)
$R_{vt}^{TC}$	The revenue generated from time chartering vessel type $v$ during the period $t$	USD	Based on the time charter rate [36]
$C_{vr}^{VY}$	The cost of a round trip for sailing route $r$ with vessel type $v$	USD	Based on port and fuel consumption cost
$C_{vt}^{BY}$	The expenditure for acquiring vessel type $v$ during the period $t$	USD	Based on depreciation calculation (5% per year)
$C_{vt}^{NW}$	The expense associated with acquiring a new vessel of type $v$ during the period $t$	USD	Tanker new building price (BIMCO)
$C_{vt}^{TC}$	The expenses associated with chartering a vessel of type $v$ during the period $t$	USD	Based on the time charter rate [36]
$C_{vt}^{OP}$	Operational costs of vessel type $v$ during the period $t$	USD	Based on vessel operating expenses per DWT [37]
$C_{vt}^{CP}$	Capital expenditures for vessel type $v$ during the period $t$	USD	80% of the acquisition price with an interest rate of 4% per year [3]

Table 5. Decision variables

Decision variable	Description	Unit
$N_{vt}^{TOT}$	Total number of vessels type $v$ utilized during the period $t$	Ship
$N_{vt}^{OWN}$	Number of vessels of type $v$ owned during the period $t$	Ship
$N_{vt}^{TCin}$	Number of vessels of type $v$ that are on time charter (charter in) during the period $t$	Ship
$N_{vt}^{TCout}$	Number of vessels of type $v$ that are under time charter (charter out) during the period $t$	Ship
$N_{vt}^{BY}$	Number of vessels of type $v$ obtained during the period $t$	Ship
$N_{vt}^{NW}$	Number of newly ordered buildings of type $v$ vessels during the period $t$	Ship
$N_{vt}^{SL}$	Number of vessels of type $v$ sold during the period $t$	Ship
$\alpha_r$	A binary variable that takes the value of 1 if route $r$ is serviced and 0 if it is not	-
$y_{vrt}$	Total number of roundtrip completed by vessel type $v$ on route $r$ during the period $t$	Roundtrip

In cases where an unserved export route exists, a specific increase in the freight rate on that route is required to boost revenue. This is done, of course, to ensure that the route can still be serviced while generating income for the shipping business. The question is, to what extent should the freight rate increase be applied to that route? This requires further

analysis, including the use of methods such as sensitivity analysis.

As mentioned before, the Indonesian government, through the Ministry of Trade, is proposing a shift in international shipping incomers, specifically for CPOs, from FOB to

CIF [31]. This policy change also drives the emergence of a beyond cabotage policy as a subsequent measure. The policy does not restrict CPO exports to specific countries; rather, it creates opportunities for shipping and transportation companies to actively participate in the CPO export business. Thus, although this research indicates the existence of underserved CPO export routes, it does not imply that these routes cannot be served. Shipping companies can cater to these routes, albeit with the requirement for a minimum increase in freight costs to achieve a balance between revenue and operational expenses.

The results generated from this research are displayed in Table 7. The table displays the fleet planning results during the planned period. This includes the total number

**Table 6.** Decision variable  $\alpha_r$

$r1$ India	$r2$ China	$r3$ Pakistan	$r4$ Dutch	$r5$ US
0	1	0	1	1

of operated vessels, the number of owned, acquired, newly built, and chartered-in/out vessels, and the number of sold vessels. In the early stages of the planning period, the fleet is prepared by chartering-in, followed by acquisition of the fleet without any new builds until the end of the planning period. Some of the acquired vessels were chartered out during this period. This demonstrates that, in addition to the CPO freight market, the charter market also offers promising revenue opportunities. Furthermore, there were several sales of owned vessels during the planning period.

Table 8 presents the number of vessels operated for each vessel alternative (fleet size and mix). Alternative vessel number 4 (v4), with a capacity of approximately 16,000 GT, emerges as the preferred option. Although the principle of economies of scale indicates that larger vessels offer better benefits, it does not imply that vessels with large capacities can be used indiscriminately. Draft limitations for vessels entering certain ports are significant factors in this decision. Vessel number 4 did not have the largest capacity but was the second-largest among the alternatives considered in

**Table 7.** Result of fleet planning (number of vessels)

Planning period	Operated	Owned	Acquired	New built	Charter in	Charter out	Sold
1	33	0	0	0	33	0	0
2	34	59	59	0	0	25	0
3	39	64	5	0	0	25	0
4	38	68	6	0	0	30	2
5	56	86	18	0	0	30	0
6	55	85	0	0	0	30	1
7	51	81	1	0	0	30	5
8	52	82	6	0	0	30	5
9	45	75	0	0	0	30	7
10	53	45	0	0	8	0	30

**Table 8.** Number of vessels operated for each vessel alternative

Period	Number of operated vessels					
	v1	v2	v3	v4	v5	v6
1	0	0	0	33	0	0
2	0	0	0	34	0	0
3	0	0	0	39	0	0
4	0	0	0	37	0	1
5	0	0	0	41	0	15
6	0	0	0	40	0	15
7	0	0	0	41	0	10
8	0	0	0	47	0	5
9	0	0	0	45	0	0
10	0	0	0	51	0	2

Table 2. This indicates that the maximum draft limitation, represented by the  $A_{vr}$  parameter in the optimization model, is appropriate. Therefore, the obtained results can be deemed feasible.

Based on the data presented in Figure 1, the existing chemical tanker fleet has an average capacity of approximately 3,600 GT, comprising 65 vessels. Meanwhile, the optimization results (Table 8) indicate a trend toward an increasing fleet size of type v4 vessels, with the overall fleet size steadily growing. The vessel type, v4, has a capacity of approximately 16,000 GT, as indicated in Table 2. This indicates a potential gap between the fleet requirements based on the optimization results and the actual conditions of the existing fleet. The composition of this fleet provides insights for shipping companies in executing CPO transportation, particularly for exports. Moreover, it serves as a focal point for the government to assess and evaluate the fleet support provided by national shipping companies in implementing beyond cabotage policy. This research, at the very least, can provide a solution to the tendency of mutual waiting between shipping companies and the government. Shipping companies await the development of the CPO shipping industry, while the government continues to wait for shipping companies to increase their fleet size to support the export of Indonesian CPO. Therefore, this research provides an overview of solutions for shipping companies to decide on acquiring fleets to support the implementation of the beyond cabotage policy advocated by the government.

#### 4. Conclusion

This study developed a strategic ship fleet planning model tailored for Indonesian CPO exports to determine the optimal number of chemical tankers required, their capacities, and the appropriate timing for chartering, purchasing, or selling vessels. The model, which is structured as MILP optimization, was designed to maximize profits while ensuring the fleet's capacity meets the CPO export demands.

The analysis revealed a significant gap between the current capabilities of the existing tanker fleet and the requirements identified by the optimization results. The existing fleet had a relatively low average capacity, which was insufficient to meet the optimal fleet needs for CPO transportation. In contrast, the optimization results indicate a clear trend toward increasing the fleet size, particularly for a specific vessel type with a much larger capacity. This disparity highlights the necessity for fleet expansion to align with the growing demand for CPO exports, emphasizing the potential for enhanced operational efficiency and profitability through strategic investments in larger, more capable vessels.

Upon careful examination of the fleet planning results outlined earlier, it is possible to derive significant

conclusions pertaining to the indispensable fleet requisites essential for bolstering Indonesian CPO export endeavors and effectively addressing the intricacies posed by “the beyond cabotage policy”. The essence of this research lies in its comprehensive exploration of strategic fleet planning concerns, encompassing not only the intricacies of ascertaining the precise number of vessels for operation but also the intricacies of determining the opportune moments for vessel acquisition or charter. Additionally, a crucial facet of this investigation involves the meticulous determination of the optimal ship capacity to ensure optimal operational efficiency. However, it is imperative to underscore the necessity for further in-depth analysis, with a particular focus on scrutinizing the dynamics of shifts in CPO demand, fluctuations in shipping costs, and the nuanced considerations surrounding ship charter expenses.

#### Footnotes

##### Authorship Contributions

Concept design: A. Riadi, Data Collection or Processing: A. Riadi, Analysis or Interpretation: A. Riadi, Literature Review: M. H. F. Ramadhan, Writing, Reviewing and Editing: A. Riadi, and M. H. F. Ramadhan.

**Funding:** This work is supported by “Hibah Publikasi Terindeks Internasional (PUTI) Q3 2020” funded by DRPM Universitas Indonesia no.: NKB-4577/UN2.RST/HKP.05.00/2020.

#### References

- [1] L. P. Koh, and D. S. Wilcove, “Is oil palm agriculture really destroying tropical biodiversity?”. *Conservation Letters*, vol. 1, pp. 60-64, Jun 2008.
- [2] M. Christiansen, K. Fagerholt, B. Nygreen, and D. Ronen, “Chapter 4 maritime transportation”. *Handbooks in Operations Research and Management Science*, vol. 14, pp. 189-284, 2007.
- [3] J. Laake, and A. Zhang, “Joint optimization of strategic fleet planning and contract analysis in tramp shipping”. *Applied Economics*, vol. 48, pp. 203-211, Jan 2016.
- [4] A. N. Perakis, and D. I. Jaramillo, “Fleet deployment optimization for liner shipping Part 1. Background, problem formulation and solution approaches”. *Maritime Policy & Management*, vol. 18, pp. 183-200, Jan 1991.
- [5] D. I. Jaramillo, and A. N. Perakis, “Fleet deployment optimization for liner shipping Part 2. Implementation and results”. *Maritime Policy & Management*, vol. 18, pp. 235-262, Jan 1991.
- [6] S.-C. Cho, and A. N. Perakis, “Optimal liner fleet routing strategies”. *Maritime Policy & Management*, vol. 23, pp. 249-259, Jan 1996.
- [7] B. J. Powell, and A. N. Perkins, “Fleet deployment optimization for liner shipping: an integer programming model”. *Maritime Policy & Management*, vol. 24, pp. 183-192, Jan 1997.
- [8] A. Imai, and F. Rivera, “Strategic fleet size planning for maritime refrigerated containers”. *Maritime Policy & Management*, vol. 28, pp. 361-374, Oct 2001.

- [9] K. Fagerholt, T. A. V. Johnsen, and H. Lindstad, "Fleet deployment in liner shipping: a case study". *Maritime Policy & Management*, vol. 36, pp. 397-409, Oct 2009.
- [10] Q. Meng, and T. Wang, "A chance constrained programming model for short-term liner ship fleet planning problems". *Maritime Policy & Management*, vol. 37, pp. 329-346, Jul 2010.
- [11] Q. Meng, and T. Wang, "A scenario-based dynamic programming model for multi-period liner ship fleet planning". *Transportation Research Part E: Logistics and Transportation Review*, vol. 47, pp. 401-413, Jul 2011.
- [12] D. F. Koza, S. Ropke, and A. Boleda Molas, "The liquefied natural gas infrastructure and tanker fleet sizing problem". *Transportation Research Part E: Logistics and Transportation Review*, vol. 99, pp. 96-114, Mar 2017.
- [13] J. Xia, K. X. Li, H. Ma, and Z. Xu, "Joint planning of fleet deployment, speed optimization, and cargo allocation for liner shipping". *Transportation Science*, vol. 49, pp. 922-938, Nov 2015.
- [14] K. Fagerholt, "Optimal policies for maintaining a supply service in the Norwegian Sea". *Omega (Westport)*, vol. 28, pp. 269-275, Jun 2000.
- [15] X. Xinlian, W. Tengfei, and C. Daisong, "A dynamic model and algorithm for fleet planning" *Maritime Policy & Management*, vol. 27, pp. 53-63, Jan 2000.
- [16] K. Fagerholt, M. Christiansen, L. Magnus Hvattum, T. A. V. Johnsen, and T. J. Vabø, "A decision support methodology for strategic planning in maritime transportation". *Omega (Westport)*, vol. 38, pp. 465-474, Dec 2010.
- [17] J. F. Alvarez, P. Tsilingiris, E. S. Engebretsen, and N. M. P. Kakalis, "Robust fleet sizing and deployment for industrial and independent bulk ocean shipping companies". *INFOR: Information Systems and Operational Research*, vol. 49, pp. 93-107, May 2011.
- [18] O. Loennechen, K. Fagerholt, B. Lagemann, and M. Stålhane, "Maritime fleet composition under future greenhouse gas emission restrictions and uncertain fuel prices". *Maritime Transport Research*, vol. 6, 100103, Jun 2024.
- [19] J. Mandal, A. Goswami, L. Thakur, and M. K. Tiwari, "Simultaneous planning of liner ship speed optimization, fleet deployment, scheduling and cargo allocation with container transshipment". Jul 2023.
- [20] L. S. de Assis, and E. Camponogara, "A MILP model for planning the trips of dynamic positioned tankers with variable travel time". *Transportation Research Part E: Logistics and Transportation Review*, vol. 93, pp. 372-388, Sep 2016.
- [21] Q. Yang, X. Xie, and W. Huo, "Modeling fleet planning strategy based on multimode investment". *Published in: 2009 Second International Symposium on Computational Intelligence and Design*, pp. 493-496, 2009.
- [22] M. Stopford, *Maritime Economics 3e*. 3rd edition, Routledge, London. 2008.
- [23] Subdirektorat Statistik Tanaman Perkebunan, *Indonesian Oil Palm Statistics 2019*. Badan Pusat Statistik, 2020.
- [24] R. Y. Priyati, "Determinants of global palm oil demand: A gravity approach". *Economic Journal of Emerging Markets*, vol. 10, pp. 148-164, Oct 2018.
- [25] Kementerian Perdagangan, *Peraturan Menteri Perdagangan No. 82*. 2017. [Online]. Available: [https://peraturan.bpk.go.id/Home/Download/119670/Permendag No. 82 Tahun 2017.pdf](https://peraturan.bpk.go.id/Home/Download/119670/Permendag%20No.%2082%20Tahun%202017.pdf)
- [26] Kementerian Perdagangan, *Peraturan Menteri Perdagangan No. 80*. [Online]. Available: [https://peraturan.bpk.go.id/Home/Download/119404/Permendag No. 80 Tahun 2018.pdf](https://peraturan.bpk.go.id/Home/Download/119404/Permendag%20No.%2080%20Tahun%202018.pdf)
- [27] Kementerian Perdagangan, *Peraturan Menteri Perdagangan No. 40*. 2020. [Online]. Available: [https://peraturan.bpk.go.id/Home/Download/152850/Permendag Nomor 40 Tahun 2020.pdf](https://peraturan.bpk.go.id/Home/Download/152850/Permendag%20Nomor%2040%20Tahun%202020.pdf)
- [28] Kementerian Perdagangan, *Peraturan Menteri Perdagangan No. 65*. 2020. Accessed: May 24, 2022. [Online]. Available: [https://peraturan.bpk.go.id/Home/Download/152883/Permendag Nomor 65 Tahun 2020.pdf](https://peraturan.bpk.go.id/Home/Download/152883/Permendag%20Nomor%2065%20Tahun%202020.pdf)
- [29] M. Reily, "Indonesia Ministry of trade answered the criticism of the obligatory insurance and sea transportation policy". Accessed: Aug 03, 2021. [Online]. Available: <https://katadata.co.id/berita/2019/01/21/kemendag-jawab-kritik-soal-kebijakan-wajib-asuransi-dan-angkutan-laut>
- [30] Staf Ahli Menteri PPN Bidang Hubungan Kelembagaan, "Kajian Tantangan dan Hambatan Pelaksanaan Beyond Cabotage di Indonesia" 2020.
- [31] World Bank, *Evaluating the Shift in Incoterms for Indonesian Export Products*. World Bank, 2016.
- [32] Departemen Perhubungan, "Indonesian flag ship database". 2021. [Online]. Available: <https://kapal.dephub.go.id/index.php/monitoring/>
- [33] Badan Pusat Statistik, "Indonesian central statistics agency". <https://www.bps.go.id/>
- [34] R. J. Hyndman, and G. Athanasopoulos, "Forecasting: Principles and Practice (2nd ed)". Accessed: May 30, 2024. [Online]. Available: <https://otexts.com/fpp2/>
- [35] Ports.com, "Sea route & distance - ports.com". Accessed: May 30, 2023. [Online]. Available: <http://ports.com/sea-route/>
- [36] E. Plomaritou, and A. Papadopoulos, *Shipbroking and Chartering Practice*. Eighth edition. | Milton Park, Abingdon, Oxon; New York, NY : Informa Law from Routledge, 2018. | Series: Lloyd's practical shipping guides: Informa Law from Routledge, 2017.
- [37] Market Realist, "Comparing Tanker Companies' Operating Expenses per DWT". Accessed: May 30, 2023. [Online]. Available: <https://marketrealist.com/2015/07/comparing-tanker-companies-operating-expenses-per-dwt/>
- [38] Mathworks, "MILP Solver MATLAB". <https://www.mathworks.com>.

# A Dynamic Discretization Algorithm for Learning BN Model: Predicting Causation Probability of Ship Collision in the Sunda Strait, Indonesia

✉ Iis Dewi Ratih<sup>1</sup>, ✉ Ketut Buda Artana<sup>1</sup>, ✉ Heri Kuswanto<sup>2</sup>, ✉ Dhimas Widhi Handani<sup>1</sup>, ✉ Renata Zahabiya<sup>3</sup>

<sup>1</sup>Institut Teknologi Sepuluh Nopember, Department of Marine Engineering, Surabaya, Indonesia

<sup>2</sup>Institut Teknologi Sepuluh Nopember, Department of Statistics, Surabaya, Indonesia

<sup>3</sup>Institut Teknologi Sepuluh Nopember, Department of Business Statistics, Surabaya, Indonesia

## Abstract

Ship collisions represent a significant category of maritime accidents with far-reaching consequences that cause damage to the involved ship and neighboring vessels. This poses a threat to the marine environment, leading to potential oil spills and the triggering of additional maritime accidents. Therefore, predicting the frequency of ship collisions by identifying the contributing factors is crucial as an initial step in preventing and mitigating their occurrence. Causation probability refers to the likelihood of events resulting from a ship collision. The contributing factors to ship collisions include weather conditions, technical failure, insufficient resources, navigation errors, human error, and the failure of other vessels. The Bayesian Network (BN) machine learning method is capable of predicting ship collisions. This method delineates the relationships among diverse and complex random variables in the form of a diagram grounded in conditional probability theory. It considers both categorical and continuous variables. The prediction of ship collisions through the application of the BN involves the use of a dynamic discretization algorithm, which offers advantages over static discretization. In this research, the causation probability of ship collisions in the Sunda Strait, Indonesia was predicted. This endeavor is necessary because of the distinct characteristics inherent to each geographical area, which implies the likelihood of varying causation probabilities across regions. The resulting predictive model for the likelihood of ship collisions in the Sunda Strait, Indonesia, derived from the implementation of the BN with the dynamic discretization algorithm, yields causation probabilities of head-on collision at  $2.74 \times 10^{-4}$ , overtaking at  $9.84 \times 10^{-4}$ , and crossing at  $8.41 \times 10^{-5}$ . The model demonstrated an overall accuracy of 94.74%.

**Keywords:** Dynamic discretization, BN, Ship collision

## 1. Introduction

Indonesia, a maritime nation consisting of an archipelago where two-thirds of its territory is water, is facing distinctive challenges. Economic activities within the country heavily rely on maritime transportation routes, resulting in significant maritime traffic, as noted by Arfian [1]. This congestion presents operational complexities for ships, frequently leading to accidents resulting in both material and human losses. From 2019 to 2022, a considerable number of maritime accidents occurred in Indonesia, as documented by the National Transportation Safety Committee (KNKT [2]). Among these incidents, 28% involved ship fires or explosions, followed by ship sinkings (27%), ship collisions

(23%), ship groundings (12%), and miscellaneous incidents (10%). Ship collisions are particularly concerning due to their notable ramifications, including loss of life, vessel damage, and environmental hazards like oil spills, as noted by Yulianti [3]. Additionally, ship collisions have the potential to trigger subsequent accidents such as sinkings, fires, and explosions. According to data from the Naval Base Command and Control Center (Puskodal) and investigations conducted by KNKT, seven ship accidents were recorded in the Sunda Strait from 2007 to 2019, with collisions being the most prevalent, contributing to four of these accidents.

The Sunda Strait is one of the most important straits in Indonesia because it is located on the shipping route



**Address for Correspondence:** Ketut Buda Artana, Institut Teknologi Sepuluh Nopember, Department of Marine Engineering, Surabaya, Indonesia  
**E-mail:** kb.artana@gmail.com  
**ORCID iD:** orcid.org/0000-0002-0302-3641

**Received:** 22.03.2024

**Last Revision Received:** 27.09.2024

**Accepted:** 22.11.2024

**To cite this article:** I. D. Ratih, K. B. Artana, H. Kuswanto, D. W. Handani, and R. Zahabiya, "A Dynamic Discretization Algorithm for Learning BN Model: Predicting Causation Probability of Ship Collision in the Sunda Strait, Indonesia." *Journal of ETA Maritime Science*, vol. 12(4), pp. 404-417, 2024.



Copyright© 2024 the Author. Published by Galenos Publishing House on behalf of UCTEA Chamber of Marine Engineers. This is an open access article under the Creative Commons AttributionNonCommercial 4.0 International (CC BY-NC 4.0) License

categorized as the Indonesian Archipelagic Sea Lane (ALKI) I from south to north with a high-density traffic route from Java Island to Sumatra Island, mostly traversed by passenger ships. As one of the straits traversed by ALKI I, the Sunda Strait has the widest shipping lane in the south with a distance of 52 nautical miles, while the narrowest shipping lane corridor in the Sunda Strait is located in the northern part with a distance of 2.2 nautical miles. The narrowness of this shipping lane is caused by several navigation hazards, such as reefs, shallows, and shipwrecks. The increase in the number of ships traversing the Sunda Strait, categorized as ALKI, prompted the Indonesian government to implement *Traffic Separation Scheme-TSS* on July 1, 2020 (Figure 1).

The noteworthy impact of ship collisions has spurred the International Maritime Organization to institute regulations specifically addressing this issue, known as The International Regulations for Preventing Collisions at Sea 1972 (Collision Regulations/COLREGS). These regulations serve as the guiding framework for all ship operational processes, mandating that ship crews have a comprehensive understanding of the established rules. Despite stringent adherence to these regulations, the practical reality is that ship collisions remain unavoidable because of other contributing factors. According to KNKT investigation reports, three primary factors stand out as the causes of ship collisions in Indonesia: human factors, technical factors, and weather factors. This underscores the necessity for regulations aimed at preventing ship collisions to be complemented by understanding the additional factors that contribute to such accidents. As a proactive measure to prevent and mitigate ship collisions, it becomes imperative to predict them through the identification of the contributing factors.

Several machine learning methodologies, including Decision Tree, Random Forest, Naïve Bayes, Bayesian Network (BN), Ensemble Bagging, and XGBoost. A comprehensive

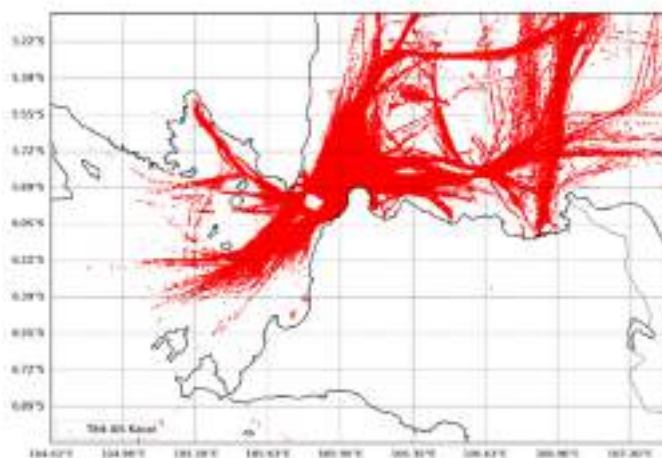


**Figure 1.** Ship trajectories along the Sunda Strait

literature review conducted by Chen et al. [4] systematically compared analytical approaches to assess the probability of ship collisions, including those based on historical data, Fault Tree Analysis (FTA), and BN modeling. Their study revealed that BN is the most effective method for estimating the likelihood of ship collisions. This conclusion finds support in the work of Hasugian et al. [5], which underscores the suitability of the BN methodology for discerning cause-and-effect relationships among factors influencing maritime accidents.

Research on ship collisions utilizing BNs has traditionally emphasized categorical variables while overlooking the impact of continuous variables, such as wind speed, wave height, and ship length, in contributing to these incidents. Although some studies have incorporated continuous variables, their use of static discretization algorithms, converting continuous variables into predefined categories, has been prevalent. An illustrative instance was observed in the study conducted by Zamzuri and Isa [6], wherein wind speed and wave height variables were discretized into categorical variables with predefined categories.

Fenton and Neil [7] posited that static discretization algorithms can compromise the accuracy of a model, which limits its applicability to real-world scenarios. To overcome these limitations, dynamic discretization algorithms offer a solution by analyzing continuous variables within BNs without requiring transformation into predefined categories. The modeling framework employing the BN method, coupled with dynamic discretization algorithms, articulates the intricate relationships among random variables through a diagram based on conditional probability theory. This method not only accommodates categorical variables and integrates continuous variables seamlessly into the modeling process.

Ship collision incidents can be broadly classified into two categories: collisions between ships and stationary objects and collisions involving two or more moving ships. This study specifically focused on the latter category, focusing on collisions among multiple moving ships. The main objective is to predict the probability of such ship collisions in the Indonesian context. This prediction can be assisted by applying a BN employing a dynamic discretization algorithm. After deriving the prediction outcomes and determining the pivotal factors contributing to the incidence of ship collisions, the resulting model can be effectively utilized for calculating the causation probabilities ( $P_c$ ). Causation Probability refers to the likelihood of events resulting from ship collisions. Karlsen and Kristiansen [8] outlined that the contributing factors to ship collisions include natural elements, technical malfunctions, insufficient resources, navigation errors, human errors, and the failure of other vessels.

Earlier investigations on the frequency of ship collisions in Indonesia relied on default values derived from IWRAP, which were determined by analyzing the causation probability in the Akashi and Dover Straits. Nevertheless, Montewka et al. [9] asserted that causation probability values should be customized according to the particular conditions of the studied waters, as each region possesses distinct characteristics, conditions, and cultures. Consequently, this study employs BN modeling to characterize and compute the causation probability in Indonesian waters, with a specific focus on the Sunda Strait as a case study. Numerous research studies have investigated the risk of ship collisions. For instance, the works of Nurmawati et al. [10], Sutrisno and Dinariyana [11], and Wuryaningrum and Handani [12] delved into ship collision risk analysis, employing default Pc values from Fuji and Shiobara [13] and Macduff [14]. These studies posit that the Pc values derived from analyses of the Akashi and Dover Strait can be universally applied. In the context of analyzing ship collisions in the Sunda Strait, several studies, including Pratiwi et al. [15], Arfian et al. [16], and Sukma et al. [17], utilized Pc values derived from modeling, employing the FTA modeling method. The modeling methodologies used in these studies entailed the determination of influencing factors and their respective probabilities, primarily referencing existing literature rather than relying on historical data from Sunda Strait accidents. Furthermore, investigations by Mulyadi et al. [18] and Purnomo et al. [19] applied the BN method to model causation probability. However, these studies adopted a simplified approach to BN modeling due to limited reference data, underscoring the need for subsequent development and updating based on the latest available data and the creation of more intricate networks, tasks that will be undertaken in the present study.

The novelty of this research, compared to previous studies, lies in the use of a BN model to capture the complex relationships between various factors influencing ship accidents, with an approach that adjusts causation probability values based on the specific conditions of the studied waters. This approach is in contrast to previous research, which often relied on default values or values derived from other regions without specific consideration of local characteristics. This research aimed to elucidate the application of BN for modeling the determinants of ship collisions and deriving Pc values for various collision scenarios (head-on, overtaking, and crossing) in Indonesian waters. Subsequently, these values were used to calculate the frequency of ship collisions in the Sunda Strait. The selection of the Sunda Strait as the focal area for this study was predicated on its status as the second-largest area in Indonesia with a notable history of ship collisions. Moreover, the strait experiences a considerable

volume of ship crossings, transporting numerous passengers daily. Therefore, a meticulous analysis of the ship collision frequency in this region is imperative to uphold safety standards and mitigate the potential losses resulting from ship collisions.

## 2. Materials and Methods

### 2.1. BN

BN is one of the simple Probabilistic Graphical Models built from graph theory and probability theory, and it serves as a well-established machine learning method by utilizing conditional probability as its foundation. In its development, the BN method, which is a BN consisting of both categorical and continuous variables, was developed [7]. A BN consists of two main parts: a qualitative part in the form of a graphical structure called a Directed Acyclic Graph (DAG) and a quantitative part in the form of a set of conditional probabilities. Figure 2 depicts the structure of the BN, which consists of nodes and edges, where  $X_i$  represents a categorical variable and  $Z_k$  represents a continuous variable. If an edge from node  $X_i$  points to node  $X_j$  then  $X_i$  is referred to as the parent and  $X_j$  is the child of  $X_i$ . Nodes without parents are called root nodes, while nodes without children are referred to as leaf nodes Korb and Nicholson [20].

In constructing a BN model, key assumptions should be considered. First, the network graph structure is directed and acyclic, facilitating the understanding of causal relationships among variables. Second, conditional independence is assumed, meaning that each variable is independent of others given its parent variables. Complete information on variable relationships is presumed to be available, facilitating risk estimation. The variables depend solely on their parent variables, without considering other variables in the network. The independence of parameters implies

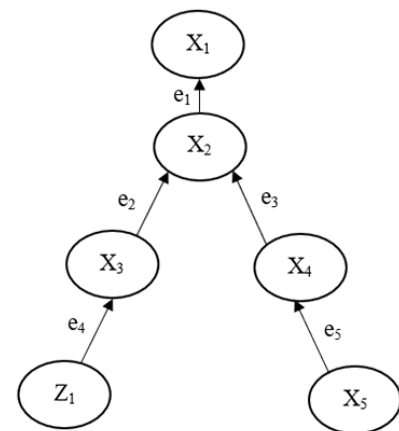


**Figure 2.** Example structure of a Directed Acyclic Graph (DAG) for a BN

that they are unrelated unless determined by the network structure. Finally, unmeasured confounding factors were assumed to be absent. Adhering to these assumptions improves the interpretation of the results, leading to more accurate conclusions about the variable relationships.

### 2.1.1. Estimation of probability values for nodes with categorical variables

BN involves estimating the probability values, starting with the determination of the prior probability values. The prior probabilities for categorical variables can be computed by utilizing straightforward probability functions, as outlined in the

$$P(X_{l(j)}) = \frac{n_{l(j)}}{n} \quad (1)$$

with  $P(X_{l(j)})$  defining the probability of the occurrence of the  $l$ -th categorical variable or the probability of the parent node's occurrence for variable  $X_j$  where  $j = 1, 2, \dots, p$  and  $l = 1, 2, \dots, p$  with  $l \neq j$ ,  $n_{l(j)}$  indicating the count of the occurrence of the  $l$ -th categorical variable, and  $n$  representing the total count of all events [21].

The structure of a BN is built using a statistical approach known as conditional probability, which is defined as the probability of an event occurring based on other events that have already occurred. If analogized in terms of parent and child, the conditional probability of the child is obtained based on the conditions experienced by the parent earlier, Sari [21]. Conditional probability values for categorical variables are presented in Equation (2).

$$P(X_j|X_{l(j)}) = \frac{P(X_j, X_{l(j)})}{P(X_{l(j)})} \quad (2)$$

with  $X_j$  indicating the categorical child node with values  $j = 1, 2, \dots, p$ ,  $X_{l(j)}$  representing the parent node of variable  $X_j$  with values  $l = 1, 2, \dots, p$  where  $l \neq j$ ,  $P(X_j|X_{l(j)})$  defining the conditional probability of  $X_j$  given the value of  $X_{l(j)}$ ,  $P(X_j, X_{l(j)})$  defining the joint probability of  $X_j$  and  $X_{l(j)}$ , and  $P(X_{l(j)})$  defining the probability value of the parent node [7].

The joint probability distribution is the probability of the simultaneous occurrence of all events. In a BN, the joint probability distribution for categorical variables is presented in Equation 3.

$$P(X_1, \dots, X_p) = P(X_1|X_2, X_3, \dots, X_p) \dots P(X_{p-1}|X_p)P(X_p) \quad (3)$$

With  $P(X_{p-1}|X_p)$  defining the conditional probability of  $X_{p-1}$  given the value of  $X_p$  and  $P(X_p)$  indicating the probability value of variable  $X_p$  Fenton and Neil [7]. If additional information is available that, when event  $X_j$  has occurred, there may be a change in the initial estimate regarding the

likelihood of event  $X_{l(j)}$  occurring, the probability of the occurrence of event  $X_{l(j)}$  now is the conditional probability due to the occurrence of event  $X_j$  and is referred to as the posterior probability. The posterior probability calculation for categorical variables is as follows:

$$P(X_{l(j)}|X_j) = \frac{P(X_j|X_{l(j)})P(X_{l(j)})}{P(X_j)} \quad (4)$$

with  $P(X_{l(j)}|X_j)$  defining the probability of  $X_{l(j)}$  given the value of  $X_j$  or the posterior of  $X_{l(j)}$  and  $P(X_{l(j)})$  indicating the prior probability of  $X_{l(j)}$  Fenton and Neil [7].

### 2.1.2. Estimation of probability values for nodes with continuous variables

The prior probability values for continuous variables in the BN follow the probability distribution of the data. The data distribution pattern must first be determined using a statistical goodness of fit test such as Kolmogorov-Smirnov test. This test is used to determine the deviation or the largest difference between the observed probability or empirical probability and the theoretical probability, Basuki et al. [22]. Conditional probability values for continuous variables in the BN are analogized in the form of parent and child, as found in the following:

$$f(Z_k|Z_{m(k)}) = \frac{f(Z_1, \dots, Z_k, \dots, Z_q)}{f(Z_{m(k)})} \quad (5)$$

with  $Z_k$  indicating the continuous child node with values  $k = 1, 2, \dots, q$ ,  $Z_{m(k)}$  representing the parent node of variable  $Z_k$  with values  $m = 1, 2, \dots, q$  where  $m \neq k$ ,  $f(Z_k|Z_{m(k)})$  defining the conditional probability of  $Z_k$  given the value of  $Z_{m(k)}$ ,  $f(Z_1, \dots, Z_k, \dots, Z_q)$  defining the joint probability, and  $f(Z_{m(k)})$  indicating the probability of the parent node. The values of the joint probability distribution for continuous variables in the BN can be expressed as follows:

$$f(Z_1, \dots, Z_q) = f(Z_1|Z_2, Z_3, \dots, Z_q) \dots f(Z_{q-1}|Z_q)f(Z_q) \quad (6)$$

With  $f(Z_{q-1}|Z_q)$  defining the conditional probability of  $Z_{q-1}$  given the value of  $Z_q$  and  $f(Z_q)$  indicating the probability value of variable  $Z_q$ , Fenton and Neil [7]. Bayes' theorem is also used to determine the posterior probability values for continuous variables, as follows:

$$f(Z_{m(k)}|Z_k) = \frac{f(Z_k|Z_{m(k)})f(Z_{m(k)})}{f(Z_k)} \quad (7)$$

With  $f(Z_{m(k)}|Z_k)$  defining the probability of  $Z_{m(k)}$  given the value of  $Z_k$  or the posterior of  $Z_{m(k)}$  and  $f(Z_{m(k)})$  indicating the prior probability of  $Z_{m(k)}$ .



**2.1.3. Estimation of probability values for mixed variables**

The probability of mixed variables in the BN can be differentiated into two cases, namely, when the continuous child node has a categorical parent node and when the categorical child node has a continuous parent node. The first condition can be explained using equation 11, and the second condition can be explained using Equation 8, Pati [23].

$$f(Z_k, X_j) = f(Z_k|X_j)P(X_j) \tag{8}$$

$$P(X_j, Z_k) = P(X_j|Z_k)f(Z_k) \tag{9}$$

Then, the posterior probability for mixed variables can be expressed in two equations, adjusting to the two conditions mentioned earlier, as found in Equations (10) and (11).

$$f(Z_k|X_{l(k)}) = \frac{P(X_{l(k)}|Z_k)f(Z_k)}{P(X_{l(k)})} \tag{10}$$

$$P(X_j|Z_{m(j)}) = \frac{f(Z_{m(j)}|X_j)P(X_j)}{f(Z_{m(j)})} \tag{11}$$

with  $Z_k$  indicating the continuous child node with values  $k = 1, 2, \dots, q$ ,  $X_j$  indicating the categorical child node with values  $j = 1, 2, \dots, p$ ,  $Z_{m(j)}$  indicating the continuous parent node for categorical variable and  $X_{l(k)}$  indicating the categorical parent node for the continuous variable.

**2.1.4. Dynamic discretization algorithm**

The dynamic discretization algorithm defines a continuous node as a simulation node. Suppose  $Z$  is a node with a continuous variable in the BN structure, where the range of  $Z$  is denoted by  $\Omega_Z$  and the Probability Density Function (PDF) of  $Z$  is denoted by  $f_Z$ . The idea behind the dynamic discretization algorithm is to estimate the value of  $f_Z$  by partitioning  $\Omega_Z$  into a set of intervals  $\Psi_Z = \{w_u\}$  and defining the local constant function  $\sim f_Z$  for the formed interval sets. This algorithm performs two main tasks: determining the optimal discretization set and determining the optimal values for the local function  $\sim f_Z$  that approximates the actual value of  $f_Z$ . Fenton, and Neil [7]. The use of a dynamic discretization algorithm can improve model accuracy compared to static discretization.

**2.2. Confusion Matrix and Sensitivity Analysis**

The confusion matrix serves as a structured table that presents the performance of a model or algorithm in a specific manner. In this matrix, each row represents the actual class of the data, and each column denotes the predicted class of the data (or vice versa), as described by Saputro and Sari [24]. A comprehensive elucidation of this matrix is presented in Table 1.

*Table 1. Confusion matrix*

Actual	Predicted	
	Collision	No collision
Collision	True Positive (TP)	False Negative (FN)
No collision	False Positive (FP)	True Negative (TN)

The four values in the confusion matrix can be utilized to compute the performance indicators of the classification models : accuracy, sensitivity, and specificity. Accuracy =  $(TP + TN) / n$ , Sensitivity =  $TP / (TP + FN)$ , and Specificity =  $TN / (TN + FP)$ .

Sensitivity analysis is a method used to determine the sensitivity of a model to changes in parameters. The main advantage of sensitivity analysis is its ability to assess model accuracy when applied to a real system. By experimenting with changes in parameters within variables, one can identify where the most significant changes occur. Sensitivity analysis was performed by altering the prior probability distribution of each node within the range of 0%-100%, Ahmadi and Manurung [25].

**2.3. Frequency Analysis**

The frequency analysis was conducted following the framework of the IALA Waterway Risk Assessment Program (IWRAP MK II). In this study, the examined frequencies encompass ship collision occurrences in the head-on, overtaking, and crossing scenarios. IWRAP is a comprehensive program designed to analyze various aspects of ship traffic movements. The proposed method takes into account factors such as hydrographic conditions, navigation channel usage, characteristics, collision risk, and other factors that influence navigational safety in specific waterways. Particularly beneficial for mapping ship movement geometries to illustrate traffic density and compute the number of potential candidate ships at risk of collision, this program is employed in our research to facilitate the calculation of the analyzed ship collision frequencies.

The computation of the collision frequency involves the use of geometric probability values, which were obtained through analysis facilitated by the IWRAP software, along with the causation probability derived from the conducted analysis. The mathematical model used to calculate the frequency is expressed as follows:

$$\lambda_{Col} = N_G \times P_c \tag{12}$$

In the given equation,  $\lambda_{Col}$  denotes the frequency of ship collisions,  $N_G$  represents the number of ships potentially at risk of collision, and  $P_c$  represents the causation probability.

The geometric probability calculations for each type of ship collision were formulated as follows:

### 2.3.1. Head-on collision

A head-on collision is a type of ship collision that occurs at the bow section between two ships moving in opposite directions. Based on the "IWRAP Mk II Working Document: Basic Modeling Principles for Prediction of Collision and Grounding Frequencies" by Hansen [26], the value of geometric probability for sailing ships potentially experiencing head-on collisions along a specified route segment is modeled as follows:

$$N_G^{head-on} = L_W \sum_{i,j} P_{G,i,j}^{head-on} \frac{V_{ij}}{V_i^{(1)} V_j^{(2)}} (Q_i^{(1)} Q_j^{(2)}) \quad (13)$$

Where  $N_{G^{head-on}}$  is the number of ships potentially at risk of a collision,  $L_W$  is Segment Length (m),  $P_G$  is the probability that two ships will collide in a head-on meeting situation,  $V_{i(1)}$  is speed of the ship on route I (m/s),  $V_{j(2)}$  is speed of the ship on route j (m/s),  $V_{ij}$  is the relative speed between the vessels (m/s),  $Q_{i(1)}$  and  $Q_{j(2)}$  is the number of passages per time unit for each ship type and size in each direction. Then to determine  $P_{G,i,j^{head-on}}$  can use the following equation:

$$P_{G,i,j}^{head-on} = \Phi\left(\frac{\bar{B}_{ij} - \mu_{ij}}{\sigma_{ij}}\right) - \Phi\left(-\frac{\bar{B}_{ij} + \mu_{ij}}{\sigma_{ij}}\right) \quad (14)$$

Where  $\Phi(x)$  is standard normal distribution function,  $\mu_{ij} = \mu_i^{(1)} + \mu_j^{(2)}$  is the mean sailing distance between the two vessels,  $\sigma_{ij} = \sqrt{(\sigma_i^{(1)})^2 + (\sigma_j^{(2)})^2}$  is the standard deviation of the joint distribution, and  $\bar{B}_{ij} = \frac{B_i^{(1)} + B_j^{(2)}}{2}$  is the average vessel breadth.

### 2.3.2. Overtaking collision

Overtaking collision is a type of ship collision that occurs when a ship is behind another and moves at a higher speed with the intention of passing the ship ahead of it in the same lane and direction. For overtaking collisions, the number of geometric collision candidates for ships sailing along the route segment in direction (1) is expressed by equation (13) using the relative speed  $V_{ij} = V_{i(1)} - V_{j(1)}$ ,  $V_{ij} > 0$ . The geometric probability of meeting [Equation (14)] becomes:

$$P_{G,i,j}^{overtaking} = P\left[y_i^{(1)} - y_j^{(1)} < \frac{B_i^{(1)} + B_j^{(1)}}{2}\right] - P\left[y_i^{(1)} - y_j^{(1)} < -\frac{B_i^{(1)} + B_j^{(1)}}{2}\right] \quad (15)$$

For normally distributed variables, the mean value in equation (14) should be replaced by  $\mu_{ij} = \mu_{i(1)} - \mu_{j(1)}$  to handle overtaking.

### 2.3.3. Crossing collision

Crossing collision is a type of ship collision that occurs between two ships moving in opposite directions relative

to each other (at an angle between  $10^\circ < |\theta| < 270^\circ$ ). The frequency of crossing collisions depends on the angle between two lanes. The geometric amount of crossing collision candidates for crossing waterways can similarly to Equation (13) be expressed as follows:

$$N_G^{crossing} = \sum_{i,j} \frac{Q_i^{(1)} Q_j^{(2)}}{V_i^{(1)} V_j^{(2)}} D_{ij} V_{ij} \frac{1}{\sin \theta} \quad \text{For } 10^\circ < |\theta| < 270^\circ \quad (16)$$

Where  $v_{ij} = \sqrt{(V_i^{(1)})^2 + (V_j^{(2)})^2 - 2V_i^{(1)}V_j^{(2)} \cos \theta}$  is the relative speed between the vessels and  $D_{ij}$  defines the apparent collision diameter. The sinus term stems from the variable transformation when integrating over the area of the joint probability distribution. Note that, contrary to head-on and overtaking collisions, the distribution of the traffic spread is not relevant for crossing collisions, except for the sinus term of course. When the crossing angle approaches zero, the length of the crossing (or the time of the crossing) goes to infinity and hence does the number of collisions. For practical reasons, it is necessary to limit the crossing angle to an interval of, for example,  $10^\circ$  to  $270^\circ$ .

As mentioned  $D_{ij}$  is the geometrical collision diameter. If it is assumed that ships can be approximated by rectangular shapes, then it can be shown that:

$$D_{ij} = \frac{L_i^{(1)} V_j^{(2)} + L_j^{(2)} V_i^{(1)}}{V_{ij}} \sin \theta + B_j^{(2)} \left\{ 1 - \left( \sin \theta \frac{V_i^{(1)}}{V_{ij}} \right)^2 \right\}^{1/2} + B_i^{(1)} \left\{ 1 - \left( \sin \theta \frac{V_j^{(2)}}{V_{ij}} \right)^2 \right\}^{1/2} \quad (17)$$

Where  $L_i$  is length of ship  $i$ ,  $L_j$  is length of ship  $j$ ,  $B_i$  is width of ship  $i$ ,  $B_j$  is width of ship  $j$ .

## 2.4. Data Sources

The dataset used in this study encompasses ship collision incidents from 2009 to 2021, consisting of a total of 44 collision cases involving two or more ships, resulting in 94 ships being involved in these collision cases. Based on the analysis, 68 ships were classified as collisions, while the remaining 26 ships were considered as non-collisions. In the accident reports, these 26 ships were determined to be innocent because they were navigating in good condition at the time. If these ships had not encountered the colliding vessels, they would not have been involved in the collision. Based on accident reports, innocent ships, namely, those that sailed in good condition or those that were stationary and then collided, were categorized as having no collision. The following gives a detailed account of the ship collision cases:

- a. There is 1 case involving 3 ships, providing a total of 3 data points.
- b. There are 3 cases involving multiple types of accidents:
  1. KMP Safira Nusantara faced a head-on collision with the LCT Sentosa Indah Sejati. Both ships, in a narrow

situation, changed course, causing KMP Safira Nusantara to experience a crossing collision with LCT Sentosa Indah Sejati. LCT Sentosa Indah Sejati overtook the ship in front, resulting in a collision (2 head-on data points, 2 crossing data points, and 1 overtaking data point).

2. KM Mochtar Prabu Mangkunegara faced a head-on collision with another ship but eventually avoided collision. KM Mochtar Prabu Mangkunegara then experienced a head-on collision with KM Sinar Jimbaran (3 head-on data points).

3. MT New Global initially faced a crossing situation with KM Maju IX. MT New Global changed course to avoid a collision, resulting in an overtaking situation that made the collision more severe (2 overtaking data points and 2 overtaking data points).

a. There were 39 cases involving 2 ships, providing a total of 78 data points.

b. There is 1 case involving only 1 ship because the captain and the first officer of the opposing ship could not be questioned as they died in the accident, so data regarding the conditions at the time of the collision could not be obtained.

The ship accident data were sourced from multiple repositories, including the following (Table 2):

The factors causing accidents used in this research are limited to those found in the chronology of ship collisions in Indonesia, as recorded in the KNKT and Maritime Court reports only. All operational definitions and categorizations related to variables are sourced from KNKT investigation reports, reports on the results of the Shipping Court's decision, COLREGS 1972, STCW, and decisions of the Minister of Transportation and Government Regulations (Table 3).

In this study, several dependent variables are treated as independent variables. One example is the ship dimension variable, which is influenced by length, breadth, draft, and Coefficient Block, as well as the maritime environment in which the ship operates. However, in this study, we assumed that this variable is independent of maneuver. This is because the selection of variables was constrained based on the accident chronology documented in the KNKT report.

*Table 2. Link to data source*

Data Source	Link
Directorate General of Sea Transportation	<a href="https://hubla.dephub.go.id/">https://hubla.dephub.go.id/</a>
Investigation reports on maritime accidents at the KNKT	<a href="https://mahpel.dephub.go.id/web/putusan/s?y=&amp;q=&amp;c=tubrukan">https://mahpel.dephub.go.id/web/putusan/s?y=&amp;q=&amp;c=tubrukan</a>
European Center for Medium-Range Weather Forecasts (ECMWF)	<a href="https://www.ecmwf.int/">https://www.ecmwf.int/</a>

*Table 3. Research variables*

Variable	Description
Y	Collision
X1	Good seamanship
X2	Crew competence
X3	Crew leadership
X4	Crew communication
X5	Understanding ship characteristics
X6	Understanding environment
X7	Inexperience
X8	Capacity in decision making
X9	Crew health
X10	Number of crew members
X11	Dual task
X12	Crew fatigue
X13	Situational awareness

Table 3. Continued

Variable		Description
X14	Visual observation	Conditions affecting the visual detection of objects around the ship, influenced by weather, screen lights, and other distractions, as well as the ability or negligence of watch officers in visual observation duties
X15	Daylight	Availability of sunlight when the ship is sailing
X16	Master presence on the bridge	Availability of the captain for guard duty and leadership on the bridge of the ship
X17	Understanding navigation and communication signs	The officer on duty's ability to understand communication and navigation codes from other ships in the form of maneuvers, light signals, or sound signals
X18	Proper utilization of navigation and communication	Navigation and communication tools for maneuvering and monitoring the movements of other ships
X19	Establish navigation and communication equipment	Complete navigation equipment required for the ship
X20	Crew responsiveness	Speed and timeliness when making decisions and taking action to avoid collisions
X21	The presence of the pilot	Availability of guides on the ship bridge when sailing in mandatory pilot waters
X22	Maneuverability	The ship's ability to change its course to avoid collision
X23	Technical failure	The ship's engine was not working properly during the operation to avoid collisions.
X24	Ship type	The type of ship involved in the collision case
X25	The type of water body	The type of water where the ship collision occurred
Z1	Wind velocity	Wind velocity at the time of collision with the ship
Z2	Wave height	The height of the water waves at the time of collision with a ship
Z3	Ship length	The horizontal distance between the leading edge of the bow height and the rear end of the stern height of the ship.
Z4	Ship breadth	The horizontal distance between the outer sides of the hull skin was measured at the main deck line.
Z5	Ship draft	The vertical distance between the waterline and the keel of the ship
Z6	Ship speed	Ship speed at the time of collision

### 3. Results and Discussion

#### 3.1. Predicting Ship Collisions using BN

The application of BN in predicting ship collisions involves a series of methodical stages. These stages comprise the development of the BN structure, the utilization of the dynamic discretization algorithm for continuous variables, the estimation of probability values for each node, the creation of a confusion matrix, the validation of the model, and the execution of the sensitivity analysis. The BN structure's variable relationships are determined based on an understanding of the collision event sequence, which is informed by prior research and expert insights. The DAG construction for the BN applied to the Indonesian ship collision data was guided by these relationships, as depicted in Figure 3.

Before parameter estimation in the BN, the dataset was partitioned into training and testing data using an 80%:20% ratio. The next step is to estimate the prior probability. The calculation of prior probabilities is only performed on the root node, as presented in Table 4 for categorical variables

and Table 5 for continuous variables. In addition, for other nodes, calculations were performed using conditional probability.

The calculation of the prior probability for continuous variables commences with the determination of the data distribution, setting the threshold value, and calculating the

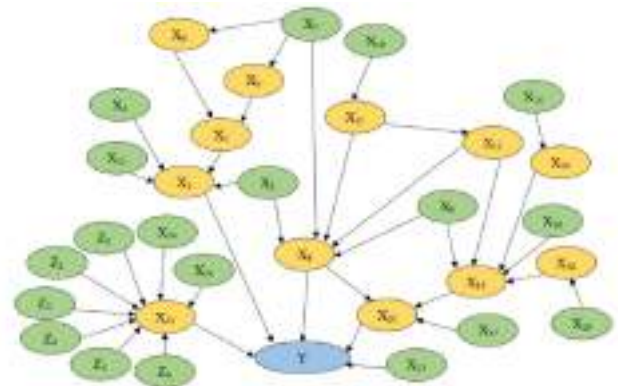


Figure 3. Ship collision DAG  
DAG: Directed acyclic graph

prior probability based on the data distribution pattern for each variable. The data patterns for each continuous variable suggest several potentially suitable data distributions, including lognormal, gamma, normal, and triangular distributions. The selection of the appropriate distribution for each continuous variable is determined through the

Kolmogorov-Smirnov test. Calculating the prior probability of continuous variables using the dynamic discretization algorithm requires threshold values that facilitate the calculation process. The thresholds for each continuous variable were determined by dividing the data for the variable according to the categories of the ship-maneuvering

**Table 4.** Prior probability of categorical variables

Variable	Category	Prior probability
Crew competence ( $X_2$ )	Proper	0.760
	Unproper	0.240
Ship communication ( $X_4$ )	Good	0.533
	Bad	0.467
Inexperience ( $X_7$ )	Yes	0.267
	No	0.733
Crew health ( $X_9$ )	Fit	0.947
	Unfit	0.053
Number of crews ( $X_{10}$ )	Proper	0.893
	Unproper	0.107
Sailing time ( $X_{15}$ )	Day	0.307
	Night	0.693
Master ( $X_{16}$ )	Available	0.760
	Not available	0.240
Understanding navigation and communication signs ( $X_{17}$ )	Good	0.787
	Bad	0.213
Navigation and communication equipment ( $X_{19}$ )	Proper	0.960
	Unproper	0.040
Pilot ( $X_{21}$ )	Available	0.320
	Charlie	0.013
	Not available	0.227
	Not required	0.440
Technical failure ( $X_{23}$ )	Yes	0.027
	No	0.973
Ship type ( $X_{24}$ )	Tanker	0.173
	Container	0.013
	General cargo	0.227
	Bulk carrier	0.027
	Passenger ship	0.080
	Ro-Ro	0.040
	Fishing ship	0.067
	Barge and tugboat	0.160
Type of water body ( $X_{25}$ )	Others	0.213
	Open sea	0.493
	River	0.467
	Coastal	0.040

ability variable, namely good and limited. The thresholds are cut-off values representing the median between the good and limited categories for each variable. The threshold values are then used to determine the prior probability of continuous variables using the PDF of each distribution of continuous variables. The obtained prior probability values for each continuous variable are presented in Table 5.

Next is to calculate the conditional probability. The conditional probability values for each child node are calculated using equation 2. The joint probability for categorical child nodes with categorical parent nodes is accomplished through the utilization of Equation 3. Conversely, for categorical child

nodes with continuous parent nodes, the determination is performed using equation 10. The final step involves computing the posterior probability. In the context of this study, posterior probability denotes the altered value following the acquisition of new information from the evidence set, constituted by the real-world data pertaining to each variable associated with the ship collision events. The computation of posterior probability for categorical variables is executed through Equation 4, whereas for mixed variables, equation 11 is employed. The outcomes of parameter estimation for each node, which have been acquired, yield a BN structure accompanied by probability values assigned to each node, as

Table 5. Prior probability of continuous variables

Variable	Units	Distribution	Parameter	Prior probability
Wind velocity ( $Z_1$ )	Knot	Triangular	$a = 0.1$ $m = 4.5$ $b = 17.50$	$f(Z \leq 8.26) = 0.6226$ $f(Z > 8.26) = 0.3774$
Wave height ( $Z_2$ )	Meter	Lognormal	$\mu = -0.509$ $\sigma = 0.779$	$f(Z \leq 0.7) = 0.5779$ $f(Z > 0.7) = 0.4221$
Ship length ( $Z_3$ )	Meter	Lognormal	$\mu = 4.315$ $\sigma = 0.661$	$f(Z \leq 101.9) = 0.6808$ $f(Z > 101.9) = 0.3192$
Ship breadth ( $Z_4$ )	Meter	Gamma	$\alpha = 4.257$ $\beta = 3.691$	$f(Z \leq 16.8) = 0.6183$ $f(Z > 16.8) = 0.3817$
Ship draft ( $Z_5$ )	Meter	Gamma	$\alpha = 3.301$ $\beta = 2.003$	$f(Z \leq 6.15) = 0.5223$ $f(Z > 6.15) = 0.4777$
Ship speed ( $Z_6$ )	Knot	Normal	$\mu = 6.811$ $\sigma = 2.878$	$f(Z \leq 6.35) = 0.4363$ $f(Z > 6.35) = 0.5637$

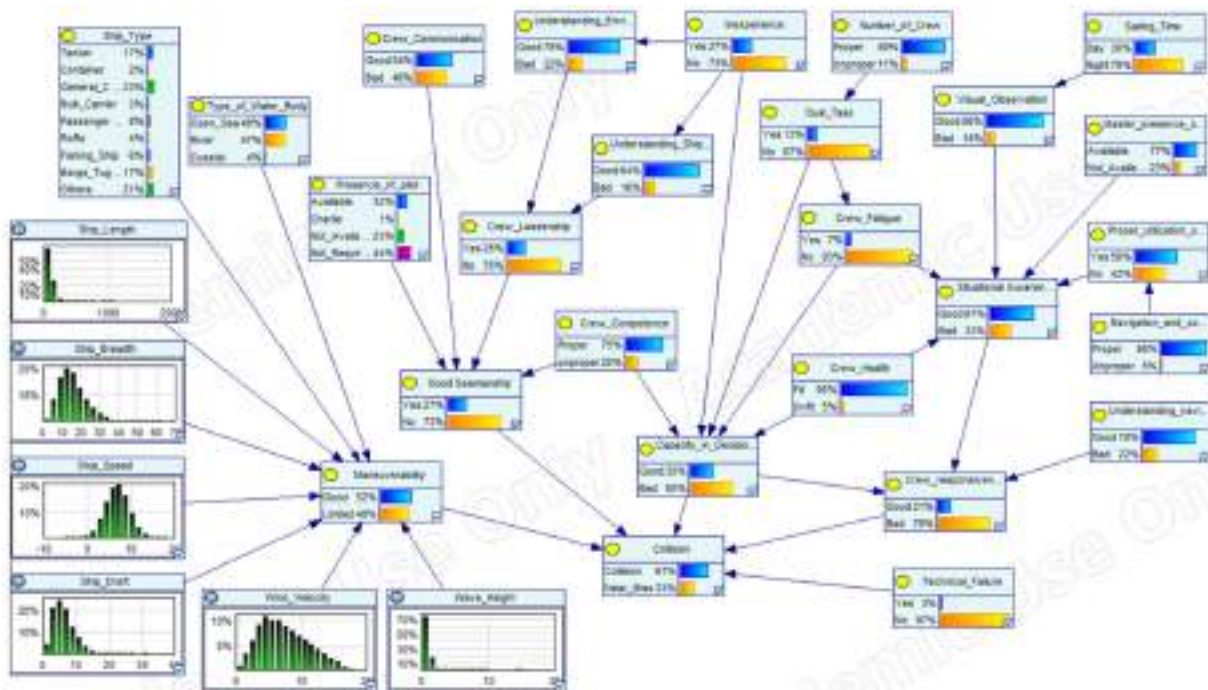


Figure 4. BN model of ship collision causes

depicted in Figure 4.

Figure 4 illustrates the configuration of the BN designed for ship collision scenarios. In this BN structure, the probability values are derived from joint probability calculations, forming the foundation for predictions when evidence pertaining to a collision case is identified to acquire posterior probability values. The construction of the BN structure is grounded in the training data, with the resultant probability values indicating a probability of 0.67 for a ship collision and a probability of 0.33 for no collision. The collision probability of 0.67 and the non-collision probability of 0.33 are derived from the sample data used to develop the BN model, which includes 68 ships that experienced collisions and 26 ships that did not (as explained in subsection 2.5). These results do not imply that the overall probability of a collision is 0.67. Instead, 0.67 represents the probability of a collision based on the causative factors identified from the sample data. Therefore, to calculate the causation

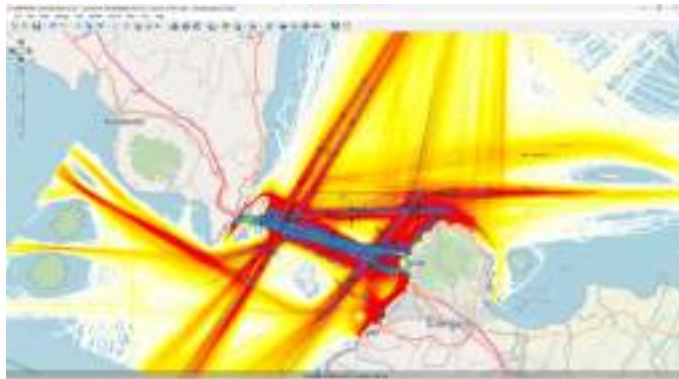


Figure 6. Mapping of traffic density in Sunda Strait waters by IWRAP MKII

probability, adjustments were made based on the number of ships passing through the Sunda Strait after obtaining this model.

Model validation was performed to evaluate the performance of the proposed classification model. Testing data consisting of 19 data points, is used to calculate the performance of the BN model by predicting ship collisions. The model accuracy was 94.74%. The sensitivity reached 100%, indicating that all ships involved in collisions were correctly predicted. The specificity is 80%, indicating that 20% of the ships not involved in collisions are incorrectly predicted as being involved, but this can serve as anticipation to avoid collisions.

The tornado diagram is presented in Figure 5 to illustrate the sensitivity analysis, where the diagram includes the top 10 scenarios that contribute the most to increasing or decreasing the probability of collision with a change of  $\pm 100\%$  for each scenario. Figure 5 illustrates that the occurrence of a collision scenario is most influenced by the watch officer failing to perform duties in line with good maritime practices, making poor decisions, being slow to take evasive action, the ship not experiencing engine failure, and possessing good ship-maneuvering abilities.

Based on the tornado diagram above, the right side is the area of increasing target probability values, whereas the left side is the opposite. The bar chart shows the impact of changes in the condition probabilities listed above on changes in the target probability values. The green and red bars indicate that the probability values of the listed conditions are increasing and decreasing, respectively. If the green bar is on the right side of the baseline, then the collision probability value will also increase. Conversely, if the green bar is on the left side, then the collision probability value will decrease.

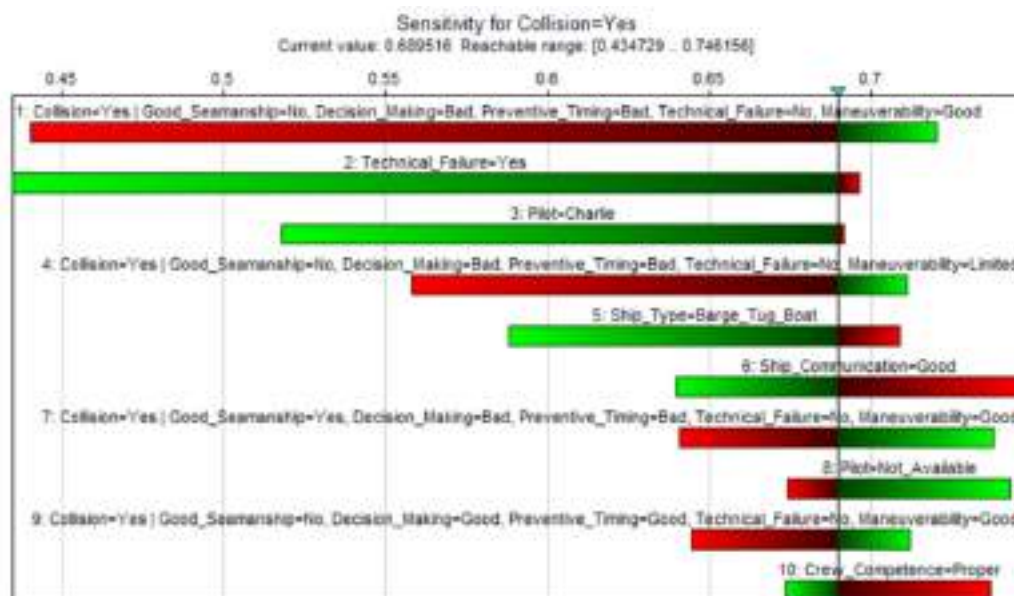


Figure 5. Tornado diagram

There exists a scenario with a change in the probability values of collisions that contradicts theoretical expectations, specifically, the scenario of technical failure with a “yes” category. Increasing the probability of this scenario from 2.7% to 100% results in a decrease in the probability of ship collisions from 68.9% to 43.5%. This discrepancy arises because of the limited data for the technical failure scenario with the “yes” category, which causes the sensitivity analysis results for this scenario to be suboptimal.

### 3.2. Causation Probability and Frequency Analysis

The causal probability ( $P_c$ ) was calculated based on a BN model that was adjusted according to the annual traffic volume of ships. Therefore, the conditional probability values for each combination of scenarios are proportional to the conditional probability values for the actual conditions that occur. In the calculation of probabilities for each state, the data are separated into data for ships that have experienced collisions and data for ships that have not experienced collisions. Probability calculations are performed separately for these segmented data, followed by the accumulation of probabilities. Upon completion of the probability calculations, akin to the methodology employed in modeling a BN classification model, the subsequent step involves determining the joint probability using a consistent approach. Table 6 presents a succinct overview of the resulting  $P_c$  values ( $P_c$  analysis) corresponding to each category of collision.

In this research, to apply the obtained  $P_c$  values, a ship collision frequency analysis was conducted in one of Indonesia’s waters, the Sunda Strait. To perform this analysis,

Automatic Identification System data on ship movements in the Sunda Strait in 2022 were required. The data were processed to create a mapping of ship density in the Sunda Strait to understand the distribution of ship density along each existing route. This step was necessary to determine the frequency values for each type of ship collision. In this process, data processing was performed with the assistance of the IWRAP MKII software to map the water density, shipping traffic distribution, and frequency values of each type of ship collision. The density mapping results in IWRAP MKII are displayed below.

From the mapping and density distribution analysis of shipping lanes in the waters of the Sunda Strait, the frequencies of ship collisions for each collision type were acquired as follows.

The results indicate that the total frequency of ship collisions is approximately 0.025 collisions/year, but according to the historical data quoted, there have been 4 collisions in 12 years (0.33 collisions/year). The very large differences between the obtained results and the actual data could occur because the causation probability used to calculate the frequency of ship collisions is obtained based on certain factors, so it does not rule out the possibility that there are other factors that also influence the causation probability and ultimately influence the frequency of ship collisions. The findings of the analysis reveal that in the Sunda Strait, the frequency of ship collisions exhibits that the causation probability for head-on collisions is notably higher than that for overtaking and crossing collisions. The following are the causation probability values obtained from the research and other regions.

*Table 6. Frequency values of ship collisions in the Sunda Strait*

Collision type	$P_c$ default IWRAP	$P_c$ analysis	Frequency ( $P_c$ default IWRAP)	Frequency analysis
Head-on	$5 \times 10^{-5}$	$2.74 \times 10^{-4}$	0.004	0.0219
Overtaking	$1.1 \times 10^{-4}$	$9.84 \times 10^{-6}$	0.002	0.000179
Crossing	$1.3 \times 10^{-4}$	$8.41 \times 10^{-5}$	0.0046	0.003

*Table 7. Causation probabilities from literature studies*

Location	$P_c$ ( $\times 10^{-4}$ )	Comment	References
Dover Strait	5.18	Head-on: no traffic separation	MacDuff [14]
Dover Strait	3.15	Head-on with traffic separation	MacDuff [14]
Dover Strait	1.11	Crossing: no traffic separation	MacDuff [14]
Dover Strait	0.95	Crossing with traffic separation	MacDuff [14]
Orsund, Denmark	0.27	Head-on	Karlson et al. [27]
Japanese Strait	0.49	Head-on	Fuji and Mizuki [28]
Japanese Strait	1.23	Crossing	Fuji and Mizuki [28]
Japanese Strait	1.10	Overtaking	Fuji and Mizuki [28]
Great Belt, Denmark	1.30	At bends in the lanes, the	Pedersen et al. [29]



The BN model for calculating accident causation probabilities has broad potential applications across various regions, not limited to just the Sunda Strait, provided that the values of condition variables and traffic density are adjusted according to the specific characteristics of the region. This adjustment is necessary to ensure that the BN model provides accurate and contextually relevant analyses. Thus, this model can serve as an effective tool for understanding and mitigating accident risks in various waterways by accounting for variations in environmental conditions and maritime activities.

#### 4. Conclusion

The conclusions from the analysis regarding the BN modeling for estimating Pc values for each type of ship collision to calculate the frequency of ship collisions in the Sunda Strait are as follows:

- In conclusion, the implementation of the BN using the dynamic discretization algorithm yielded an accuracy of 94.74%, sensitivity of 100%, and specificity of 80%. The predominant factors contributing to ship collisions are good seamanship, decision-making, preventive timing, technical failure, and maneuverability.
- Based on the analysis and BN modeling, the causation probability values obtained for the Sunda Strait are as follows: Pc Head-on, Pc Overtaking, and Pc Crossing are  $2.74 \times 10^{-4}$ ,  $9.84 \times 10^{-6}$ , and  $8.41 \times 10^{-5}$ , respectively, with a model accuracy of 93.75%.
- The frequency of ship collisions in the Sunda Strait for each type of collision (Head-on, Overtaking, and Crossing) using the default Pc values from IWRAP is as follows: 0.004 collisions/year, 0.002 collisions/year, and 0.0046 collisions/year, respectively. Meanwhile, based on the BN modeling results, the frequency values are 0.0219, 0.000179, and 0.003 collisions/year, respectively.

The research findings offer practical recommendations, emphasizing the importance of ship crew members fulfilling their duties in line with good maritime practices, possessing the ability to make sound decisions, acting promptly and accurately to avert collisions, conducting regular inspections and maintenance of ship engines, and maintaining good maneuverability to mitigate the potential for ship collisions. The study acknowledges limitations due to data constraints, which result in some unavailable combinations in conditional probability calculations. As a result, the BN model may not be applicable to certain ship collision scenarios. Future research should address these limitations by expanding the dataset and/or involving expert opinion to encompass all potential collision scenarios for more robust and optimal outcomes.

#### Footnotes

##### Authorship Contributions

Concept design: I. D. Ratih, K. B. Artana, and H. Kuswanto, Data Collection or Processing: I. D. Ratih, and R. Zahabiya, Analysis or Interpretation: I. D. Ratih, K. B. Artana, H. Kuswanto, D. W. Handani, and R. Zahabiya, Literature Review: I. D. Ratih, K. B. Artana, H. Kuswanto, and D. W. Handani, Writing, Reviewing and Editing: I. D. Ratih, K. B. Artana, H. Kuswanto, and D. W. Handani.

**Funding:** The authors did not receive any financial support for the research, authorship and/or publication of this article.

#### References

- [1] Z. Arfian, *Penilaian Risiko Tubrukan Kapal Akibat Instalasi Anjungan Lepas Pantai di Dekat Alur Pelayaran Barat Surabaya*, Surabaya: Institut Teknologi Sepuluh Nopember, 2017. [Online]. Available: <https://api.semanticscholar.org/CorpusID:115277737>
- [2] KNKT, "Laporan dan Informasi Statistik Kecelakaan", 2023. [Online]. Available: <https://knkt.go.id/statistik>
- [3] Yulianti, "Prosedur dan Penanggulangan Keadaan Darurat di Kapal KM. Mutiara Ferindo III", UNIMAR AMNI, Semarang, 2019. [Online]. Available: <http://repository.unimar-amni.ac.id/id/eprint/2482>
- [4] P. Chen, Y. Huang, J. Mou, and P. V. Gelder, "Probabilistic risk analysis for ship-ship collision: State-of-the-art". *Safety Science*, vol. 117, pp. 108-120, Aug 2019.
- [5] S. Hasugian, M. Rahmawati, A. I. S. Wahyuni, I. Suwondo, and I. Sutrisno, "Analysis the risk of the ship accident in Indonesia with BN model approach". *Annals of the Romanian Society for Cell Biology*, vol. 25, pp. 3341-3356, 2021.
- [6] Z. H. Zamzuri and Z. Isa, "Pengukuran risiko menggunakan rangkaian Bayes: aplikasi kepada data pelanggaran kapal di Malaysia [English: Risk measurement using Bayesian networks: applications to ship collision data in Malaysia]". *Sains Malaysiana*, vol. 51, pp. 2305-2314, Apr 2022.
- [7] N. Fenton, and M. Neil, *Risk Assessment and Decision Analysis with BN*, Boca Raton: CRC Press, 2013.
- [8] J. E. Karlsen, and S. Kristiansen, *Analysis of Causal Factors and Situation Dependent Factors. Project: Cause Relationships of Collisions and Groundings*, Report 80-1144, Det Norske Veritas, Høvik, Norway, 1980. [Online]. Available: <https://api.semanticscholar.org/CorpusID:108479276>
- [9] J. Montewka, F. Goerlandt, and P. Kujala, "A new definition of a collision zone for a geometrical model for ship-ship collision probability estimation". *TransNav, the International Journal on Marine Navigation and Safety of Sea Transportation*, vol. 5, no. 4, pp. 497-504, 2011.
- [10] Nurmawati, K. B. Artana, and T. Pitana, "Penilaian risiko tubrukan kapal di sekitar buoy 12 perairan selat madura melalui proses formal safety assessment (FSA), [English: Risk assessment of ship collision around buoy 12 madura strait through formal safety assessment (FSA) process]". 2015.
- [11] J. Sutrisno, and A. A. B. Dinariyana, "Risk assessment of ship collision and grounding in Surabaya west access channel due to the existence of shipwrecks". 2018.

- [12] N. D. Wuryaningrum, and D. W. Handani, "Frequency analysis of ship collision and its impact on the fulfillment of supporting facilities and route changes due to implementation of Sunda Strait TSS". *IOP Conference Series: Earth and Environmental Science*, 2020.
- [13] Y. Fujii, and R. Shiobara, "The analysis of traffic accidents". *Journal of Navigation*, vol. 24, pp. 534-543, 1971.
- [14] T. MacDuff, "The probability of vessel collisions". *Ocean Industry*, vol. 9, pp. 144-148, Sep 1974.
- [15] E. Pratiwi, K. B. Artana, and A. A. B. Dinariyana, "Ship collision frequency during pipeline decommissioning process on Surabaya west access channel (SWAC)". *Journal of Engineering Science and Technology*, vol. 14, pp. 2013-2033, Aug 2019.
- [16] Z. Arfian, K. B. Artana, and A. A. B. Dinariyana, "Penilaian risiko tubrukan kapal akibat instalasi anjungan lepas pantai di dekat alur pelayaran barat Surabaya". Jul 2017.
- [17] R. A. Sukma, D. W. Handani, and T. F. Nugroho, "Risk assessment of ship collision on FSO Pertamina abherka and oil spill modelling due to structural damage". 2021.
- [18] Y. Mulyadi, E. Kobayashi, N. Wakabayashi, T. Pitana, and Wahyudi, "Development of ship sinking frequency model over subsea pipeline for Madura Strait using AIS data". *WMU Journal of Maritime Affairs*, vol. 13, pp. 43-59, 2013.
- [19] D. A. Purnomo, A. A. B. Dinariyana, and K. B. Artana, "Formal safety assessment for ship collision in Bali strait". 2019.
- [20] K. Korb, and A. Nicholson, *Bayesian Artificial Intelligence*, 2nd ed., CRC Press, 2010.
- [21] A. N. Sari, *Model Prediksi Kondisi Perkerasan Jalan dengan Metode Dynamic BN*, Surabaya: Institut Teknologi Sepuluh Nopember, 2016. [Online]. Available: <http://repository.its.ac.id/id/eprint/167>
- [22] I. Basuki, Winarsih, and N. L. Adhyani, "Analisis periode ulang hujan maksimum dengan Berbagai metode". *J Agroment*, vol. 23, pp. 76-92, 2009.
- [23] D. Pati, "Jointly distributed random variables". pp. 1-4, 2012.
- [24] I. W. Saputro, and B. W. Sari, "Uji performa algoritma naïve bayes untuk prediksi masa studi mahasiswa". *Citec Journal*, vol. 6, pp. 5, Jan-Jun 2019.
- [25] B. W. Ahmadi, and O. S. M. Manurung, "Aplikasi model BN dalam perhitungan performansi operasi keamanan laut yang dihasilkan TNI AL di wilayah timur dengan pendekatan causal mapping". *Asro Journal*, p. 63, 2015.
- [26] P. Friis-Hansen, "Basic modelling principles for prediction of collision and grounding frequencies". Technical University of Denmark, 2007. [Online]. Available: [https://iala.int/wiki/iwrap/images/2/2b/IWRAP\\_Theory.pdf](https://iala.int/wiki/iwrap/images/2/2b/IWRAP_Theory.pdf)
- [27] M. Karlson, F. Rasmussen, and L. Frisk, "Verification of ship collision frequency model". Proceeding of the International Symposium on Advances in Ship Collision Analysis, Copenhagen, Denmark, pp. 117-121, 1998. [Online]. Available: <https://api.semanticscholar.org/CorpusID:197512444>
- [28] Y. Fujii, and N. Mizuki, "Design of VTS systems for water with bridges". Proceeding of the International Symposium on Advances in Ship Collision Analysis, Copenhagen, Denmark, pp. 177-190, 1998. [Online]. Available: <https://api.semanticscholar.org/CorpusID:188357660>
- [29] P. T. Pedersen, P. F. Hansen, and L. Nielsen, "Probabilistic analysis of collision damages with application to passenger Ro-Ro vessels". Safety of Passenger Ro-Ro Vessels. Dept. of Naval Architecture and Ocean Eng. Doc. pac- 001. 1995

# Analysis of the Strain-Dependent Damping of Paulownia Wood to Reduce Vibrations in Maritime Transport

✉ Jürgen Göken<sup>1</sup>, ✉ Nicolas Saba<sup>2</sup>

<sup>1</sup>University of Applied Sciences Emden/Leer Faculty of Maritime Sciences, Leer, Germany

<sup>2</sup>University of Balamand Faculty of Engineering, Department of Mechanical Engineering, Tripoli, Lebanon

## Abstract

The shipping industry is striving to optimise efficiency and safety regarding sound and vibration protection through innovations. A key aspect of these innovations is the development of new insulation materials that help minimise vibrations and noise. In addition to protecting the ship's structures, the protection of the crew members is also of great importance. Noise pollution and persistent vibrations can adversely affect the health and well-being of the crew. This, in turn, can reduce performance and responsiveness in critical situations. Paulownia wood is an innovative natural product and a fast-growing and lightweight wood that can be cultivated worldwide. In light of the increasing interest in sustainable building materials and the growing demand for lightweight construction solutions, especially in shipbuilding, it is crucial to better analyse and hence understand the damping potential of Paulownia wood which significantly affects its acoustic behaviour. Damping was investigated by measuring the logarithmic decrement of freely decaying bending oscillations as a function of the maximum strain amplitude. The measurements were carried out on a common Paulownia species (obtained from plantations in Georgia, Italy, and Spain) and a new species of Paulownia obtained from a plantation in Germany. It was found that all damping curves exhibited a strain-independent and a strain-dependent range. Moreover, it was shown that the influence of the fibre orientation on the damping behaviour was less than expected.

**Keywords:** Wood, Bio-based materials, Damping, Dynamic mechanical analysis

## 1. Introduction

Sustainable thinking and action are gaining increasing importance in society. This is evident, for example, in shipping, where the recycling of ship parts plays a significant role [1]. Therefore, it is advisable to consider resource-saving and easily recyclable materials during the construction phase of the ships. Ecological action is accompanied by an increased demand for sustainable and renewable raw materials. Wood is one of these raw materials.

Something that is often forgotten: Wood has a long and significant tradition in shipbuilding and played a crucial role for centuries. The oldest known boats are dugouts, which were used before Christ. Boats from ancient Egypt, built from Cedar wood imported from Lebanon, are also of historical importance. They were used for transport, hunting, and exploration [2]. Even in modern times, wood holds a significant position in shipbuilding and is employed in various

areas. Wood is often deployed in the interior design of ships due to its aesthetics and structural properties. Its high-quality appearance gives wood a warm look and creates a luxurious atmosphere [3].

The shipping industry is working towards becoming eco-friendlier without compromising on safety standards for ships and their crews. Reducing vibrations and noise is essential to safeguard the ship's structure and the health and well-being of crew members. These challenges are managed according to recognised international regulations [4-6]. To comply with these standards, it is vital to conduct studies on renewable materials and their properties.

A fast-growing raw material is the wood of the Paulownia tree. This tree is also known as the Empress tree, Royal Paulownia, or Kiri. In one year, this tree grows an average of 4 metres in height and about 2 centimetres in width. After approximately



**Address for Correspondence:** Jürgen Göken, University of Applied Sciences Emden/Leer Faculty of Maritime Sciences, Leer, Germany

**E-mail:** juergen.goeken@hs-emden-leer.de

**ORCID iD:** orcid.org/0000-0002-4847-2870

**Received:** 25.09.2024

**Last Revision Received:** 10.12.2024

**Accepted:** 11.12.2024

**To cite this article:** J. Göken, and N. Saba, "Analysis of the Strain-Dependent Damping of Paulownia Wood to Reduce Vibrations in Maritime Transport." *Journal of ETA Maritime Science*, vol. 12(4), pp. 418-426, 2024.



Copyright© 2024 the Author. Published by Galenos Publishing House on behalf of UCTEA Chamber of Marine Engineers. This is an open access article under the Creative Commons AttributionNonCommercial 4.0 International (CC BY-NC 4.0) License

a period of 10 years, 0.5 m<sup>3</sup> to 1.5 m<sup>3</sup> of wood can be harvested [7]. With a specific density of about 250 kg/m<sup>3</sup> (see Table 1), this wood is also considered very light. Paulownia wood is gaining significant attention in technical fields because of its impressive strength-to-density ratio. In addition to this, the large size of its leaves gives the Paulownia tree a key position in terms of photosynthetic efficiency. One Paulownia tree can absorb daily up to 22 kg of CO<sub>2</sub> and produce approximately 6 kg of O<sub>2</sub>. In comparison, a mature tree absorbs approximately 22 kg of CO<sub>2</sub> from the atmosphere annually [8].

As the Paulownia tree is better known worldwide as the Kiri tree, this name will be retained in the following. In Table 1 some essential properties about Kiri wood are listed.

Kiri wood is utilised in various applications. Some fields of its use including concrete examples are shown in Table 2.

For the maritime industry, the damping properties and density of wood are of particular interest. However, these properties are still largely undetermined. Establishing these properties will enable a definitive conclusion on the suitability of Kiri wood for noise and vibration insulation. Potential areas of application include cabins on cruise ships and yachts. The potential use of this renewable raw material in shipbuilding concerns, for example, the cladding of cabins or its utilization as a structured wall element.

The fire hazard on board ships is generally a significant concern. Thus, the International Maritime Organization developed fire safety regulations, including the “International Code for Application of Fire Test Procedures” (FTP Code

[11]. Since wood is already being used (e.g., in the interiors of yachts), there are no new regulatory barriers to the use of Kiri wood to overcome in this regard.

Its low density makes it ideal for a variety of lightweight construction projects. Furthermore, that the lower weight results in reduced fuel consumption, enabling a more environmentally friendly journey [12]. In addition to its low density, Kiri wood is highly recyclable, setting it apart from other materials [13].

In this work, the assessment of the suitability of Kiri wood for damping vibrations is performed based on strain-dependent damping measurements. These measurements were executed at room temperature and constant moisture content.

## 2. Experimental Details

### 2.1. Material

It was important to obtain Kiri wood from different growing regions, as the growth conditions (e.g., nutrient content of the soil) and climatic circumstances influence the structural development of the wood [14]. The Kiri wood to be analysed was provided by a supplier specialising in Kiri wood from controlled European sources. This company has access to various plantations across Europe.

Tested samples were taken from Kiri trees originating from plantations in a) Italy, b) Spain, c) Georgia, and d) Germany. Note: The Kiri trees from German plantation are considered non-invasive species (called NordMax21<sup>®</sup>) and are a hybrid of Paulownia tomentosa and Paulownia fortunei. The genetic

*Table 1. Properties of Kiri wood [9]*

Property	Description of Kiri wood
Specific density	About 250 kg/m <sup>3</sup> ; comparison: oak: ~ 770 kg/m <sup>3</sup> ; beech: ~ 720 kg/m <sup>3</sup> ; pine ~ 480 kg/m <sup>3</sup> ; spruce: ~ 450 kg/m <sup>3</sup> → Low weight saves transport and energy costs.
Strength	Honeycomb-like cell structure → Kiri wood is very strong and stable in relation to its weight.
Dimensional stability	Extremely low swelling and shrinking behaviour → This makes Kiri wood the first choice in environments with changing humidity levels.
Thermal conductivity	Only 0.09 W/mk → Kiri wood stores a lot of air in its vacuoles and therefore insulates more than twice as well as oak or beech.
Weather-proof	No splitting, no cupping, no warping
Knot occurrence	Completely knot-free assortment is possible → The delicate grain and pleasantly smooth feel make it attractive for different areas of application.
Processing	Does not splinter, can be easily processed manually and mechanically, can easily absorb glazes and varnishes, and is very good for gluing

*Table 2. Application areas of Kiri wood [10]*

Mobility	Construction	Lifestyle
Ship and boat construction, surfboards, model and glider airplanes, caravan manufacturing	Ceilings, stairs, windows, modular buildings, tiny houses, wooden facades, structures for trade shows, events, and stages	Furniture, home accessories such as vases and bowls, garden furniture, packaging and storage containers

influence of *Paulownia tomentosa* provides this hybrid breed with particularly wide site tolerance and high frost resistance. The cross-breeding partner, *Paulownia fortunei*, dominates the straight, robust, and homogeneous stem growth of this variety [15]. Samples of this special variety (location of the German plantation: Ladenburg, growing time: 11 to 12 years) were harvested for the first time and made available for this study.

All samples used in this work were sourced from wood harvested about a year ago. The Kiri wood was delivered as boards which were cut in the direction of the tree trunk's growth. The cutting direction was not necessarily the growth direction of the tree. This resulted in an inconsistent fibre orientation of the samples which were used as bending beams. The designation of the fibre orientations is shown in Figure 1.

## 2.2. Measuring Procedure

Damping measurements were carried out at room temperature and constant moisture content [equilibrium moisture content  $\sim 10\%$  (accompanied by randomised corresponding measurements)] using wooden samples with rectangular shape and the following dimensions: thickness  $a$  about 3 mm, width  $b$  of 10 mm and total length  $l$  of 120 mm. The specially configured experimental damping setup is shown in Figure 2. A metallic cylinder is rotated using a hand crank. On this cylinder, a bevelled cuboid touches the free end of the bending sample and sets it into vibration. Depending on the degree of overlap between the bevelled cuboid and the free end of the bending beam, a variation in the initial amplitude can be achieved. When contact with the sample is lost, the deflected bending beam undergoes free damped harmonic oscillation. The oscillation amplitude is measured using a laser triangulation sensor (model: ILD1320-100,

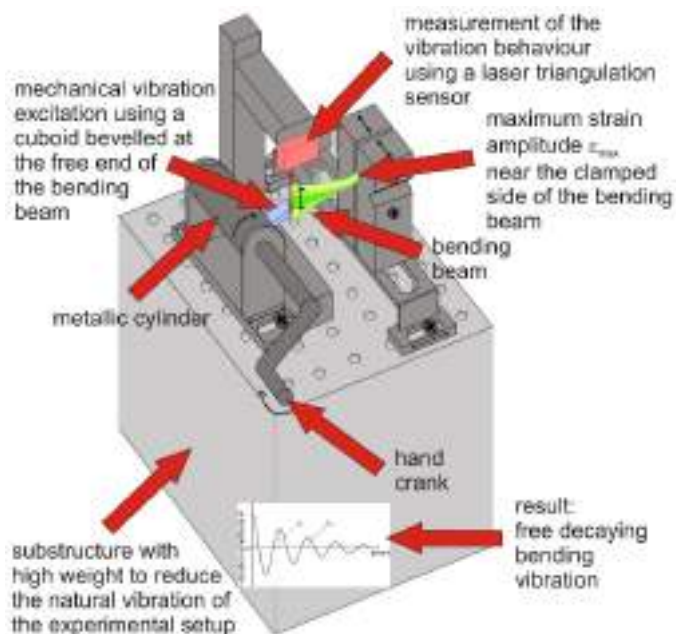


Figure 2. Experimental damping setup. Adopted from [16] (modified)

Micro-Epsilon, Ortenburg, Germany) with a set sampling rate of 2000 measurement points per second. It is attached above the free end of the sample and records the vibration data as a function of time by measuring distance data. The laser software transfers the data to a PC and visualises it.

According to Figure 2, the maximum strain  $\epsilon_{max}$  is generated near the clamped side of the bending beam, which is used as a reference value for amplitude-dependent damping measurements.

Material damping was measured in terms of the logarithmic decrement  $\delta$  which is defined by [17]:

$$\delta = \frac{1}{k} \ln \left( \frac{A_n}{A_{n+k}} \right) \quad (1)$$

and represents the measure of the rate of decay in vibration amplitude of a harmonically decaying oscillation. In Equation (1), the vibration amplitude  $A_n$  at time  $nT$  ( $T$ : periodic time) and  $A_{n+k}$ , the vibration amplitude after  $k$  oscillation periods at time  $(n+k)T$ , are shown, where  $n$  and  $k$  are whole numbers. To obtain the current damping behaviour of a damped system, two consecutive oscillation amplitudes are therefore considered [18].

Damping is subject to the superposition principle, meaning that various external damping mechanisms (such as apparatus damping and air damping) can overlap and thus distort material damping. It is not trivial to detect this additional damping, and in individual cases it may be difficult to determine. This makes it challenging to compare absolute damping values.

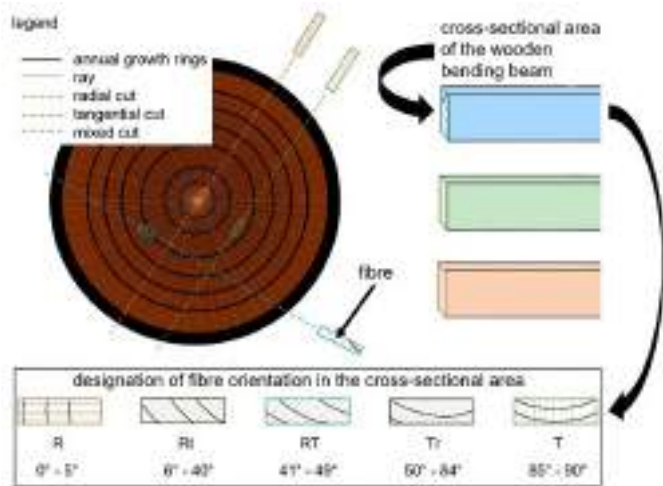


Figure 1. Fibre orientations of the bending beams and designation of the fibre orientation. Adopted from [16] (modified)

Relative changes between damping data naturally remain even if the apparatus damping is retained.

As the bending sample exhibits approximately harmonic decaying behaviour immediately after vibration excitation, the vibration frequency  $f$  can be calculated according to  $f = 1/T$  ( $T$ : periodic time). Knowing  $f$  and the specific density  $\rho$ , the bending modulus  $E_{bend}$  (here in the unit N/mm<sup>2</sup> (or MPa)), can be determined as [19]

$$E_{bend} = 10^{-12} 4\pi^2 f^2 \frac{l^4 \rho ab}{c^4 I_y} \quad (2)$$

where  $c$  is a constant (eigenvalue) taken from the modal analysis of a cantilever beam. Using  $c = 1.875$  the first vibration mode of such a beam is described.  $I_y$  is the area moment of inertia of a rectangle ( $\rightarrow$  end face of the bending beam) with respect to the resistance to bending around the Y-axis, with  $I_y = (a^3 b)/12$  ( $a$ : thickness,  $b$ : width).

More detailed information about the experimental setup and the extensive data analysis (using self-written software) can be found in another own work [20]. A key component of the software is the consideration of possible offsets and noise when recording the vibration amplitudes. Ignoring offsets and noise can lead to excessively high values of the logarithmic decrement due to the logarithmization [see Equation (1)].

### 3. Results

In Figure 3, the strain-dependent damping of Kiri wood from Georgia can be seen. The bending modulus  $E_{bend}$  was calculated according to Equation (2) and added as well.

The damping curves can be divided into a strain-independent

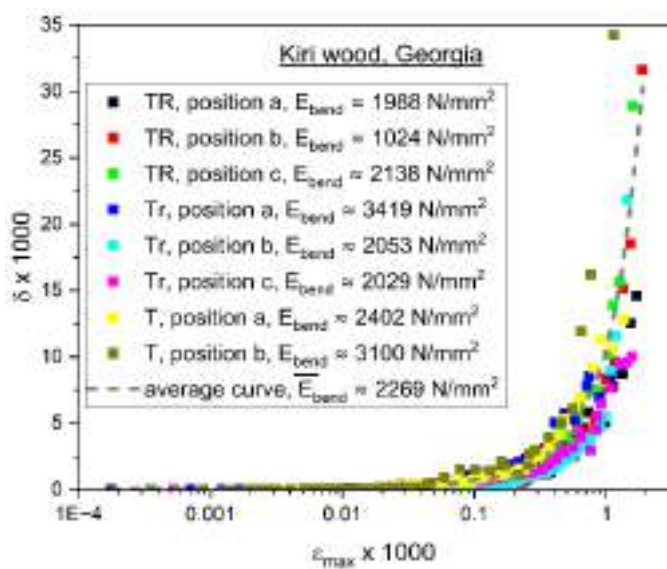


**Figure 3.** Strain-dependent damping of Kiri wood from Georgia in consideration of the fibre orientation. The calculated bending modulus  $E_{bend}$  is added

range ( $\delta_0 \rightarrow$  parallel to the X-axis) and a strain-dependent range ( $\delta_h(\epsilon_{max}) \rightarrow$  increase with increasing maximum strain amplitude) where  $\delta_h$  is the hysteretic damping (structural damping). Such behaviour is well known for strain-dependent damping measurements of metals [21]. A noticeable increase in material damping is observed at a maximum strain amplitude of approximately 0.1 (in terms of  $\epsilon_{max} \times 1000$ ). The tangential fibre orientation T appears to result in a higher material damping at the same strain amplitude.

Kiri wood from Germany (Figure 4) shows the same curve progression as Kiri wood from Georgia. Here, TR and Tr are the directions that lead to increased damping. The curve profile, represented by the averaged curve, is similar to the profile of the averaged curve of Georgian wood. The bending modulus of the Kiri wood sample from Germany is higher

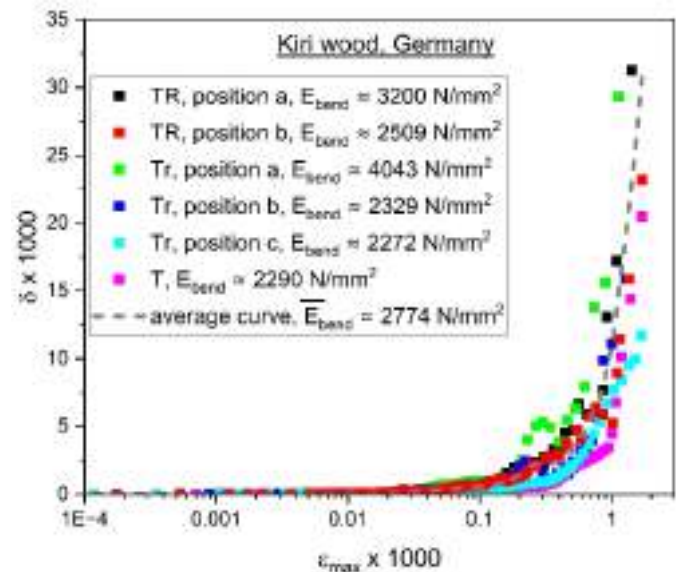


**Figure 4.** Strain-dependent damping of Kiri wood from Germany in consideration of the fibre orientation. The calculated bending modulus  $E_{bend}$  is added

than that of the Georgian wood, resulting in slightly higher strength.

A significant difference in both the strain-dependent damping and the bending modulus can be observed in the Italian Kiri wood samples, Figure 5. The bending modulus is significantly lower than that of the Georgian or German samples. For example, when considering the logarithmic decrement at maximum strain amplitude with a value of 1 (in terms of  $\epsilon_{max} \times 1000$ ), an approximately 30% lower value of material damping is recorded. The maximum damping is only reached at higher maximum strain amplitudes. Moreover, the wood tested is less rigid than the samples from Georgia and Germany.

Figures 6-8 show the results of strain-dependent damping measurements of Kiri wood samples from Spain. There was mainly a radial fibre orientation present. In all cases, the bending modulus is greater than the value of the samples from Italy, Germany, and Georgia. In the higher strain range, a comparatively high damping is revealed.

Figure 9 illustrates the respective averaged strain-dependent damping curves. It becomes clear once again that the damping of the Kiri wood samples from Georgia and Germany are very similar. To illustrate the difference in damping data, the data

was taken at maximum strain amplitudes of 0.1 and 1 (in terms of  $\epsilon_{max} \times 1000$ , see also reference lines) and are shown in Table 3. It is evident that the samples from Spain have approximately double the values of strain-independent damping compared to the other samples. In the strain-dependent damping range, the samples from Italy exhibit lower damping than the samples from Georgia and Germany. However, the damping values of the samples from Spain at this maximum strain amplitude is approximately double that of the others.

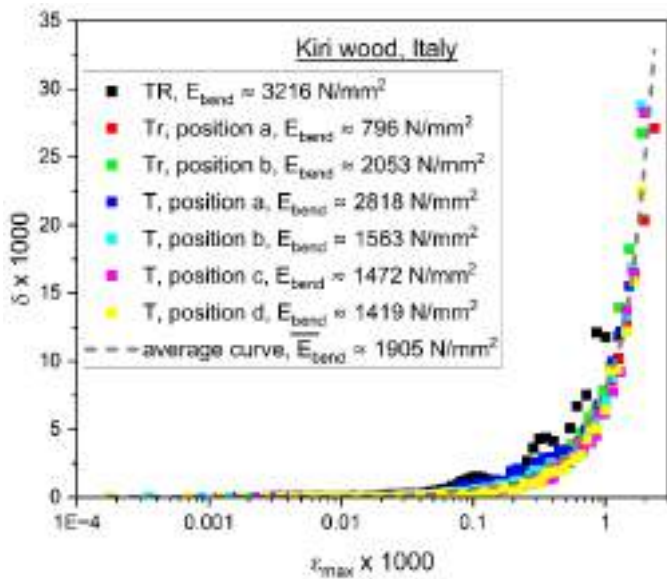


Figure 5. Strain-dependent damping of Kiri wood from Italy in consideration of the fibre orientation. The calculated bending modulus  $E_{bend}$  is added

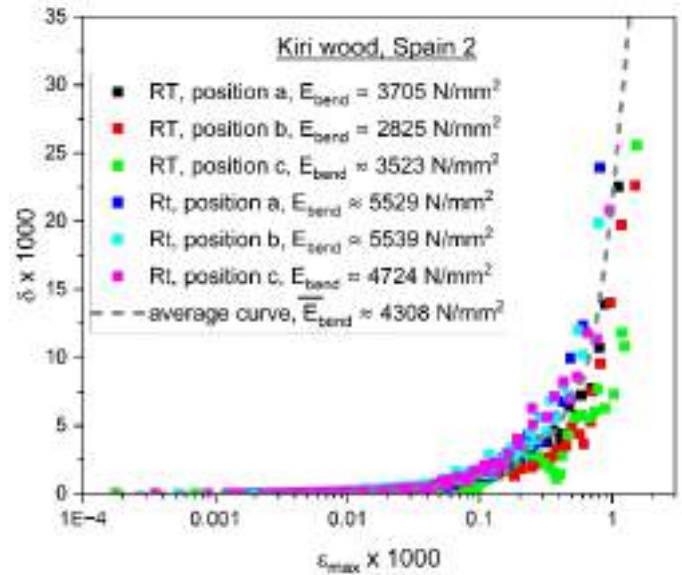


Figure 7. Strain-dependent damping of Kiri wood from Spain (2) in consideration of the fibre orientation. The calculated bending modulus  $E_{bend}$  is added

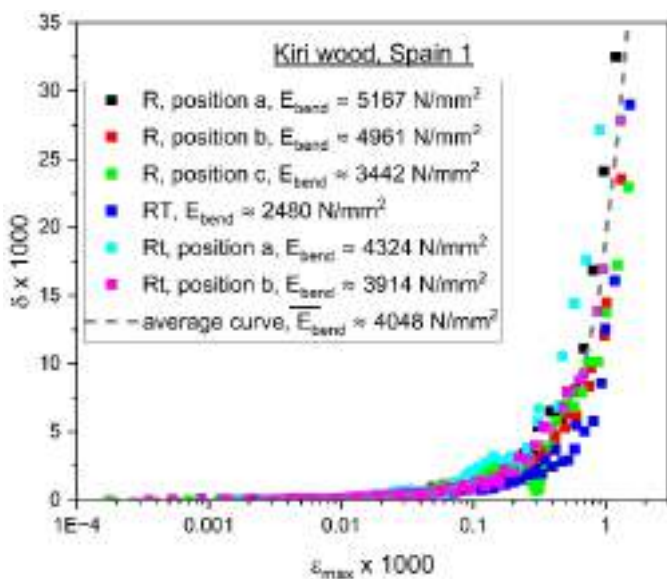


Figure 6. Strain-dependent damping of Kiri wood from Spain (1) in consideration of the fibre orientation. The calculated bending modulus  $E_{bend}$  is added

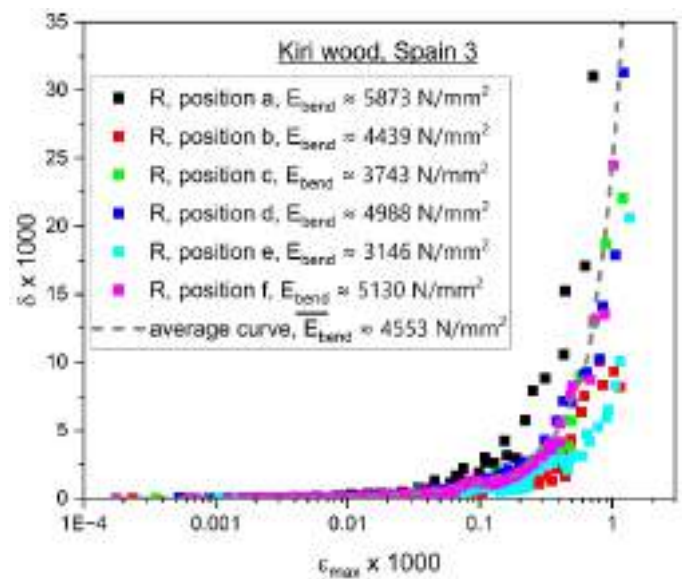


Figure 8. Strain-dependent damping of Kiri wood from Spain (3) in consideration of the fibre orientation. The calculated bending modulus  $E_{bend}$  is added

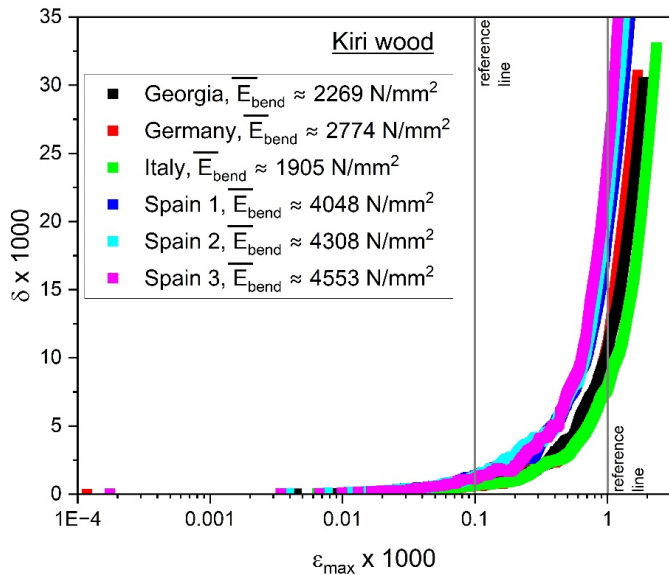


Figure 9. Mean strain-dependent damping curves of Kiri wood. The calculated mean bending modulus  $\bar{E}_{bend}$  is added

#### 4. Discussion

According to Golovin [22], a damping categorization can be made on the basis of the damping value at  $\epsilon_{max}$  of about 0.1% (see Table 3). Based on this, Kiri wood can be regarded as a medium damping material.

It is necessary to classify the results of the strain-dependent damping of Kiri wood. In this context, the results of the non-invasive German variant of Kiri wood are compared to the strain-dependent damping of the softwood pine and the hardwood beech. This comparison is shown in Figure 10.

It is obvious that the bending modulus of beech wood and pine wood depends on the fibre direction and ranges from approximately 9000 N/mm<sup>2</sup> to 13800 N/mm<sup>2</sup> for beech wood (literature value for American beech: 11900 N/mm<sup>2</sup> [23]) and between 9000 N/mm<sup>2</sup> and 12500 N/mm<sup>2</sup> for pine wood (literature value: 8500 N/mm<sup>2</sup> - 13700 N/mm<sup>2</sup> [23]). The observed differences in the bending modulus of the Kiri wood samples from different regions might be attributed to the influence of varying site conditions (e.g., nutrient or water content of the soil) leading to individual structural changes in the wood [24].

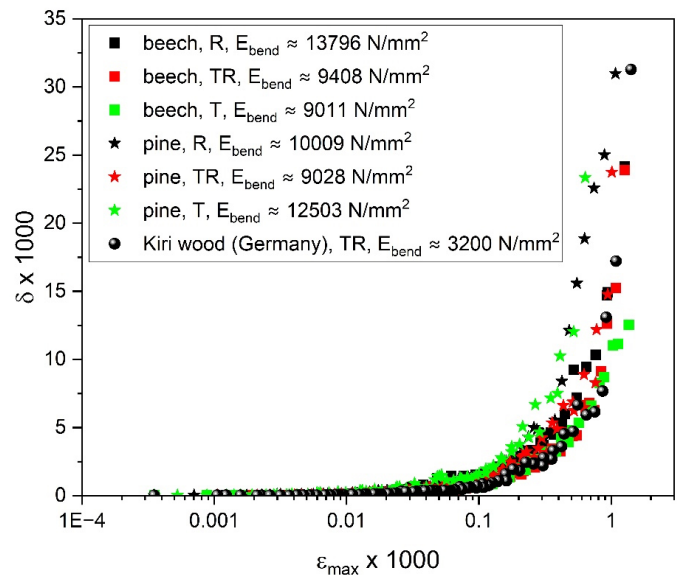


Figure 10. Strain-dependent damping of different woods. The calculated bending modulus  $E_{bend}$  is added

Kiri wood has an average bending modulus of around 3200 N/mm<sup>2</sup> and is therefore to be described as soft. According to literature, its bending modulus ranges from 2651 N/mm<sup>2</sup> to 4917 N/mm<sup>2</sup> [25]. Both beech wood and pine wood are used as tonewoods. The damping behaviour of Kiri wood is very similar to that of beech wood. So, it is not surprising that Kiri wood is used as tonewood, too. Its damping properties, combined with its climate friendliness and the possibility of local cultivation (resulting in a short logistics chain), make it suitable for areas requiring higher sound absorption, especially in the shipping industry.

As shown in Figures 3-8, all damping curves have the same shape, indicating a similar damping mechanism. Figure 11 illustrates the assumed mechanical reaction of the wood's honeycomb-like cell structure to an external force. It is surmised that the cell wall acts as a spring, with an external force causing displacement. The restoring force (referred to as "internal force") attempts to restore the cell wall's original shape. However, this mechanism represents elastic behaviour and cannot be considered the cause of the damping.

Table 3. Comparison of damping data at different maximum strain amplitudes

$\epsilon_{max} \times 1000$	$\epsilon_{max}$ in %	$\delta \times 1000$ , Georgia	$\delta \times 1000$ , Germany	$\delta \times 1000$ , Italy	$\delta \times 1000$ , Spain 1	$\delta \times 1000$ , Spain 2	$\delta \times 1000$ , Spain 3
0.1	0.01	0.74	0.61	0.63	1.36	1.33	1.16
1	0.1	10.52	10.92	7.83	19.19	21.41	24.46



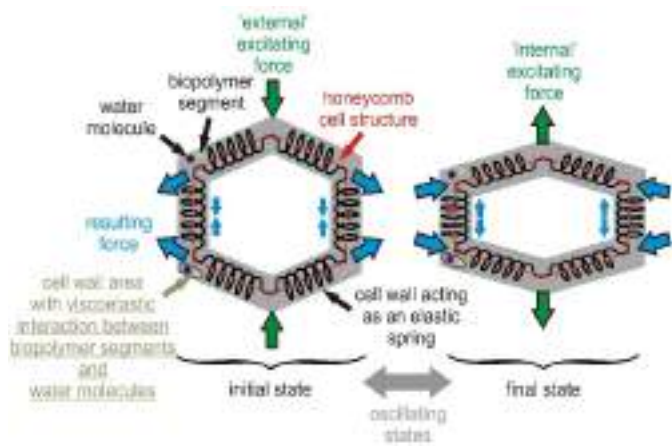


**Figure 11.** Visualization of the effect of an external force on the honeycomb cell structure of Kiri wood

The actual causes of the damping are the water molecules and segments of biopolymers present in the wood's cell wall. It is assumed that a primarily viscoelastic interaction occurs between the biopolymers and water molecules. However, a secondary viscoelastic interaction among the biopolymers cannot be ruled out. Therefore, wood damping is largely determined by the components present in the cell wall structure and their interactions.

In metals, the strain amplitude dependency of the loss tangent observed in this study is known from an unpinning process from obstacles (e.g., impurity atoms or precipitates) as explained in the Granato and Lücke [26] theory of dislocation damping. Following this approach, a similar mechanism is assumed here, where the obstacles are clusters consisting of connections of biopolymer segments with water molecules.

As shown in Figure 12, for small maximum strain amplitudes  $\varepsilon_{max}$ , it is presumed that mainly biopolymer segments exert a small movement (bowing out mechanism). If the maximum strain amplitude increases, weaker bonds between the biopolymer segments are occasionally broken. These bonds are referred to as 'potential' bonds, as they cannot be completely excluded. The stronger bond between the biopolymer segments and the water molecules (referred to as 'real' bonds) becomes progressively strained. Ultimately, this bond is also broken, leaving behind an unavoidable bond between the water molecules themselves. Meanwhile, new pairings of biopolymer segments with water molecules, as well as among the biopolymer segments themselves, have formed. The damping of wood is therefore significantly dependent on the moisture content and the proportion of biopolymers present in the cell structure. The lengths  $L$  and  $l$  declared in the figure ( $L$ : mean distance of the water

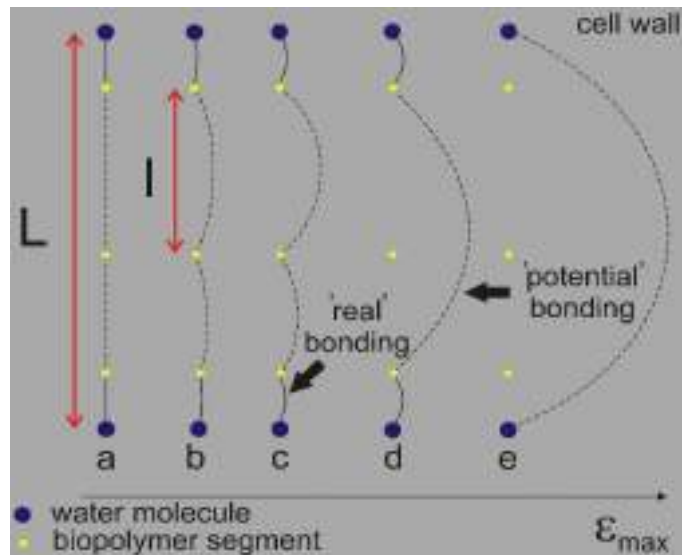


**Figure 12.** Interaction between biopolymer segments with water molecules in the wood's cell wall (see also Figure 11). An unpinning mechanism takes place at increasing maximum strain amplitude  $\varepsilon_{max}$

molecules,  $l$ : mean distance of the biopolymer segments) can thus be interpreted as content statements concerning the respective water molecules and biopolymers.

This approach is based on studies of Becker and Noack [27]. They point out that groups of molecules from parts of cellulose, hemicellulose, and lignin (structural components of the wood cell wall) can move. Furthermore, water molecules connected to these groups by sorption forces influence the distance between molecules, their mobility, orientation, and the dipole moment of polar groups. In the wood fibre system, the potential adsorption sites are the hydroxyl groups and the carboxyl groups [28]. Amorphous wood polymers or segments have a higher affinity to form a bond with water [29]. Therefore, the moisture content has a significant influence on the wood damping. This was shown in a former own work [30].

Ashby has compiled a large number of material properties in the form of materials selection maps. Figure 13 shows such an "Ashby chart". In this chart, the damping of various materials is plotted against the Young's modulus. As there is hardly any damping data available for Kiri wood to date, and the vibration experiments carried out allowed the bending modulus to be determined, the damping data for the strain range listed in Table 3 was inserted in Figure 13.

When comparing the range determined for Kiri wood with that of Pine wood, a higher damping is expected for Pine wood, according to Figure 13. This result is confirmed by the damping data for Pine wood obtained in Figure 10 compared to Kiri wood.

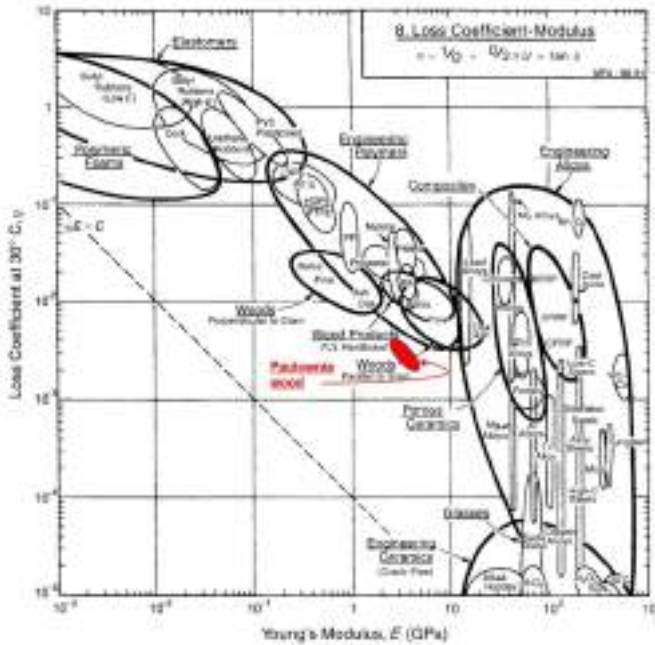


**Figure 13.** Material property chart “Ashby chart”. The loss coefficient  $\eta$  is plotted versus the Young’s modulus. Own damping data (taken from Table 3; note:  $\eta = \delta/\pi$ ) and data of the bending modulus (taken from Figure 9; note: bending modulus = Young’s modulus) of Kiri wood are added. Adopted from [31] (modified)

Wood typically exhibits a rectangular cell structure, causing anisotropy in the mechanical properties. A round cell structure would result in isotropic mechanical properties. In the case of Kiri wood, the honeycomb shape of the cell structure can be seen as a mixture of rectangular and round shapes. Despite different fibre orientations, Kiri wood demonstrates a quasi-isotropic damping behaviour, allowing for more universal use.

## 5. Conclusion

A fast-growing timber which is designated as climate tree and demonstrably enables plantation cultivation is Paulownia wood. It is also known as Kiri wood. The usual varieties are considered invasive. A new non-invasive Paulownia variety is called Paulownia NordMax21<sup>®</sup> and is a German hybrid of Paulownia tomentosa and Paulownia fortunei. Its damping behaviour was investigated and compared with common Paulownia varieties harvested in Georgia, Italy and Spain.

The damping was measured as logarithmic decrement of freely decaying bending vibrations and determined as a function of the maximum strain amplitude. All damping curves could be divided into a strain-independent and a strain-dependent range where the latter one is interpreted as hysteretic damping. Such behaviour is well known for strain-dependent damping measurements of metals where pinning/unpinning of defects from pinning points in the structure (e.g., dislocations) can be found (Granato-Lücke

model). A similar approach was introduced. It is assumed that biopolymer segments and water molecules form a bond. A weaker bond may also occur between biopolymer segments. With increasing maximum strain amplitude, these bonds are stressed and can fail (unpinning mechanism). This leads to viscoelastic material behaviour, which manifests itself in the form of damping.

It is therefore hardly surprising that moisture content significantly influences the wood damping. However, Kiri wood is the first choice in environments with changing humidity levels (e.g., like on board ships) due to its extremely low swelling and shrinking behaviour. Consequently, a relatively constant damping value is to be expected despite fluctuations in humidity.

The damping data, along with the determined bending moduli, were added to an existing “ashby chart”. Although the damping of Kiri wood is lower than that of balsa wood, it shows less dependence on the fibre orientation (leading to a quasi-isotropic damping behaviour), which might be attributed to the honeycomb structure of the Kiri wood.

Since wood is a renewable resource, particularly with Kiri wood, it combines properties of sustainability, aesthetics, and functionality. Especially Kiri wood is lightweight, which means less energy is needed in transporting this material. The advantage of weight savings is particularly significant in different areas like: construction (e.g., tiny houses, wooden facades), mobility (e.g., model and glider aircraft, caravan construction) and lifestyle (e.g., furniture, home accessories such as vases and bowls). Kiri wood has enormous application potential in these areas and also opens up a large field of research.

## Acknowledgements

Prof. Dr. Jürgen Göken would like to thank the KIRITEC GmbH (Tönisvorst, Germany) for providing the Kiri wood used in this work. The Meyer Möbelmanufaktur GmbH (Westoverledingen, Germany) is thanked for producing the Kiri wood samples. Special thanks go to the students Ms. A. Liehm and Mr. K. Legene, who carried out the recording of the raw data as part of their respective bachelor thesis.

## Footnotes

### Authorship Contributions

Concept design: J. Göken, and N. Saba, Data Collection or Processing: J. Göken, Analysis or Interpretation: J. Göken, and N. Saba, Literature Review: J. Göken, and N. Saba, Writing, Reviewing and Editing: J. Göken, and N. Saba.

**Funding:** The authors did not receive any financial support for the research, authorship and/or publication of this article.

## References

- [1] International Maritime Organization (IMO), *The Hong Kong international convention for the safe and environmentally sound recycling of ships*. London, UK: IMO, 2009.
- [2] C. Ward, "Building pharaoh's ships: Cedar, incense and sailing the Great Green". *British Museum Studies in Ancient Egypt and Sudan*, vol. 18, pp. 217-232, Aug 2012.
- [3] J. Rice, R. A. Kozak, M. J. Meitner, and D. H. Cohen, "Appearance wood products and psychological well-being". *Wood and Fiber Science*, vol. 38, pp. 644-659, Oct 2006.
- [4] ISO Standard, *ISO 2923:1996: Acoustics - Measurement of Noise on board vessels*. Geneva, Switzerland: International Organization for Standardization, 1996.
- [5] International Labour Organisation, *ILO Code of practice: protection of workers against noise and vibration in the working environment*. Geneva, Switzerland: International Labour Organisation, 1984.
- [6] UK. International Maritime organization (IMO), *code on noise levels on board ships*. London: IMO Resolution A.468(XII); 1981. [Online]. Available: [https://wwwcdn.imo.org/localresources/en/KnowledgeCentre/IndexofIMOResolutions/AssemblyDocuments/A.468\(12\).pdf](https://wwwcdn.imo.org/localresources/en/KnowledgeCentre/IndexofIMOResolutions/AssemblyDocuments/A.468(12).pdf). [Accessed: Sep 13, 2024].
- [7] R. Mosandl, and B. Stimm, "Kurzportrait Blauglockenbaum (Paulownia tomentosa)". 2015. [Online]. Available: <https://www.waldwissen.net/de/waldwirtschaft/waldbau/kurzportrait-blauglockenbaum> [Accessed: Sep 13, 2024].
- [8] *Trees Help Tackle Climate Change*. [Online]. Available: <https://www.eea.europa.eu/articles/forests-health-and-climate-change/key-facts/trees-help-tackle-climate-change>. [Accessed: Sep 13, 2024].
- [9] *Eigenschaften und Fakten Kiri Holz*. [Online]. Available: <https://www.kiritec.eu/kiriholz-eigenschaften/>. [Accessed: Sep 13, 2024].
- [10] *Kiri Wood - A Demanded RRaw material with many positive properties*. [Online]. Available: <https://wegrow-croptec.com/en/how-to-grow-2/kiri-wood/>. [Accessed: Sept. 13, 2024].
- [11] Resolution MSC.307(88), *International Code for application of fire test procedures*, 2010. [Online]. Available: <https://wwwcdn.imo.org> [Accessed: Nov 19, 2024].
- [12] H. N. Psaraftis, and C. A. Kontovas, "Balancing the economic and environmental performance of maritime transportation". *Transportation Research Part D: Transport and Environment*, vol. 15, pp. 458-462, Dec 2010.
- [13] C. A. Welter, D. T. de Farias, P. H. G. de Cademartori, C. de Bona da Silva, and C. Pedrazzi, "Valorization of Paulownia tomentosa wood wastes to produce cellulose nanocrystals". *CERNE*, vol. 30, e-103343, Sep 2024.
- [14] J. Gadermaier, et al., "Soil water storage capacity and soil nutrients drive tree ring growth of six European tree species across a steep environmental gradient". *Forest Ecology and Management*, vol. 554, 121599, Feb 2024.
- [15] *NordMax 21*. [Online]. Available: <https://www.paulownia.at/product/nordmax-21/>. [Accessed: Sep 13, 2024].
- [16] A. Liehm, *Messungen der dehnungsabhängigen Dämpfung von Paulownia-Holz (Measurements of the strain-dependent damping of Paulownia wood)*, Bachelor thesis, Faculty of Maritime Sciences, Laboratory of Materials Physics, University of Applied Sciences Emden/Leer, Leer, Germany, 2024. (in German).
- [17] Z. Trojanová, P. Palček, P. Lukáč, and M. Chalupová, "Internal friction in magnesium alloys and magnesium alloy-based composites". in *Magnesium Alloys*, M. Aliofkhazraei, Ed. London, UK: IntechOpen Limited, 2017, ch. 2.
- [18] M. S. Blanter, I. S. Golovin, H. Neuhäuser, and H.-R. Sinning, *Internal Friction in Metallic Materials - A Handbook*. Berlin, Germany: Springer, 2007.
- [19] S. Sohn, "Feasibility study on the use of wireless accelerometers in the experimental modal testing". *The Journal of Supercomputing*, vol. 72, pp. 2848-2859, Jan 2016.
- [20] J. Göken, and N. Saba, "Strain-dependent damping of Paulownia wood at room temperature and constant moisture content". *Romanian Journal of Physics*, 2024.
- [21] Z. Trojanová, P. Lukáč, J. Džugan, and K. Halmešová, "Amplitude dependent internal friction in a Mg-Al-Zn alloy studied after thermal and mechanical treatment". *Metals*, vol. 7, 433, Oct 2017.
- [22] I. S. Golovin, "Damping mechanisms in high damping materials". *Key Engineering Materials*, vol 319, pp. 225-230, Sep 2006.
- [23] D. E. Kretschmann, "Mechanical properties of wood". In *Wood Handbook: Wood as an Engineering Material*, U.S. Department of Agriculture, Forest Service, Forest Products Laboratory, Ed. Madison, WI, USA: General Technical Report FPL-GTR-190, 2010, ch. 5.
- [24] T. dos Santos Angélico, C. R. Marcati, S. Rossi, M. R. da Silva, and J. Sonsin-Oliveira, "Soil effects on stem growth and wood anatomy of tamboril are mediated by tree age". *Forests*, vol. 12, 1058, Aug 2021.
- [25] M. Jakubowski, "Cultivation potential and uses of Paulownia wood: a review". *Forests*, vol. 13, 668, Apr 2022.
- [26] A. Granato, and K. Lücke, "Theory of mechanical damping due to dislocations". *Journal of Applied Physics*, vol. 27, pp. 583-593, Jun 1956.
- [27] H. Becker, and D. Noack, "Studies on dynamic torsional viscoelasticity of wood". *Wood Science and Technology*, vol. 2, pp. 213-230, Sep 1968.
- [28] A.-M. Olsson, and L. Salmén, "The association of water to cellulose and hemicellulose in paper examined by FTIR spectroscopy". *Carbohydrate Research*, vol. 339, pp. 813-818, Mar 2004.
- [29] E. T. Englund, L. G. Thygesen, S. Svensson, and C. A. S. Hill, "A critical discussion of the physics of wood-water interactions". *Wood Science and Technology*, vol. 47, pp. 141-161, 2013.
- [30] J. Göken, N. Saba, and I. S. Golovin, "Damping of spruce wood at different strain amplitudes, temperatures and moisture contents". *Romanian Journal of Physics*, vol. 68, 903, 2023.
- [31] M. F. Ashby, *Materials Selection in Mechanical Design, 2<sup>nd</sup> edition*. Oxford, UK: Butterworth-Heinemann, 1999, pp. 48

# Strategic Management Modeling for Offshore Tugboat and Support Vessel Operations: A Hybrid SWOT-TOWS Fuzzy DEMATEL-TOPSIS Framework

● Ali Burçin Eke<sup>1</sup>, ● Ozan Batmaz<sup>2</sup>, ● Muhammed Fatih Gülen<sup>1</sup>, ● Esmâ Uflaz<sup>1</sup>, ● Özcan Arslan<sup>1</sup>

<sup>1</sup>Istanbul Technical University Faculty of Maritime, Department of Maritime Transportation and Management Engineering, İstanbul, Türkiye

<sup>2</sup>Dokuz Eylül University Faculty of Maritime, Department of Maritime Transportation and Management Engineering, İzmir, Türkiye

## Abstract


The maritime sector, particularly in offshore tugboat and support vessel operations, faces multifaceted strategic management challenges due to rapid technological advancements, environmental regulations, and market conditions. This paper introduces an innovative strategic decision-making framework for this industry, integrating Strengths, Weaknesses, Opportunities, and Threats (SWOT) analysis with Fuzzy Decision Making Trial and Evaluation Laboratory-DEMATEL and Order of Preference by Similarity to Ideal Solution-TOPSIS methodologies. A thorough extensive literature review and expert contributions identified 20 key factors impacting the sector across 4 SWOT categories, with balanced weights of 25.14% (strengths), 25.32% (weaknesses), 24.68% (opportunities), and 24.86% (threats). The hybrid approach uniquely highlights the interdependencies among these factors, offering a prioritized list of 8 strategic options. The analysis revealed that the WO1 strategy (focusing on cost reduction through technological innovation) emerged as the most effective strategy with a closeness coefficient of 0.798, followed by SO2 (operational efficiency enhancement) at 0.642, and ST1 (leveraging experienced crew and advanced technology) at 0.550. These results show that operational cost reduction through technological innovation and emerging market entry is a strategic priority. This study contributes significantly to the existing literature by providing a robust strategic management model tailored to address the unique challenges of offshore maritime operations. These insights are useful for improving operational efficiency for industrialists with sustainability-related concerns and for furthering their competitive advantage in an increasingly dynamic global environment. Moreover, the study also provides a replicable model that can be applied to other industries where similarly complex decisions can be made.

**Keywords:** SWOT, TOWS fuzzy DEMATEL, TOPSIS, Strategic management, Offshore tugboat and support vessel operations

## 1. Introduction

Sea trade has also, for a very long time, played the role of a building block in shaping trade, travel, and transportation among people. One of the defining attributes of this great industry is its towage services [1]. A tugboat can be described as a handy vessel built to pull or push other vessels

through harbors, coastal areas and rivers [2]. In particular, tugboats are responsible for ensuring the safety and efficiency of congested ports and narrow channels during ships' movements [3]. With the increasing volumes of global maritime trade, the volume of work also increases for each port, which serves to connect land transport with that of the

 **Address for Correspondence:** Esmâ Uflaz, İstanbul Technical University Faculty of Maritime, Department of Maritime Transportation and Management Engineering, İstanbul, Türkiye  
**E-mail:** uflaz16@itu.edu.tr  
**ORCID iD:** orcid.org/0000-0003-2229-8242

**Received:** 12.09.2024  
**Last Revision Received:** 09.12.2024  
**Accepted:** 16.12.2024

**To cite this article:** A. B. Eke, O. Batmaz, M. F. Gülen, E. Uflaz, and Ö. Arslan, "Strategic Management Modeling for Offshore Tugboat and Support Vessel Operations: A Hybrid SWOT-TOWS Fuzzy DEMATEL-TOPSIS Framework." *Journal of ETA Maritime Science*, vol. 12(4), pp. 427-445, 2024.

 Copyright© 2024 the Author. Published by Galenos Publishing House on behalf of UCTEA Chamber of Marine Engineers. This is an open access article under the Creative Commons AttributionNonCommercial 4.0 International (CC BY-NC 4.0) License

sea. Tugboats, as essential port services, support vessels by escorting, towing, berthing, and departure, especially in congested narrow waterways where maneuverability is impeded. Without the assistance of tugboats, large vessels risk losing control. This can lead to collisions with nearby vessels, docks, and other port facilities. Therefore, tugboat operations are crucial for the safe and efficient management of ports [4].

Climate change is among the global problems that humanity is currently facing. The port industry by its nature related to international trade, contributes to greenhouse gas emissions through the operational functions of tugboats. These emissions raise environmental and health hazards, particularly in highly populated ports, and are one of the causes of climate change. Environmental measures such as switching to cleaner and more renewable energy sources are therefore being sought by port authorities and tugboat operators [5]. Technological changes characterize modern-day towage services. The invention of modern tugboats operating in traditional and hazardous waters has improved the safety and efficiency of the maritime industry [1]. Although emission control technologies are widely applied to ships, very few are applied to tugboats [6]. This means that the development of transport systems, including maritime transport, needs to be directed toward alternative low-carbon fuels, like Liquefied Natural Gas (LNG) and hydrogen [7]. Today, LNG has gained popularity in the maritime industry because of its cleaner energy benefits. It helps reduce harmful emissions like nitrogen oxides, sulfur dioxide, and particulate matter. This, in turn, improves the air quality in ports [8]. Most fuel-powered tugboats emit substances into the atmosphere, which are related to environmental concerns in the maritime field. More eco-friendly technologies, such as electric tugboats, are therefore being increasingly used to address these issues. Electric tugboats greatly minimize harmful emissions and further improve air quality and environmental sustainability, mainly at busy ports [9].

Tugboats, with their high engine power, consume a great deal of fuel and emit huge emissions [10]. Reducing environmental impact and ensuring operational efficiency have gained much importance in the shipping industry. The utilization of hybrid power systems in tugboats is considered beneficial due to several factors, including emission reduction, fuel economy, cost-saving on maintenance, and workplace health improvement [11]. These hybrid systems contribute a great deal to the environment in that they show considerable improvements in terms of emissions when using normal conventional fuels, hence ensuring better air quality. They also reduce operating costs by improving fuel economy and lowering maintenance requirements. As a result, their operational efficiency is enhanced. For instance, the tugboat

Carolyn Dorothy is based on an award-winning dolphin series by Robert Allan Ltd. for its prime power and positioning in restricted waterways. Wider adoption of hybrid propulsion systems can improve the shipping industry's efficiencies with fewer environmental impacts [11].

This research attempts to fill this critical gap in the existing literature by presenting an integrated strategic management framework, specifically designed for offshore tugboat and support vessel operations. Therefore, the major objectives of this study are to identify and prioritize key factors affecting the industry, to analyze their complex relationships, and to prioritize strategic options according to their impact magnitudes. The present study exploits the complementarity of Strengths, Weaknesses, Opportunities, and Threats-Threat, Opportunity, Weakness and Strength (SWOT-TOWS) analysis, Fuzzy Fuzzy Decision Making Trial and Evaluation Laboratory (DEMATEL), and Order of Preference by Similarity to Ideal Solution (TOPSIS) for new synthesis; it therefore provides an in-depth and detailed strategic landscape. Thus, it would help the sector address its issues, such as operational efficiency, cost reduction, improved profitability, and environmental concerns. This study contributes to strategic management literature by providing a strong and quantitative decision-making (DM) framework tailored to the peculiarities of maritime operations. From an industrial practitioner's perspective, it is a useful tool in making difficult strategic choices and setting higher benchmarks with respect to operational and environmental performance. The remainder of this paper is structured as follows: Section 2 reviews the related literature; Section 3 outlines the methodology, and Section 4 presents the findings and discussion. The conclusions and suggestions for future research are presented in Section 5.

## 2. Literature Review

Strategic management businesses first explore changes in the environment and opportunities, along with risks from competition. This step then completes an in-depth analysis of the competitive environment concerning industrial characteristics, competitor activities, and consumer behavior and preferences. Furthermore, they evaluate their resources and capabilities in terms of strengths and weaknesses to meet strategic goals. Based on this, corporations devise special value propositions to retain customer loyalty and generate a sustainable competitive advantage. Strategic management also strives to design policies and methods to improve efficacy, reduce costs, and streamline operations. Together, these interconnected elements constitute the cornerstone of the strategic management process, facilitating businesses in attaining and retaining competitive advantage [12].

Kuzu [13] explored the application of the Fuzzy DEMATEL method to understand and resolve issues in shipbuilding and

structural research. Shi et al. [14] developed a quantitative risk analysis approach using complex networks and DEMATEL to manage ship collision risks, identifying 46 risk-influencing factors (RIFs) and highlighting 10 key RIFs from a global network perspective and 11 from a causality perspective. Liu et al. [15] examined the maritime supply chain's resilience post-coronavirus disease-2019 using Analytic Hierarchy Process-Quality Function Deployment-DEMATEL (AHP-QFD-DEMATEL) to analyze critical resilience factors. Torkayesh et al. [16] proposed an extended DEMATEL method with type-2 neutrosophic numbers and K-means to identify barriers to renewable fuels in Germany's transportation sector. Umut [17] used DEMATEL to evaluate factors causing navigation equipment failures and recommended preventive measures. Guan et al. [18] used Fuzzy DEMATEL to assess barriers to blockchain adoption in port logistics, identifying cause-effect relationships among barriers. Ayaz et al. [19] identified barriers to integrating ports into eco-friendly systems using Fuzzy DEMATEL, highlighting long payback periods and high investment costs as key triggers. Özdemir and Güneroglu [20] employed DEMATEL and Analytic Network Process (ANP) to evaluate human factors in maritime accidents. Durán et al. [21] analyzed strategic synergy within port communities using DEMATEL, emphasizing technological integration and coordination among port actors. Lin [22] developed a new methodology using Balanced Scorecard, DEMATEL, and ANP for risk analysis in maritime accidents. Chen et al. [23] proposed a model for vulnerability assessment based on DEMATEL, Interpretive Structural Modeling, and AHP-entropic weight method in the context of the maritime transportation system. Sun et al. [24] integrated QFD, Multiple Criteria Decision Making (MCDM), and Intuitionistic Fuzzy Sets with DEMATEL to tackle uncertainty and complexity in the bauxite maritime supply chain. Muravev et al. [25] indicated several issues regarding the China Railway Express and proposed the DEMATEL-Multi Atributive Ideal-Real Comparative Analysis for optimizing the locations of international logistics centers. Hossain et al. [26] used SWOT analysis regarding shipbuilding companies in China in view of the shifting trends of the shipbuilding industry to Asia, based on global economic conditions and trends in shipbuilding orders.

Cheng and Ouyang [27] combined decision matrix and SWOT analyses to develop strategic policies for unmanned autonomous ships, marking a novel approach in this area. Tseng and Pilcher [28] analyzed, from a corporate perspective, the business potential of the Kra Canal using a combined Political, Economic, Societal, Technological, Environmental, Legal and Ethical and SWOT analysis for companies, ports and countries. Vorkapić et al. [29] proposed a framework for

shipboard energy efficiency monitoring while systematically observing internal and external environments and using SWOT to spot strengths, weaknesses, opportunities, and threats. Bauk [30] analyzed the performance of unmanned aerial and underwater vehicles for maritime surveillance, employing SWOT to position these technologies effectively. Aleksanyan [31] conducted a SWOT analysis of autonomous navigation systems based on expert opinions and the influence of reduced crews associated with increased automation. Serra et al. [32] used SWOT analysis and described how blockchain technology affects port and general maritime digitalization, pointing to practical applications and barriers. Papaioannou et al. [33] evaluated the potential of Mobility as a Service in passenger transport, focusing on coastal shipping in Greece's Aegean Islands, through expert interviews and SWOT analysis. Kelfaoui et al. [34] applied SWOT analysis to revitalize rural tourism in Algeria's Great Kabylie community, leveraging a combination of literature review, field research, and analytical approaches. Mafrisal et al. [35] assessed the potential of marine resources to enhance community welfare in Indonesia's Makassar archipelago using integrated planning and SWOT analysis. Oral and Paker [36] identified and prioritized security risks in container shipping between Turkey and the Far East, employing the Delphi technique and SWOT analysis. Palmén et al. [37] evaluated energy sources for an Arctic research icebreaker by conducting a SWOT analysis on fuel options, infrastructure suitability, and operational resilience, followed by a comprehensive assessment of fuel tank space, lifetime costs, and CO<sub>2</sub> emissions. Kizielewicz and Sałabun [38] investigated the impact of using information-based methods, such as entropy and standard deviation, for re-identifying criterion weights in multi-criterion decision analysis when expert input was limited. Gazi et al. [39] identified key criteria for women's empowerment in sports by employing literature review, expert opinions, and direct interactions with sector professionals and applied the DEMATEL method with pentagonal fuzzy sets to address uncertainties, thereby providing strategic decision support. Elraaid et al. [40] explored the development of construction projects in Libya's Misrata Free Zone, addressing the challenges encountered and utilizing the AHP to identify the role of the Project Management Office in overcoming these obstacles and developing strategic solutions. Kannan et al. [41] developed the Linear Diophantine Fuzzy Set as an extension to traditional fuzzy sets to address uncertainty in human DM and integrated it with the Combinative Distance-based Assessment method, proposing a novel approach for solving complex DM problems characterized by uncertainty and imprecision.

The existing literature offers significant insights into

various dimensions of strategic management, technological advancements, and environmental challenges within the offshore tugboat and support vessel industry. Nevertheless, a critical gap persists in the integration of these diverse elements into a holistic strategic management framework specifically designed for the maritime sector. While individual studies have separately applied SWOT analysis, Fuzzy DEMATEL, and TOPSIS within maritime contexts, the combined and synergistic use of these methodologies to address the complex challenges in offshore support vessel operations remains underexplored. It is also an industry that is dynamic, where continuous change due to technological innovation, strict environmental legislation, and changes in market conditions require a more sophisticated and agile approach to strategic DM. This study aims to fill these gaps by designing an integrated framework that not only highlights and prioritizes strategic factors but also focuses on their complex interrelationships and provides a quantitative basis for the selection of strategies. The basis of this research is embedded in the theoretical discourse on strategic management in specialized maritime operations, while providing relevant tools for industry practitioners to effectively address the complications of their operational environment. The methodology used and findings that directly address these identified gaps are discussed in the following sections, along with specific details.

### 3. Methodology

Most strategic management of offshore tugboats and their support vessels is complex in nature and requires a multifaceted analytical approach. In this respect, the research incorporates SWOT-TOWS analysis, Fuzzy DEMATEL, and TOPSIS to provide in-depth analyses of internal and external factors, the interrelations among these factors, and the determination of priorities in strategic alternatives.

#### 3.1. SWOT-TOWS Analysis

SWOT analysis includes four factors: strengths, weaknesses, opportunities, and threats. The strengths and weaknesses are internal factors, and opportunities and threats are external environmental factors. The SWOT is illustrated as a four-quadrant matrix that categorizes and summarizes these factors for quick comprehension [42]. SWOT analysis examines internal strengths and weaknesses, as well as external opportunities and threats. This analysis aims to leverage strengths, minimize weaknesses, maximize opportunities, and overcome threats [43].

The advantages of SWOT analysis are its simplicity and ease of understanding. It can be used at more than one level within an organization, and the depth can range from a quick assessment to an in-depth analysis. In addition, it links well with corporate objectives and strategies, and the format

is visual, facilitating communication. However, SWOT has notable disadvantages. It often relies on qualitative and subjective data, leading to broad generalizations. The process is susceptible to biases and can confuse data collection and DM. Misapplication is common, especially when fundamental principles and methods are ignored, sometimes resulting in it being considered a significant time-consuming task if not properly facilitated [44]. In particular, when developing alternative strategies based on SWOT analysis, the TOWS matrix is an invaluable tool. As presented by Ghazinoory et al. [45] and shown in Table 1, the TOWS matrix aids in formulating effective strategies by systematically examining SWOT-identified factors. This framework facilitates the creation of effective strategies by systematically assessing the factors identified through SWOT analysis. Specifically, Strengths and Opportunities (SO) strategies are designed to leverage organizational strengths to capitalize on available opportunities. Weaknesses and Opportunities (WO) strategies leverage opportunities to address various weaknesses, preventing potential weaknesses from becoming actual challenges. Strengths and Threats (ST) strategies utilize strengths to overcome or avoid threats, ensuring the organization remains resilient in hostile and adverse environments. Finally, Weaknesses and Threats (WT) strategies call for exploiting defensive measures with respect to both weaknesses and external threats to reduce the risks from such combined threats. This approach promotes a structured methodology for strategic planning that is both adaptive and proactive. This ensures that all critical aspects are considered, providing a comprehensive framework for effective DM [45].

#### 3.2. Fuzzy-DEMATEL

DEMATEL was developed in 1973 by Gabus and Fontela [46] as an MCDM technique. Similar to other MCDM methods, DEMATEL analyses expert opinions and solves DM problems. DEMATEL will be able to measure the weights of the relationships among criteria, considering cause-and-effect relationships among the complex and multiple criteria. DEMATEL is applied in group decisions, such as finding the critical factors influencing the systems of disaster operations management, hospital service quality, industrial symbiosis networks, sustainable supply chains, emergency management, supplier and truck selection, and electric vehicle [47]. The fuzzy DEMATEL method was

*Table 1. TOWS matrix*

Objectives	Strengths (S)	Weaknesses (W)
Opportunities (O)	SO Strategies	WO Strategies
Threats (T)	ST Strategies	WT Strategies
TOWS: Threat, Opportunity, Weakness and Strength		

applied to analyze the complex interrelationships among the SWOT factors. The fuzzy logic was implemented to bear with the uncertainty and subjectivity that would arise in expert judgments.

### 3.3. TOPSIS

The Technique for Order Preference by Similarity to Ideal Solution (TOPSIS) is a multi-criteria DM method that evaluates alternatives based on their proximity to an ideal solution. The ideal solution represents the best possible values for each criterion, while the anti-ideal solution reflects the worst. TOPSIS selects the alternative that minimizes the geometric distance from the ideal solution and maximizes the distance from the anti-ideal solution. One of the primary advantages of TOPSIS is its ability to reduce subjectivity, confining it mostly relies on assigning weights to criteria. This method is also considered to be logically sound because it coincides with rational choice and has the advantage of computational simplicity and ease of implementation. Therefore, it is practical for real applications. The results of TOPSIS can be represented graphically, especially for lower dimensions, which improves interpretability. However, TOPSIS has some limitations, challenges in calculating criteria weights and ensuring decision consistency. Whatever the difficulties related to such issues may imply, TOPSIS's efficiency regarding the complexity-usability trade-off placed it among the most frequently used techniques in multi-criteria decision analysis [48].

### 3.4. Integrated Methodology

This section describes the integration of SWOT-TOWS based fuzzy-DEMATEL and TOPSIS methodologies. The framework of the integrated methodology is presented in Figure 1.

The integration of these methods provides a comprehensive framework for strategic DM. The SWOT analysis provides the foundational factors, and the TOWS matrix enables the identification of initial strategies. The Fuzzy DEMATEL analysis then offers insights into the complex interrelationships among these factors. Finally, TOPSIS uses these insights to quantitatively rank strategic alternatives. This integrated approach overcomes the limitations of using each method in isolation, providing a more robust and nuanced analysis. In addition, all computational steps are presented in this section.

**Step 1. Building the SWOT matrix:** A robust strategic approach requires a comprehensive analysis. Therefore, the first step is to build a solid SWOT matrix. Thus, appropriate subfactors are identified through literature data and expert judgment. The matrix is then completed by identifying alternative strategies. In particular, when alternative strategies are to be developed as a result of SWOT analysis, the TOWS matrix appears as a useful tool. The TOWS matrix

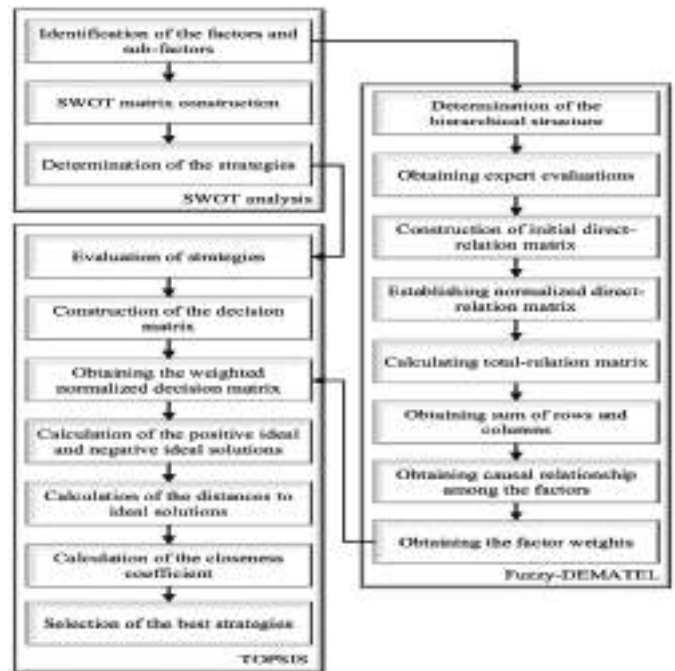


Figure 1. Framework of the integrated methodology

proposed by Ghazinoory et al. [45] is shown in Table 1.

This framework allows effective strategies to be developed by evaluating all factors that emerge from an SWOT analysis. SO strategies use strengths to leverage opportunities. WO strategies focus on eliminating weaknesses by taking advantage of opportunities. ST strategies use strengths to avoid exposure to threats. Finally, WT strategies can be used to develop defensive measures to avoid weaknesses and threats.

**Step 2. Determination of the hierarchical structure:** In this step, the hierarchical structure between the goal, factors, and sub-factors is established.

**Step 3. Obtaining expert evaluations:** The pairwise comparison matrices constructed for the identified SWOT factors and subfactors were evaluated by the experts. For this purpose, a DM group of experts with relevant knowledge and experience is selected. DMs defined their judgments using the linguistic scale presented in Table 2.

**Step 4. Construction of initial direct-relation matrix:** Once the DM assessments are obtained, the linguistic expressions are quizzified and aggregated to establish a direct-relation matrix ( $A$ ).  $A = [a_{ij}]$  is a  $(n \times n)$  non-negative matrix, where  $a_{ij}$  is the direct impact of factor  $i$  on factor  $j$ . The diagonal elements of matrix  $A$  (where  $i = j$ ) are equal to zero.

**Step 5. Establish a normalized direct-relation matrix:** In this step, the normalized direct-relation fuzzy matrix ( $D$ ) is established. Where,  $D = [d_{ij}]$ , all diagonal elements are equal to zero, and all elements are complying with  $d_{ij} \in [0,1]$ .  $D$  can be obtained using Equation 1.



**Table 2.** Linguistic scale for expert judgments

Linguistic scale	Definition	Triangular fuzzy numbers
No	No influence	(0, 0, 0.25)
VL	Very low influence	(0, 0.25, 0.50)
L	Low influence	(0.25, 0.50, 0.75)
H	High influence	(0.50, 0.75, 1)
VH	Very high influence	(0.75, 1, 1)

$$D = \frac{1}{\max_{1 \leq i \leq n} \sum_{j=1}^n a_{ij}} \quad (1)$$

**Step 6. Calculating the total-relation matrix:** After normalizing the initial direct-relation matrix, the next step is to calculate the total-relation matrix. The total-relation matrix,  $T$ , is calculated using Equation 2.

$$T = D(I - D)^{-1} \quad (2)$$

where,  $D$  is the normalized direct-relation fuzzy matrix, and  $I$  stands for a  $n \times n$  identity matrix.

**Step 7. Obtaining  $r_i$  and  $c_j$  values:** In this step, the values of  $r_i$  and  $c_j$  are calculated using Equations 3 and 4.

$$r_i = \sum_{1 \leq j \leq n} t_{ij} \quad (3)$$

$$c_j = \sum_{1 \leq i \leq n} t_{ij} \quad (4)$$

where,  $r_i$  denotes all influence given by criterion  $i$  to all other factors,  $c_j$  indicates the degree of influence. Then the  $r_i$  and  $c_j$  values defuzzified using the Center of Area technique shown in Equation 5.

$$A = \int a \frac{\mu_x(a) da}{\int \mu_x da} \quad (5)$$

**Step 8. Obtaining the causal relationship:** Once the  $r_i$  and  $c_j$  values are obtained,  $(r_i + c_j)$  and  $(r_i - c_j)$  values are calculated to obtain the causal relationship among the factors.  $(r_i + c_j)$  denotes the mutual influence of criterion  $i$  and other system factors,  $(r_i - c_j)$  represents the net influence of criterion  $i$  on the system. If  $r_i - c_j > 0$ , the factor  $i$  is in the cause group, while if  $r_i - c_j < 0$ , the factor  $i$  is in the effect group. Then, a causal diagram is constructed based on these values to simply visualize the complex interrelationships between the factors.

**Step 9. Calculating weights:** In this step, the weights of the factors and sub-factors are calculated using Equations 6 and 7 [49].

$$\omega_i = \sqrt{(r_i + c_j)^2 + (r_i - c_j)^2} \quad (6)$$

$$\tilde{\omega}_i = \frac{\omega_i}{\sum_{i=1}^n \omega_i} \quad (7)$$

where,  $\omega_i$  denotes importance of any factor,  $\tilde{\omega}_i$  stands for the final local weights of the factors and subfactors obtained from the normalization of  $\omega_i$  values. Finally, the local weights of the subfactors are multiplied by the local weights of the relevant factors to obtain the global weights ( $W_j$ ) of each subfactor.

**Step 10. Evaluation of strategies:** In this step, DMs evaluate the relevance of the strategies identified in the first step to SWOT factors using the linguistic scale presented in Table 3.

**Step 11. Construction of the decision matrix:** Once the DM evaluations are obtained from each expert, the decision matrix,  $X = [x_{ij}]$ , is derived by quizzifying the linguistic values.

**Step 12. Obtaining the weighted normalized decision matrix:** The normalized decision matrix,  $\tilde{X} = [\tilde{x}_{ij}]$ , is calculated by using Equation 8.

$$\tilde{x}_{ij} = \frac{x_{ij}}{\sqrt{\sum_{i=1}^n x_{ij}^2}} \quad (8)$$

Then, the factor weights obtained in step 7,  $\tilde{\omega}_i$ , are multiplied with the  $\tilde{x}_{ij}$  values to calculate the weighted normalized decision matrix,  $\tilde{\tilde{X}} = [\tilde{\tilde{x}}_{ij}]$ .

$$\tilde{\tilde{x}}_{ij} = \tilde{x}_{ij} \otimes \tilde{\omega}_i \quad (9)$$

**Step 13. Calculation of the positive and negative ideal solutions:** In this step, the positive and negative ideal solutions,  $A^+$  and  $A^-$ , calculated by using Equations 10 and 11.

$$A^+ = (\tilde{\tilde{x}}_1^+, \tilde{\tilde{x}}_2^+, \dots, \tilde{\tilde{x}}_n^+) = \{max(\tilde{\tilde{x}}_{ij})\} \quad (10)$$

$$A^- = (\tilde{\tilde{x}}_1^-, \tilde{\tilde{x}}_2^-, \dots, \tilde{\tilde{x}}_n^-) = \{min(\tilde{\tilde{x}}_{ij})\} \quad (11)$$

**Step 14. Calculation of the distances to ideal solutions:** The distances of each alternative to the ideal solutions,  $D_i^+$  and  $D_i^-$ , are obtained using Equations 12 and 13.

$$D_i^+ = \sqrt{\sum_{j=1}^n (\tilde{\tilde{x}}_{ij} - \tilde{\tilde{x}}_j^+)^2} \quad (12)$$

$$D_i^- = \sqrt{\sum_{j=1}^n (\tilde{\tilde{x}}_{ij} - \tilde{\tilde{x}}_j^-)^2} \quad (13)$$

**Table 3.** Linguistic scale for TOPSIS

Scale	Linguistic variables
1	Very low
2	Low
3	Moderate
4	High
5	Very high

TOPSIS: Order of Preference by Similarity to Ideal Solution

where  $D_i^+$  is the distance from  $A^+$ , and  $D_i^-$  is the distance from  $A^-$ .

**Step 15. Calculation of the closeness coefficient:** Then, the relative closeness to the ideal solution,  $\mathcal{C}_i^*$ , is calculated using Equation 14.

$$\mathcal{C}_i^* = \frac{D_i^+}{D_i^+ - D_i^-} \quad (14)$$

**Step 16. Selection of the best strategies:** Finally, the strategies are ranked in descending order according to their  $\mathcal{C}_i^*$  values. The strategies with the highest  $\mathcal{C}_i^*$  values are the closest to the ideal solution, i.e., they were considered the best strategies.

## 4. Practical Implementation of the Methodology

### 4.1. Numerical Analysis

This section describes the application of the integrated methodology for the strategic management of offshore tugboat and support vessel operations. Initially, a group of 5 experts with in-depth knowledge and experience on the subject was formed to contribute to the DM process. The detailed DM profiles are presented in Table 4.

Then, the computational steps of the integrated methodology presented in section 3.4 are applied.

A comprehensive literature review formed the initial framework for identifying key SWOT factors by drawing on relevant studies on maritime operations, strategic management, and offshore vessel operations. In this study, the selection of experts was crucial to ensure the validity and reliability of the SWOT-TOWS and DEMATEL analyses. Twelve experts were chosen from various maritime industry segments to create the SWOT matrix, including senior managers from companies like ALP Maritime, Boskalis, Spanopoulos, Iskolden, Tüpraş, Uzmar, and Ata Offshore, as well as academic researchers, technical experts, and industry consultants. These experts were selected based on their extensive knowledge, experience, and active involvement in the maritime sector. A comprehensive questionnaire was designed to identify and evaluate relevant SWOT factors

for offshore tugboat and support vessel operations. The questionnaire was distributed electronically to the selected experts. As an initial analysis step, a third-party analysis helped compile a SWOT list highlighting the most significant strengths, weaknesses, opportunities, and threats relevant to offshore operations. A total of 20 factors were identified and are presented in Table 5.

**Step 1. Building the SWOT matrix:** Based on the literature data and expert consultations, internal (strengths and weaknesses) and external (opportunities and threats) factors related to offshore tugboat and support vessel operations were identified. Thus, a SWOT matrix was created by identifying five subfactors for each factor. Finally, the SWOT matrix was constructed by identifying eight alternative strategies within the framework of the TOWS matrix presented in Table 1. The final TOWS matrix is presented in Table 5.

**Step 2. Determination of the hierarchical structure:** The hierarchical structure based on SWOT factors and subfactors is presented in Figure 2.

**Step 3. Obtaining expert evaluations:** To determine the hierarchy between SWOT factors and subfactors, DMs performed pairwise comparisons using the linguistic scale presented in Table 2. The data of the “Strengths” factor obtained from five DMs is shared as an example in Table 6. Pairwise comparisons were also performed for the main factors, weaknesses, threats, and opportunities identified by all DMs.

**Step 4. Construction of initial direct-relation matrix:** After obtaining the evaluations from all five DMs, the linguistic values were aggregated by converting them into triangular fuzzy numbers according to the scale in Table 2. Thus, five separate initial direct-relation fuzzy matrices were constructed for the goal and each factor. As an example, the fuzzification of the linguistic assessment from DM1 is presented in Table 6. After the evaluations of the other four DMs are quizzified in the same manner, the aggregated expert evaluation matrix (i.e., the initial direct-relation matrix) is obtained by averaging all evaluations. The initial direct-relation matrix of the strengths is shown in Table 6 as an example.

*Table 4. Profile of the DMs*

DM	Professional rank	Sea experience	Current profession	Educational level
1	Master	10	Operation Manager	BSc
2	Chief Officer	7	Academician	PhD
3	Master	12	Fleet Manager	MSc
4	Master	21	Chartering Manager	BSc
5	Master	15	Fleet Manager	MSc
DMs: Decision-makings				

Table 5. SWOT matrix

	Strengths		Weaknesses	
SWOT	S <sub>1</sub>		<b>Experienced Crew:</b> Skilled personnel with expertise in handling complex offshore operations [50].	W <sub>1</sub> <b>High Operational Costs:</b> Significant expenses related to fuel, maintenance, and crew wages reduce overall profitability [51].
	S <sub>2</sub>		<b>Advanced technology:</b> Modern tugboats equipped with state-of-the-art technology, enhancing safety and efficiency [6].	W <sub>2</sub> <b>Dependency on a Single Market:</b> Heavy reliance on the oil and gas sector makes businesses in this industry vulnerable to market fluctuations in this industry [52].
	S <sub>3</sub>		<b>Strong Client Relationships:</b> Established long-term contracts and trusted partnerships with leading oil and gas companies [53].	W <sub>3</sub> <b>Vulnerability to Weather Conditions:</b> Operations are highly susceptible to disruptions caused by adverse weather conditions, which affect service delivery [3].
	S <sub>4</sub>		<b>Diversified Service Offerings:</b> Provide a wide range of services, including towing, escorting, and offshore support, to enhance market adaptability [54].	W <sub>4</sub> <b>High-capital investment:</b> Significant capital investment required for fleet maintenance, upgrades, and expansion, which may strain financial resources [55,56].
	S <sub>5</sub>		<b>Innovation in Vessel Design and Efficient Resource Management:</b> Continuous improvement and modernization of vessel designs, coupled with optimized use of fuel, spare parts and other resources, enhance operational efficiency and reduce costs while meeting evolving industry standards and client needs [57].	W <sub>5</sub> <b>Limited Innovation Culture and Research Gaps:</b> A lack of a proactive approach toward innovation and insufficient research in the literature related to offshore tugboat and support vessel operations may hinder the adoption of new technologies and best practices, impacting the company's ability to remain competitive and efficient [58].
Opportunities	SO <sub>1</sub>		Leverage strong client relationships and diversified service offerings to expand into emerging markets and meet increasing demand for offshore services. By capitalizing on existing relationships and diverse capabilities, the company can broaden its market presence and secure more stable revenue streams.	WO <sub>1</sub> Address high operational costs and dependency on a single market by adopting technological advancements that improve fuel efficiency, reduce maintenance expenses, and support diversification into renewable energy projects and emerging markets. Additionally, they should enhance crew retention programs and adopt new training methods that utilize government incentives aimed at workforce development.
O <sub>1</sub>	<b>Expanding renewable energy sources:</b> The growing demand for offshore windfarms and other renewable energy projects offers new avenues for diversification and growth [59].			
O <sub>2</sub>	<b>Technological Advancements &amp; Fleet Modernization:</b> Opportunities to adopt cutting-edge technologies, such as autonomous vessels and advanced navigation systems, to enhance operational efficiency. In addition, there are opportunities to invest in new, energy-efficient vessels that reduce operating costs and improve competitiveness [60].			

Table 5. Continued

		Strengths		Weaknesses	
$O_3$	<b>Emerging Markets:</b> Expansion into developing regions with increasing offshore exploration and production activities, providing access to new markets [61].	$SO_2$	Enhance operational efficiency and vessel design innovation while implementing eco-friendly operations to capitalize on technological advancements and fleet modernization. This strategy also involves aligning with government incentives to further the use of alternative energy sources and reduce environmental impact, thus ensuring a competitive edge.	$WO_2$	Improve marketing strategies and strengthen vulnerability to weather conditions by investing in fleet modernization and adopting advanced navigation systems and weather forecasting technologies, thereby ensuring better operational resilience and market adaptability.
$O_4$	<b>Increased demand for offshore services:</b> The growing global energy demand, particularly in offshore oil and gas, could lead to an increased need for support vessels [62].				
$O_5$	<b>Rising Importance of Maritime Safety:</b> An increasing focus on maritime safety and risk management could create a demand for specialized services, such as emergency response and safety training [63].				
Threats	$ST_1$				
$T_1$	<b>Market Volatility:</b> Fluctuations in global oil prices could reduce demand for offshore support services, affecting revenue stability [64].	$ST_2$	Using experienced crew members, advanced technology, and innovation in vessel design and resource management to maintain operational efficiency, mitigate the impacts of market volatility, and stay ahead of technological disruptions, ensuring long-term competitiveness.	$WT_1$	Reduce high operational costs and streamline logistics by implementing cost-saving technologies and automated systems, addressing the threats of intense competition and environmental risks. This involves developing contingency plans for weather-related disruptions.
$T_2$	<b>Environmental Regulations:</b> Increasingly stringent environmental regulations may increase operational costs and challenges [65].				
$T_3$	<b>Geopolitical Risks:</b> Political instability in key operational regions can disrupt activities and affect the stability of contracts [66].	$ST_2$	Strengthen strong client relationships and resilient fleet to secure contracts in politically stable regions while minimizing the risks associated with geopolitical instability while optimizing operational costs to reduce the financial impact of economic downturns.	$WT_2$	Mitigate the risks associated with high capital investments and address the research gaps by securing long-term financing options and exploring strategic alliances, while improving marketing strategies to enhance brand visibility and counter market volatility.
$T_4$	<b>Environmental Risks:</b> The potential for environmental incidents, such as oil spills, poses a risk to reputation and financial stability [67].				
$T_5$	<b>Economic Downturns:</b> Global economic downturns could reduce investment in offshore projects, impacting demand for services [68].				

SWOT: Strengths, Weaknesses, Opportunities, and Threats

**Step 5. Establish a normalized direct-relation matrix:** The initial direct-relation matrices were normalized by applying Equation 1. The normalized direct-relation matrix calculated for the strengths is shown in Table 6 as an example.

**Step 6. Calculating the total-relation matrix:** After obtaining the normalized direct-relation matrix, the total-relation matrix was calculated using Equation 2. The total relation matrix calculated for strengths is presented as an example in Table 6.

**Step 7. Obtaining  $r_i$  and  $c_j$  values:** In this step,  $r_i$  and  $c_j$  values were obtained and defused by using Equations 3-5. The calculated strength values are shown in Table 6 as an example.

**Step 8. Obtaining the causal relationship:** Once the  $r_i$  and  $c_j$  values are obtained,  $(r_i + c_j)$  and  $(r_i - c_j)$  values are calculated to obtain the causal relationship among the factors. The causal relationship among strength subfactors is presented in Table 6 as an example.

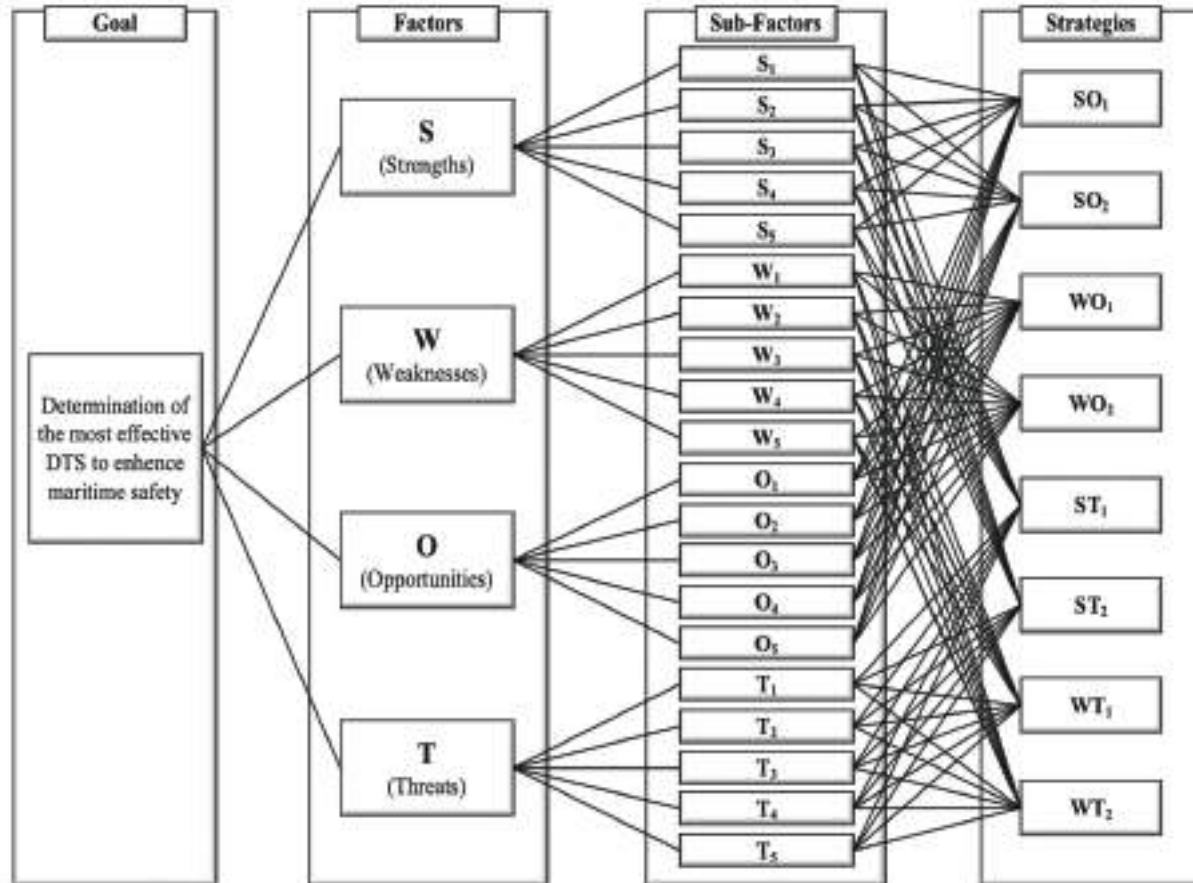


Figure 2. Hierarchical structure

**Step 9. Calculate the weights:** After  $r_i$  and  $c_j$  values, the weights of the goal and each factor were calculated using Equations 6 and 7. The calculated local and global weights ( $W_j$ ) are shown in Table 7 and also illustrated in Figures 3 and 4.

**Step 10. Evaluation of strategies:** The DMs were asked to assess the relevance of the identified strategies to SWOT factors using the linguistic scale presented in Table 3.

**Step 11. Construction of the decision matrix:** After obtaining the DM evaluations, the linguistic expressions were quantified according to the scale presented in Table 3. Then, all matrices were aggregated, and the decision matrix presented in Table 8 was constructed.

**Step 12. Obtaining the weighted normalized decision matrix:** The decision matrix was normalized using Equations 8 and 9. Then, the normalized decision matrix is weighted with the global weight values ( $W_j$ ) obtained in Step 9. Thus, the weighted-normalized decision matrix presented in Table 9 was constructed.

**Step 13. Calculation of the positive and negative ideal solutions:** The positive ( $A^+$ ) and the negative ( $A^-$ ) ideal

solutions were calculated using Equations 10-11.  $A^+$  and  $A^-$  values are presented in Table 9.

**Step 14. Calculation of distance to ideal solutions:** The distances  $D_i^+$  and  $D_i^-$ , of each alternative to the ideal solutions were calculated using Equations 12 and 13. The results are presented in Table 10.

**Step 15. Calculation of the closeness coefficient:** Then, the relative closeness to the ideal solution,  $C_i^*$ , is calculated using Equation 14.  $C_i^*$  values of each strategy are also shown in Table 10.

**Step 16. Selection of the best strategies:** Finally, all alternative strategies were ranked in descending order according to their  $C_i^*$  values. The prioritized order of the strategies is obtained as  $WO_1 > SO_2 > ST_1 > WT_2 > ST_2 > SO_1 > WT_1 > WO_2$ . Results and the prioritized order of the strategies are also illustrated in Figure 5.

These values, derived from the TOPSIS analysis, provide a quantitative measure of each strategy's effectiveness in addressing the complex challenges identified through the SWOT-TOWS and Fuzzy DEMATEL analyses. This prioritization serves as a valuable guideline for decision-

Table 6. DEMATEL application steps for the strengths

DMs' pairwise comparison matrices of DMs for strengths																									
DM <sub>1</sub>					DM <sub>2</sub>					DM <sub>3</sub>					DM <sub>4</sub>					DM <sub>5</sub>					
	S <sub>1</sub>	S <sub>2</sub>	S <sub>3</sub>	S <sub>4</sub>	S <sub>5</sub>	S <sub>1</sub>	S <sub>2</sub>	S <sub>3</sub>	S <sub>4</sub>	S <sub>5</sub>	S <sub>1</sub>	S <sub>2</sub>	S <sub>3</sub>	S <sub>4</sub>	S <sub>5</sub>	S <sub>1</sub>	S <sub>2</sub>	S <sub>3</sub>	S <sub>4</sub>	S <sub>5</sub>	S <sub>1</sub>	S <sub>2</sub>	S <sub>3</sub>	S <sub>4</sub>	S <sub>5</sub>
S <sub>1</sub>	NO	L	VH	H	H	NO	VL	VH	VH	VH	NO	L	H	H	H	NO	H	VH	L	H	NO	L	VH	H	L
S <sub>2</sub>	VH	NO	VH	H	VH	H	NO	H	H	H	VH	NO	VH	VH	VH	VH	NO	VH	H	VH	VH	NO	VH	L	VH
S <sub>3</sub>	NO	H	NO	NO	VL	NO	H	NO	VL	NO	VL	VH	NO	NO	VL	NO	H	NO	VL	NO	L	L	NO	NO	VL
S <sub>4</sub>	H	NO	L	NO	L	VH	VL	VL	NO	L	H	NO	H	NO	VL	L	NO	L	NO	L	H	VL	L	NO	H
S <sub>5</sub>	NO	VH	VL	H	NO	VL	H	VL	VH	NO	NO	VH	L	H	NO	VL	VH	VL	L	NO	NO	VH	NO	H	NO
Fuzzified pairwise comparison matrix of DM <sub>i</sub> for strengths																									
	S <sub>1</sub>					S <sub>2</sub>					S <sub>3</sub>					S <sub>4</sub>					S <sub>5</sub>				
S <sub>1</sub>	(0, 0, 0.25)					(0.25, 0.5, 0.75)					(0.75, 1, 1)					(0.5, 0.75, 1)					(0.5, 0.75, 1)				
S <sub>2</sub>	(0.75, 1, 1)					(0, 0, 0.25)					(0.75, 1, 1)					(0.5, 0.75, 1)					(0.75, 1, 1)				
S <sub>3</sub>	(0, 0, 0.25)					(0.5, 0.75, 1)					(0, 0, 0.25)					(0, 0, 0.25)					(0, 0.25, 0.5)				
S <sub>4</sub>	(0.5, 0.75, 1)					(0, 0, 0.25)					(0.25, 0.5, 0.75)					(0, 0, 0.25)					(0.25, 0.5, 0.75)				
S <sub>5</sub>	(0, 0, 0.25)					(0.75, 1, 1)					(0, 0.25, 0.5)					(0.5, 0.75, 1)					(0, 0, 0.25)				
Initial direct-relation matrix of the strengths																									
	S <sub>1</sub>					S <sub>2</sub>					S <sub>3</sub>					S <sub>4</sub>					S <sub>5</sub>				
S <sub>1</sub>	(0, 0, 0.25)					(0.25, 0.5, 0.75)					(0.7, 0.95, 1)					(0.5, 0.75, 0.95)					(0.5, 0.75, 0.95)				
S <sub>2</sub>	(0.7, 0.95, 1)					(0, 0, 0.25)					(0.7, 0.95, 1)					(0.5, 0.75, 0.95)					(0.7, 0.95, 1)				
S <sub>3</sub>	(0.05, 0.15, 0.4)					(0.5, 0.75, 0.95)					(0, 0, 0.25)					(0, 0.1, 0.35)					(0, 0.15, 0.4)				
S <sub>4</sub>	(0.5, 0.75, 0.95)					(0, 0.1, 0.35)					(0.25, 0.5, 0.75)					(0, 0, 0.25)					(0.25, 0.5, 0.75)				
S <sub>5</sub>	(0, 0.1, 0.35)					(0.7, 0.95, 1)					(0.05, 0.25, 0.5)					(0.5, 0.75, 0.95)					(0, 0, 0.25)				
Normalized direct-relation matrix for strength																									
	S <sub>1</sub>					S <sub>2</sub>					S <sub>3</sub>					S <sub>4</sub>					S <sub>5</sub>				
S <sub>1</sub>	(0, 0, 0.06)					(0.1, 0.14, 0.18)					(0.27, 0.26, 0.24)					(0.19, 0.21, 0.23)					(0.19, 0.21, 0.23)				
S <sub>2</sub>	(0.27, 0.26, 0.24)					(0, 0, 0.06)					(0.27, 0.26, 0.24)					(0.19, 0.21, 0.23)					(0.27, 0.26, 0.24)				
S <sub>3</sub>	(0.02, 0.04, 0.1)					(0.19, 0.21, 0.23)					(0, 0, 0.06)					(0, 0.03, 0.08)					(0, 0.04, 0.1)				
S <sub>4</sub>	(0.19, 0.21, 0.23)					(0, 0.03, 0.08)					(0.1, 0.14, 0.18)					(0, 0, 0.06)					(0.1, 0.14, 0.18)				
S <sub>5</sub>	(0, 0.03, 0.08)					(0.27, 0.26, 0.24)					(0.02, 0.07, 0.12)					(0.19, 0.21, 0.23)					(0, 0, 0.06)				
Total-relation matrix of strengths																									
	S <sub>1</sub>					S <sub>2</sub>					S <sub>3</sub>					S <sub>4</sub>					S <sub>5</sub>				
S <sub>1</sub>	(0.15, 0.24, 0.66)					(0.28, 0.41, 0.83)					(0.42, 0.53, 0.91)					(0.34, 0.45, 0.89)					(0.33, 0.45, 0.87)				
S <sub>2</sub>	(0.43, 0.51, 0.86)					(0.26, 0.36, 0.78)					(0.5, 0.6, 0.96)					(0.41, 0.52, 0.94)					(0.46, 0.56, 0.93)				
S <sub>3</sub>	(0.1, 0.18, 0.49)					(0.25, 0.33, 0.64)					(0.11, 0.17, 0.52)					(0.09, 0.18, 0.54)					(0.1, 0.2, 0.54)				
S <sub>4</sub>	(0.25, 0.33, 0.68)					(0.11, 0.23, 0.62)					(0.21, 0.34, 0.72)					(0.1, 0.19, 0.61)					(0.18, 0.31, 0.7)				
S <sub>5</sub>	(0.17, 0.25, 0.59)					(0.37, 0.44, 0.76)					(0.2, 0.33, 0.69)					(0.33, 0.41, 0.77)					(0.16, 0.24, 0.61)				
Results of applying DEMATEL to the strengths																									
	r <sub>i</sub>					c <sub>j</sub>					(r <sub>i</sub> + c <sub>j</sub> )					(r <sub>i</sub> - c <sub>j</sub> )									
S <sub>1</sub>	2.588					1.960					4.548					0.629									
S <sub>2</sub>	3.036					2.225					5.261					0.812									
S <sub>3</sub>	1.474					2.405					3.879					-0.931									
S <sub>4</sub>	1.863					2.259					4.122					-0.396									
S <sub>5</sub>	2.102					2.215					4.317					-0.114									
DEMATEL: Fuzzy Decision Making Trial and Evaluation Laboratory, DMs: Decision-makings																									

Table 7. Local and global weights

Factors	Local Weights ( $\tilde{a}_i$ )	Sub-Factors	Local Weights ( $\tilde{a}_i$ )	Global Weights ( $W_i$ )
S	0.2514	S <sub>1</sub>	0.2053	0.052
		S <sub>2</sub>	0.2380	0.060
		S <sub>3</sub>	0.1784	0.045
		S <sub>4</sub>	0.1852	0.047
		S <sub>5</sub>	0.1931	0.049
W	0.2532	W <sub>1</sub>	0.2247	0.057
		W <sub>2</sub>	0.2306	0.058
		W <sub>3</sub>	0.1285	0.033
		W <sub>4</sub>	0.2285	0.058
		W <sub>5</sub>	0.1877	0.048
O	0.2468	O <sub>1</sub>	0.1795	0.044
		O <sub>2</sub>	0.2100	0.052
		O <sub>3</sub>	0.2222	0.055
		O <sub>4</sub>	0.1931	0.048
		O <sub>5</sub>	0.1951	0.048
T	0.2486	T <sub>1</sub>	0.2253	0.056
		T <sub>2</sub>	0.1748	0.043
		T <sub>3</sub>	0.1844	0.046
		T <sub>4</sub>	0.1977	0.049
		T <sub>5</sub>	0.2178	0.054

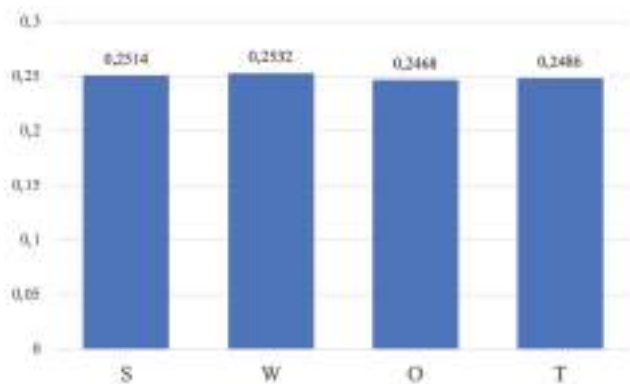


Figure 3. Weighting of the SWOT factors

makers in the offshore tugboat and support vessel industries, providing a rational, data-driven foundation for strategic planning and resource allocation. However, it is important to consider that although this ranking presents a clear priority order, the implementation of these strategies should be tailored to the specific context of each organization. In addition, the industry environment may change rapidly,

necessitating continuous evaluation and adaptation of strategic plans.

#### 4.2. Sensitivity Analysis

This section presents a sensitivity analysis that explores the effects of the weights obtained using the SWOT-TOWS-DEMATEL method on the prioritization of strategies. In addition to the results of the numerical analysis (i.e., the base case, eleven more different cases with alternative local weights ( $\tilde{a}_i$ ) of the SWOT factors were created (Büyüközkan et al., 2021). The alternative cases are listed in Table 11.

Then, subfactor global weights ( $W_i$ ) are calculated with reference to the factor weights determined for each alternative case (Table 12).

The TOPSIS method is then reapplied by revising the global weights to obtain strategy prioritizations for each case.

The  $C_i^*$  values of the strategies for all the different cases are presented in Table 13, and the final prioritization of the strategies for all the different cases is presented in Table 14.

The prioritization of strategies for each case is illustrated in Figure 6. It can be seen that there are small differences in the ranking of the strategies. These small changes do not affect validity. For example, the WO1 strategy was calculated as the most prioritized strategy in 10 out of 11 alternative cases. Thus, the results of the base case study can be validated. Furthermore, WO1 emerged as the best strategy in 11 cases, followed by SO2 and ST1 as the other suitable strategies.

### 5. Findings and Discussion

Adopting advanced technologies to improve fuel efficiency and reduce maintenance costs is a key strategy that should help to overcome the significant challenges brought by high operational expenses and market dependencies [69,70]. This issue is central to achieving sustainable growth in the industry, and the WO1 strategy aims at innovative, particularly ecological, solutions to alleviate these cost-related challenges. By focusing on reducing expenses related to fuel, maintenance, and crew wages, this approach not only promises substantial cost savings but also aligns companies with global sustainability goals. This emphasis on cost-effectiveness and sustainability enhances competitive advantage in a market that is increasingly shaped by these factors. The SO2 strategy focuses on improving operational efficiency through innovative vessel designs, including eco-friendly practices, and modernizing the fleet with advanced technologies. This is in conjunction with government incentives for autonomous vessels and advanced navigation systems, which positions the company to further lead efforts toward sustainable fleet

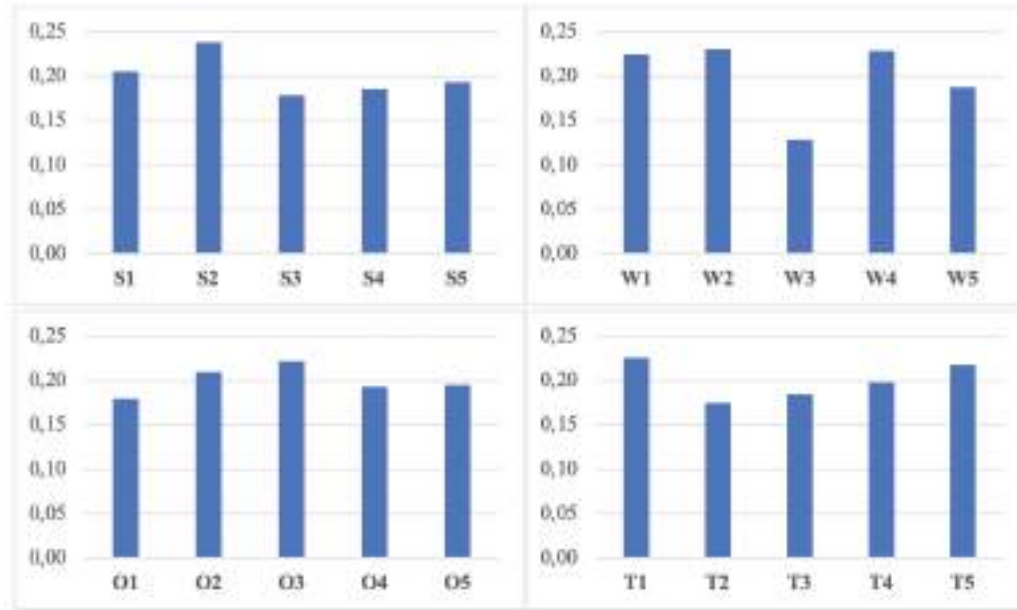


Figure 4. Weights of the SWOT subfactors

Table 8. Initial decision matrix

	SO <sub>1</sub>	SO <sub>2</sub>	WO <sub>1</sub>	WO <sub>2</sub>	ST <sub>1</sub>	ST <sub>2</sub>	WT <sub>1</sub>	WT <sub>2</sub>
S <sub>1</sub>	4.40	4.60	4.40	1.20	4.20	4.80	4.60	3.20
S <sub>2</sub>	4.20	4.60	4.60	4.20	4.80	4.60	4.60	4.60
S <sub>3</sub>	4.60	4.80	4.40	1.80	4.80	4.80	3.80	4.20
S <sub>4</sub>	4.80	2.80	4.60	3.40	4.80	4.80	3.80	4.80
S <sub>5</sub>	4.60	4.60	4.60	4.80	4.60	4.80	4.80	4.60
W <sub>1</sub>	3.40	4.80	4.60	3.80	2.80	3.20	4.80	3.60
W <sub>2</sub>	4.80	2.80	5.00	4.60	4.20	4.60	4.20	4.20
W <sub>3</sub>	1.20	4.20	4.20	1.20	4.40	2.20	1.40	3.80
W <sub>4</sub>	2.80	3.80	4.60	2.80	2.80	3.60	3.80	4.80
W <sub>5</sub>	4.80	4.80	4.60	4.60	4.80	4.20	4.80	4.20
O <sub>1</sub>	4.80	4.60	4.80	4.80	4.20	4.80	4.80	4.80
O <sub>2</sub>	4.80	4.80	4.60	4.80	4.80	4.60	4.80	4.60
O <sub>3</sub>	2.20	3.80	3.80	2.20	2.40	2.20	1.80	2.40
O <sub>4</sub>	2.80	3.20	4.20	2.80	2.20	3.40	1.80	2.20
O <sub>5</sub>	4.80	4.80	4.80	4.80	4.80	2.80	2.80	3.20
T <sub>1</sub>	3.80	4.20	4.80	2.80	4.60	2.80	3.20	4.80
T <sub>2</sub>	4.80	4.60	4.80	4.80	4.80	4.80	4.80	4.80
T <sub>3</sub>	3.80	2.80	2.80	2.80	3.80	4.60	2.80	2.80
T <sub>4</sub>	3.20	4.80	4.60	4.80	4.60	3.80	4.80	4.80
T <sub>5</sub>	4.80	4.20	4.80	4.20	3.80	3.80	4.20	4.80

modernization [71]. Continuous innovation empowers the industry to meet increasing market and regulatory demands, reduce environmental impact, and maintain leadership by attracting new and existing clients.

The competitive advantage can be fueled not only by enabling a skilled crew but also by using advanced technology and practicing resource management innovation in the continuously volatile market with fast changes in technologies to ensure long-term success [72,73]. Such a strategy positions the industry not only to respond to but also to predict changes in the market and technology. Such strategic direction enables companies to surmount challenges and maintain leadership in a dynamic environment.

Companies can mitigate risks associated with high capital investments and research gaps and enhance brand visibility by securing long-term financing options and forming strategic alliances [74]. A strong financial foundation strengthens a company’s position against market volatility and builds resilience to sustain growth. According to Pringpong et al. [75], the risks associated with geopolitical instability and financial stressors due to economic decline can be mitigated by strengthening client relationships and optimizing operational costs. This ensures that firms remain resilient even when such unexpected external shocks occur because their revenue streams are stable and efficient. Those firms that focus on retaining clients and optimizing costs can better navigate economically ambiguous climates to sustain their competitive advantage.

It would ensure a stable revenue stream by leveraging strong client relationships and diversified service offerings and expanding into growth markets with increasing demand for offshore services [76]. This strategy capitalizes on growth opportunities in emerging markets and establishes a robust global presence. Diversifying business services and building deep customer relationships enhance the ability to



**Table 9.** The weighted-normalized decision matrix

	$W_i$	$SO_1$	$SO_2$	$WO_1$	$WO_2$	$ST_1$	$ST_2$	$WT_1$	$WT_2$	$A^+$	$A^-$
$S_1$	0.052	0.020	0.021	0.020	0.005	0.019	0.021	0.021	0.014	0.021	0.005
$S_2$	0.060	0.020	0.021	0.021	0.020	0.022	0.021	0.021	0.021	0.022	0.020
$S_3$	0.045	0.017	0.018	0.016	0.007	0.018	0.018	0.014	0.016	0.018	0.007
$S_4$	0.047	0.018	0.011	0.018	0.013	0.018	0.018	0.015	0.018	0.018	0.011
$S_5$	0.049	0.017	0.017	0.017	0.018	0.017	0.018	0.018	0.017	0.018	0.017
$W_1$	0.057	0.017	0.024	0.023	0.019	0.014	0.016	0.024	0.018	0.024	0.014
$W_2$	0.058	0.023	0.013	0.024	0.022	0.020	0.022	0.020	0.020	0.024	0.013
$W_3$	0.033	0.004	0.015	0.015	0.004	0.016	0.008	0.005	0.014	0.016	0.004
$W_4$	0.058	0.015	0.021	0.025	0.015	0.015	0.020	0.021	0.027	0.027	0.015
$W_5$	0.048	0.018	0.018	0.017	0.017	0.018	0.015	0.018	0.015	0.018	0.015
$O_1$	0.044	0.016	0.015	0.016	0.016	0.014	0.016	0.016	0.016	0.016	0.014
$O_2$	0.052	0.019	0.019	0.018	0.019	0.019	0.018	0.019	0.018	0.019	0.018
$O_3$	0.055	0.016	0.027	0.027	0.016	0.017	0.016	0.013	0.017	0.027	0.013
$O_4$	0.048	0.016	0.018	0.024	0.016	0.013	0.020	0.010	0.013	0.024	0.010
$O_5$	0.048	0.019	0.019	0.019	0.019	0.019	0.011	0.011	0.013	0.019	0.011
$T_1$	0.056	0.019	0.021	0.024	0.014	0.023	0.014	0.016	0.024	0.024	0.014
$T_2$	0.043	0.015	0.015	0.015	0.015	0.015	0.015	0.015	0.015	0.015	0.015
$T_3$	0.046	0.018	0.014	0.014	0.014	0.018	0.022	0.014	0.014	0.022	0.014
$T_4$	0.049	0.012	0.019	0.018	0.019	0.018	0.015	0.019	0.019	0.019	0.012
$T_5$	0.054	0.021	0.019	0.021	0.019	0.017	0.017	0.019	0.021	0.021	0.017

**Table 10.** Ranking strategies

Strategies	$D_i^+$	$D_i^-$	$C_i^*$	Prioritization
$SO_1$	0.025	0.026	0.511	6
$SO_2$	0.018	0.032	0.642	2
$WO_1$	0.009	0.037	0.798	1
$WO_2$	0.033	0.016	0.329	8
$ST_1$	0.023	0.028	0.550	3
$ST_2$	0.023	0.027	0.539	5
$WT_1$	0.028	0.023	0.450	7
$WT_2$	0.022	0.026	0.546	4

adapt and make future profits. The adoption of cost-saving technologies and automation may facilitate cost operations, augmenting the resistance to competition and environmental variables, and even provide an opportunity for weather disruption [77]. Fleet modernization with good navigation systems will increase operational resilience and market adaptability; for example, a critical factor influencing a company’s ability to cope with weather variables [78]. In recent years, when world trade has faced the challenges of climate change and intensifying competition, results have

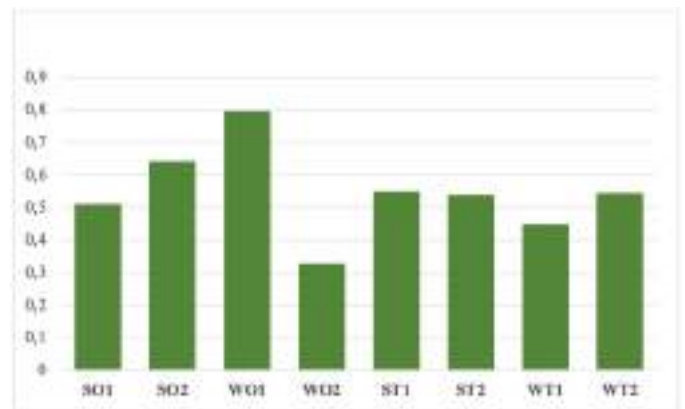


**Figure 5.** Results and prioritized order of strategies

been obtained that emphasize how conservative methods used in current management systems should be used to make operational management systems more environmentally friendly, competitive, and efficient with the development of technology. Based on the results, we can expect that the implementation of environmentally friendly technologies in new offshore vessel construction and design will increase operational efficiency and profitability. Companies that are uncertain about investing in such technological advancements will likely accelerate their orientation toward

*Table 11. All cases with different SWOT factor weights*

SWOT factor	Base	Case 1	Case 2	Case 3	Case 4	Case 5	Case 6	Case 7	Case 8	Case 9	Case 10	Case 11
S	0.251	0.250	0.400	0.200	0.200	0.200	0.400	0.400	0.100	0.400	0.100	0.100
W	0.253	0.250	0.200	0.400	0.200	0.200	0.400	0.100	0.400	0.100	0.400	0.100
O	0.247	0.250	0.200	0.200	0.400	0.200	0.100	0.400	0.100	0.100	0.400	0.400
T	0.249	0.250	0.200	0.200	0.200	0.400	0.100	0.100	0.400	0.400	0.100	0.400

*Table 12. Sub-factor weights for all cases*

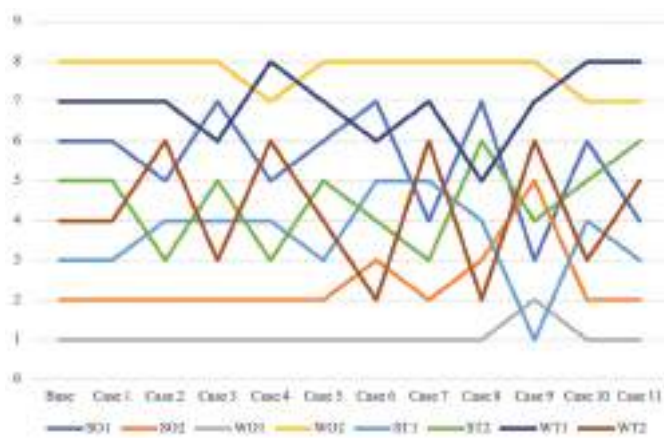
Sub-factor	Base	Case 1	Case 2	Case 3	Case 4	Case 5	Case 6	Case 7	Case 8	Case 9	Case 10	Case 11
S <sub>1</sub>	0.052	0.051	0.082	0.041	0.041	0.041	0.082	0.082	0.021	0.082	0.021	0.021
S <sub>2</sub>	0.060	0.060	0.095	0.048	0.048	0.048	0.095	0.095	0.024	0.095	0.024	0.024
S <sub>3</sub>	0.045	0.045	0.071	0.036	0.036	0.036	0.071	0.071	0.018	0.071	0.018	0.018
S <sub>4</sub>	0.047	0.046	0.074	0.037	0.037	0.037	0.074	0.074	0.019	0.074	0.019	0.019
S <sub>5</sub>	0.049	0.048	0.077	0.039	0.039	0.039	0.077	0.077	0.019	0.077	0.019	0.019
W <sub>1</sub>	0.057	0.056	0.045	0.090	0.045	0.045	0.090	0.022	0.090	0.022	0.090	0.022
W <sub>2</sub>	0.058	0.058	0.046	0.092	0.046	0.046	0.092	0.023	0.092	0.023	0.092	0.023
W <sub>3</sub>	0.033	0.032	0.026	0.051	0.026	0.026	0.051	0.013	0.051	0.013	0.051	0.013
W <sub>4</sub>	0.058	0.057	0.046	0.091	0.046	0.046	0.091	0.023	0.091	0.023	0.091	0.023
W <sub>5</sub>	0.048	0.047	0.038	0.075	0.038	0.038	0.075	0.019	0.075	0.019	0.075	0.019
O <sub>1</sub>	0.044	0.045	0.036	0.036	0.072	0.036	0.018	0.072	0.018	0.018	0.072	0.072
O <sub>2</sub>	0.052	0.052	0.042	0.042	0.084	0.042	0.021	0.084	0.021	0.021	0.084	0.084
O <sub>3</sub>	0.055	0.056	0.044	0.044	0.089	0.044	0.022	0.089	0.022	0.022	0.089	0.089
O <sub>4</sub>	0.048	0.048	0.039	0.039	0.077	0.039	0.019	0.077	0.019	0.019	0.077	0.077
O <sub>5</sub>	0.048	0.049	0.039	0.039	0.078	0.039	0.020	0.078	0.020	0.020	0.078	0.078
T <sub>1</sub>	0.056	0.056	0.045	0.045	0.045	0.090	0.023	0.023	0.090	0.090	0.023	0.090
T <sub>2</sub>	0.043	0.044	0.035	0.035	0.035	0.070	0.017	0.017	0.070	0.070	0.017	0.070
T <sub>3</sub>	0.046	0.046	0.037	0.037	0.037	0.074	0.018	0.018	0.074	0.074	0.018	0.074
T <sub>4</sub>	0.049	0.049	0.040	0.040	0.040	0.079	0.020	0.020	0.079	0.079	0.020	0.079
T <sub>5</sub>	0.054	0.054	0.044	0.044	0.044	0.087	0.022	0.022	0.087	0.087	0.022	0.087

*Table 13. C<sub>i</sub><sup>\*</sup> values of the DTSs for all cases*

Sub-factor	Base	Case 1	Case 2	Case 3	Case 4	Case 5	Case 6	Case 7	Case 8	Case 9	Case 10	Case 11
SO <sub>1</sub>	0.511	0.511	0.625	0.444	0.476	0.503	0.546	0.590	0.416	0.656	0.408	0.457
SO <sub>2</sub>	0.642	0.642	0.671	0.611	0.688	0.597	0.638	0.720	0.562	0.632	0.651	0.649
WO <sub>1</sub>	0.798	0.798	0.824	0.837	0.848	0.705	0.877	0.891	0.732	0.718	0.909	0.746
WO <sub>2</sub>	0.329	0.329	0.257	0.349	0.374	0.328	0.285	0.309	0.352	0.239	0.392	0.381
ST <sub>1</sub>	0.550	0.549	0.650	0.509	0.478	0.578	0.595	0.571	0.524	0.726	0.443	0.485
ST <sub>2</sub>	0.539	0.537	0.660	0.497	0.479	0.504	0.624	0.600	0.452	0.645	0.433	0.433
WT <sub>1</sub>	0.450	0.447	0.557	0.476	0.330	0.422	0.592	0.438	0.459	0.562	0.360	0.264
WT <sub>2</sub>	0.546	0.543	0.589	0.600	0.432	0.561	0.654	0.471	0.626	0.616	0.488	0.437

*Table 14. Prioritization of DTSs in all cases*

Sub-factor	Base	Case 1	Case 2	Case 3	Case 4	Case 5	Case 6	Case 7	Case 8	Case 9	Case 10	Case 11
SO <sub>1</sub>	6	6	5	7	5	6	7	4	7	3	6	4
SO <sub>2</sub>	2	2	2	2	2	2	3	2	3	5	2	2
WO <sub>1</sub>	1	1	1	1	1	1	1	1	1	2	1	1
WO <sub>2</sub>	8	8	8	8	7	8	8	8	8	8	7	7
ST <sub>1</sub>	3	3	4	4	4	3	5	5	4	1	4	3
ST <sub>2</sub>	5	5	3	5	3	5	4	3	6	4	5	6
WT <sub>1</sub>	7	7	7	6	8	7	6	7	5	7	8	8
WT <sub>2</sub>	4	4	6	3	6	4	2	6	2	6	3	5

*Figure 6. Changes in the prioritization of the strategies for all cases*

these innovations, based on the evidence presented in this study.

This strategic framework is crucial for decision makers guiding the offshore tugboat and support vessel industries. Companies in this sector can overcome contemporary challenges and seize emerging opportunities by prioritizing technological innovation, operational efficiency, and market diversification. Strategies should be tailored to individual organizations' unique strengths, weaknesses, and market positions.

## 6. Conclusion

This study investigates critical issues related to strategic maritime management, especially offshore operations. This study highlights the critical role of adopting advanced technologies and innovative strategies to address the challenges faced by the offshore tugboat and support vessel industries. Prioritizing fuel efficiency, maintenance cost reduction, and fleet modernization not only ensures operational sustainability but also aligns with global environmental and market trends. By incorporating SWOT-TOWS analysis into Fuzzy DEMATEL and TOPSIS

methods, this study develops an integrated framework that, in detail, represents strategic priorities and their interlinkages of various complexities. While the proposed integrated methodology provides valuable insights, certain limitations should be acknowledged. The DEMATEL method's reliance on subjective expert judgments and the complexity of pairwise comparisons with an increasing number of factors may influence the precision of results, although our sensitivity analysis demonstrates robust outcomes across different scenarios. A state-of-the-art critical literature review and industry experts' insights into the most influential factors shaping the maritime sector are presented in this study. Its core objective is to provide hands-on tools and strategic frameworks for industry leaders to address current challenges and prepare for future opportunities. These advanced DM techniques rank strategic options effectively in this research, emphasizing cost reduction through technology and market diversification. The results of this study confirm that innovation and sustainability are imperative for the maritime sector to maintain competitiveness in an increasingly dynamic global market. This research fills an important gap in the literature on strategic management by providing a customized DM model for maritime operations.

Future studies applying this framework to different maritime scenarios or similar industries are desirable. A long-term study of the effects of some of these emerging technologies, such as AI and automation, on mariners' operations would provide valuable insights. Additionally, further investigation into the role of strategic alliances and client relationship management in mitigating geopolitical and economic uncertainties will provide valuable insights for strengthening the resilience and adaptability of the sector. It would be interesting to conduct longitudinal analyses on how these strategies could contribute to operational efficiency and resilience.

In summary, this research contributes to strategic management in maritime organizations and provides a

practical framework for complex DM to navigate the constant changes and challenges of the global marketplace.

### Acknowledgments

This article is partly produced from a Ph.D. thesis entitled “Strategic management modeling of Offshore Tugboats and Support Vessels Management” which has been executed in a Ph. D. Program in Maritime Transportation Engineering at the Graduate School, İstanbul Technical University.

### Footnotes

### Authorship Contributions

Concept design: A. B. Eke, O. Batmaz, M. F. Gülen, E. Uflaz, and Ö. Arslan, Data Collection or Processing: A. B. Eke, O. Batmaz, M. F. Gülen, and E. Uflaz, Analysis or Interpretation: A. B. Eke, O. Batmaz, M. F. Gülen, E. Uflaz, and Ö. Arslan, Literature Review: A. B. Eke, O. Batmaz, and M. F. Gülen, Writing, Reviewing and Editing: A. B. Eke, O. Batmaz, M. F. Gülen, E. Uflaz, and Ö. Arslan,

**Funding:** The İstanbul Technical University Scientific Research Projects Coordination Office supported this article (project no. MAB-2024-45613).

### References

- [1] O. Drobitko, and N. Drobitko, “Legal regulation of sea towage contracts in the EU countries”. *Lex Portus*, vol. 7, pp. 37-64, Dec 2021.
- [2] B. Dwibastyantoro, “Feasibility study for tugboat expansion project using capital budgeting and sensitivity analysis (Case Study: PT. ABC)”. *International Journal of Current Science Research and Review*, vol. 06, pp. 1816-1847, Feb 2023.
- [3] M. Höffmann et al., “Wind affected maneuverability of tugboat-controlled ships”. *IFAC-PapersOnLine*, vol. 54, pp. 70-75, 2021.
- [4] C. Sun, M. Li, L. Chen, and P. Chen, “Dynamic tugboat scheduling for large seaports with multiple terminals”. *Journal of Marine Science and Engineering*, vol. 12, pp. 170, Nov 2024.
- [5] A. Ortega-Piris, E. Diaz-Ruiz-Navamuel, A. H. Martinez, M. A. Gutierrez, and A.-I. Lopez-Diaz, “Analysis of the concentration of emissions from the Spanish fleet of tugboats”. *Atmosphere (Basel)*, vol. 13, 2109, Dec 2022.
- [6] H. Wang, P. Zhou, Y. Liang, B. Jeong, and A. Mesbahi, “Optimization of tugboat propulsion system configurations: A holistic life cycle assessment case study”. *Journal of Cleaner Production*, vol. 259, 120903, Jun 2020.
- [7] W. Koznowski, and A. Lebkowski, “Port tugboat formation multi-agent control system”. *TransNav, the International Journal on Marine Navigation and Safety of Sea Transportation*, vol. 15, pp. 807-814, 2021.
- [8] S. Lebedevas, L. Norkevičius, and P. Zhou, “Investigation of effect on environmental performance of using LNG as fuel for engines in seaport tugboats”. *Journal of Marine Science and Engineering*, vol. 9, pp. 123, Nov 2021.
- [9] K. T. Gillingham, and P. Huang, “Long-run environmental and economic impacts of electrifying waterborne shipping in the United States”. *Environmental Science & Technology*, vol. 54, pp. 9824-9833, Aug 2020.
- [10] V. Paulauskas, D. Paulauskas, and V. Paulauskas, “Impact of port clearance on ships safety, energy consumption and emissions”. *Applied Sciences*, vol. 13, 5582, Apr 2023.
- [11] S. Hayman, and J. Stratton, “Hybrid-Powered Marine Vessels”. Proceedings of the ASME/USCG 2010 2nd Workshop on Marine Technology and Standards. ASME/USCG 2010 2nd Workshop on Marine Technology and Standards. Washington, DC, USA. July 29-30, 2010. pp. 39-47.
- [12] C. White, “Strategic Management.”
- [13] A. C. Kuzu, “Risk analysis of break-in-two accident of ships using fuzzy DEMATEL method”. *Ocean Engineering*, vol. 235, 109410, Sep 2021.
- [14] J. Shi et al., “Evolutionary model and risk analysis of ship collision accidents based on complex networks and DEMATEL”. *Ocean Engineering*, vol. 305, 117965, Aug 2024.
- [15] J. Liu, J. Wu, and Y. Gong, “Maritime supply chain resilience: From concept to practice”. *Computers & Industrial Engineering*, vol. 182, 109366, Aug 2023.
- [16] A. Ebadi Torkayesh, S. Hendiani, G. Walther, and S. Venghaus, “Fueling the future: Overcoming the barriers to market development of renewable fuels in Germany using a novel analytical approach”. *European Journal of Operational Research*, vol. 316, pp. 1012-1033, Aug 2024.
- [17] T. Umut, “Fuzzy DEMATEL approach to assess factors leading to navigational equipment defect”. *Transactions on Maritime Science*, vol. 11, pp. 16-27, Apr 2022.
- [18] P. Guan, L. C. Wood, J. X. Wang, and L. N. K. Duong, “Barriers to blockchain adoption in the seaport industry: A fuzzy DEMATEL analysis”. *Mathematical Biosciences and Engineering*, vol. 20, pp. 20995-21031, Nov 2023.
- [19] İ. S. Ayaz, U. Bucak, and S. Esmer, “How to integrate ports into the EU ETS: the CAS approach perspective”. *The International Journal of Logistics Management*, vol. 35, pp. 719-735, Jan 2024.
- [20] Ü. Özdemir, and A. Güneroglu, “Strategic approach model for investigating the cause of maritime accidents”. *Promet-traffic & Transportation*, vol. 27, pp. 113-123, 2015, [Online]. Available: <https://api.semanticscholar.org/CorpusID:42718898>
- [21] C. Durán, J. Sepúlveda, and R. Carrasco, “Determination of technological risk influences in a port system using DEMATEL”. *Decision Science Letters*, vol. 7, pp. 1-12, Nov 2017.
- [22] W. Lin, “Maritime environment assessment and management using through balanced scorecard by using DEMATEL and ANP technique”. *International Journal of Environmental Research and Public Health*, vol. 19, pp. 2873, Mar 2022.
- [23] Y.-J. Chen, Q. Liu, C. Wan, Q. Li, and P.-W. Yuan, “Identification and analysis of vulnerability in traffic-intensive areas of water transportation systems”. vol. 7, pp. 174, Nov 2019.
- [24] J. Sun, H. Wang, and Z. Cui, “Alleviating the bauxite maritime supply chain risks through resilient strategies: QFD-MCDM with intuitionistic fuzzy decision approach”. *Sustainability*, vol. 15, 8244, 2023.
- [25] D. Muravev, H. Hu, H. Zhou, and D. Pamucar, “Location optimization of CR express international logistics centers”. *Symmetry (Basel)*, vol. 12, 143, Nov 2020.
- [26] K. A. Hossain, N. M. G. Zakaria, and M. A. R. Sarkar, “SWOT analysis of China shipbuilding industry by third eyes”. *Procedia Engineering*, vol. 194, pp. 241-246, 2017.

- [27] H.-H. Cheng, and K. Ouyang, "Development of a strategic policy for unmanned autonomous ships: a study on Taiwan". *Maritime Policy & Management*, vol. 48, pp. 1-15, Nov 2020.
- [28] P.-H. Tseng, and N. Pilcher, "Examining the opportunities and challenges of the Kra Canal: a PESTELE/SWOT analysis". *Maritime Business Review*, vol. 7, pp. 161-174, Jan 2022.
- [29] A. Vorkapić, R. Radonja, and S. Martinčić-Ipšić, "A framework for the application of shipboard energy efficiency monitoring, operational data prediction and reporting". *Pomorstvo*, vol. 35, pp. 3-15, Jun 2021.
- [30] S. Bauk, "Performances of some autonomous assets in maritime missions". *TransNav, International Journal on Marine Navigation and Safety of Sea Transportation*, vol. 14, pp. 875-881, Nov 2021.
- [31] A. Aleksanyan, "Unmanned navigation system". *Journal of Physics: Conference Series*, Volume 2061, International Conference on Actual Issues of Mechanical Engineering (AIME 2021) 15-16 June 2021, Novorossiysk, Russia vol. 2061, 012119 Nov 2021.
- [32] P. Serra, G. Fancello, R. Tonelli, and L. Marchesi, "Application prospects of blockchain technology to support the development of interport communities". *Computers*, vol. 11, pp. 24, Apr 2022.
- [33] G. Papaioannou, A. Polydoropoulou, A. Tsirimpa, and I. Pagoni, "Assessing the potential of 'mobility as a service' in passenger maritime transport". *Frontiers in Future Transportation*, vol. 2, Jan 2022.
- [34] A. Kelfaoui, M. A. Rezzaz, and L. Kherrou, "Revitalization of mountain rural tourism as a tool for sustainable local development in Kabylie (Algeria). The case of Yakouren municipality". *Geojournal of Tourism and Geosites*, vol. 34, pp. 112-125, 2021.
- [35] Mafrisal, M. Jinca, M. Ali, and M. Asdar, "Strategies for enhancing inter-island transportation performance in Makassar, Indonesia: An integrated planning approach". *International Journal of Transport Development and Integration*, vol. 8, pp. 79-89, Nov 2024.
- [36] F. Oral, and S. Paker, "Risk assessment for maritime container transportation security". *Journal of ETA Maritime Science*, vol. 11, pp. 304-316, Dec 2023.
- [37] M. Palmén, A. Lotrič, A. Laakso, V. Bolbot, M. Elg, and O. Valdez Banda, "Selecting appropriate energy source options for an Arctic research ship". *Journal of Marine Science and Engineering*, vol. 11, 2337, Dec 2023.
- [38] B. Kizielewicz, and W. Sařabun, "SITW method: a new approach to re-identifying multi-criteria weights in complex decision analysis". *Spectrum of Mechanical Engineering and Operational Research*, vol. 1, pp. 215-226, Nov 2024.
- [39] K. H. Gazi, N. Raisa, A. Biswas, F. Azizzadeh, and S. P. Mondal, "Finding the most important criteria in women's empowerment for sports sector by pentagonal fuzzy DEMATEL methodology". *Spectrum of Decision Making and Applications*, vol. 2, pp. 28-52, Aug 2024.
- [40] U. Elraaid, I. Badi, and M. B. Bouraima, "Identifying and addressing obstacles to project management office success in construction projects: An AHP approach". *Spectrum of Decision Making and Applications*, vol. 1, pp. 33-45, Jul 2024.
- [41] J. Kannan, V. Jayakumar, and M. Pethaperumal, "Advanced fuzzy-based decision-making: the linear diophantine fuzzy CODAS method for logistic specialist selection". *Spectrum of Operational Research*, vol. 2, pp. 41-60, Aug 2024.
- [42] E. Gürel, "SWOT analysis: a theoretical review". *Journal of International Social Research*, vol. 10, pp. 994-1006, Nov 2017.
- [43] G. M. Ravanavar, "Strategic formulation using TOWS matrix - a case study". [Online]. Available: <https://api.semanticscholar.org/CorpusID:53660848>
- [44] A. Sarsby, *A useful guide to SWOT analysis*. Pansophic Online, 2012.
- [45] S. Ghazinoory, M. Abdi, and M. Azadegan-Mehr, "Swot methodology: A state-of-the-art review for the past, a framework for the future". *Journal of Business Economics and Management*, vol. 12, pp. 24-48, Apr 2011.
- [46] A. Gabus, and E. Fontela, "Perceptions of the world problematique: communication procedure, communicating with those bearing collective responsibility". 1973. [Online]. Available: <https://api.semanticscholar.org/CorpusID:157271447>
- [47] Y.-W. Du, and W. Zhou, "New improved DEMATEL method based on both subjective experience and objective data". *Engineering Applications of Artificial Intelligence*, vol. 83, pp. 57-71, Aug 2019.
- [48] A. Borawska, "Multiple-criteria decision analysis using TOPSIS method for interval data in research into the level of information society development". *Folia Oeconomica Stetinensia*, vol. 13, Jan 2014.
- [49] A. Baykasođlu, V. Kaplanoglu, Z. D. U. Durmuşoglu, and C. Şahin, "Integrating fuzzy DEMATEL and fuzzy hierarchical TOPSIS methods for truck selection". *Expert Systems with Applications*, vol. 40, pp. 899-907, Feb 2013.
- [50] D. Abreu, M. Maturana, E. Droguett, and M. Ramos Martins, "Human reliability analysis of ship maneuvers in harbor areas". *Journal of Offshore Mechanics and Arctic Engineering*, vol. 142, pp. 1-31, May 2020.
- [51] G. C. de Bittencourt, et al., "A solution framework for the integrated problem of cargo assignment, fleet sizing, and delivery planning in offshore logistics". *Computers & Industrial Engineering*, vol. 161, 107653, 2021.
- [52] A. Riaz, L. Xingong, Z. Jiao, and M. Shahbaz, "Dynamic volatility spillover between oil and marine shipping industry". *Energy Reports*, vol. 9, pp. 3493-3507, Dec 2023.
- [53] K. Vedat, "IoT in the OSV sector". Paper presented at the Abu Dhabi International Petroleum Exhibition & Conference, Abu Dhabi, UAE, November 2020. Nov 2020.
- [54] L. Lu, G. D. Gregory, L. V. Ngo, and R. P. Bagozzi, "Managing customer uncertainty in making service offshoring decisions". *Journal of Service Research*, vol. 24, pp. 500-519, Mar 2021.
- [55] W. Gleißner, T. Günther, and C. Walkshäusl, "Financial sustainability: measurement and empirical evidence". *Journal of Business Economics*, vol. 92, pp. 467-516, Apr 2022.
- [56] J. C. Gleissner Harald and Femerling, "Investment and financing in logistics", in *Logistics: Basics — Exercises — Case Studies*, Cham: Springer International Publishing, 2013, pp. 225-243, Jan 2013.
- [57] N. Diniz, D. Cunha, M. Porte, and C. Oliveira, "Disclosure of the sustainable development goals in the maritime industry and port sector". *Revista de Gestão e Secretariado (Management and Administrative Professional Review)*, vol. 14, pp. 8129-8149, Nov 2023.
- [58] D. Chadee, R. R. Sharma, and H. Banjo Roxas, "Linking and leveraging resources for innovation and growth through collaborative value creation: A study of Indian OSPs". *Asia Pacific Journal of Management*, vol. 34, pp. 777-797, Dec 2017.

- [59] E. Faraggiana, G. Giorgi, M. Sirigu, A. Ghigo, G. Bracco, and G. Mattiazzo, "A review of numerical modelling and optimisation of the floating support structure for offshore wind turbines". *Journal of Ocean Engineering and Marine Energy*, vol. 8, pp. 433-456, 2022.
- [60] N. Agarwala, "Technological trends for ocean research vessels", in *Proceedings of the Fourth International Conference in Ocean Engineering (ICOE2018)*, V. and S. A. and S. N. Murali K. and Sriram, eds., Singapore: Springer Singapore, 2019, pp. 435-452.
- [61] Y. Luo, S. L. Wang, Q. Zheng, and V. Jayaraman, "Task attributes and process integration in business process offshoring: A perspective of service providers from India and China". *Journal of International Business Studies*, vol. 43, pp. 498-524, Apr 2012.
- [62] C. Yin, "International law regulation of offshore oil and gas exploitation". *Environmental Impact Assessment Review*, vol. 88, 106551, 2021.
- [63] S. S. Pettersen, J. J. Garcia Agis, C. F. Rehn, and S. O. Erikstad, "Latent capabilities in support of maritime emergency response". *Maritime Policy & Management*, vol. 47, pp. 479-499, 2020.
- [64] Md. S. Islam, F. Ahmed, Md. M. Islam, A. ur Rehman, and Md. F. Alam, "The impact of oil price shocks on oil and gas production amidst geopolitical risk in OPEC: Insights from method of moments quantile regression". *Journal of the Knowledge Economy*, Aug 2024.
- [65] M. Albeldawi, "Chapter 10 - Environmental impacts and mitigation measures of offshore oil and gas activities". *Developments in Petroleum Science*, vol. 78, pp. 313-352, 2023.
- [66] "The impact of geopolitical factors and trade risks on global supply chain", 2024. [Online]. Available: <https://www.grandviewresearch.com/research-insights/geopolitical-factors-trade-risks-impact-supply-chain>
- [67] M.-G. Seo, N. Kim, Y.-G. Lee, S. Y. Hong, and H.-J. Choi, "Experimental and numerical study of towing characteristics of damaged ship". Paper presented at the 32nd International Ocean and Polar Engineering Conference, Shanghai, China, June 2022, ISOPE-I-22-510.
- [68] S. Mahmood, P. Misra, H. Sun, A. Luqman, and A. Papa, "Sustainable infrastructure, energy projects, and economic growth: mediating role of sustainable supply chain management". *Annals of Operations Research*, Jan 2024.
- [69] K. Ismoyo, Muhajirin, Iskendar, K. Ajidarmo, Triyanto, and A. Muis, "Analysis of technology readiness level of dual fuel harbor tug boat research achievement". The 7th International Conference on Marine Technology (SENTA 2022) 20/10/2022 Surabaya, Indonesia *IOP Conference Series: Earth and Environmental Science*, vol. 1166, 12004, May 2023.
- [70] J. Li, X. Duan, Z. Xiong, and P. Yao, "Tugboat scheduling method based on the NRPER-DDPG algorithm: an integrated DDPG algorithm with prioritized experience replay and noise reduction". *Sustainability*, vol. 16, 3379, Apr 2024.
- [71] J. Ang, C. Goh, and Y. Li, "Hull form design optimisation for improved efficiency and hydrodynamic performance of 'ship-shaped' offshore vessels". Sep 2015.
- [72] F. Mauro, and R. Nabergoj, "A global operability index for an offshore vessel". Proceedings paper, Paper No: OMAE2020-18650, V001T01A025; 8 pages. Dec 2020.
- [73] M. Gutsch, S. Steen, and F. Sprenger, "Operability robustness index as seakeeping performance criterion for offshore vessels". *Ocean Engineering*, vol. 217, 107931, Dec 2020.
- [74] M. Arrfelt, R. M. Wiseman, and G. T. M. Hult, "Looking backward instead of forward: Aspiration-driven influences on the efficiency of the capital allocation process". *Academy of Management Journal*, vol. 56, pp. 1081-1103, Aug 2013.
- [75] S. Pringpong, S. Maneenop, and A. Jaroenjitrkam, "Geopolitical risk and firm value: Evidence from emerging markets". *The North American Journal of Economics and Finance*, vol. 68, 101951, 2023.
- [76] F. Chien, M. Sadiq, H. W. Kamran, M. A. Nawaz, M. S. Hussain, and M. Raza, "Co-movement of energy prices and stock market return: environmental wavelet nexus of COVID-19 pandemic from the USA, Europe, and China". *Environmental Science and Pollution Research*, vol. 28, pp. 32359-32373, 2021.
- [77] A. B. Saroha Anil K. and Pal, "Industry 4.0: applications in oil and gas industry". In: *Handbook of Smart Materials, Technologies, and Devices: Applications of Industry 4.0*, P. Hussain Chaudhery Mustansar and Di Sia, Ed., Cham: Springer International Publishing, 2020, pp. 1-27.
- [78] S. S. Pettersen, and B. Asbjørnslett, "Designing resilient fleets for maritime emergency response operations". 2016.

# Close Contact Tracing and Risky Area Identification Using Alpha Shape Algorithm and Binary Contact Detection Model Based on Bluetooth 5.1

Qianfeng Lin<sup>1</sup>, Jooyoung Son<sup>2</sup>

<sup>1</sup>National Korea Maritime and Ocean University, Department of Computer Engineering, Busan, South Korea

<sup>2</sup>National Korea Maritime and Ocean University, Department of Marine IT Engineering, Busan, South Korea

## Abstract

This study presents a novel approach to managing disease outbreaks on cruise ships by integrating Bluetooth 5.1 technology, a Binary Contact Detection Model, and an alpha shape algorithm. By harnessing the precise data capture capabilities of Bluetooth 5.1, this study accurately tracks interpersonal interactions and delineated high-risk areas, effectively enhancing close contact tracing and disease surveillance efforts. The Binary Contact Detection Model utilizes In-phase (I) and Quadrature (Q) data to identify close contacts with high accuracy, while the alpha shape algorithm helps in mapping out areas most susceptible to disease transmission. The combined use of these technologies represents a significant advancement in public health surveillance, offering a method to enhance safety and mitigate the spread of infections on cruise ships.

**Keywords:** Bluetooth 5.1 technology, Binary contact detection model, Alpha shape algorithm, Cruise ship disease management

## 1. Introduction

The motivation for this paper stems from the urgent need to enhance infectious disease management on cruise ships, as illustrated by recent outbreaks, such as the one at the Celebrity Summit.

Recent incidents, such as the outbreak onboard Celebrity Cruises' Celebrity Summit during its May 24, 2024, voyage, have highlighted the urgent need for effective disease management strategies on cruise ships. According to the Centers for Disease Control and Prevention, 68 out of the 2,264 passengers and five crew members contracted the virus, highlighting the complexity of controlling infectious diseases in such environments [1]. Cruise ships are unique environments that combine the characteristics of residential communities and transient hubs, presenting distinct challenges for disease control. The motivation for this study stems from the urgent need to enhance infectious disease management on cruise ships, as illustrated by recent outbreaks, such as the one at the Celebrity Summit.

The confined and highly interactive nature of cruise ships exacerbates the difficulty of traditional epidemiological tracking and containment. For instance, the mobility and interaction patterns of passengers and crew in shared spaces like dining rooms, pools, and theaters significantly increase the risk of widespread exposure [2]. In this environment, precise tools are required to monitor and control the spread of pathogens.

Effective disease management on cruise ships requires two critical strategies: close contact tracing and identification of high-risk areas. Close contact tracing involves accurately identifying individuals who have interacted with infected persons, which is essential for implementing effective quarantine measures and preventing further spread [3]. Additionally, identifying areas aboard ships that present higher transmission risks can guide targeted sanitization efforts and the implementation of specific restrictions to manage outbreaks efficiently [4].

In response to these challenges, this paper proposes an integrated technological approach that utilizes Bluetooth



**Address for Correspondence:** Jooyoung Son, National Korea Maritime and Ocean University, Department of Marine IT Engineering, Busan, South Korea  
**E-mail:** mmlab@kmou.ac.kr  
**ORCID iD:** orcid.org/0000-0001-7851-9214

**Received:** 18.08.2024

**Last Revision Received:** 15.10.2024

**Accepted:** 12.11.2024

**To cite this article:** Q. Lin, and J. Son, "Close Contact Tracing and Risky Area Identification Using Alpha Shape Algorithm and Binary Contact Detection Model Based on Bluetooth 5.1." *Journal of ETA Maritime Science*, vol. 12(4), pp. 446-465, 2024.



Copyright© 2024 the Author. Published by Galenos Publishing House on behalf of UCTEA Chamber of Marine Engineers. This is an open access article under the Creative Commons AttributionNonCommercial 4.0 International (CC BY-NC 4.0) License

5.1 technology. The proposed technology enhances position tracking capabilities with high accuracy, which is crucial for the automatic logging of spatial interactions among passengers and crew [5]. The Binary Contact Detection Model proposed in this paper operates using In-phase and Quadrature (IQ) data from Bluetooth 5.1 signals to capture precise interaction data. This model is further complemented by the alpha shape algorithm, which facilitates the sophisticated delineation of high-risk areas on ships [6].

The combination of these technologies represents a significant advancement in public health surveillance on cruise ships. By employing these tools, we aim to not only rapidly identify potentially infected individuals and areas of high risk but also improve the precision and efficiency of public health interventions. This proactive approach to health management is vital for ensuring passenger safety, maintaining safe navigation, and enhancing the overall customer service experience on cruise ships. Moreover, it supports cruise companies by fostering a sense of corporate responsibility and enhancing consumer trust, which is crucial in today's competitive tourism market [7].

Finally, by implementing these strategies, cruise companies can not only effectively control and prevent the spread of disease but also foster a sense of corporate responsibility and enhance consumer trust, thus maintaining a competitive edge in the intense tourism market. This proactive approach to health management may also become a crucial factor for passengers when choosing a cruise line, especially in today's context of prominent global health issues [8].

Therefore, close contact tracing and risky area identification on cruise ships are not only practical necessities for addressing public health emergencies but are also integral parts of cruise operations, vital for ensuring public health, maintaining safe navigation, and enhancing customer service experiences [9].

Bluetooth 5.1 enhances position tracking capabilities with high accuracy, facilitating the automatic logging of spatial interactions among passengers and crew. Bluetooth 5.1 technology significantly enhances the use of IQ data in signal processing [10]. The IQ data are crucial for defining the amplitude and phase of the Bluetooth signal, which can be used to derive more precise information.

To effectively utilize Bluetooth 5.1 technology in close contact tracing, we propose the implementation of a Binary Contact Detection Model. The proposed model operates by utilizing the IQ data from the Bluetooth 5.1 signal, which is pivotal for capturing precise and granular interaction data. Alongside the Binary Contact Detection Model, integrating the alpha shape algorithm allows for sophisticated delineation of high-risk areas on the ship. This integrated approach not only facilitates the rapid identification of potentially infected individuals and high-risk areas and significantly improves the precision and

efficiency of public health interventions. By implementing these advanced technological tools, we can better manage and contain outbreaks in complex environments like cruise ships, thereby ensuring passenger safety and public health. To address these pressing challenges, technological innovations that provide more accurate and automated solutions. This necessity forms the basis for the proposed Binary Contact Detection Model, which is designed to harness advanced Bluetooth 5.1 technology to realize more precise interaction tracking.

The primary contribution of this paper is the proposed Binary Contact Detection Model, which is designed to enhance disease management on cruise ships. This model is then innovatively integrated with Bluetooth 5.1 technology and the alpha shape algorithm, enabling precise tracking of interpersonal interactions and detailed mapping of high-risk areas. By leveraging Bluetooth 5.1's advanced signal processing capabilities, including IQ data, this approach offers a novel method for accurately identifying close contacts and potential transmission hotspots. Consequently, it provides a more effective strategy for outbreak containment and management onboard cruise ships, significantly improving public health surveillance.

The paper is structured to provide a comprehensive understanding of the study, and its findings as follows: Section 2, entitled "Previous Works", reviews the existing literature to highlight past methodologies and technologies used in tracking and managing disease outbreaks, setting the stage for the innovations introduced in this paper. Section 3, "Close Contact Tracing and Risky Area Identification", details the implementation of Bluetooth 5.1 technology integrated with the Binary Contact Detection Model and the alpha shape algorithm, describing how these tools are specifically applied to cruise ships. Section 4, "Performance Evaluation", presents an analysis of the effectiveness of the proposed models in real-world scenarios. Section 5, "Discussion", briefly addresses the implications of the results and identifies potential areas for improvement. Finally, Section 6 presents the conclusions, summarizing the key findings and suggesting directions for future research.

## 2. Previous Works

In ship environments, Bluetooth is favored over alternative wireless technologies for health monitoring and contact tracing because of its numerous benefits, such as low power usage, affordability, easy setup, spatial flexibility, precision, immediacy in data transmission, and robust privacy and security features. In particular, the Bluetooth Low Energy (BLE) variant is tailored for short-distance communications and consumes minimal power, enabling prolonged operation of devices without the need for frequent recharging [11]. These devices are cost-effective



and can be extensively implemented throughout a cruise ship without significant upfront investment. Unlike more complex technologies like Wi-Fi, Bluetooth is easier to configure and maintain, which is essential for swift deployment and usability on cruise ships by staff without technical expertise [12].

Bluetooth technology enables direct device-to-device communication without relying on internet connectivity, thereby safeguarding data privacy and security-critical for handling sensitive personal health information. These attributes make Bluetooth the optimal choice for executing health surveillance and epidemic tracking onboard ships [13]. Bluetooth-enabled devices such as wristbands or badges are employed to track interaction patterns among passengers and crew, thereby facilitating the identification of close contacts. This technology's capability for quick and automated data collection diminishes the need for manual documentation and enhances the accuracy and efficiency of tracking efforts. Furthermore, Bluetooth can monitor and analyze movements and congregations on the ship, thereby identifying areas of high risk. When infections are identified, these data becomes essential for swift implementation of control measures like quarantines and sanitation procedures. Employing this technology not only aids in curbing the spread of infectious diseases but also bolsters the ability to manage public health crises, significantly supporting health and safety management on ships [14].

In ship environments, Bluetooth is chosen over other wireless technologies as the primary tool for health monitoring and close contact tracing primarily due to its advantages in low power consumption, cost-effectiveness, ease of deployment, spatial adaptability, accuracy, real-time capabilities, and privacy and security. Bluetooth, especially the BLE version, is designed for short-range communication and consumes very little power, allowing devices to operate for extended periods without frequent charging. Moreover, Bluetooth devices are generally low-cost and can be deployed on a large scale across a cruise ship without substantial investment. Compared to Wi-Fi, Bluetooth is simpler to configure and maintain, which is crucial for rapid deployment and operation on cruise ships, even by non-technical personnel [15]. Bluetooth technology allows direct communication between devices without the need for internet connectivity, enhancing the privacy and security of data, which is especially important for applications involving personal health data [16]. Collectively, these factors make Bluetooth an ideal choice for health surveillance and epidemic tracking in ship environments.

Research on Bluetooth technology in ship environments for health primarily involves real-time monitoring and data collection to support epidemic management and control measures. By using Bluetooth devices, such as wristbands or badges, the contact patterns of passengers and crew aboard

a ship can be tracked, thereby aiding in the identification of close contacts [17]. The application of this technology allows for the rapid and automatic collection of contact data, thus reducing reliance on manual recording and improving the accuracy and efficiency of tracking. Additionally, Bluetooth technology can be used to monitor and analyze the movement and gathering of people on the ship, thereby identifying high-risk areas. When cases are detected, this information is crucial for quickly implementing control measures such as lockdowns and disinfection. The use of this technology not only helps control the spread of infectious diseases but also improves the capacity to handle public health emergencies, providing significant support for health and safety management on ships [18].

Studies on the spatial transmission of contagious diseases have extensively utilized Global Positioning System data from mobile devices to track human movement and identify infectious sites, proving critical in monitoring and predicting virus spread based on subjects' position histories during key infection periods [19]. Explores the use of BLE technology for close contact tracing, highlighting challenges due to varying signal strengths influenced by handset models, orientations, physical obstructions, and environmental reflections, which complicate accurate proximity detection necessary for effective coronavirus disease-2019 (COVID-19) contact tracing efforts [20]. Focuses on leveraging BLE technology for proximity detection, emphasizing the need for efficient, privacy-preserving methods and exploring various machine learning classifiers to enhance the accuracy and reliability of detecting high-risk contacts based on proximity data collected from smartphones [21]. Investigates smartphone-based applications utilizing both geolocation and Bluetooth technologies aimed at identifying and mitigating the spread of COVID-19, raising concerns regarding their practical implementation in densely populated areas and potential privacy issues associated with the tracking technologies [22]. Explores Bluetooth-based and decentralized approaches to balance effectiveness with privacy concerns, focusing on minimizing reliance on central authorities while addressing device compatibility and the operational complexities introduced by decentralized models [23]. Primarily focused on using BLE technology to estimate proximity through signal attenuation, with many studies highlighting its limitations under various environmental conditions and proposing enhancements involving machine learning models to leverage additional signal features and contextual data from smartphones to improve accuracy in both indoor and outdoor settings [24]. Utilized device-to-device interactions via technologies like Bluetooth, facing challenges such as low interoperability, modest user adoption, and privacy concerns [25]. There is an increasing focus on enhancing these

systems through epidemiological modeling and integration of environmental data to improve effectiveness and adoption rates.

Previous studies have laid a solid foundation in the use of technology for disease surveillance; however, they also reveal significant gaps in current methodologies, particularly in environments as complex as cruise ships. We provide the Binary Contact Detection Model. The integration of the alpha shape algorithm with the Binary Contact Detection Model represents an evolution in the field, aimed at overcoming this limitation.

Bluetooth 5.1 technology has been increasingly adopted in consumer electronic products, especially smartphones and wearable devices. However, considering the diversity of devices carried by cruise ship passengers, our system design does not require passengers to purchase Bluetooth 5.1 devices. Instead, the system simply needs to attach low-cost tags to the smartphones of passengers to enable positioning functionality. This approach not only reduces the barrier for passengers but also ensures broad device compatibility.

Implementing Bluetooth 5.1 AoA positioning technology involves certain costs, primarily based on the procurement of locators and tags. The cost of locators is relatively high; however, the cost of tags is relatively low. In a ship environment, cruise companies can significantly reduce overall costs by purchasing bulk tags. Additionally, the lightweight and easy-to-distribute nature of the tags simplifies logistics management, allowing cruise companies to distribute tags uniformly to passengers upon boarding, thereby ensuring efficient system operation.

The placement of antenna arrays plays a crucial role in the positioning accuracy of Bluetooth 5.1 AoA. However, antenna array optimization typically requires hardware adjustments and upgrades. Although optimizing the locator deployment positions can improve the positioning accuracy, the need to frequently adjust the locator positions in the highly dynamic environment of a ship presents certain operational challenges and limitations.

Although Bluetooth 5.3 introduces several enhancements, such as improved power efficiency, faster data transmission, and better connection stability, it does not offer specific improvements in indoor positioning accuracy compared to Bluetooth 5.1. The key feature for high-precision indoor positioning, namely the AoA functionality, is introduced in Bluetooth 5.1 and remains the core technology for accurate position tracking.

To address this issue, we adopt machine learning algorithms, such as the Random Forest (RF) algorithm, to mitigate the impact of environmental changes on positioning accuracy. Specifically, by filtering out noise features before model

training, we can enhance the quality of the input data to ensure that the model can maintain high positioning accuracy in dynamic environments. The proposed method reduces the reliance on frequent hardware adjustments, thereby allowing the system to more flexibly adapt to environmental changes while still providing reliable positioning results.

### 3. Close Contact Tracing and Risky Area Identification

In this section, we present our comprehensive approach for tracing close contacts and identifying risky areas on cruise ships. Given the unique challenges posed by the cruise ship environment—such as high-density populations, enclosed spaces, and complex interpersonal interactions—it is essential to employ advanced technologies and models to effectively monitor and control the spread of infectious diseases. Our method integrates Bluetooth 5.1 technology for precise in-ship positioning, a Binary Contact Detection Model for accurate identification of close contacts, and an alpha shape algorithm to delineate high-risk areas based on the spatial distribution of individuals. The following subsections describe each component of the proposed approach.

#### 3.1. Problem Definition

The rapid spread of infectious diseases in cruise ship environments poses a significant public health challenge. As a closed and densely populated setting, a cruise ship's unique environmental conditions—such as high-density interpersonal interactions and frequent social activities—greatly increase the risk of disease transmission. Traditional disease monitoring and control methods often fail to address the rapid spread of diseases within high-density, enclosed spaces, making efficient tracking and control difficult. Specifically, the critical issue that needs to be addressed is how to effectively and accurately track close contacts and identify high-risk transmission areas on a cruise ship. In the cruise ship environment, traditional contact tracing methods primarily rely on manual records or low-precision technological means, which are insufficient for handling the complex and variable patterns of interpersonal interactions inherent to cruise ships. Additionally, the enclosed environment facilitates the widespread dissemination of pathogens, further complicating disease control efforts.

To address these challenges, this study proposes an innovative approach that integrates Bluetooth 5.1 technology, a Binary Contact Detection Model, and the alpha shape algorithm to enhance disease monitoring and response capabilities on cruise ships. Specifically, the proposed method leverages the high-precision data capture capabilities of Bluetooth 5.1 in combination with a Binary Contact Detection Model to achieve accurate tracking of interactions between individuals. Concurrently, the alpha shape algorithm helps identify

areas most susceptible to disease transmission, providing an effective means to quantify the risk of infectious disease spread on cruise ships.

Through this comprehensive technological approach, our research aims to play a crucial role in disease prevention and control by slowing the rate of virus transmission and containing the spread within defined limits, thereby ensuring the health and safety of cruise passengers and staff. This not only offers an advanced disease monitoring solution for the cruise industry but also provides valuable insights for controlling infectious diseases in other high-density, enclosed environments.

### 3.2. In-Ship Positioning Using Bluetooth 5.1

Bluetooth 5.1's AoA indoor positioning technology is an advanced wireless positioning method that primarily determines a device's position by measuring the angles of incoming wireless signals [26]. In an AoA positioning system, a positioning tag (e.g., a device equipped with a Bluetooth transmitter) emits signals at specific frequencies. The signals are captured by a receiver equipped with multiple antennas. The receiver utilizes its antenna array to measure the angles of arrival of the signals, which includes both the azimuth angle (the angle on the horizontal plane) and the elevation angle (the angle on the vertical plane) [27]. This measurement typically involves advanced signal processing techniques, such as phase-difference measurements, where the receiver calculates the differences in signal arrival times across various antennas to infer the angles of arrival. By integrating multiple angle measurements, the system can accurately calculate the tag position in 3D space.

The internal environment of ships is complex, with many metallic structures and devices that can affect the propagation of wireless signals. Bluetooth 5.1 technology can provide more accurate positioning in such environments because it does not rely on signal strength. Known for its low

energy consumption, Bluetooth technology is well-suited for long-term operation in environments with limited power sources, which is a significant advantage for devices on ships. Compared to other advanced positioning technologies like Wi-Fi or Ultra-Wideband, Bluetooth devices generally have lower costs and are easier to deploy on a large scale. Bluetooth technology supports a wide range of devices and applications, is easy to integrate into existing ship management systems, and can support future expansions and upgrades.

Figure 1's left side shows a direction-finding antenna array labeled with specific antenna numbers from 1 to 16. This array is used to capture signals sent from various angles. Each antenna's position and angle are designed to maximize the capability to receive signals from different directions. When a tag with a Bluetooth transmitter emits a signal, the antenna receives the signal and calculates the angle of arrival based on the differences in the signal arrival times. The middle panel of Figure 1 displays a three-dimensional view of the positioning principle.

Figure 1 illustrates the AoA positioning technique used in Bluetooth 5.1 for indoor positioning. The left schematic in Figure 1 shows the direction-finding antenna array used to detect the AoA of the Bluetooth signal. The schematic on the right of Figure 1 shows how the system determines the tag's position in a three-dimensional space (X, Y, Z planes) using the elevation and azimuthal angles. By measuring the angle between the Bluetooth tag and multiple locators, the system can calculate the tag's precise position. The locators are placed at different positions, which allows the system to triangulate the tag's position using these angle measurements. Figure 1 highlights the tag's positioning in relation to the locators and explains how the azimuthal and elevation angles contribute to determining the position of the tag within the indoor environment.

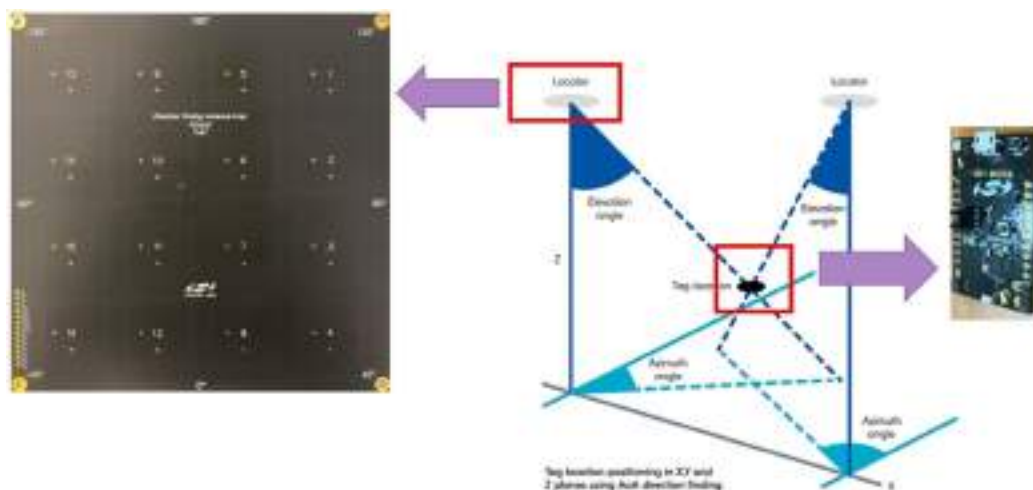


**Figure 1.** Illustration of how Bluetooth 5.1 uses the angle of arrival technique for precise indoor positioning by measuring the arrival angles of signals at a receiver antenna array

The hardware shown on the right side of Figure 1 is actually a tag equipped with a Bluetooth chip, which is used to emit signals containing specific frequencies and coding information. This transmitter is likely designed to have low power consumption and is therefore suitable for applications requiring long run times. Its main function is to continuously emit signals that are received by the direction-finding antenna array. With the combination of precise hardware and complex signal processing algorithms, high-precision position information can be obtained in complex environments. This technology is particularly suitable for scenarios requiring precise positioning, such as on ships, in large factories, or in other environments with complex physical structures. With Bluetooth 5.1 indoor positioning technology, devices can achieve efficient spatial position monitoring and management with low energy consumption [28].

### 3.3. Methods to Obtain IQ Data

Constant Tone Extension (CTE) is a technology used in Bluetooth signal transmission, specifically designed to support AoA indoor positioning functions [29]. Essentially, CTE is a continuous single-frequency tone appended at the end of a data packet. The primary function of the proposed system is to provide a stable reference point, enabling receiving devices to precisely measure the signal angle of arrival by analyzing its phase information [30]. A tag emits a Bluetooth signal containing CTE, which, following conventional data, such as device ID and other communication information, includes the additional CTE portion, as shown in Figure 2. Locators equipped with multiple antennas receive the transmitted signal. Each antenna records the signal arrival time and phase information upon receipt. The processing system within the locator calculates the phase differences of the signals received by each antenna.

Because CTE is a continuous single-frequency tone, it makes the phase information very clear and stable, thereby facilitating high-precision measurements. By analyzing the phase differences received from different antennas, the locator can determine the signal's angle of arrival, including both azimuth and elevation angles. These angles are determined based on the relative positions of the signal to each antenna. By combining the angle information provided by more locators, the system uses geometric triangulation to calculate the exact position of the tag. If the locators are fixed and their positions are known, then the exact coordinates of the tag in 3D space can be accurately determined.

Through this method, CTE enables Bluetooth technology to achieve precision positioning similar to that of radar and sonar. This high-precision angle measurement capability is particularly suitable for complex environments such as ships and large factories. Therefore, CTE not only improves the accuracy of Bluetooth positioning technology and expands its application scenarios, making it a versatile and efficient positioning tool.

In Bluetooth technology, the relationship between IQ data and CTE is central to the implementation of high-precision positioning technologies, such as AoA positioning. IQ data represent the I and Q components of a signal. These components are used to describe the signal's amplitude and phase and are fundamental to signal analysis in wireless communication. Using these data, the signal's waveform can be reconstructed and its transmission characteristics analyzed. Thus, IQ data form the basis for implementing various signal processing techniques, including frequency modulation, phase modulation, and other complex modulation-demodulation methods [31].

The antenna arrays capture CTE signals, recording the I and Q components of the signal received by each antenna.

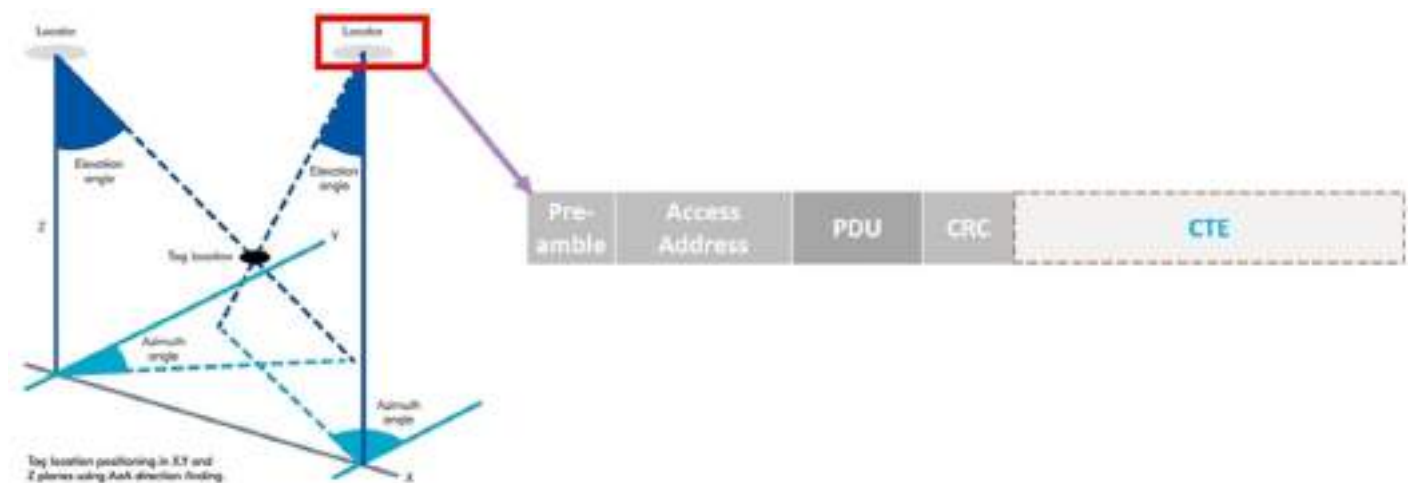


**Figure 2.** IQ sampling upon receiving CTE packets

*IQ: In-phase and Quadrature, CTE: Constant Tone Extension*

Analysis software or hardware devices use the collected IQ data to calculate the signal's phase and amplitude [32]. For AoA positioning, phase differences are particularly important because they can reveal the angle of the transmitter's position relative to the receiver. Because CTE provides a continuous and stable signal, the receiver can perform multiple measurements, thereby enhancing the angle estimation accuracy. Accurate capture of IQ data is crucial to this process. In real environments, multipath effects and environmental noise may interfere with the accuracy of IQ data; thus, high-quality signal processing algorithms and hardware are necessary to ensure correct signal interpretation and precise calculation of phase differences. The combination of IQ data and CTE achieves high-precision three-dimensional positioning in Bluetooth technology, providing an effective solution for tracking and locating devices in complex environments.

The right panel of Figure 3 illustrates the data points of the I and Q components changing over time. The blue curve represents the I data, indicating changes in the I component over time, while the orange curve represents the Q data, indicating changes in the quadrature component. The fluctuations of these two curves depict the dynamic characteristics of the signal, with each point's vertical position representing the amplitude of the component at specific moments in time.

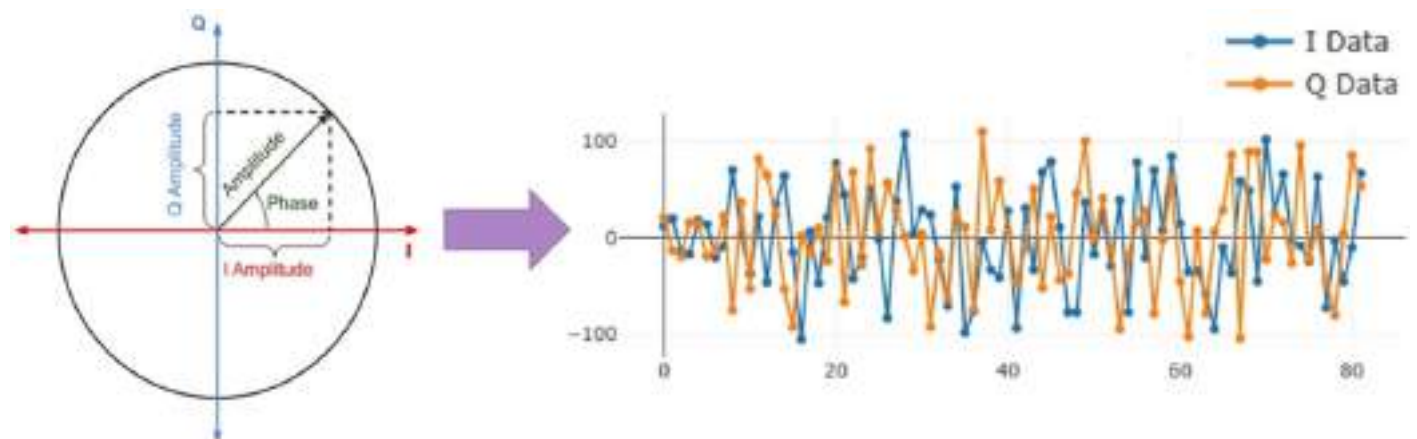


**Figure 3.** Visualization of IQ data

*IQ: In-phase and Quadrature*

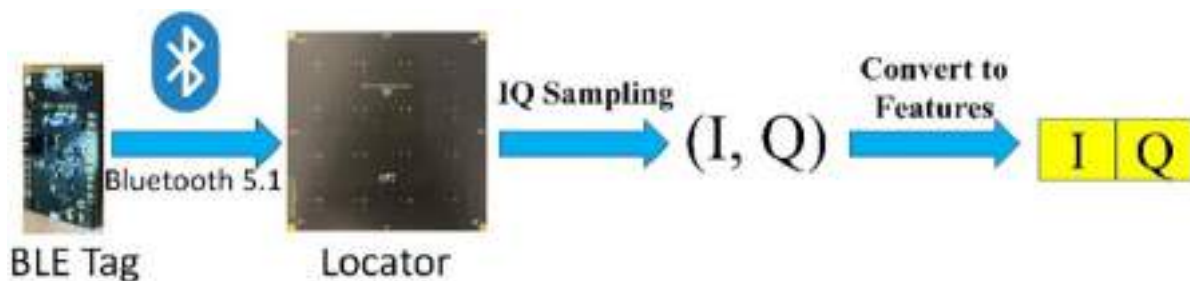


**Figure 4.** The IQ data processing flow from BLE tag to model-ready features

*IQ: In-phase and Quadrature, BLE: Bluetooth Low Energy*

### 3.4. Pairwise Combined IQ Data

The Binary Contact Detection Model identifies close contacts using Pairwise Combined IQ Data. The proposed method combines the identification results from the Binary Contact Detection Model and the corresponding positions with the alpha shape algorithm to identify risky areas. Positions are precisely determined by affixing BLE tags to user smartphones and leveraging Bluetooth 5.1 technology for data acquisition. The core concept of directly converting IQ data into features acceptable by a model lies in fully utilizing the rich information contained within the IQ data to simplify the data processing workflow and enhance model performance. IQ data can comprehensively describe the amplitude and phase information of signals, which is crucial for many applications. By directly using these raw IQ data as input features for models, more useful information can be retained, thereby avoiding information loss during the data preprocessing stage and simplifying the complexity of data processing. Directly using IQ data as features can also improve the predictive performance of the model, as these data contain complete signal information that helps in more accurately capturing signal characteristics.

Figure 4 illustrates the entire process of transmitting IQ data from a BLE Tag to a Locator via Bluetooth 5.1 and eventually

converting it into features acceptable to the model. The icon on the left represents the BLE Tag, which transmits data via Bluetooth 5.1. The icon in the middle panel of Figure 4 represents the locator. The locator receives the signals transmitted from the BLE Tag and performs IQ sampling. IQ sampling is achieved by extracting the I and Q components from the received signal. The arrow labeled “IQ Sampling” in Figure 4 illustrates this process, with the (I, Q) symbols next to it representing the collected IQ data.

Subsequently, these IQ data are converted into features that can be directly used as model input. The arrow labeled “Convert to Features” in Figure 4 indicates this conversion process. The converted feature data are shown in the yellow box on the right (labeled I and Q, indicating the directly used feature data). The key to this step is that it does not require complex feature extraction methods; it simply involves using raw IQ data directly as model input, which simplifies the data processing workflow.

Figure 4 shows the process of transmitting signals from the Tag device via Bluetooth 5.1, performing IQ sampling with the locator, and eventually converting these IQ data into features for direct use in model input. This approach not only simplifies the data processing workflow but also retains crucial signal information, potentially enhancing model performance and enabling functionalities such as localization and signal classification.

IQ data between close contacts may be similar or exhibit certain patterns. Therefore, assuming that we already know that an individual is a COVID-19 patient or has close contact with other individuals, we can combine the IQ data of other individuals with the IQ data of the known individual in pairs to provide input features to the model. If the model outputs a result of 1, then the individual and the known close contact are also closely connected. Until the identification results of all individuals are obtained, all individuals are considered potential close contacts.

Specifically, the first step is to identify and confirm COVID-19 patients or known close contacts whose IQ data served as the reference baseline. Then, the IQ data of other individuals are combined with the IQ data of a known individual in pairs to form new feature pairs. These paired IQ data can be used as input features for the machine learning model, which makes predictions based on them. If the model outputs a result of 1, it indicates that the individual has close contact with a known close contact; if the result is 0, it indicates no close contact. Based on the model prediction results, new close contacts can be identified and marked. Until the identification results of all individuals are obtained, all individuals are considered potential close contacts.

During data collection and preprocessing, IQ data can be normalized or standardized to reduce noise and interference effects on the model, thereby improving the prediction accuracy and stability of the model. Using the data of known COVID-19 patients and close contacts, the machine learning model can be trained to recognize patterns in the IQ data. An RF classifier can be used to train and optimize the model. After training the model, it can be tested using a validation dataset to evaluate its accuracy. By continuously adjusting the model parameters and improving the algorithms, the model’s performance can be enhanced.

Deploy the trained model into practical applications and monitor its prediction results in real time to ensure that it accurately identifies potential close contacts. Continuously collect new IQ data to update and optimize the model, and address any changes or challenges that may arise. Through these steps and methods, an efficient COVID-19 close-contact identification system can be established to help promptly detect and isolate potential infected individuals, effectively controlling the spread of the pandemic. This approach not only simplifies the data processing workflow but also improves identification accuracy and efficiency, thus contributing to public health management and pandemic prevention.

Figure 5 illustrates the concept of using the IQ data of already labeled close contacts to identify potential close contacts. At the top of Figure 5, the IQ data of close contacts (represented by blue dots) are displayed. The middle panel of Figure 5 presents two sets of IQ data: the upper panel presents the IQ data of known close contacts (blue dots), and the lower panel presents the IQ data of potential close contacts (red dots). The bottom section of Figure 5 provides a solution, indicating that the IQ data of known and potential close contacts should be considered as one group and input into a classifier for identification. This process is further emphasized by a yellow arrow, explaining the specific operation of combining the two sets of IQ data and inputting them into the model for classification. To expand on this, the workflow depicted in Figure 5 involves several key steps. First, the IQ data from known close contacts, represented by blue dots, are used as baseline data. Then, the IQ data of potential close contacts (red dots) are paired with these known data to form new data pairs. Next, these paired data are input into a classification model for training and prediction. By learning the features within these IQ data pairs, the model can identify which individuals are likely to be new, close contacts.

The underlying logic of the proposed method is that the IQ data of close contacts may exhibit similar feature patterns. By using a machine learning model, these feature patterns can be recognized automatically, thereby allowing accurate identification of potential close contacts.

### 3.5. Binary Contact Detection Model

The sigmoid function is a commonly used activation function in machine learning and neural networks. The characteristics of the sigmoid function make it particularly suitable for binary classification problems, where it can map input real numbers to a range of (0,1), representing the probability of a particular class. For example, in binary classification models, the output processed by the sigmoid function can be interpreted as the probability that a sample belongs to a certain class. However, in some practical applications, the standard sigmoid function may not sufficiently meet the requirements; thus, we propose the Shifted-Scaled Sigmoid Function.

The proposed Shifted-Scaled Sigmoid Function is proposed because the standard sigmoid function may have limitations in some application scenarios and may not fully meet the actual requirements. The standard sigmoid function is centered at 0, which means that its symmetry is centered around 0. The standard sigmoid function has an output range of (0,1) with a smooth transition at 0.5, which is an ideal threshold. However, in many cases, the distribution of input data is not symmetric, or the characteristics of the data are not suitable for being centered around 0.

For example, in some detection and classification tasks, the mean or median of the input data may be offset from 0. In such cases, using the standard sigmoid function would lead to biased classification results and would not accurately reflect the actual situation. Therefore, adjusting the position of the sigmoid function so that its symmetry is centered around the median of the data can improve the model’s prediction accuracy. Furthermore, the steepness of the standard sigmoid function is fixed; thus, it may not provide sufficient discriminative power for tasks requiring

more sensitive threshold transitions. In these tasks, we want the function to have a more rapid transition near a specific point, which allows the model to make clearer classifications for data points close to the threshold. This requires adjusting the steepness of the function to accommodate different application requirements. Table 1 provides a detailed description of the symbols and notations used throughout this paper.

In Equation (1), we define “prediction<sub>i</sub>” as the models predicted output for the *i*-th sample, which is expressed as

$$prediction_i = f(x_i) \tag{1}$$

where *f* represents the model’s prediction function, and *x<sub>i</sub>* is the input feature vector of the *i*-th sample.

By employing the Shifted-Scaled Sigmoid Function, we can shift the center of the sigmoid function from 0 to other specific values in the data, thereby making the classification threshold more reasonable and accurate. Before introducing the Shifted-Scaled Sigmoid Function, we first need to understand two important parameters: *k* and *x* (Equation 2).

$$x = \frac{\sum_{i=1}^k prediction_i}{k} \tag{2}$$

where *k* is the amount of input data. *x* is the cumulative average of the model’s output values. After introducing *k* and *x*, we introduce the Shifted-Scaled Sigmoid Function. The Shift-Scaled Sigmoid Function is formulated as Equation (3).

$$Shifted - Scaled Sigmoid Function = \frac{1}{1+e^{-k(x-0.5)}} \tag{3}$$

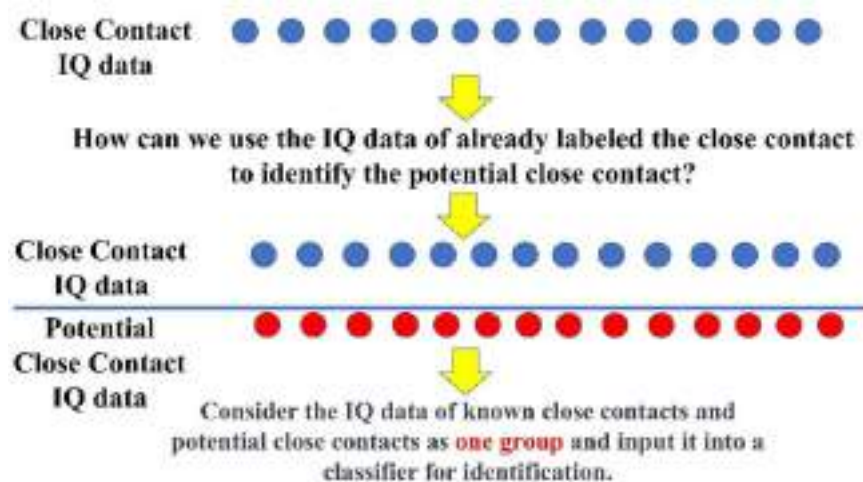


Figure 5. Using IQ data on labeled close contacts to identify close contacts

*IQ: In-phase and Quadrature*

where the shift parameter 0.5 moves the center from 0 to 0.5, thereby making the function symmetrical around 0.5. The choice of 0.5 as the shift parameter is intended to align the decision threshold of the sigmoid function with the standard for binary classification problems, thereby enhancing classification accuracy and interpretability while ensuring model consistency and natural symmetry. The scaling parameter  $k$  controls the function steepness. Larger  $k$  values make the function steeper at approximately 0.5, which makes the distinction between 0 and 1 in classification tasks more clear. Therefore, if the output value is greater than 0.5, it is classified as 1; otherwise, it is classified as 0.

For example, the distribution of Pairwise Combined IQ Data may be asymmetric, and the feature center of the data may deviate from 0. By using the Shifted-Scaled Sigmoid Function, we can ensure that the model's classification threshold is closer to the actual data feature center, thereby avoiding classification errors caused by the standard sigmoid function's center deviation. At the same time, by adjusting the scaling parameter  $k$ , the model can more flexibly adapt to different data distributions, which improves the accuracy and stability of the classification results.

In summary, the shift-scaled sigmoid function overcomes the limitations of the standard sigmoid function in terms of center position and steepness by shifting and scaling it, making it better suited for various practical applications. By adjusting the values of  $x$  and  $k$ , the model's classification accuracy and stability can be improved, making it suitable for tasks that require flexible adjustment of classification thresholds and rapid response to changes.

Cruise ships are constructed with extensive metal structures, including hulls, decks, and bulkheads, which can cause

significant signal reflection, absorption, and multipath propagation. These metal surfaces can distort Bluetooth signals, leading to errors in the angle estimation and reduced reliability of AoA measurements. Additionally, the complex layout of ships, with numerous confined spaces and obstacles such as walls, furniture, and equipment, contributes to signal obstructions. The dynamic movement of passengers and crew members adds another layer of complexity, as human bodies can absorb and reflect signals, causing fluctuations in signal strength and quality.

To mitigate these environmental factors and enhance the accuracy of Bluetooth 5.1 AoA technology on cruise ships, this study employs a method that involves optimizing the features of the input signal. Signal data are used as features and input to machine learning algorithms, such as the Light Gradient Boosting Machine (LightGBM), to perform feature filtering. This process forms a feature filter that removes noisy features, effectively addressing the inherent interference problem. By filtering out these noisy features—which represent manifestations of environmental interference—the overall impact of interference in the ship environment can be mitigated. This optimization enhances the quality of the data used for angle estimation, leading to more reliable AoA measurements and improved positioning accuracy. Moreover, our approach does not require the assistance of the Wireless Fidelity (WiFi) and the Radio Frequency Identification (RFID) to improve accuracy, thereby avoiding increased hardware costs.

The Binary Contact Detection Model is a machine learning model designed to identify close contacts. Its core idea is to use Pairwise Combined IQ Data as features, undergo a series of feature selection and classification processing

**Table 1.** Notations and symbol descriptions

Symbol	Description
$f(x_i)$	The function represents the model's prediction function, and is the input feature vector of the $i$ -th sample
prediction <sub><math>i</math></sub>	The models predicted output for the $i$ -th sample
$k$	Amount of input data used to calculate the average prediction
$x$	Cumulative average of the model's output values
$h(p)$	Prediction function for close contact between devices
$e_i$	The positional coordinate of the $i$ -th device pair is predicted as "1" (close contact)
$E$	Set of positional coordinates of all device pairs predicted as "1"
$\sigma$	A simplex with a circumcircle radius in the Delaunay triangulation
$Del(E)$	Delaunay triangulation of position set $E$ , a geometric structure that connects points to form triangles where no point is inside the circumcircle of any triangle
$r(\sigma)$	The radius of the circumcircle
Alpha	The parameter that controls the tightness of the shape
$n$	Number of positions in the input set $E$
$\gamma$	Adjustment factor for the alpha value (typically set to 1)



steps, and finally use the Shifted-Scaled Sigmoid Function to output the result, determining whether an individual is in close contact. The specific process is as follows: first, the IQ data are paired to form Pairwise Combined IQ Data, which generates the initial feature set. Then, through Controllable Feature Selection (CFS), including feature importance calculation using LightGBM, sorting features by importance in descending order, forward feature selection, and RF classifier validation, the optimal feature set is finally output. The optimal feature set forms a feature filter that screens the most important features. The features processed by the Feature Filter are then input into a trained RF classifier for initial classification, and the final classification result is input into the Shift-Scaled Sigmoid Function. If the output is 1, the individual is considered to have close contact; if the output is 0, the individual is considered to have no close contact.

Figure 6 illustrates the overall process of the Binary Contact Detection Model, including two main stages: the offline and online stages, used to identify close contacts. In the offline stage, IQ data are paired to form Pairwise Combined IQ Data, generating the initial feature set. Next, CFS is performed, which includes feature importance calculation, sorting features by importance in descending order, forward feature selection, and RF classifier validation. These steps ultimately output the optimal feature set.

In the online stage, the input Pairwise Combined IQ Data is represented by green dots. First, this data is screened through a feature filter formed using the optimal feature set obtained in the offline stage to filter out important features. Then, the features processed by the Feature Filter are input to a trained RF classifier for initial classification. The classification result is then processed by the Shift-Scaled Sigmoid Function, which ultimately outputs 0 or 1. If the result is 1, the individual is judged to have close contact; if the result is 0, the individual is judged to have no close contact.

Through this process, the Binary Contact Detection Model can effectively identify close contacts, improving the model's classification accuracy and stability, making it suitable for public health management and epidemic prevention.

### 3.6. System Model

In this study, a risky area is defined as the convex hull polygon formed by a set of positions of close contacts. Therefore, we propose an innovative model that combines an alpha shape algorithm and the output of a Binary Contact Detection Model to precisely identify and mark risky areas. This method is particularly suitable for disease transmission and public health management, especially in environments where rapid identification and response to infectious disease outbreaks. The Binary Contact Detection Model, which is based on IQ data received from the locator, predicts whether

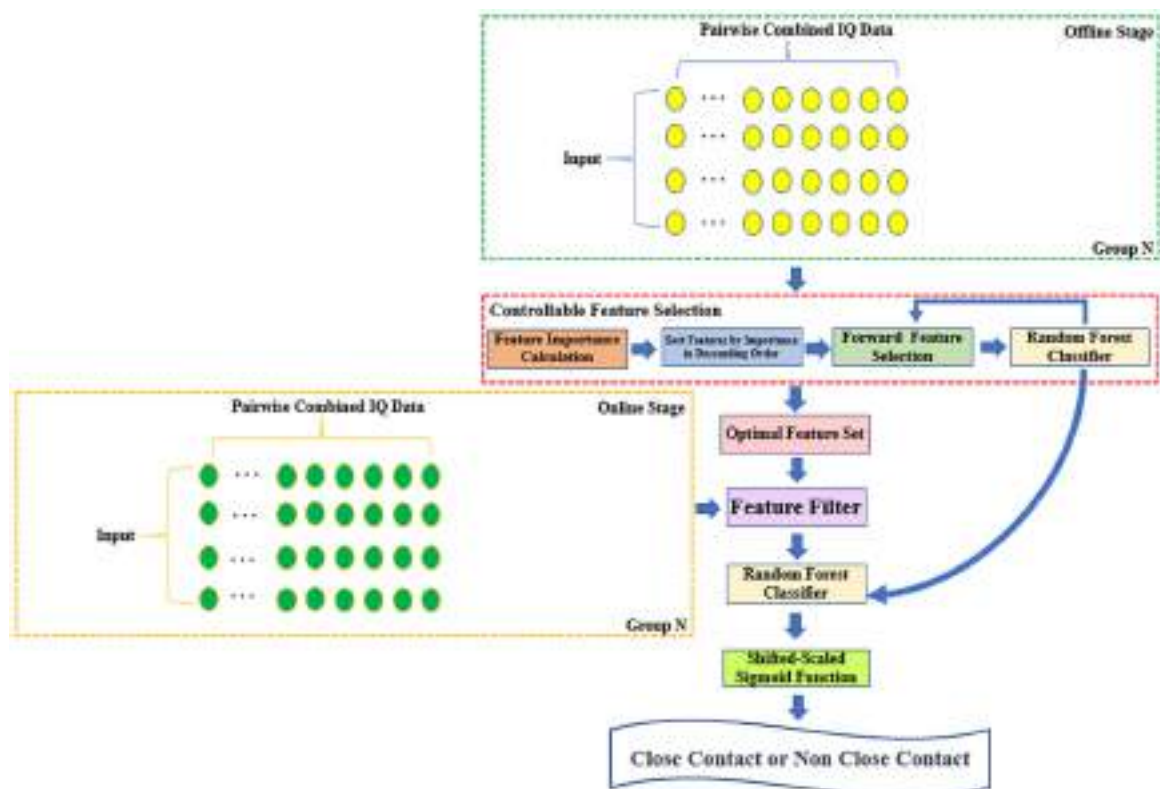


Figure 6. Binary Contact Detection Model

there is close contact between individuals based on the BLE Tags they carry. The model outputs a binary value-1 or 0. Here, “1” indicates that there is close contact between two devices, and “0” indicates non-close contact. This step is crucial for identifying risky areas.

All device pairs marked as “1” in the Binary Contact Detection Model are considered close contacts. The positional coordinates of these devices are extracted as inputs to the subsequent alpha shape algorithm. This selection process ensures that the alpha shape algorithm is applied only to the points most likely to be mediators of disease transmission, thereby enhancing the efficiency and focus of the overall analysis.

The Binary Contact Detection Model predicts the likelihood of close contact between each pair of individuals based on the IQ data from their devices. The output value of “1” indicates close contact, while “0” indicates non-close contact. Let  $\{p_1, p_2, \dots, p_n\}$  be the set of positions, and the prediction function  $h(p)$  is given by Equation (4).

$$h(p) = \begin{cases} 1, & \text{if close contact between devices} \\ 0, & \text{if non - close contact} \end{cases} \quad (4)$$

The positional coordinates of all device pairs predicted as “1” form the input position set  $E$  for the alpha shape algorithm, that is Equation (5).

$$E = \{e_i | h(p_i) = 1\} \quad (5)$$

Given a set of positions  $E$  the alpha shape algorithm is used to identify the shape formed by these positions. An appropriate alpha value is selected that determines the tightness of the algorithm boundary. The convex hull contains all the positions in the set. The Convex Hull is a special case of the alpha shape; specifically, it is the alpha shape when the alpha tends toward infinity. In this limit, all positions are included in a single convex shape without considering any internal structure or holes within the set of positions. The larger the alpha value, the more the resulting alpha shape tends to approximate the convex hull of the position set.

Alpha shape is used to determine the shape of a position set by analyzing its Delaunay triangulation. The construction of the alpha shape is based on the Delaunay triangulation of the position set. The Delaunay triangulation provides a well-defined circumcircle for each triangle, characterized by not containing any other positions. Alpha shapes compare the radius of these circumcircles with a given threshold alpha to decide which triangles should be included in the final shape [33]. Technically, if the circumcircle radius of a simplex (an edge or triangle) in the Delaunay triangulation

is less than or equal to alpha, then that simplex is included in the alpha shape [34]. When the alpha value is small, only positions that are very close to each other are connected, resulting in a tighter, more detailed shape that may exhibit more non-convex features. As the alpha value increases, more simplices are included, and the alpha shape gradually expands until it becomes the convex hull of the position set when the alpha value is sufficiently large to exceed the maximum distance between any positions.

Using position set  $E$  as input, the alpha shape algorithm is used to determine the boundary of the area formed by these close contacts. Let  $Del(E)$  represent the Delaunay triangulation of the position set  $E$ , and let simplex  $\sigma \in Del(E)$  have a circumcircle with radius  $r(\sigma)$ . The alpha shape can be described by Equation (6) [35].

$$A_{Alpha} = \cup\{\sigma \in Del(E) | r(\sigma) \leq Alpha\} \quad (6)$$

where  $\sigma$  represents a simplex (an edge or triangle) within the Delaunay triangulation,  $r(\sigma)$  is the radius of the circumcircle, and alpha is the parameter that controls the tightness of the shape. In the alpha shape algorithm, triangles whose circumcircle radius is less than or equal to alpha are selected as part of the alpha shape. Each triangle in Delaunay triangulation undergoes a filtering process, ultimately forming a shape that describes the original set of positions.

In the traditional alpha shape algorithm, alpha represents the radius of the largest circle (or sphere) used in the construction of the shape. As the number of positions involved in the calculation increases, the complexity of the Delaunay triangulation also increases. If the alpha value is kept constant, new positions may be added that form new simplices whose circumcircle radii exceed the current alpha value, thereby refining the alpha shape. However, if the alpha value increases with the number of positions, more triangles can be maintained within the alpha shape, making the shape more likely to encompass the Convex Hull, which includes all positions. Here,  $n$  is the number of positions in input set  $E$ .

$$n = |E| \quad (7)$$

$$Alpha = \gamma \times n \quad (8)$$

where  $\gamma$  is an adjustment factor that can be modified based on the specific characteristics of the dataset, which is typically set to 1. This dynamic adjustment of the alpha shape’s size adapts to changes in the size of the position set, thus more

effectively reflecting the spatial structure and characteristics of the dataset. This setting allows the value of alpha to grow linearly with the number of positions while maintaining sufficient flexibility and coverage while avoiding overly complex shapes. In many practical application scenarios, the collection of positions is not static, but can change over time or under different conditions. Setting alpha proportional to the number of positions, scaled by  $\gamma$ , provides a natural mechanism by which the alpha shape dynamically adapts to changes in the number of positions.

Through this approach, the combination of the alpha shape algorithm and Binary Contact Detection Model not only provides precise delineation of risky areas but also makes the management of these areas more scientific and systematic, thereby effectively supporting the formulation and implementation of disease prevention and control measures.

Figure 7 illustrates a process for identifying risky areas, where the output of the Binary Contact Detection Model is used in the alpha shape algorithm to calculate risky areas. In this model, the output of the Binary Contact Detection Model is 0 or 1, indicating whether close contact exists between device pairs. If the model output is 1, then the two devices are determined to be in close contact, and their positions are marked and extracted.

Next, the positions of all devices marked as 1 by the Binary Contact Detection Model are collected from position set

$E$ , which is then inputted into the alpha shape algorithm. The alpha shape algorithm determines the shape boundaries by computing the Delaunay triangulation of these positions and by filtering out triangles or edges whose circumcircle radii do not exceed alpha.

In particular, Delaunay triangulation is first performed for position set  $E$ . Delaunay triangulation is a special type of triangular mesh in which no positions from the set are inside the circumcircle of any triangle. Next, alpha is calculated based on the number of positions  $n$  in the set  $E$  and the factor  $\gamma$ . Then, the alpha shape is constructed by filtering out triangles and edges from the Delaunay triangulation whose circumcircle radii are less than the alpha radii. The filtered simplices form the alpha shape.

Through these steps, the alpha shape algorithm generates a shape boundary that includes all positions from point set  $E$ . The final output risky area is indicated by the red boundary in Figure 7. This method, by combining the output of the Binary Contact Detection Model with the alpha shape algorithm, not only dynamically adjusts the shape to adapt to changes in the dataset but also precisely identifies and marks the risky areas. This is of significant importance for public health management and disease prevention and control, as it helps to detect and isolate close contacts to prevent the spread of epidemics.

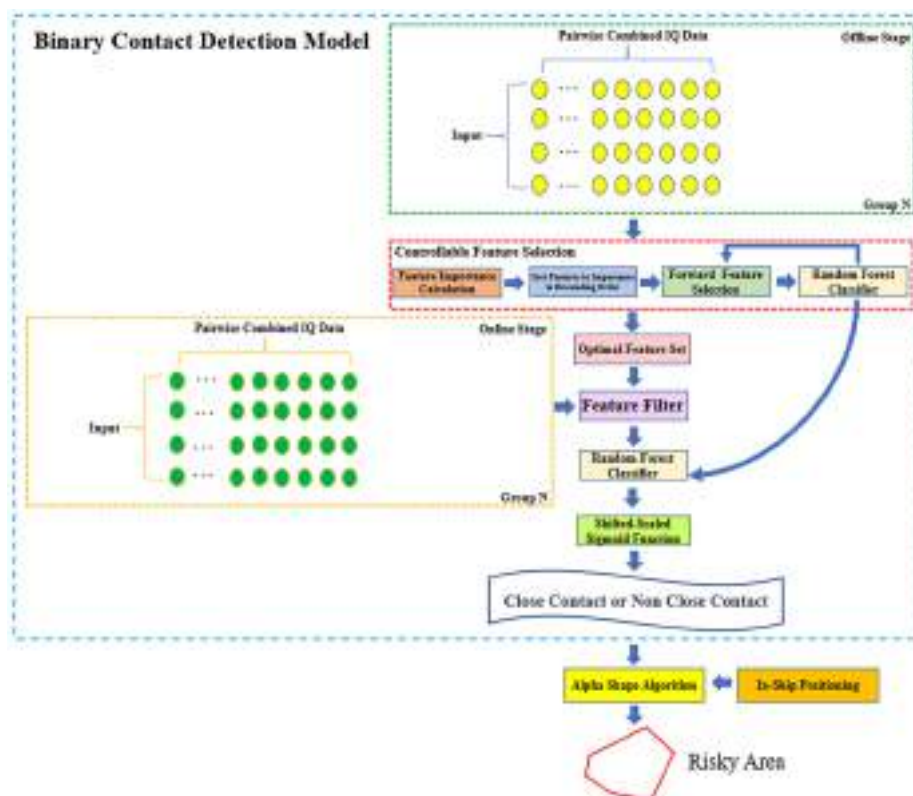


Figure 7. Risky area identification process based on alpha shape algorithm and binary contact detection model

### 4. Performance Evaluation

Figure 8 shows the layout of the upper deck of the HANNARA ship used to collect IQ data for the close-contact experiments. In this experiment, BLE Tags are placed in various positions on the deck, and user positions (blue markers) are recorded, allowing the capture and recording of individual BLE tag IQ data. The experiment focused on pairs of individuals within a distance of 1.5 m. These individuals are considered to have close contacts because their physical distance falls within the possible range of disease transmission. Through this experimental layout and data collection, we can use the collected IQ data to train and validate the Binary Contact Detection Model.

In Figure 8, “2-12” indicates that individuals 2 and 12 form a group called group 1, which is abbreviated as “g\_1”. Therefore, there are 8 groups of close contacts and 8 groups of non-close contacts, totaling 16 groups. The 8 groups of close contacts are “g\_1, g\_2, g\_3, g\_4, g\_5, g\_6, g\_7, g\_8”, while the 8 groups of non-close contacts are “g\_9, g\_10, g\_11, g\_12, g\_13, g\_14, g\_15, g\_16”. Table 2 summarizes the key experimental parameters and model configurations used in this study, including the environment, model types, dataset size, and performance metrics.

In Figure 9, the x-axis represents the relative importance calculated by the Binary Contact Detection Model, indicating

the relative importance of each feature. This value is typically computed based on how the feature improves the model’s predictive performance, for example, in decision trees, it can be based on the gain during node splits. The y-axis lists the names of the features used for learning and prediction in the Binary Contact Detection Model. This graph shows the contribution of IQ data to the decisions made by the Binary Contact Detection Model. The Binary Contact Detection Model uses 144 IQ data points as features. For ease of display, the graph only lists the top 20 features. For example, “IQ\_data\_1\_I\_24” represents the I data of the 24<sup>th</sup> IQ data point from BLE Tag 1. In a ship scenario, these features can represent data points used to identify close contacts. The

Table 2. Experimental setup

Parameter	Description
Environment	Python
Model type	LightGBM, Random Forest
Number of samples	23,932
Feature count	144
Train-test split ratio	70% training and 30% testing
Performance metrics	Accuracy, AUC, precision, recall, F1 score, receiver operating characteristic
LightGBM: Light Gradient Boosting Machine, AUC: Area Under the Curve	

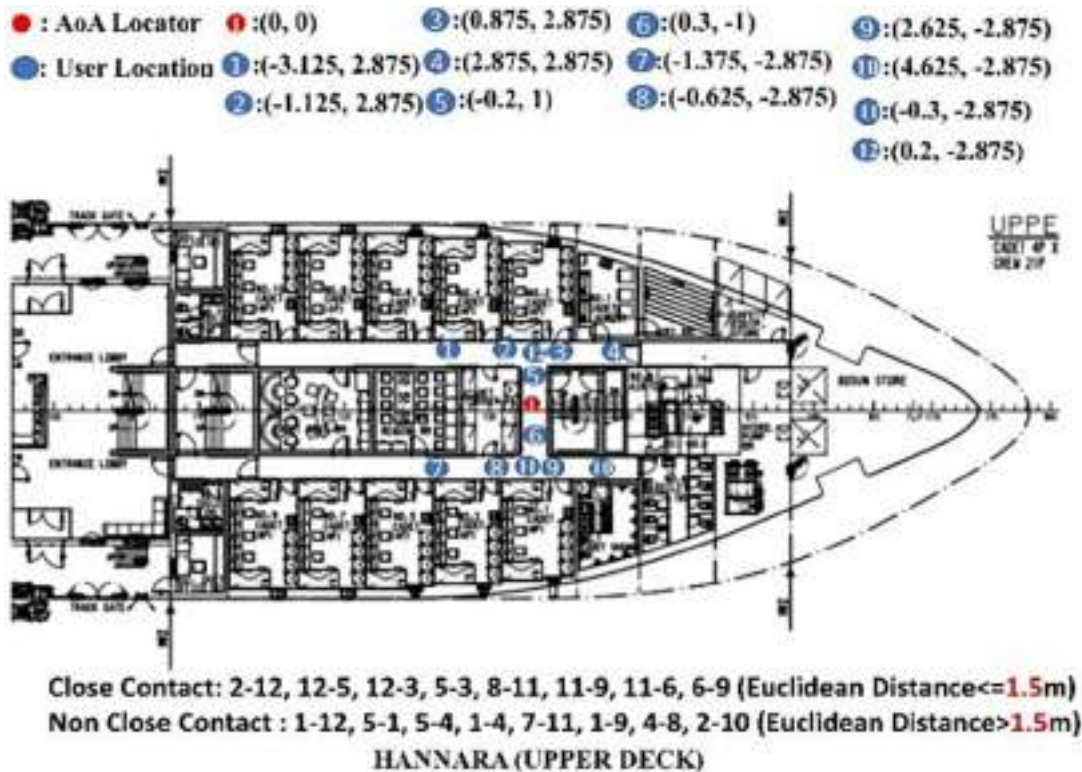


Figure 8. HANNARA ship upper deck layout for a close contact experiment

features are sorted by their relative importance, with the most important features playing a more significant role in the predictions made by the Binary Contact Detection Model. This means that these features provide the most information when identifying close contacts.

An in-depth examination of Figure 9 reveals that the top-ranked features have a significantly higher relative importance than the others. This indicates that a small subset of IQ data points strongly influences the model's predictive

ability. By focusing on these key features, we can potentially streamline the model for faster computation without sacrificing accuracy. Additionally, understanding the most impactful features can provide insights into the underlying patterns that signify close contacts, thereby improving feature engineering and data collection strategies in future implementations.

As shown in Figure 10, as the number of sorted features increases, the key evaluation metrics such as test accuracy,

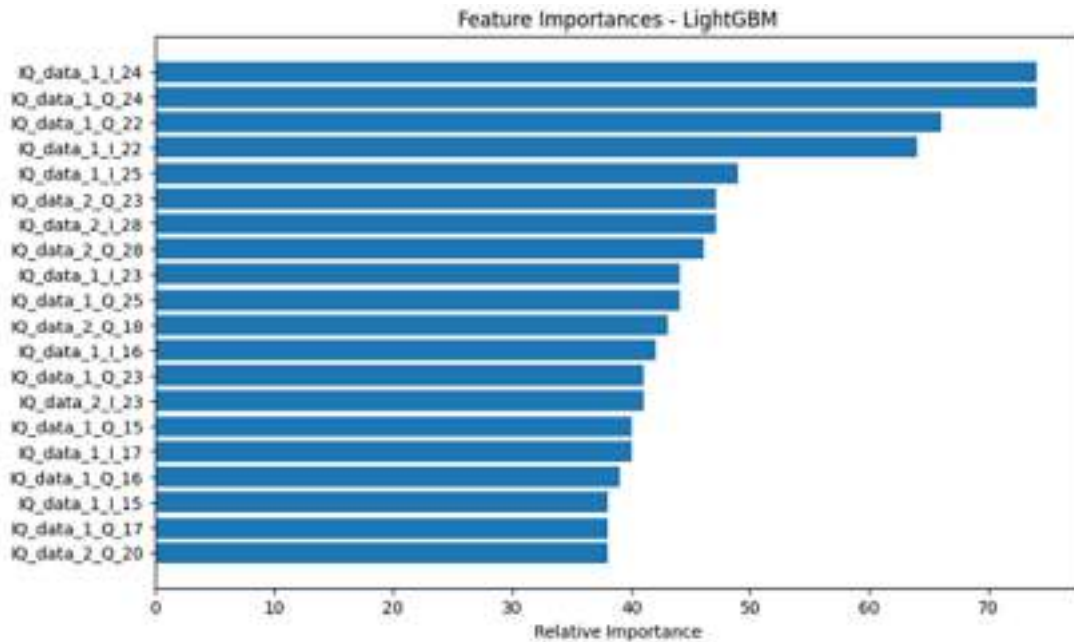


Figure 9. A graph showing the contribution of IQ data to the model's decision IQ: In-phase and Quadrature

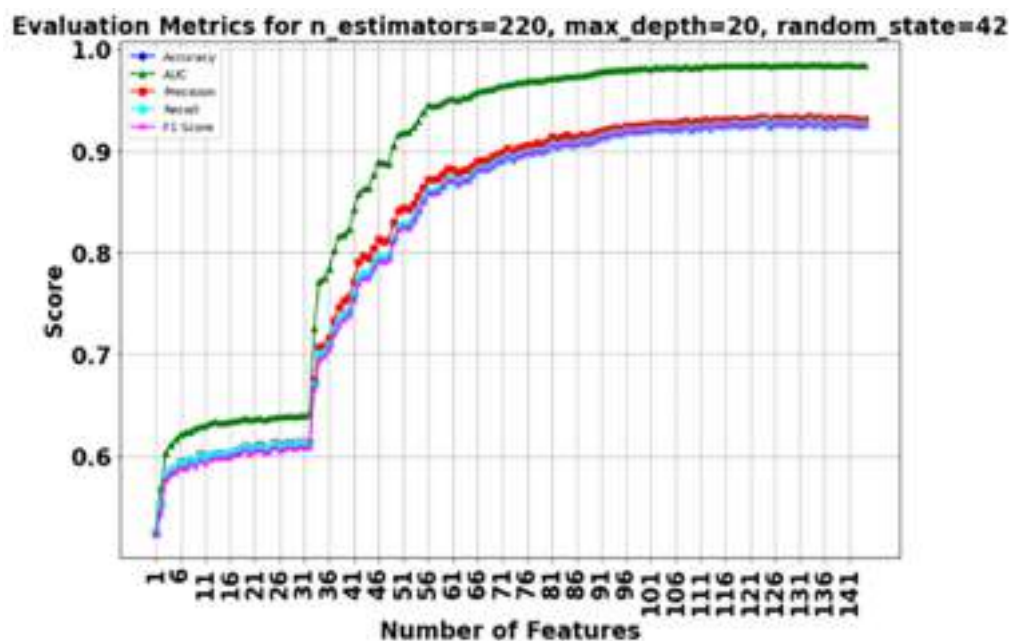


Figure 10. Impact of sorted number of features on model evaluation metrics

Area Under the Curve (AUC), precision, recall, and F1 score, of the model initially show signs of improvement; however, these performance metrics stabilize after reaching a certain point. The x-axis represents the “Number of Features” used by the Binary Contact Detection Model for prediction. These features may be columns of the dataset, which the model uses to make predictions. The y-axis represents the “Score”, which measures the performance of the model. The score ranges from 0 to 1, with a score closer to 1 indicating better model performance.

In particular, the data demonstrate that when the number of features reached above 33, the model performance significantly improved. Starting from the 33 features, all major performance metrics (accuracy, AUC, precision, recall, F1 score) increased significantly. This trend indicates that initially increasing the number of features can provide more information to the model, thereby enhancing its predictive capability. However, after reaching a certain number of features, performance improvement becomes very limited. In particular, when the number of features is small, model performance improved significantly, especially as the number of features started to increase from a lower range. In particular, model performance improved noticeably before reaching a certain threshold. This threshold represents the turning point at which the model transitions from acquiring essential information to approaching its performance ceiling. The test accuracy and AUC initially improved with an increase in the number of features, indicating that the model’s ability to distinguish between different categories is enhanced. However, after the number of features increases to a certain level, the improvement in these metrics diminishes and eventually stabilizes, which indicates that the model has reached its potential limit in distinguishing capability.

The precision, recall, and F1 scores also demonstrate noticeable improvements when the number of features is small, followed by a slowdown in performance enhancement and stabilization as the number of features continues to increase. As the model processes more information, its ability to classify positive and negative samples reaches a certain balance. The results demonstrate that adding features significantly improves model performance when the number of features is small. However, beyond a certain threshold, the performance improvement diminishes and stabilizes, emphasizing the importance of fine feature selection to add necessary information while avoiding excessive noise or irrelevant information.

Ultimately, Figure 10 underscores the principle of the “curse of dimensionality”, where adding too many features can lead to diminishing returns or even degrade model performance due to overfitting or increased noise. This highlights the necessity of an optimal feature set that balances the amount of information provided and the potential for introducing irrelevant data. This balance ensures that the model remains both efficient and effective, maximizing the predictive accuracy while minimizing the computational complexity.

Figure 11 shows the receiver operating characteristic (ROC) curve, which shows the performance of the classification model at all possible classification thresholds. The AUC is a metric used to measure the performance of a classifier, with higher AUC values indicating better classifier performance. An ideal ROC curve bends toward the top left corner of the plot, which means that the classifier can achieve a high True Positive Rate (TPR) with a low False Positive Rate (FPR).

In Figure 11, the ROC curve is displayed in orange, starting from (0,0), rapidly rising to near the (0,1) point, and then

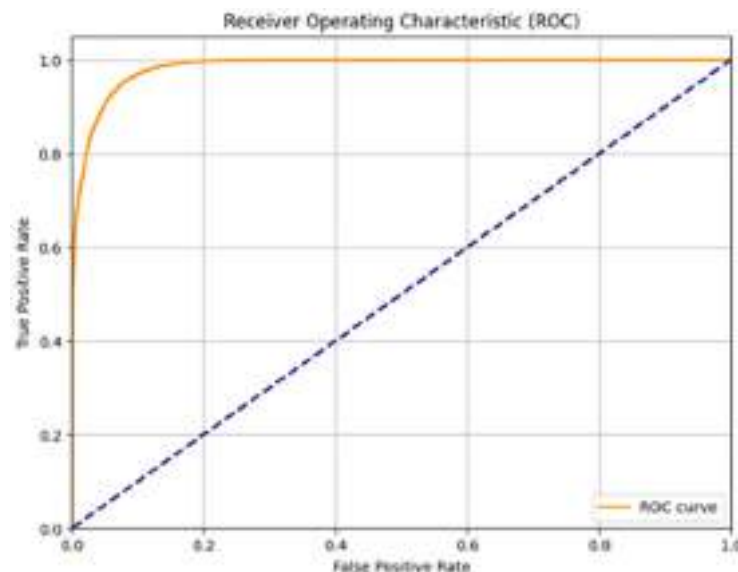


*Figure 11. Receiver operating characteristics*

gradually approaching (1,1) to the right. The blue dashed line represents the performance of a Random Classifier (RF), essentially the result of random guessing, and the slope of this line is 1, indicating that the TPR and FPR are equal for the classifier. Ideally, the ROC curve should be above the blue dashed line, indicating that the classifier's performance is better than random guessing. In Figure 11, the ROC curve is clearly above the blue dashed line, indicating that the classifier exhibits good classification performance.

The sharp ascent of the ROC curve in Figure 11 toward the top left corner demonstrates the model's strong ability to distinguish between the positive and negative classes. The substantial AUC indicates that the model performs significantly better than random guessing. This high AUC value signifies that the model exhibits a high TPR while maintaining a low FPR across various thresholds. Such performance is crucial in applications like close contact detection on ships, where accurately identifying potential risks without generating excessive false alarms is essential for effective disease prevention and control measures.

Figure 12 shows the results of 8 overlapping risky areas on the HANNARA upper deck. The x-axis represents the pixel width, which can be understood as the horizontal resolution of the image, and the y-axis represents the pixel height, corresponding to the vertical resolution of the image. This is the visual overlap of 8 risky areas identified by the model. The risky areas are determined based on the likelihood of close contact, which involves disease prevention and ship safety monitoring. In the daily operation of a ship, these results can be used to monitor the flow and activities of personnel to ensure the safety of passengers and crew. If a specific area is marked as high-risk, measures can be taken

to restrict access to that area or increase the frequency of cleaning and disinfection. This not only provides an intuitive representation of the risky areas but also helps managers take preventive measures to reduce health risks on the ship. By monitoring and adjusting the usage patterns of the ship, the spread of diseases onboard can be effectively controlled and prevented.

## 5. Discussion

Our experimental results demonstrate that after filtering out noise features, the model's performance improved significantly as the number of features increased from a lower range [36]. This indicates that utilizing more relevant information greatly enhances the model's ability to identify close contacts. This trend emphasizes the importance of providing the model with sufficient and relevant information to ensure accurate identification of close contacts and areas of transmission risk.

Our goal is to first filter out noise features and optimize the feature set, thereby ensuring that the model receives only effective information that contributes to improved identification accuracy. Filtering out noise features not only reduces the model's complexity but also enhances its robustness when handling high-density, complex interpersonal interaction environments [37]. Subsequently, as the number of features increases, the model leverages more relevant information to further enhance its ability to identify close contacts and transmission risky areas. The proposed method effectively combines feature selection and feature expansion to ensure that the model remains efficient and precise while being information rich.

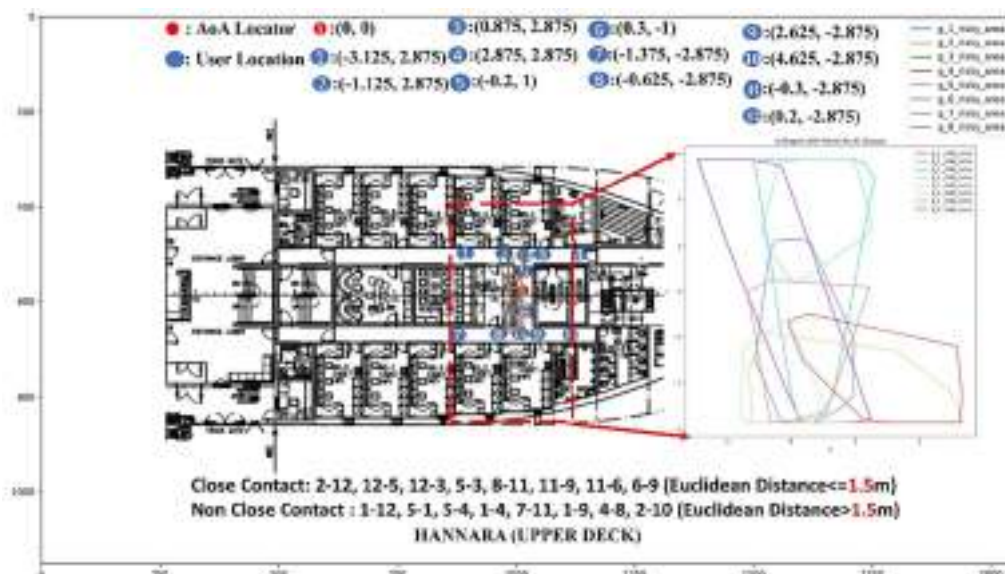


Figure 12. Results of 8 risky areas on the HANNARA upper deck

The proposed method primarily relies on Bluetooth 5.1 technology to track close contact between individuals and employs a Binary Contact Detection Model to analyze these data. Although this technology is highly effective at detecting direct interpersonal contact, it does not capture pathogens transmitted through the air. However, timely identification of close contacts can still significantly reduce the speed of virus transmission and help control the spread of infection.

Noise primarily causes errors in positioning systems, which is a challenge in any environment [38]. The proposed model has a strong ability to filter out noise, which improves accuracy in any setting. While testing in different ship environments is desirable and can provide additional insights, it is not essential for demonstrating the effectiveness of our noise-filtering approach. The key contribution of our work lies in the model's capability to handle noise effectively, which we have thoroughly validated through our experiments. The HANNARA training ship accommodates hundreds of students, each with their own living space. This high-density passenger environment closely resembles actual operational scenarios of cruise ships, effectively simulating the movements and close contact among passengers of real cruise ships.

Compared to existing technologies for contact tracing and risky area identification, such as WiFi-based positioning systems and RFID tracking, the proposed solution using Bluetooth 5.1 technology combined with machine learning-based feature filtering offers superior accuracy, energy efficiency, and ease of deployment in the complex environment of a cruise ship. WiFi-based positioning systems, while utilizing existing infrastructures, consume significant power, making them unsuitable for the long-term tracking of contacts. High power consumption poses challenges for continuous operation over extended periods. In contrast, Bluetooth technology offers lower power consumption and wider device coverage, facilitating easy deployment for continuous monitoring. Bluetooth devices are energy-efficient, enabling long-term tracking without frequent battery replacements or recharging [39].

In addition, ordinary devices can be converted into Bluetooth Tags by modifying the communication protocols, thus eliminating the need for specialized hardware and simplifying deployment. This adaptability allows for cost-effective implementation and scalability across different ship sizes and configurations. Traditional BLE methods without AoA capabilities rely on the Received Signal Strength Indicator values and are highly sensitive to environmental factors, leading to unreliable proximity detection. The proposed method mitigates these limitations by effectively filtering out noisy features that represent environmental interference, thereby enhancing the quality of angle estimations and

improving the positioning accuracy, which is crucial for close contact detection [40]. While the initial investment and requirement for specific hardware are considered, the increased accuracy, robustness to interference, energy efficiency, and ease of deployment of our system present significant advantages over existing solutions, providing a robust and adaptable approach tailored to the unique challenges of the ship environment.

In subsequent practical applications, data anonymization techniques are employed to encrypt and hash passengers' unique identifiers (such as device IDs) and remove sensitive information related to personal identities, thereby ensuring data privacy. All data are securely stored in high encrypted databases using advanced encryption algorithms (such as AES-256), and only authorized personnel have access. Additionally, the system design strictly adheres to relevant data protection regulations, including the European Union's General Data Protection Regulation, to ensure that data processing activities are lawful, transparent, and fair [41]. Upon boarding, we ensure that passengers fully understand the purposes, scope, and rights of data collection and usage through clear notifications and easy-to-understand consent processes, allowing them to voluntarily participate in the system's use. To prevent potential misuse of the technology, the system design incorporates multiple protective measures, such as strict access controls, data usage monitoring, and anomaly detection, to ensure that data are used solely for legitimate purposes. Implementing the proposed solution requires an initial investment in Bluetooth 5.1 devices, specifically locators and tags, and the necessary infrastructure on cruise ships [42]. While this upfront cost is a consideration, the system's ability to rapidly identify and isolate close contacts can significantly reduce the spread of diseases, leading to substantial savings from preventing outbreaks and minimizing disruptions to cruise operations. Ongoing operational costs, such as maintenance and staff training, can be offset by these potential savings. Furthermore, the system is designed to be scalable and adaptable to ships of different sizes and passenger capacities; by adjusting the number of locators and tags deployed, the solution can be efficiently scaled, ensuring both cost-effectiveness and optimal performance across various ship configurations.

## 6. Conclusion

This study effectively integrates Bluetooth 5.1 technology with a Binary Contact Detection Model and an alpha shape algorithm to enhance disease surveillance on cruise ships. The key results demonstrate that when the model uses more than 33 features, there is a significant improvement in performance metrics-including accuracy, AUC, precision,



recall, and F1 score-leading to more accurate detection of close contacts. In addition, the alpha shape algorithm successfully identified eight overlapping high-risk areas on the ship's upper deck. The main contributions of this paper are the development of a precise and efficient real-time monitoring system that reduces false detections and enhances disease control capabilities in complex, high-density environments, ensuring passenger safety through targeted interventions. Future work will focus on refining the algorithms to further enhance accuracy and reduce false positives, integrating machine learning techniques to predict outbreak patterns, and expanding the system's application to other high-density settings. Collaborations with public health authorities will be essential to develop standardized protocols for data sharing and privacy protection, maximizing the system's effectiveness while ensuring ethical considerations are met.

## Footnotes

### Authorship Contributions

Concept design: Q. Lin, and J. Son, Data Collection or Processing: Q. Lin, Analysis or Interpretation: Q. Lin, and J. Son, Literature Review: Q. Lin, and J. Son, Writing, Reviewing and Editing: Q. Lin, and J. Son.

**Funding:** This research was supported by Basic Science Research Program through the National Research Foundation of Korea (NRF) funded by the Ministry of Education (grant number: 2021R111A3056125).

## References

- [1] N. Diller, "Nearly 70 celebrity cruises guests sick in norovirus outbreak". *USA TODAY*, Jun 2024.
- [2] E. Dahl, "Coronavirus (COVID-19) outbreak on the cruise ship Diamond Princess". *International Maritime Health*, vol. 71, pp. 5-8, Mar 2020.
- [3] K. Ritos, D. Drikakis, and I. W. Kokkinakis, "Virus spreading in cruiser cabin". *Physics of Fluids*, vol. 35, pp. 1-16, Oct 2023.
- [4] W. Ahmed et al., "Detection of SARS-CoV-2 RNA in commercial passenger aircraft and cruise ship wastewater: a surveillance tool for assessing the presence of COVID-19 infected travelers". *Journal of Travel Medicine*, vol. 27, pp. 1-11, Aug 2020.
- [5] T. Sekizuka, et al., "Haplotype networks of SARS-CoV-2 infections in the Diamond Princess cruise ship outbreak". *Proceedings of the National Academy of Sciences*, vol. 117, pp. 20198-20201, Aug 2020.
- [6] K. Gravningen, et al., "Risk factors, immune response and whole-genome sequencing of SARS-CoV-2 in a cruise ship outbreak in Norway". *International Journal of Infectious Diseases*, vol. 118, pp. 10-20, May 2022.
- [7] L.-S. Huang, L. Li, L. Dunn, and M. He, "Taking account of asymptomatic infections: A modeling study of the COVID-19 outbreak on the Diamond Princess cruise ship". *PLoS ONE*, vol. 16, pp. 1-10, Mar 2021.
- [8] A. J. Kucharski, et al., "Early dynamics of transmission and control of COVID-19: a mathematical modelling study". *The Lancet Infectious Diseases*, vol. 20, pp. 553-338, Mar 2020.
- [9] X. Liu, and Y. C. Chang, "An emergency responding mechanism for cruise epidemic prevention—taking COVID-19 as an example". *Marine Policy*, vol. 119, pp. 1-11, Sep 2020.
- [10] Q. Lin, J. Son, and H. Shin, "A self-learning mean optimization filter to improve Bluetooth 5.1 AoA indoor positioning accuracy for ship environments". *Journal of King Saud University-Computer and Information Sciences*, vol. 35, pp. 59-73, Mar 2023.
- [11] S. J. Curtis, et al., "Feasibility of bluetooth low energy wearable tags to quantify healthcare worker proximity networks and patient close contact: A pilot study". *Infection, Disease & Health*, vol. 27, pp. 66-70, May 2022.
- [12] L. Reichert, S. Brack, and B. Scheuermann, "A survey of automatic contact tracing approaches using bluetooth low energy". *ACM Transactions on Computing for Healthcare*, vol. 2, pp. 1-33, Mar 2021.
- [13] F. Daniş, and A. Cemgil, "Model-based localization and tracking using bluetooth low-energy beacons". *Sensors*, vol. 17, pp. 1-23, Oct 2017.
- [14] Z. Su, K. Pahlavan, and E. Agu, "Performance evaluation of COVID-19 proximity detection using bluetooth LE signal". *IEEE Access*, vol. 9, pp. 38891-38906, Oct 2021.
- [15] Q. Lin, and J. Son, "A close contact tracing method based on bluetooth signals applicable to ship environments". *KSI Transactions on Internet and Information Systems*, vol. 17, pp. 1-19, Feb 2023.
- [16] Q. Lin, and J. Son, "A close contact identification algorithm using kernel density estimation for the ship passenger health". *Journal of King Saud University - Computer and Information Sciences*, vol. 35, pp. 101564-101564, Jun 2023.
- [17] V. Bianchi, P. Ciampolini, and I. De Munari, "RSSI-based indoor localization and identification for ZigBee wireless sensor networks in smart homes". *IEEE Transactions on Instrumentation and Measurement*, vol. 68, pp. 566-575, Feb 2019.
- [18] M. S. Munir, D. H. Kim, A. K. Bairagi, and C. S. Hong, "When CVaR meets with bluetooth PAN: a physical distancing system for COVID-19 proactive safety". *IEEE Sensors Journal*, vol. 21, pp. 13858-13869, Jun 2021.
- [19] H. Ghayvat, M. Awais, P. Gope, S. Pandya, and S. Majumdar, "ReCognizing SUSpect and PredictiNg The SpRead of Contagion Based on Mobile Phone LoCation DaTa (COUNTERACT): a system of identifying COVID-19 infectious and hazardous sites, detecting disease outbreaks based on the internet of things, edge computing, and artificial intelligence". *Sustainable Cities and Society*, vol. 69, pp. 1-11, Jun 2021.
- [20] D. J. Leith and S. Farrell, "Coronavirus contact tracing". *ACM SIGCOMM Computer Communication Review*, vol. 50, pp. 66-74, Oct 2020.
- [21] P. C. Ng, P. Spachos, and K. N. Plataniotis, "COVID-19 and your smartphone: BLE-based smart contact tracing". *IEEE Systems Journal*, pp. 1-12, Dec 2021.
- [22] M. T. Rahman, R. T. Khan, M. R. A. Khandaker, M. Sellathurai, and M. S. A. Salan, "An automated contact tracing approach for controlling Covid-19 spread based on geolocation data from mobile cellular networks". *IEEE Access*, vol. 8, pp. 213554-213565, Dec 2020.

- [23] A. Berke, K. Larson, A. S. Pentland, M. Bakker, P. Vepakomma, and D. Calacci, "Assessing disease exposure risk with location data: A proposal for cryptographic preservation of privacy". *Mitmedialab*, vol. 1, pp. 1-15, Mar 2020, arXiv preprint arXiv:2003.14412.
- [24] P. G. Madoery, et al., "Feature selection for proximity estimation in COVID-19 contact tracing apps based on bluetooth low energy (BLE)". *Pervasive and Mobile Computing*, vol. 77, pp. 1-14, Oct 2021.
- [25] G. Barthe, et al., "Listening to bluetooth beacons for epidemic risk mitigation". *Scientific Reports*, vol. 12, pp. 1-14, Apr 2022.
- [26] Q. Lin, and J. Son, "Sustainable ship management post COVID-19 with in-ship positioning services". *Sustainability*, vol. 14, pp. 1-23, Dec 2021.
- [27] Q. Lin, J. Son, and H. Shin, "A mean optimization filter to improve bluetooth aoa indoor positioning accuracy for ship environments". *IPIN-WiP*, vol. 1, pp. 1-16, Sep 2022.
- [28] Q. Lin, and J. Son, "An in-ship localization algorithm for close contact identification". *Journal of Theoretical and Applied Information Technology*, vol. 100, pp. 1706-1717, Mar 2022.
- [29] N. B. Suryavanshi, K. Viswvardhan Reddy, V. R. Chandrika, "Direction finding capability in Bluetooth 5.1 standard". *Ubiquitous Communications and Network Computing: Second EAI International Conference*, Feb 2019.
- [30] P. Sambu, and M. Won, "An experimental study on direction finding of Bluetooth 5.1: indoor vs outdoor". *2022 IEEE Wireless Communications and Networking Conference (WCNC)*, Apr 2022.
- [31] Y. Zhuang, C. Zhang, J. Huai, Y. Li, L. Chen, and R. Chen, "Bluetooth localization technology: principles, applications, and future trends". *IEEE Internet of Things Journal*, vol. 9, pp. 23506-23524, Dec 2022.
- [32] F. A. Toasa, L. Tello-Oquendo, Carlos Ramiro Peñafiel-Ojeda, and G. Cuzco, "Experimental demonstration for indoor localization based on AoA of Bluetooth 5.1 using software defined radio". *IEEE 18th Annual Consumer Communications & Networking Conference (CCNC)*, Jan 2021.
- [33] H. Edelsbrunner, and E. P. Mücke, "Three-dimensional alpha shapes". *ACM Transactions on Graphics*, vol. 13, pp. 43-72, Jan 1994.
- [34] H. Edelsbrunner, "Alpha shapes-a survey". In: *Tessellations in the Sciences: Virtues, Techniques and Applications of Geometric Tilings*, vol. 1, pp. 1-25, Dec 2011.
- [35] N. Akkiraju, H. Edelsbrunner, M. Facello, P. Fu, E. P. Mücke, and C. Varela, "Alpha shapes: definition and software". In *Proceedings of the 1st international computational geometry software workshop*, Sep 1995.
- [36] G. K. Rajbahadur, S. Wang, G. A. Oliva, Y. Kamei, and A. E. Hassan, "The impact of feature importance methods on the interpretation of defect classifiers". *IEEE Transactions on Software Engineering*, vol. 48, pp. 2245-2261, Feb 2021.
- [37] D. Rengasamy, et al., "Feature importance in machine learning models: A fuzzy information fusion approach". *Neurocomputing*, vol. 511, pp. 163-174, Sep 2022.
- [38] X. Zhu, J. Yi, J. Cheng, and L. He, "Adapted error map based mobile robot UWB indoor positioning". *IEEE Transactions on Instrumentation and Measurement*, vol. 69, pp. 6336-6350, Jan 2020.
- [39] B. Etzlinger, B. Nußbaumüller, P. Peterseil, and K. A. Hummel, "Distance estimation for BLE-based contact tracing—a measurement study". *2021 Wireless Days (WD)*, Aug 2021.
- [40] B. Nußbaumüller, B. Etzlinger, and K. A. Hummel, "BLE-based contact tracing: characterization of distance estimation errors and mitigation options". *IEEE Pervasive Computing*, vol. 22, pp. 7-14, Nov 2023.
- [41] C. Badii, P. Bellini, A. Difino, and P. Nesi, "Smart city IoT platform respecting GDPR privacy and security aspects". *IEEE Access*, vol. 8, pp. 23601-23623, Jan 2020.
- [42] D. Antonioli, N. O. Tippenhauer, K. B. Rasmussen, and M. Payer, "BLURtooth: exploiting cross-transport key derivation in bluetooth classic and bluetooth low energy". In *Proceedings of the 2022 ACM on Asia Conference on Computer and Communications Security*, Jun 2022.

# Challenges and Facilitators in Professional Pursuits: A Qualitative Exploration of Work Experiences in Türkiye and Perspectives of Seaborne Professionals

Özgür Sert, İbrahim Sani Mert

Antalya Bilim University Faculty of Economics, Administrative and Social Sciences, Department of Business Administration, Antalya, Türkiye

## Abstract

To understand the challenges and facilitators of the business climate in Türkiye from an outsider's perspective, this qualitative and conceptual research examines foreign seaborne business professionals. The main goal is to explore the challenges and opportunities faced by male and female professionals using feedback from 37 international participants working within the Türkiye business realm. The analysis was based on a comprehensive qualitative content analysis conducted with the help of Maxqda software, which helped unveil prominent themes that define the Türkiye corporate world as expressed by the views and experiences of the respondents. This paper highlight and exposes the contrasts and similarities between expatriates' and their Turkish counterparts' experiences in seaborne business in Türkiye. Therefore, it contributes to knowledge of the operational mechanics of the Turkish business environment. The outcome of this research indicates that situational diversity, as well as flexible organizational practices, contribute significantly to creating a sustainable business environment and ensuring international business success. Türkiye's business culture offers both possibilities and problems for foreign professionals. Given these circumstances, research has established that a full-fledged global business requires sensitivity to the business culture and understanding local business practices, along with areas for improvement. This study is perceived to provide valuable perspectives for entrepreneurs who aspire to facilitate and improve the business climate in Türkiye, as well as policymakers and other administrators. In addition, it contributes to more comprehensive discussions related to Türkiye's international business environment.

**Keywords:** Turkish seaborne business environment, Challenges and facilitators in Türkiye, Qualitative analysis of Turkish business environment, Content analysis, Grounded theory

## 1. Introduction

The rationale behind this research stems from a significant gap in the literature regarding the business environment of seaborne professionals in Türkiye. The growing interest in understanding how business practices adapt to different cultural and economic environments highlights the necessity of this research, and it contributes to the literature on international business, Foreign Direct Investment (FDI), and management by providing empirical insights into the Turkish business environment from the perspectives and experiences of foreign professionals. Understanding the Turkish business environment is critically important for

global and multinational businesses. Türkiye's geographical location, serving as a strategic bridge between Europe and Asia, is of significant importance to international business and diplomacy. This study aims to fill this gap in the existing research by providing a detailed examination of the working environment of seaborne professionals in Türkiye. This highlights the importance of cultural sensitivity and adaptation to local business practices. By leveraging insights from industry and academia, this research offers valuable perspectives for entrepreneurs, policymakers, and international managers, contributing to more comprehensive discussions related to Türkiye's international business environment.



**Address for Correspondence:** Özgür Sert, Antalya Bilim University Faculty of Economics, Administrative and Social Sciences, Department of Business Administration, Antalya, Türkiye  
**E-mail:** capt.ozgursert@gmail.com  
**ORCID iD:** orcid.org/0000-0002-7393-8011

**Received:** 22.01.2024

**Last Revision Received:** 31.05.2024

**Accepted:** 17.12.2024

**To cite this article:** Ö. Sert, and İ. S. Mert, "Challenges and Facilitators in Professional Pursuits: A Qualitative Exploration of Work Experiences in Türkiye and Perspectives of Seaborne Professionals." *Journal of ETA Maritime Science*, vol. 12(4), pp. 466-476, 2024.



Copyright© 2024 the Author. Published by Galenos Publishing House on behalf of UCTEA Chamber of Marine Engineers. This is an open access article under the Creative Commons AttributionNonCommercial 4.0 International (CC BY-NC 4.0) License

The general landscape of Türkiye's business world is shaped by its strategic geographic location, dynamic economy, and cultural richness, offering a unique combination of opportunities and challenges. This qualitative research explores the experiences of foreign business professionals operating in or with partners in Türkiye, focusing on identifying the facilitators and challenges they encounter. The rationale behind this research stems from the growing interest in understanding how business practices adapt to different cultural and economic environments. Türkiye offers a distinct business environment that can be both challenging and rewarding for foreign professionals. This research contributes to the literature on international business and FDI and management by providing empirical insights into the Turkish business environment from the perspectives and experiences of foreign professionals [1].

In the 1980s, Türkiye adopted economic liberalization policies and an openness to globalization. This has increased the presence of foreign investors and integrated Türkiye into international trade. Relations with the European Union, in particular, gained importance during this period. Foreign capital is concentrated mainly in the finance, telecommunications, and energy sectors. Today, Türkiye is recognized as a strategic location and dynamic market for foreign investors. As part of global economic integration, foreign investors play a significant role in diversifying the Turkish economy and accelerating technological innovation [2].

The importance of the Turkish business environment for global and multinational businesses can be assessed as follows: Türkiye's geographical location, serving as a strategic bridge between the continents of Europe and Asia, is of significant importance to international business and diplomacy. This position makes Türkiye a physical and cultural connection between the two continents. Economically, Türkiye is a significant transit point for trade and investment between the East and the West. Understanding the Turkish business environment is critically important for global and international relations. Hosting various cultural and commercial interactions throughout history, Türkiye's rich heritage shapes its business practices and position in international relations [3].

On the other hand, Türkiye's political and economic structure enables it to establish relations with developing and developed economies. Türkiye plays an active role in significant international economic platforms like the OECD and G-20. In addition, it maintains close ties with regional organizations such as the Organization of Islamic Cooperation. This dual approach allows Türkiye to become an influential player in global and regional economic systems. Additionally, connections such as the customs union with the EU and NATO membership facilitate

Türkiye's integration with both the western and the Eastern blocs. Thus, understanding the Turkish business world means comprehending this multifaceted and strategic network of relationships. Türkiye's role in global trade and politics, especially regarding energy lines and logistical routes, necessitates a deep understanding of its business environment. Understanding the business environment of Türkiye in the context of the global business world and international relations can be seen not only as an economic necessity but also as a strategic advantage [4].

It is appropriate to conduct exploratory research to understand and analyze healthily the matters experienced and encountered by foreign professionals with Turkish professionals, partners, and affiliates of their companies. When the existing scientific literature is examined, it is seen that the motivation sources of foreign investors and the issue of prioritizing them are focused on [5-7]. This research, which adopts the grounded theory approach, provides a general picture of the business environment and business culture of Türkiye. Both general trends and essential themes within this context were identified from the interviews conducted [8,9]. Our research, which examines the business environment in Türkiye and the problems and perspectives that foreign maritime business professionals face when operating in this environment, leverages theories of intercultural business management and adaptation as the core theoretical basis. The theory of intercultural business management explores how to deal with relationships among individuals from different cultural backgrounds. It can help shed light on how foreign professionals adjust to Türkiye's business environment and cultural challenges. In contrast, adaptation theories investigate how individuals and organizations adapt to new environmental conditions. The theory explains how expatriates can thrive or overcome problems they might experience in Türkiye's business climate and culture [10]. As this research identified, cultural sensitivity and the accommodation of Turkish business norms are vital variables to consider. This conceptual framework is intended to give insights into the complex aspects of the business environment in Türkiye as well as help understand how foreign business professionals can deal with these challenges [11].

Seaborne business professionals possess industry expertise and experience in shipping, logistics, trade, and other associated operations through the sea. Such professionals include individuals in ship management, maritime transportation, port management, maritime law, international maritime trade, maritime and port goods and services manufacturers, maritime security, and marine logistics. These professionals play significant roles where their skills are required to efficiently handle the movement

of goods and services via sea routes, resolve the challenges encountered in maritime transportation, and ensure compliance with complex rules governing global trade by sea. These professionals are vital workers who strongly influence international trade and economic indicators and have the right to receive a large amount of world trade by sea. Therefore, they were selected as the specific target group of research in the Turkish maritime business sector to help identify and analyze impediments and facilitators in the Business Environment of Türkiye. Their efficiency means they can provide recommendations and insights from various holistic and diversified perspectives.

Additionally, this paper helps explain how the findings can assist various stakeholders, such as foreign investors, policymakers, business educators, and international managers, in developing practical applications and strategies. This framework emphasizes the importance of cultural diversity and adaptation in the business world and enables foreign business professionals to develop the skills and techniques necessary to succeed in Türkiye. When the scientific literature is examined, it is generally seen that the comparative valuations of professionals and business environments stand out when deciding on investments. Since the 1970s, significant decreases in profitability rates have been observed in industrial sectors, especially in manufacturing, in developed countries. This situation is related to various social, political, and economic factors, such as production stagnation, changes in the capital-labor structure, and increased competition between domestic and international entrepreneurs [1,12].

Firms must restructure their production processes by moving to regions with lower production costs or closer to potential markets. This process has led developing countries to provide branch opportunities to multinational and small-and medium-sized enterprises in developed countries. In the 1980s, along with technological innovations in developed countries, manufacturing activities increased in intensity, leading to the globalization of some advanced technology industries. Looking at Türkiye from 1923 to the 1970s, except for a short liberalization period in 1950-53, economic policy was largely inward-looking and dependent on intergovernmental relations [13].

Opportunities for direct foreign investments and international business in Türkiye were limited during this period. However, the situation changed with the start of Türkiye's liberalization programs in 1980 and its adaptation to changes in the world economy. Türkiye became open to foreign capital, although investment values remained low compared to those in the Central and Eastern European markets [14].

Nevertheless, Türkiye's success in attracting foreign capital is noteworthy. The motivations of multinational corporations

for international production and the economic theory of this process have been addressed through an analysis of property rights and production locations [15]. Host country theories have been integrated into the economic theory of multinational corporations, and it has been emphasized that location decisions and internalization decisions continuously interact with each other [16,17].

Some studies into factors that influence FDIs have examined variables such as corruption, political risk, market size, human capital, and economic freedom. Notably, several findings indicate that although corruption negatively impacts foreign investments, it has the potential to encourage foreign investment. Another factor affecting investment is corruption in the investor's home country. The analyses thus reveal that dissimilar elements impinge on FDI performance due to their different characteristics. One of this paper's key findings is Türkiye's unique business environment, which presents opportunities and challenges for foreign professionals. The degree of adaptability to the business culture in a new market and sensitivity to local business practices can determine the success of any globalization operation. In this regard, one of the most valuable aspects is identifying the key stakeholders who will benefit from the research and determining how such findings can influence their decisions and strategies.

According to the research, Türkiye is one of the most favorable countries for business, based on its strategic location and its ability to adapt to foreign investment. The research pointed out the need to make foreign investors adaptable to Türkiye's business culture and practices. Such information can aid foreign investors in creating suitable adaptation strategies to be effective in their investment schemes in Türkiye. The findings of this research can contribute to policymakers' establishment of policies to support foreign business ventures and enhance the ease of doing business. Given the challenges and opportunities within Türkiye's business environment, policymakers can easily develop more valuable strategies. For business educators, the research offers helpful information on the peculiarities of Türkiye's business world and cultural patterns, which are essential to help them understand how these factors impact businesses in Türkiye. Therefore, the educators will use this knowledge to provide future business leaders with the skills and academic backgrounds required to meet global standards and successfully operate in other countries. Gaining insights into the Turkish business environment and culture can help international managers create an effective global-local balance in the formulation of business strategies. In connection with this, we would like to add that executives can use the results of our investigation as an effective tool for adapting to the Turkish business world. Consequently, these results may enable stakeholders to make more accurate decisions and correctly identify the business

environment in Türkiye. Therefore, to develop successful strategies.

This article examines the issues and dynamics of foreign maritime business professionals and companies' business operations in Türkiye and their Turkish counterparts. By analyzing these dynamics from both sides and exploring how local team members, partners, and employees perceive these factors, a comprehensive understanding. It is also a matter of increasing real-world significance because foreign businesses conduct their activities in various contexts influenced by unique mechanisms and perspectives that govern different markets [18].

## 2. Literature Review

Since the late 1970s, a significant decline in profitability rates has been observed in many industries in developed countries, particularly in the manufacturing sector. This phenomenon, including stagnation in productivity growth, disruption in the capital-labor structure, and intensifying competition among domestic and international entrepreneurs, results from complex social, political and economic factors that have emerged in developed countries. Many firms have been forced to rationalize their production processes by relocating to areas with lower production costs or greater access to potential markets.

Additionally, the development of modern communication and transportation technologies has enabled the geographical expansion of production. Consequently, many developing countries have hosted branch facilities of multinational corporations and small- and medium-sized enterprises from developed countries. Initially, this globalization process in output occurred in labor-intensive manufacturing industries. In the 1980s, due to technological innovations in developed countries, manufacturing activities increased in intensity, leading to the globalization of some advanced technology industries. Therefore, despite the economic slowdown in the 1980s, these countries received significant FDI from developed countries. However, developing countries have gradually pushed labor-intensive industries to other developing countries with lower levels of technological development and cheaper labor [19].

However, the situation in Türkiye from the establishment of the new Republic in 1923 until the late 1970s (except for the short period of liberalization in 1950-53), Türkiye had an inward-looking economic policy that was largely dependent on intergovernmental relations [9]. As in many developing countries, the Turkish public sector was the primary trade provider during the initial period. Direct foreign investments and international business in Türkiye were limited.

The environment changed in 1980 with Türkiye's stabilization, adapting to the changes in the world and the

workings of FDI and partnerships, and began implementing liberalization programs. A series of legislative changes in Türkiye liberalized the conditions for direct foreign investment, leading to a continued, even accelerated, increase in multinational business activity into the early 2000s. Despite a dramatic increase in the number of foreign capital ventures in Türkiye, the total value of foreign investment is relatively low compared to emerging markets in the Far East and Latin America. However, when evaluated in different periods, Türkiye's success in attracting foreign capital is remarkable [20].

Analyzing the current situation in Türkiye, along with the foundations and criteria of importance to FDI and foreign professionals in the existing business literature in foreign countries, the economic theory of multinational enterprise (MNE) addresses two main aspects of international production: The ownership of assets used in overseas production and the location of such production activities. Several scholars have analyzed motivations for international output using the transaction cost paradigm [15].

Cost minimization implies that a company chooses the least costly location for its production activities [16]. Thus, the elements of host country location theories have been integrated into the economic theory of MNE, where location decisions continuously interact with internalization decisions. Similarly, location factors have also been included in Dunning's eclectic paradigm of international production, consisting of ownership and internalization factors, where each group of factors moves in connection [17].

Wheeler and Moody [21] used data from the United States to conduct company-level analyses. They discovered that FDI was not significantly impacted by "corruption" in the host nation. Erramilli and Rao [22] asked 14 service companies about entering overseas markets. They examined firms' preferences for shared and complete control entry modes. One of the research's conclusions was that FDI is hampered by sovereign risk. Multinational corporations were advised against investing in host nations with a high "political risk" profile [21].

Singh and Jun [23] empirically analyzed macroeconomic and socio-political factors influencing the spatial distribution of FDI in 31 countries between 1970 and 1993. They discovered that the BERII "political risk" index positively impacted FDI [23]. The study conducted by Noorbakhsh et al. [24] investigated the correlation between a host country's level of human capital and the spatial allocation of FDI. Thirty-six developing countries from Latin America, Asia, and Africa were included in this study. The empirical results show that Human capital is one of the most significant and statistically significant predictors of FDI; human capital is becoming increasingly vital. The report also claims that political risk factors and democracy have no discernible effect on

FDI [24]. In a study published in 2002, Kolstad and Tondel examined 61 developing countries between 1989 and 2000 and found that externality variables and market size had a significant impact on FDI. Furthermore, no discernible link was discovered between socio-economic circumstances and FDI. The study found that corruption was not a significant factor. However, it affected FDI when considered alongside other control variables [25]. FDI and corruption were negatively correlated. This implies that FDI increases with corruption. Using the same corruption measure, Wei's [26] research produced results that conflict with these findings. Internal conflict, disputes between different religions and ethnic groups, political rights, civil liberties, and democratic accountability are critical factors that impact FDI. Based on these findings, nations that grant their citizens greater political and civil rights typically attract more foreign direct investors. Democracy, internal strife, and ethnic tension affect the admission of FDI. However, FDI requires more than political authority, bureaucracy, external conflicts, and the rule of law [26].

Between 1995 and 2003, Van Wyk and Lal [27] studied how institutional and macroeconomic factors affected FDI in 31 developing countries. According to the study, political risk discourages investments, whereas economic freedom encourages FDI. This study concludes that FDI increase with decreasing political risk. The findings also indicate a favorable correlation between GDP growth rate, FDI, and market size. These findings show that low inflation, rising value of the host nation's currency, and a low current account balance all promote FDI [27].

Using the panel gravity approach, Subasat and Bellos [28] examined the relationship between governance and FDI in a few Latin American countries between 1985 and 2008 [26]. The findings demonstrate how poor governance in target countries attracts more FDI. Governance variables had negative and significant coefficients, except for "democratic accountability", a correlation between high amounts of FDI and weak governance. "Democratic Accountability" was a slightly yet auspicious sign. These findings imply that Latin America and transitioning nations benefit from FDI promoted by poor governance. Additionally, a negative and marginally significant sign for the "Regulatory Quality" variable, suggesting that lax regulations do not discourage FDI. According to the findings, high levels of corruption in source nations have prompted multinational corporations to increase their investments in Latin America. The source had higher "democratic accountability" and "bureaucratic quality".

### 3. Materials and Methods

#### 3.1. Theoretical Framework

In this research, by adopting the Grounded Theory Approach, the methodology provides flexibility and a unique research process [29].

The Grounded Theory Approach aims to uncover an event or situation and develop a theory explaining its social processes by identifying concepts that describe the process through comparative data analysis. In Grounded Theory, data collection and analysis are expressed as interrelated processes. The approach focuses the researcher on collecting and analyzing qualitative data to understand and explain social issues. In Grounded Theory, phenomena are compared in terms of similarities and differences. Concepts are labeled, compared with pre-existing concepts, and grouped. The Grounded Theory Approach offers an exploratory and qualitative research method for understanding and explaining phenomena [30].

In this study, we examine the challenges and facilitating factors in the business world of Türkiye from the perspectives of foreign professionals, grounding our analysis primarily on two scientific theories:

The first is the Theory of Cross-Cultural Business Management, which investigates how business relationships between individuals from different cultural backgrounds are managed. This research focuses on the interaction among people from diverse cultures and how such interaction impacts business outcomes. Our research uses this theory to understand how foreign professionals adapt to Türkiye's business environment and cultural challenges. Geert Hofstede defined the dimensions of national cultures to understand how different cultures behave in work environments. Hofstede's Cultural Dimensions Theory is a framework used to measure intercultural communication in any business, institution, or individual within a social structure [31-33]. Fons Trompenaars, who extended Hofstede's work, addressed intercultural differences and challenges encountered in the business world. Trompenaars' approach focuses on various cultural dimensions, analyzing how cultures create conflict and cooperation. His dimension provide a deeper understanding of cultural diversity and business interactions. These dimensions allow business leaders and managers to develop more effective communication and collaboration strategies in different cultural contexts. Trompenaars highlighted the importance of cultural richness and diversity in business [34]. Additional research within this management theory by Edward T. Hall has developed concepts like high-context and low-context cultures, which are fundamental to intercultural communication. Hall, emphasizes the importance of awareness of these concepts and developing

culturally sensitive approaches to effective communication in different cultural contexts. His work shows that increasing cultural awareness and sensitivity are essential for successful international cooperation and communication. Understanding these two contexts in intercultural communication paves the way for more effective and meaningful interactions among people of different cultural backgrounds [22]. Hall stressed that not recognizing the differences between these two communication styles can lead to misunderstandings and conflicts in international relations and intercultural interactions [35].

The second theory this study is based on is Adaptation Theory. This theory explains how individuals and organizations adapt to changing environmental conditions. In the context of business and management, it mainly focuses on cultural adaptation and organizational adaptation. John Kotter and Leonard Schlesinger have significantly contributed to organizational change and adaptation. They concentrated on how organizations should approach change processes and facilitate employee adaptation. The core elements of Kotter and Schlesinger's adaptation theory are the Causes of Resistance to Change, Change Management Strategies, the Importance of Communication, Participative Approaches, and the emphasis on Flexibility and Dynamic Management. Their approaches help organizations understand the challenges they face in change processes and manage them more effectively. This theory offers valuable guidance for managers and leaders, especially in today's rapidly changing and adaptation-demanding business world [36].

The theories and models mentioned above are widely used to understand and manage cultural differences in the global business world. This research supports foreign business professionals in developing the necessary skills and strategies to succeed in Türkiye by highlighting Türkiye's strengths and weaknesses in the business world. This study emphasizes cultural sensitivity and the importance of adapting to local business practices, highlighting the need for foreign business professionals to develop skills and strategies essential for success in Türkiye. These theories, forming the foundation of the research with their theoretical framework emphasizing cultural diversity and adaptation, provide valuable insights for foreign business professionals aiming for success in Türkiye. This study explores how foreigners conducting business in Türkiye perceive the business environment and culture. Participants were informed about the purpose and nature of the research. After posing questions, the participants were given time to gather their thoughts. The participants' opinions were recorded through interviews, and notes taken at the end of the interview were shared for confirmation [23,37].

### 3.2. Procedures and Sample

Data were collected from 37 participants using structured interviews during the research process. Care was taken to ensure that the participants were completely voluntary and willing, and all participants were informed about the purpose and goals of the research. The research sample consisted of participants from as many countries and sub-sectors of the maritime industry as possible to ensure diversity in the data collection. Participants were included in the study using a convenience sampling method, and interviews were conducted in a single session lasting 15-20 minutes. Interviews were conducted independently to prevent mutual influence.

Participants were from the UK, Singapore, Netherlands, France, Belgium, Spain, Saudi Arabia, Switzerland, Luxembourg, Germany, India, Norway, and Pakistan. They also stated that they were in middle and upper management roles in maritime businesses. It is observed that the participants, who were interviewed through convenience sampling, were well-informed about the business environment in Türkiye due to the maritime industries they work in. Participants' companies' areas in seaborne businesses are mainly seaborne logistics, shipping agencies, ship software producers, shipowners, and consulting companies.

The responses of the participants were subject to content analysis. The analysis was conducted using Maxqda 20 The Analytics Pro software was used, and care was taken to ensure as much original coding as possible.

In analyzing interviews and participants' responses, existing literature codings were evaluated to discover themes and codes, and participants' statements were divided into meaningful smaller units and subgroups. Two evaluators and coders independently and individually coded the participants' expressions.

After the initial coding phase, the codes identified by the two evaluators were carefully compared in terms of what they represented, and a reduction and augmentation process was performed. Subsequently, the evaluators re-coded all interviews using mutually agreed codes.

Subsequently, the formula proposed by Miles and Huberman [38]  $[(\text{Consensus})/(\text{Disagreement} + \text{Consensus})] \times 100$  was used to determine the consistency and evaluator reliability in these codes and themes. As a result of the analysis, 133 of the expressions evaluated from the research were in consensus, while the remaining five disagreed. Thus, the reliability coefficient between the evaluators was 96%. This acceptable level of reliability [39] was considered sufficient for the reliability of the study. In addition, the 5-coding differences between the evaluators were understood and resolved.



As a result of applying the stages of the Grounded Theory Approach, the codes mutually agreed upon by the evaluators were linked to create a higher-level structure; thus, the codes were categorized. The evaluators worked separately to determine the names of the established codes and the codes under them and then again collectively re-determined the themes and their subdivisions.

This study used MAXQDA, a robust qualitative data analysis tool, for multiple purposes, including coding and classification. The Maxqda algorithm enabled us to code qualitative data such as interview transcripts, open-ended survey responses, and focus group discussions. The codes were then organized into categories to identify patterns and themes. Text Analysis: This software helps extract essential themes, concepts, and relationships from textual data. It supports various text analysis methods, such as word frequency analysis and contextual keyword search. Memo writing: The Maxqda function for writing memos and comments. The researchers used these features to record their thoughts, reflections, and insights during the data analysis. Visualization Tools: This software includes mind mapping, concept mapping and network diagrams, which help visualize the connections between different topics and concepts. Data Organization: Maxqda helps organize qualitative data into manageable chunks and group data according to demographics, project stage or other relevant criteria. By leveraging these capabilities, we ensure a comprehensive, systematic qualitative data analysis approach, increasing the depth and reliability of the results.

#### 4. Findings

The segmentations (themes) of foreign professionals' experiences and perceptions and the coding related to

these components are detailed in Table 1. The frequencies of these codes are also displayed in the table. Accordingly, the evaluations of professionals regarding the business environment in Türkiye have been divided into the following themes: Regulatory and government Factors, economic and financial perspectives, human factors, and Workplace.

Upon examining the codes in Table 1, it is observed that the most frequently used codes in the participants' interviews, in order of frequency, are adaptability, highly skilled labor, motivation, resilience and non-structural practices. These five codes are more prominent than the others. Therefore, evaluations related to human factors were predominantly positive (47% of all themes and codes). However, assessments concerning the workplace and Regulatory and government Factors are perceived as unfavorable.

In Figure 1, the components displayed in terms of frequency are adaptability (16%, highly skilled labor 9%, motivated 9%, non-structural policies (8%), resilient (8%), excessive uncertainty (6%), lack of rule of law (5%), regulatory difficulties (5%), and overbureaucratization (4%).

The relationships between evaluations of Turkish business life can be understood through the thickness of lines. Notably, the thickness of these lines is generally more pronounced between adaptability, resilience, motivation, highly skilled labor, and non-structural practices. In other words, participants more frequently associated these business life components with each other (Figure 2).

However, when we carefully examine the participants' statements, it is observed that the abilities and capabilities related to Turkish professionals are collectively expressed, and there is a significant concentration. For example,

*Table 1. Codes and themes*

Codes	Frequency	Codes	Frequency
<b>Regulatory and Government Factors</b>		<b>Human Factors</b>	
Lack of the rule of law	7	Adaptability	22
Regulatory difficulties	7	Motivated	12
Over-bureaucratization	5	Highly skilled labor	12
Government instability	4	Being resilient	11
Labor legislation advantages	1	Extraversion	3
Responsive-bureaucracy	1	Innovative	3
<b>Economic and Financial Perspectives</b>		<b>Workplace</b>	
Fertile environment	3	Non-Structural practices	11
Embracing new opportunities	3	Excessive uncertainty	8
Strong financial system	3	Chaotic order	4
Currency and exchange complexities	2	Unethical situations and demands	3
Non-existence of difficulty	2	Robust structure	4
Economic instability	1	Inadequate infrastructure	1

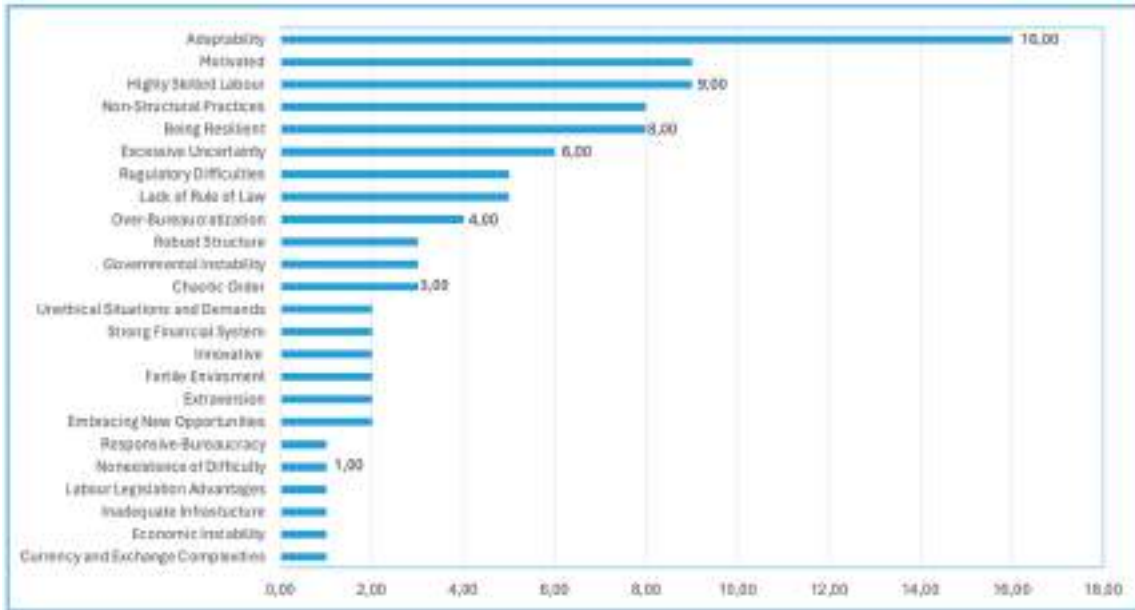


Figure 1. Code statistics

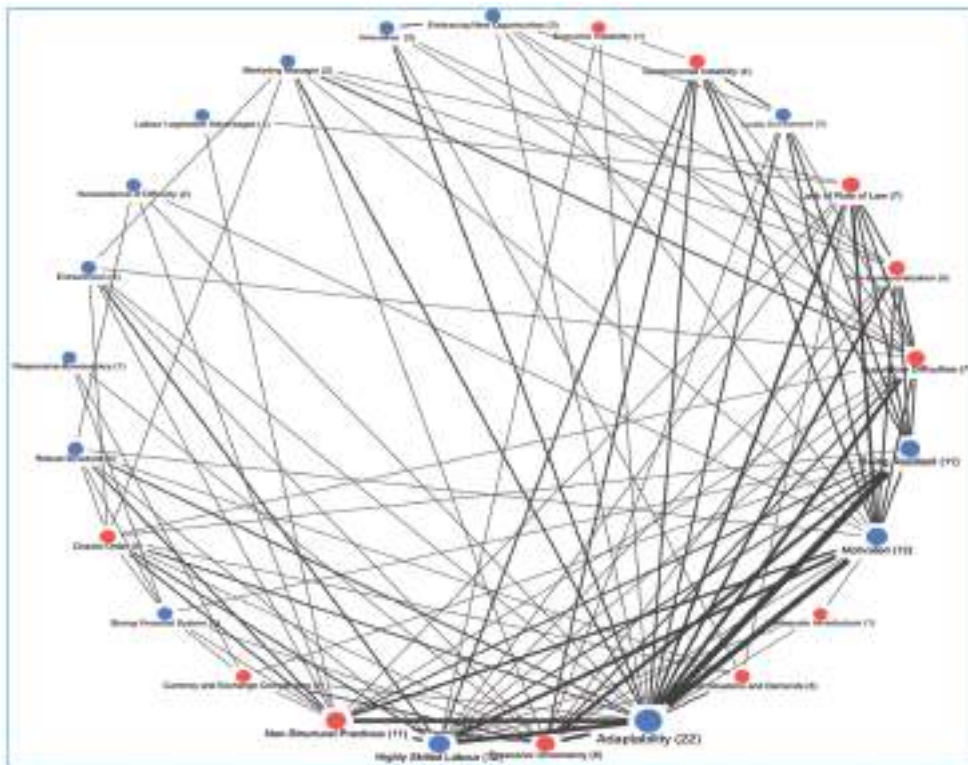


Figure 2. Relationship between codes

Participant #2’s statement is as follows: “Skilled & Educated & Hardworking Workforce. We often have the chance to business with highly educated people. Our Turkish partners are extremely experienced and talented. We can reach our team in Türkiye even on weekends and in the evening. They never quit or take a break until the job is completed”. On the

other hand, in Participant #3’s statement: “The adaptability of the workforce and the Turkish business world is quite high, despite everything, the business focus is very high// Despite the ongoing crises, it is seen that effective crisis management is developed in every event and situation, and its adaptation power is high”.

When we analyzed the coding results, we observed a high concentration of coding and factors related to human factors. Furthermore, it is noticeable that all these factors can be positively evaluated in Turkish business life. The experiences and perceptions regarding human factors in Turkish business life are positive and well-positioned compared to other elements. When we evaluate the results related to the working environment, it is observed that 27 out of the 31 codes are related to negatives in business life. Similarly, when “Regulatory & Government Factors” are evaluated, 23 out of 25 codes are related to negative factors affecting the business environment. When considering the “Economical & Financial” category, only 3 out of 15 codings can be said to exhibit negative characteristics.

## 5. Discussion

### 5.1. Interpretation of Results

This study strives to contribute to the literature on international business, FDI, and management by leveraging insights from the perspectives and experiences of foreign business professionals. This chapter seeks to provide significant insights into the Turkish business environment and Turkish Business Culture. Furthermore, it is believed to offer various experiences and viewpoints that help analyze the complexities and conveniences brought by working with Turkish business partners and in Türkiye. These insights aid in better understanding the interactions among global business strategies [38].

### 5.2. Theoretical Implications

The Theory of Cross-Cultural Business Management addresses how individuals from different cultural backgrounds perceive and manage business relationships. The observations and findings of participants, predominantly engaged in business within the EU, as included in this research article, distinctly illustrate how cultural awareness, diversity, and sensitivity influence modes of conducting business. This scenario serves as a fitting practical example of the proposed theory. Adaptation theory explores how individuals and organizations adjust to new environmental conditions. Specifically, cultural sensitivity and adaptation to local business practices, as observed in this study, hold significant roles in facilitating and overcoming business success. Moreover, this research underscores the emphasis in adaptation theory on adapting to environmental conditions, flexibility, and resilience. It highlights that the ability to swiftly adapt in the presence of uncertainties, unpredictability, and even chaotic environments-aspects negatively perceived in this research-is a skill developed by Turkish business professionals. This aspect demonstrates that Turkish business practices exemplify the characteristics and outcomes that support adaptation theory [40].

### 5.3. Managerial and Practical Implications

The study results have significant implications for managers of multinational corporations operating or considering business in Türkiye. The dynamics of the Turkish business environment, with its strengths and weaknesses, enable decision-makers to adopt proactive approaches and implement measures to maximize potential benefits.

Specific areas and topics are the focus when Turkish professionals and culture are analyzed by foreign professionals. The perception of Turkish professionals and culture, which can be summarized as adaptation, crisis management, and resilience to crises, is considered beneficial in comparison to those considering doing business in Türkiye and/or in regions including the Balkans, the Middle East, and West Asia [41].

Additionally, legislators and administrators in Türkiye need to improve certain areas to enhance business culture development, increase FDIs, and achieve a higher level of integration in Turkish business life [42]. The existence of a legal system, the effectiveness and efficiency of bureaucracy, and the creation of a more predictable business environment, as evaluated by foreign professionals, should be prioritized by the Turkish Republic’s authorities and incorporated into short- and medium-term legislative and executive programs [43,44].

Foreign business professionals and companies wishing to establish or expand their operations in Türkiye are seen to benefit from conducting detailed risk analyses on matters evaluated in the research under the headings of A- “Regulatory & Government Factors”, B- “Economical/ Financial Perspective”, and C- “Workplace”. This approach can prevent potential difficulties and facilitate the development of healthier business plans, growth strategies in Türkiye, and business development. Furthermore, under D- “Human Factors”, developing plans for adapting and effectively utilizing the skilled Turkish workforce and providing training to align existing management with the Turkish business environment and its people are seen as beneficial [45,46].

## 6. Limitations of Study and Future Studies

This research contributes significantly to both theory and practice. However, it has certain limitations. First, the use of non-probability sampling techniques in this research limits the generalizability of the findings. The sample size in this research needs to be more prominent due to difficulties in attracting competent business professionals and convincing them to participate. For the results to be more widely applicable, future researchers should consider replicating this study with a more extensive and diverse sample, including business professionals from different sectors and

regions. A comparative analysis with other countries or a quantitative approach to validate the qualitative findings could be considered.

Additionally, in this study, comparative analyses can be conducted with quantitative research on the prominent characteristics of Turkish business professionals and areas for improvement in Turkish business life. Such research can also be expanded to influence policymakers and civil society organizations.

## 7. Conclusion

The research's exploratory nature makes it possible to arrive at tentative conclusions based on the observations and experiences of foreign seaborne business professionals in Türkiye. Furthermore, information obtained from the interviews provides a basis on which more rigorous investigations can be built in the future. Türkiye, with its location bridging Europe and Asia, not only offers advantages as a part of the EU Customs Union agreements but is also thought to provide a suitable and effective business environment for foreign partners and investors, thanks to its talented and accessible workforce and dynamic business climate. As far as can be seen from the experiences and perceptions of foreign professionals, the Turkish seaborne business world and culture emphasize vital aspects like a skilled and efficient workforce and resilience to crises, which lawmakers and administrators prioritize. The international nature of maritime affairs and maritime trade indicates that foreign professionals involved in maritime activities provide invaluable sources of experience and knowledge about the Turkish business world. However, there is a need to prioritize and work on areas that need improvement in Turkish business life and its elements in terms of administrative, legal, and structural aspects. The governance and regulatory factors in Türkiye can address prominent issues such as economic/financial perspectives and workplace conditions, working conditions, administrative order, and legal matters by developing skills and "strategy improvements" while considering vital aspects like adaptability, resilience, and motivation. In this context, the success of foreign business professionals in Türkiye depends on their thorough understanding of the current situation. Therefore, foreign investors and professionals with high situational awareness can produce better and more effective results in Türkiye.

## Footnotes

### Authorship Contributions

Concept design: Ö. Sert, and İ. S. Mert, Data Collection or Processing: Ö. Sert, Analysis or Interpretation: Ö. Sert, and İ. S. Mert, Literature Review: Ö. Sert, and İ. S. Mert, Writing, Reviewing and Editing: Ö. Sert.

**Funding:** The authors did not receive any financial support for the research, authorship and/or publication of this article.

## References

- [1] A. Buğra, and O. Savaşkan, "Politics and class: the Turkish business environment in the neoliberal age". *New Perspectives on Turkey*, vol. 46, pp. 27-63, Spring 2012.
- [2] T. Szigetvári, "The changing role of the state in the Turkish economy". Seeking the best master: state ownership in the varieties of capitalism, M. Szanyi, Ed., Central European University Press, 2019, pp. 297-324. [Online]. Available: <http://www.jstor.org/stable/10.7829/j.ctv138wqt7.14>. [Accessed: Dec 17, 2024].
- [3] E. P. Dal and S. Dipama, "Economic enterprise of the international relations council: re-scaling and globalizing EU-Turkey bilateral relations in the changing global political landscape". *Europe*, vol. 20, pp. 35-50, 2023.
- [4] Z. Önis, "Power, interests and coalitions: the political economy of mass privatisation in Turkey". *Third World Quarterly*, vol. 32, pp. 707-724, 2011.
- [5] J. Deichmann, S. Karidis, and S. Sayek, "Foreign direct investment in Turkey: regional determinants". *Applied Economics*, vol. 35, pp. 1767-1778, 2003.
- [6] E. Tatoglu, and K. W. Glaister, "Determinants of foreign direct investment in Turkey". *Thunderbird International Business Review*, vol. 40, pp. 279-314, 1998.
- [7] M. Afşar, "The causality relationship between economic growth and foreign direct investment in Turkey". *Selçuk Üniversitesi Sosyal Bilimler Enstitüsü Dergisi*, vol. 20, pp. 1-9, 2008.
- [8] R. D. Hisrich, B. Bucar, S. Oztark, and M. Chair, "A cross-cultural comparison of business ethics: cases of Russia, Slovenia, Turkey, and United States". *Cross Cultural Management An International Journal*, vol. 10, pp. 3-28, Mar 2003.
- [9] K. Olofsdotter, "Foreign direct investment, country capabilities and economic growth". *Weltwirtschaftliches Archiv*, 1998. [Online]. Available: <https://www.jstor.org/stable/40440664>
- [10] A. Ersoy, "The role of cultural intelligence in cross-cultural leadership effectiveness: a qualitative study in the hospitality industry 1". *Journal of Yasar University*, vol. 9, pp. 6099-6260, 2014.
- [11] A. K. Mercül, "Foreign direct investment in Turkey in the framework of candidacy to the EU". *Marmara Journal of European Studies*, vol. 9, pp. 155-173, Dec 2001.
- [12] A. Dicle, and U. Dicle, "Effects of government export policies on Turkish export trading companies". *International Marketing Review*, vol. 9, Mar 1992.
- [13] J. P. Doh, and H. Teegen, "Nongovernmental organisations as institutional actors in international business: theory and implications". *International Business Review*, vol. 11, pp. 665-684, Dec 2002.
- [14] E. T. Aydoğan, "Foreign direct investment in Turkey: a comparison with the central and Eastern European countries". *Economics Bulletin*, vol. 626, pp. 89-101, Apr 2017.
- [15] K. D. Brouthers, and J. F. Hennart, "Boundaries of the firm: insights from international entry mode research". *Journal of Management*, vol. 33, pp. 395-425, Jun 2007.

- [16] P. J. Buckley, C. le Pass, and K. Prescott, "Measures of international competitiveness: a critical survey\*†". *Journal of Marketing Management*, vol. 4, pp. 175-200, 1988.
- [17] J. H. Dunning, "The eclectic paradigm of international production: a restatement and some possible extensions". *Journal of International Business Studies*, vol. 19, pp. 1-31, Mar 1988.
- [18] D. S. Ones, H. K. Sinangil, and B. M. Wiernik, "Validity of big five personality traits for expatriate success: results from Turkey". In book: *Managing Expatriates: Success Factors in Private and Public Domains*, pp. 83-102, Jan 2018.
- [19] H. Amirahmadi, and W. Wu, "Foreign direct investment in developing countries". *The Journal of Developing Areas*, vol. 28, pp. 167-190, 1994.
- [20] A. Kazaz, and S. Ulubeyli, "Strategic management practices in Turkish construction firms". *Journal of Management in Engineering*, vol. 25, pp. 185-194, Sep 2009.
- [21] D. Wheeler, and A. Mody, "International investment location decisions: The case of U.S. firms". *Journal of International Economics*, vol. 33, pp. 57-76, 1992.
- [22] M. K. Erramilli, and C. P. Rao, "Service firms' international entry-mode choice: a modified transaction-cost analysis approach". *Journal of Marketing*, vol. 57, pp. 19-38, Jul 1993.
- [23] H. Singh and K. W. Jun, "Some new evidence on determinants of foreign direct investment in developing countries". *World Bank Working Paper*, no. 1531, Washington, DC, USA, 1995.
- [24] F. Noorbakhsh, A. Paloni, and A. Youssef, "Human capital and FDI inflows to developing countries: new empirical evidence". *World Development*, vol. 29, pp. 1593-1610, Sep 2001.
- [25] I. Kolstad, L. Tøndel, and Chr. Michelsen Institutt, "Social development and foreign direct investments in developing countries". Chr. Michelsen Institute, Development Studies, and Human Rights, 2002.
- [26] S.-J. Wei, "How taxing is corruption on international investors?". *The Review of Economics and Statistics*, vol. 82, pp. 1-11, Feb 2000.
- [27] J. Van Wyk, and A. K. Lal, "Risk and FDI flows to developing countries". *South African Journal of Economic and Management Sciences*, vol. 11, pp. 511-527, 2008.
- [28] T. Subasat, and S. Bellos, "Economic freedom and foreign direct investment in Latin America: a panel gravity model approach". *Economics Bulletin*, vol. 31, pp. 2053-2065, 2011.
- [29] E. Şener, "Using grounded theory approach in management research". *Qualitative Social Sciences*, vol. 1, pp. 22-47, Apr 2019.
- [30] O. O. Kocabıyık, "Phenomenology and grounded theory: a comparison of certain features". *Trakya University Journal of Education Faculty*, vol. 6, pp. 55-66, 2015.
- [31] G. Hofstede, *Culture's consequences: International differences in work-related values*, 2nd ed. Beverly Hills, CA: SAGE Publications, 1984.
- [32] G. Hofstede, *Culture's consequences: Comparing values, behaviours, institutions, and organisations across nations*, 2nd ed. Thousand Oaks, CA: SAGE Publications, 2001.
- [33] G. Hofstede, G. J. Hofstede, and M. Minkov, *Cultures and organizations: software of the mind*, 3rd ed. New York: McGraw-Hill, 2010.
- [34] F. Trompenaars and C. Hampden-Turner, *Riding the waves of culture: understanding diversity in global business*, Nicholas Brealey International, 2011.
- [35] H. Erkekoğlu, "Do political risks affect the foreign direct investment inflows to host countries?". *Journal of Business, Economics & Finance*, vol. 5, pp. 218-232, 2016.
- [36] J. P. Kotter, and L. A. Schlesinger, "Choosing strategies for change". *Harvard Business Review*, vol. 57, pp. 106-114, Mar-Apr 1979.
- [37] E. Tatoglu, K. W. Glaister, and F. Erdal, "Determinants of foreign ownership in Turkish manufacturing". *Eastern European Economics*, vol. 41, pp. 5-41, 2003.
- [38] M. B. Miles, and A. M. Huberman, "Drawing valid meaning from qualitative data: toward a shared craft". *Educational Researcher*, vol. 13, pp. 20-30, 1984.
- [39] M. Owusu Ansah, and L. Louw, "The influence of national culture on the organisational culture of multinational companies". *Cogent Social Sciences*, vol. 5, Jun 2019.
- [40] M. T. Birgonul, and I. Dikmen, "Neural network model to support international market entry decisions". *Journal of Construction Engineering and Management-Asce*, vol. 130, pp. 59-66, 2001.
- [41] Z. Önis, and U. Türem, "Business, globalization and democracy: a comparative analysis of Turkish business associations". *Turkish Studies*, vol. 2, pp. 94-120, 2001.
- [42] K. Cagiltay, B. Bichelmeyer, and G. Kaplan Akilli, "Working with multicultural virtual teams: critical facilitation, satisfaction, and success factors". *Smart Learning Environments*, vol. 2, 11, Jun 2015.
- [43] M. Demirbağ, and H. Mirza, "Factors affecting international joint venture success: an empirical analysis of foreign-local partner relationships and performance in joint ventures in Turkey". *International Business Review*, vol. 9, pp. 1-35, Feb 2000.
- [44] A. Osman Gürbüz, and A. Aybars, "The impact of foreign ownership on firm performance, evidence from an emerging market: Turkey". *American Journal of Economics and Business Administration*, vol. 2, pp. 350-359, 2010.
- [45] C. Hampden-Turner, and F. Trompenaars, *Riding the waves of culture: Understanding diversity in global business*, Hachette UK, 2020.
- [46] S. Togan, "Technical barriers to trade: the case of Turkey and the European Union". *Journal of Economic Integration*, vol. 30, pp. 121-147, 2015.

---

## Reviewer List of Volume 12 Issue 4 (2024)

---

Abdullah Aık	Dokuz Eylöl University	Türkiye
Ali Doğrul	National Defense University	Türkiye
Aykut Korkmaz	Dokuz Eylöl University	Türkiye
Aysu Göçer	İzmir University of Economics	Türkiye
Bulut Ozan Ceylan	Bandırma Onyedi Eylöl University	Türkiye
Burak Kundakçı	İskenderun Technical University	Türkiye
Cihad Delen	İstanbul Technical University	Türkiye
Coşkan Sevgili	Zonguldak Bülent Ecevit University	Türkiye
Davut Pehlivan	Mersin University	Türkiye
Dragan Pamucar	University of Belgrade	Serbia
Göl Denктаş Şakar	Dokuz Eylöl University	Türkiye
Joe Ronald	Korea Maritime & Ocean University	South Korea
Kadriye Oya Turhaner	Yaşar University	Türkiye
Kubilay Bayramođlu	Zonguldak Bülent Ecevit University	Türkiye
Marcin Przywarty	Maritime Univeristy of Szczecin	Poland
Mehmet Doymuş	Dokuz Eylöl University	Türkiye
Melek Ertođan	İstanbul Technical University	Türkiye
Michel Daaboul	University of Balamand	Lebanon
Muammer Nurduhan	Dokuz Eylöl University	Türkiye
Nergis Özispa	Mersin University	Türkiye
Nesrin Alptekin	Anadolu University	Türkiye
Nguyen Thi Le Thuy	Ho Chi Minh City Open University	Vietnam
Ođuzhan Kırıkbaş	Istanbul Technical University	Türkiye
Olgun Konur	Dokuz Eylöl University	Türkiye
Ömer Melih Göl	Istanbul Technical University	Türkiye
Özdal Gökdal	Adnan Menderes University	Türkiye
Ratna Purwaningsih	Diponegoro University	Indonesia
Saly Yaacoub	University of Balamand Issam Fares	Lebanon
Serim Paker	Dokuz Eylöl University	Türkiye
Seyid Mahmud Esad Demirci	Sakarya University of Applied Sciences	Türkiye
Umut Taç	Piri Reis University	Türkiye
Umut Yıldırım	Karadeniz Technical University	Türkiye
Yaser Farag	University of Strathclyde	Scotland

---

## 2024 Reviewer Index

---

Abbas Mamudu	Fuat Alarçin	Oğuzhan Kırıkbaş
Abdullah Açık	Gökçe Çiçek Ceyhun	Olgun Konur
Achraf Touil	Gökhan Budak	Onur Yüksel
Ali Can Takinacı	Gül Denктаş Şakar	Ömer Arslan
Ali Doğrul	Güven Gonca	Ömer Kemal Kınacı
Ali Tehci	Hasan Gökhan Güler	Ömer Melih Gül
Amellal Issam	Hasan Ölmez	Özdal Gokdal
Arda Toygar	Hasan Uğurlu	Özgür Kırca
Asım Sinan Karakurt	Hüseyin Gençer	Özkan Uğurlu
Ayfer Ergin	Indra Gunawan	Quang Thang Do
Aykut Korkmaz	İshak Altınpınar	Ramazan Şener
Ayman Sabry Karim	Joe Ronald	Ratna Purwaningsih
Aysu Göçer	José A Orosa	Refik Özyurt
Ayşe Yüksel Ozan	Kadriye Oya Turhaner	Saly Yaacoub
Barış Ufuk Şentürk	Koray Şahin	Samet Biçen
Buğra Çelebi	Kubilay Bayramoğlu	Sedat Baştuğ
Bulut Ozan Ceylan	M. Imron Masud	Serdar Kum
Burak Kundakçı	Mahmut Ali Gökçe	Serdar Turgut İnce
Burcu Aracıoğlu	Marcin Przywarty	Serdar Yıldız
Burhan Kayıran	Mehmet Doymuş	Serim Paker
Cemile Solak Fışkın	Meisam Mahboubi Niazmandi	Seyid Mahmud Esad Demirci
Cihad Delen	Melek Ertoğan	Simone Mancini
Cihan Şahin	Michel Daaboul	Soner Esmer
Coşkan Sevgili	Mihaela Greti Manea	Tahsin Görmüş
Çağatay Kandemir	Momoko Kitada	Tamer Mahmoud Ahmed
Dahlia El-manstrly	Mouhsene Fri	Taner Çoşgun
Davut Pehlivan	Muammer Nurduhan	Theophilus Chinoyerem Nwokedi
Deniz Bayraktar Bural	Muhammet Aydın	Uğur Can
Doğan Kısacık	Muhammet Boran	Umut Taç
Dragan Pamucar	Muhammet Gül	Umut Yıldırım
Elif Arslan	Mustafa Nuran	Veysi Başhan
Emin Deniz Özkan	Mustafa Taşkın	Volkan Efecan
Emrah Erginer	Müge Büber	Yasemin Arıkan Özden
Emre Kahramanoğlu	Naz Yılmaz	Yasemin Nemlioğlu Koca
Emre Pesman	Nergis Özispa	Yaser Farag
Erdem Kan	Neslihan Paker	Yavuz Hakan Özdemir
Erkan Çakır	Nesrin Alptekin	Yunus Emre Şenol
Fatih Cüneyt Korkmaz	Nguyen Thi Le Thuy	Zdeslav Juric
Ferdi Çakıcı	Nur Jale Ece	

---

## 2024 Author Index

---

Abdullah Aık.....	106	Heri Kuswanto.....	404
Achmad Riadi.....	395	Hwanseong Kim.....	169
Afşin Baran Bayezit.....	365	I Made Ariana.....	277
Aguk Zuhdi Muhammad Fathallah.....	277	Igor De Souza Pinto.....	310
Ahmad Irham Jambak.....	365	Iis Dewi Ratih.....	404
Ahmed S. A. Ibrahim.....	116	Ismail Bayezit.....	346
Ahmet Kaan Karabüber.....	365	İbrahim Sani Mert.....	466
Aleksei Dobrodeev.....	358	İsmail Çiçek.....	377
Ali Burin Eke.....	427	Jin Wang.....	156
Ali Yasin Kaya.....	156	Jooyoung Son.....	446
Almudena Filgueira-Vizoso.....	36	Jürgen Göken.....	418
Anak Agung Bagus Dinariyana.....	253	Ketut Buda Artana.....	253, 404
Anas M. El Molla.....	116	Kirill Sazonov.....	358
Anh Dan Nguyen.....	2	Koena Mukherjee.....	144
Aydın Bozkurt.....	74	Kubilay Bayramođlu.....	128
Aykut Öler.....	224	Laura Castro-Santos.....	36
Barış Barlas.....	224	Leonardo Braga.....	310
Batuhan Çullu.....	186	Luidmyla Leonidovna Nikolaieva.....	25
Brais Preto-Fernández.....	36	Maruf Gögebakan.....	213
Bünyamin Ustalı.....	365	Mateus Carvalho Amaral.....	310
Can Özsoy.....	238	Mehmet Akif Uđur.....	365
Cüneyt Baykal.....	238	Mehmet Utku Öđür.....	365
Dhimas Widhi Handani.....	404	Melek Ertogan.....	64, 74
Elvan Deniz.....	319	Mikhail Gapanovich.....	287
Emrah Akdamar.....	213	Minh Tuan Vu.....	295
Emre Kahramanođlu.....	14, 365	Mohd Rashdan Saad.....	83
Emre Sayın.....	346	Mohd Rosdzimin Abdul Rahman.....	83
Eralp Özkaya.....	156	Muhammad Hanif Fajri Ramadhan.....	395
Ersin Fırat Akgül.....	213	Muhammed Fatih Gülen.....	427
Esma Uflaz.....	427	Natalia Paleo-Mosquera.....	36
Evgenia Rabenok.....	287	Nergis Özispa.....	186
Evrin Işık.....	213	Ngoc Cuong Truong.....	169
Fatih Tonođlu.....	156	Nicolas Saba.....	418
Febro Helios Javanica.....	253	Nikolay Sinyavsky.....	287
Ferdi Çakıcı.....	14, 365	Noh Zainal Abidin.....	83
Firly Irhamni Ahsan.....	277	Nur Jale Ece.....	50
Fuat Peri.....	365	Nurten Vardar.....	332
Gamze Arabelen.....	186	Ođuzhan Kırıkbaş.....	199
Giri Ram.....	83	Oksana Synashenko.....	287
Gonca Tuncel.....	319	Oleksandr Viktorovich Haichenia.....	25
Hany G. I. Ahmed.....	116	Omar Djecevic.....	377
Hasan Uđurlu.....	377	Orun Gündođan.....	92



---

## 2024 Author Index

---

Ozan Batmaz .....	427	Soner Esmer .....	319
Ömer Sinan Şahin.....	365	Şakir Bal .....	199
Özcan Arslan .....	427	Tabassum Rasul .....	144
Özgür Sert .....	466	Taner Çoşgun .....	332
Özgür Yalçinkaya .....	319	Taras Yurievitch Omelchenko .....	25
Özkan Uğurlu .....	156	Taufik Fajar Nugroho.....	253
Paulo Apicelo De Souza Pereira .....	310	Tolga Aycı.....	224
Pavel Burakovskiy.....	136	Toorban Mitra.....	263
Philip A. Wilson.....	64	Tuba Keçeci.....	92
Phung Hung Nguyen .....	169	Viet Thanh Nguyen .....	2, 295
Qianfeng Lin .....	446	Vinh An Le.....	2
Ramón Yáñez-Brage.....	36	Yen Thi Pham .....	169
Renata Zahabiya .....	404	Yves Lacroix.....	295
Rodolfo Cardoso .....	310	Zayyan Fakhri Suwardana.....	253
Savaş Sezen.....	14		
Selçuk Nas .....	1, 115, 237, 357		

---

## 2024 Subject Index

---

Adaptive control.....	144	Damietta port .....	116
Adaptive cumulative prospect theory.....	169	Damping.....	418
Air pollution .....	156	DARPA Suboff.....	199
Alpha shape algorithm.....	446	Data-driven control.....	144
Alternative fuels .....	128	Decision-making.....	169
Ammonia .....	128	Dielectric constant.....	287
Annular flow .....	332	Dielectric loss tangent .....	287
Automatic identification system.....	156	Digitalization.....	92
Autonomous underwater vehicle.....	64, 144	Dinh An estuary.....	2
Availability .....	310	Double-cycling.....	319
Bearing capacity.....	136	Dynamic discretization.....	404
Beyond cabotage policy.....	395	Dynamic mechanical analysis.....	418
Binary contact detection model.....	446	Dynamic path planning .....	377
Bio-based materials .....	418	Dynamic position control.....	64
Black box modelling.....	64	Energy security.....	106
Black Sea.....	156	Exergy analysis.....	128
Bluetooth 5.1 technology.....	446	Failures.....	310
BN .....	404	FEM .....	136
Breakwater .....	83	Field modeling.....	224
Carbon fiber .....	277	Fire dynamics simulation.....	224
Cascade control.....	346	Fire safety.....	224
CFD .....	14	Fishing vessels.....	156
CFRP propeller.....	277	Fluid-structure interaction .....	277
Challenges and facilitators in Türkiye.....	466	Genetic algorithm .....	346
Chi-square test.....	50	Giens tombolo.....	295
Collision avoidance .....	377	Grounded theory.....	466
Collision frequency.....	253	Heavy-tonnage vessel.....	358
Collision Risk Index (CRI) .....	377	Hierarchical management system .....	25
COLREGs .....	377	Hull form.....	358
Competitiveness factor.....	36	Hydrodynamic.....	2, 295
Computational fluid dynamics .....	74, 93, 332	Hydrodynamic performance.....	83
Concentric annulus .....	332	Hydrogen.....	128
Conductivity .....	287	Ice basin .....	358
Container terminal.....	319	Ice navigation .....	74
Content analysis .....	466	Interpersonal relationship.....	263
Corrugated bulb.....	136	IWRAP.....	253
COVID-19.....	263	Kalman filter .....	365
CRITIC.....	213	Leximancer .....	186
Crude palm oil.....	395	Liquefied natural gas.....	106
Cruise ship disease management.....	446	LQG.....	365
Cumulative prospect theory.....	169	Maneuvering coefficient.....	199
Daily profit model.....	169	Marine motor oils .....	287

---

## 2024 Subject Index

---

Marine propeller .....	74	Sediment transport rate.....	295
Marine transportation .....	395	Service quality perception .....	186
Marine-propeller.....	277	Shallow neural networks.....	64
Maritime piracy .....	50	Ship collision.....	404
Maritime security.....	50	Ship collisions.....	136
Maritime trade .....	50, 213	Ship domain .....	377
Maritime traffic.....	253	Ship emissions.....	156
Maritime transport logistics .....	92	Ship heading control.....	346
MIKE21.....	116	Shipbuilding .....	36, 106
Mixed integer linear programming.....	395	Shipping network .....	169
Model tests.....	358	Shipyards .....	36
Model-based simulation .....	346	Shoreline change model.....	238
Multi-level control system .....	25	Simulation .....	319
Numerical model.....	295	SLR .....	295
Oceans.....	36	Stern tube .....	332
Offshore breakwater.....	238	Strategic management.....	427
Offshore renewable energies.....	36	Strategic ship fleet planning.....	395
Offshore tugboat and support vessel operations.....	427	Structural equation modeling (SEM).....	92
Open water test.....	277	Structural equation modelling .....	263
OpenFOAM.....	199	Structure analysis .....	74
Operational characteristics .....	25	Submarine.....	14
Optimization .....	395	Sustainability index.....	128
Oscillating buoy .....	83	SWOT.....	427
Particle swarm optimization.....	346	Taylor-Couette-Poiseuille flow.....	332
Passenger ships .....	224	Technology acceptance model (TAM) .....	92
Personality traits.....	263	TOPSIS .....	427
Plastic limit analysis .....	136	TOWS fuzzy DEMATEL .....	427
Port call .....	213	Tra Vinh province .....	2
Port container terminals.....	25	Trend analysis .....	116
Propulsion in ice.....	358	Turbulence.....	332
Qualitative analysis of Turkish business environment....	466	Turkish seaborne business environment.....	466
Quasi-2DH.....	238	Unfalsified control .....	144
Quay crane .....	319	User generated content.....	186
RBM.....	310	Vertical maneuvering derivatives .....	14
Roll stabilization.....	365	VIKOR.....	213
Rotating arm .....	199	Wave .....	116
Routeing measures.....	253	Wave energy converter.....	83
ROV.....	310	Wood .....	418
Scale effect .....	14		
Sediment transport.....	2, 116, 238		

---

Volume 12 Issue 4 (2024) is indexed in

---



**TRID**

the TRIS and ITRD database



TÜBİTAK

**ULAKBİM**



**Scopus**

---

## JEMS's Sponsors

---

**INCE SHIPPING  
GROUP**



**GEMLIK PILOTS**



**DENİZ ÇALIŞANLARI  
DAYANIŞMA DERNEĞİ**



**EGE GAZ INC.**



**SEFİNE SHIPYARD**



**GÜRDESAN SHIP MACHINERY CORP.**



**ER SHIPPING**



**ONURSAN**



# ONURSAN

40  
YEĞER

*Istanbul / Türkiye*

[onursan@onursan.net](mailto:onursan@onursan.net)



## SAFETY FIRST



*Istanbul / Türkiye*

[info@gepafiberglass.com](mailto:info@gepafiberglass.com)



*Houston / Texas*

[sales@americanmarinesafety.com](mailto:sales@americanmarinesafety.com)



*Rotterdam / Netherlands*

[rotterdam@onursan.net](mailto:rotterdam@onursan.net)





**GEMLIK PILOTS**  
Gemlik Pilotage and Tugboat Services Inc.

**GEMLIK Pilotage  
and Tugboat  
Services Inc.,**

provides the highest  
level of navigation  
and maneuvering  
safety, which aims  
to continuous  
training and  
development, in  
Gemlik Bay.

**GEMLIK PILOTS**  
**GEMLIK Pilotage and Tugboat Services Inc.**

Adress : Ata Mh. Sanayi Cd. No:4 İç Kapı No:9  
Gemlik / BURSA Phone : 0224 524 77 35 - 0224 524 77 36  
Fax : 0224 524 77 64  
e-mail : pilotage@geptco.com

